Characterising the role of the nsP3 macro domain in Chikungunya virus replication

Grace Charlotte Roberts

Submitted in accordance with the requirements for the degree of
Doctor of Philosophy

The University of Leeds
Faculty of Biological Sciences
School of Molecular and Cellular biology

November 2018

The candidate confirms that the work submitted is their own, except where work which has formed part of jointly-authored publications has been included. The contribution of the candidate and the other authors to this work has been explicitly indicated below. The candidate confirms that appropriate credit has been given within the thesis where reference has been made to the work of others.

Chapter 3 within this thesis has been based on work from a jointly-authored publication:

Grace C. Roberts, Carsten Zothner, Roland Remenyi, Andres Merits, Nicola J. Stonehouse & Mark Harris (2017). Evaluation of a range of mammalian and mosquito cell lines for use in Chikungunya virus research. Scientific Reports DOI: 10.1038/s41598-017-15269-w

- All experiments were performed by GCR
- CZ and RR assisted in optimisation of the CHIKV systems used in the study
- AM provided methods and reagents
- NJS and MH provided supervision and co-authored the paper

Acknowledgements

Abstract

Chikungunya virus (CHIKV) causes an acute fever with debilitating joint pain. Spread by the *Aedes* species of mosquito, recent increases in global temperature, and mutations in the viral glycoproteins have facilitated outbreaks worldwide with huge economic burden. Despite the recent resurgence of CHIKV, there are currently no vaccines or antiviral agents available.

CHIKV, an alphavirus, possesses a positive sense, single stranded RNA genome that encodes four non-structural proteins (nsPs). The CHIKV nsP3 possesses an N-terminal macro domain, a domain found in the proteins of all species, and are defined by their ability to bind ADP-ribose. It is unclear what role the nsP3 macro domain contributes to CHIKV replication.

Initially, a panel of cell lines was validated in terms of their physiological relevance and ability to support the replication of the CHIKV replicon and infectious virus. The phenotypes of a panel of mutants in the ADP-ribose binding pocket of the nsP3 macro domain were assessed in the context of a sub-genomic replicon and infectious virus in a range of relevant cell lines. Comparison of this data to the known biochemical properties of the nsP3 macro domain from the literature, indicated that ADP-ribose binding was crucial to CHIKV replication. In addition, this data suggested a role for the nsP3 macro domain in antagonising cellular innate immune pathways. ADP-ribose signalling has been implicated in the activation of the NFκB pathway therefore potential for the nsP3 macro domain to interfere with this cell signalling pathway was investigated. It was demonstrated that CHIKV did not activate the pathway and that expression of nsP3 actively was inhibitory. Furthermore, macro domain mutants with reduced ADP-ribose binding were unable to inhibit the pathway. It is therefore proposed that the CHIKV nsP3 macro domain is a virulence factor, able to suppress the host NFκB pathway to facilitate viral replication.

Table of Contents

List of Figures

List of Tables

List of Equations

Abbreviations

+ssRNA	Positive sense, single stranded RNA
26S	CHIKV subgenomic RNA encoding for the structural proteins
A	Ampere
Å	Angstrom
ADAR	Adenosine deaminase
ADP	Adenosine diphosphate
ADPR	ADP-ribose
Ae	*Aedes*
APS	Ammonium persulfate
ARTD	ADP-ribosyltransferase diphtheria toxin like
ATPSβ	ATP synthase beta subunit
AUD	Alphavirus unique domain
BHK	Baby hamster kidney cells
Bin1	Bridging Integrator 1
BSA	Bovine serum albumin
BSL	Biosafety level
C	Core
CFAV	Cell fusing agent virus
CHIKV	Chikungunya virus
CIP	Calf intestinal phosphatase
CME	Clathrin mediated endocytosis
CMV	Cytomegalovirus
CNS	Central nervous system
CoVs	Coronaviruses
CPV	Cytopathic vacuole
DAPI	4′,6-diamidino-2-phenylindole
DePC	Diethyl pyrocarbonate
dLuc	Dual luciferase
DMSO	Dimethyl sulfoxide
DNA	Deoxyribose nucleic acid
dNTP	deoxynucleoside triphosphate
dsRNA	Double stranded RNA
E1	Envelope protein 1
E2	Envelope protein 2
E3	Envelope protein 3

ECSA	East/central/southern African
EDTA	Ethylenediaminetetraacetic acid
EEEV	Eastern encephalitis virus
EGFP	Enhanced green fluorescent protein
ER	Endoplasmic reticulum
FBS	Fetal bovine serum
FLuc	FIrefly luciferase
G3BP	GAP SH3 domain binding protein
GAGs	Glycosaminoglycans
GBS	Guillain-Barre syndrome
GFP	Green fluorescent protein
GTase	Guanylytransferase
h	Hours
HCV	Hepatitis C virus
HEK	Human embryonic kidney
HEV	Hepatitis E virus
HIV	Human immunodeficiency virus
hpe	Hours post electroporation
hpi	Hours post infection
hpt	Hours post transfection
Hsp70	Heat shock protein 70
HTNV	Hantaan virus
HVD	Hypervariable domain
HVR	Hypervariable region
IBV	Infectious bronchitis virus
ICA	Infectious centre assay
ICRES	"Integration of Chikungunya research" virus strain
IF	Immunofluorescence
IFIT-1	Interferon induced protein with tetratricopeptide repeats 1
IFN	Interferon
Ifnar	IFN α/β receptor
IKK	IκB kinase
IOL	Indian ocean lineage
IPS-1	IFN promoter stimulator 1
IRES	Internal ribosomal entry site
IRF-1	IFN regulatory factor 1
IRF3	IFN regulatory factor 3
ISGs	IFN stimulated genes

IκB	Inhibitor of kappa B
JAK	Janus kinases
kDa	Kilodaltons
KLD	Kinase ligase DPNI
LB	Lysogeny broth
LC3	Light chain 3
LSM	Laser scanning microscope
MAR	Mono-ADP-ribose
MAVS	Mitochondrial anti-viral signalling protein
MAYV	Mayaro virus
MC	Methyl cellulose
min	Minutes
miR	microRNA
MLV	Murine leukaemia virus
MOI	Multiplicity of infection
MOPS	3-(N- morpholino)propanesulfonic acid
mRNA	Messenger RNA
ms	Milliseconds
MTase	Methyltransferase
NAD	Nicotinamide adenine dinucleotide
NEB	New England Biolabs
NEMO	NFκB essential modulator
NFκB	Nuclear factor kappa light chain enhancer of activated B cells
ns	Not significant
nsPs	Non-structural proteins
ONNV	O'nyong nyong virus
ORF	Open reading frame
PAR	Poly-ADP-ribose
PARG	PAR glycohydrolase
PARP	Poly-ADP-ribose polymerase
PBS	Phosphate buffered saline
PCR	Polymerase Chain Reaction
PFA	Para-formaldehyde
PFU	Plaque forming units
pH	Potential hydrogen
PLB	Passive lysis buffer
Poly(I:C)	Polyinosinic acid:polycytidylic acid
PVDF	Polyvinylidene difluoride

qRT-PCR	Quantitative, reverse transcriptase PCR
RdRp	RNA dependent RNA polymerase
RIG-I	Retinoic acid-inducible gene I
RLuc	Renilla luciferase
RNA	Ribose nucleic acid
RNAi	RNA interference
RRV	Ross river virus
RSV	Respiratory syncytial virus
rt	Room temperature
SDS	Sodium dodecyl sulfate
SDS-PAGE	SDS polyacrylamide gel electrophoresis
SG	Subgenomic
SGR	Subgenomic replicon
SH3	SRC Homology 3 Domain
SINV	Sindbis virus
STAT	Signal transducer and activator of transcription proteins
SUMO	Small ubiquitin-like modifier
SV40	Simian virus 40
TBS	Tris buffered saline
TDP1	Tyrosyl DNA phosphodiesterase 1
TEMED	Tetramethylethylenediamine
TIM-1	T cell immunoglobulin mucin domain 1
TLR	Toll-like receptor
TNFα	Tumour necrosis factor α
tRNA	Transfer RNA
UTR	Untranslated region
VEEV	Venezuelen equine encephalitis virus
VLP	Virus like particle
VR	Variable region
VZV	Varicella zoster virus
WEEV	Western equine encephalitis virus
wt	Wildtype
YBX1	Y-box binding protein
ZAP	Zinc anti-viral protein

Chapter 1 Introduction

1.1 Chikungunya virus

1.1.1 Identification and classification

Chikungunya virus (CHIKV) was first isolated and identified in Tanzania in 1952 (Lumsden, 1955) where a large outbreak occurred that resembled Dengue fever. The name 'Chikungunya' comes from the local Kimakonde language which roughly translates to 'bent upwards,' describing the appearance from those suffering with the painful joint symptoms of the disease.

CHIKV is in the *Alphavirus* genus of the *Togaviridae* family (Chen *et al.*, 2018). The majority of alphaviruses, including CHIKV, are mosquito-borne, and are alternately transmitted between the mosquito vector and vertebrate hosts. In addition to CHIKV, there are eight alphaviruses that are human pathogens and these are further separate into "new world" and "old world" alphaviruses defined by their genomic sequence, disease pathology and their geographical distribution (Zumla, 2010). Old world alphaviruses are mostly found in Africa, Asia, and Australia and cause disease of high fever, arthralgia and rashes. This group includes CHIKV, O'nyong-nyong virus (ONNV), Semliki forest virus (SFV) Mayaro virus (MAYV), Ross river virus (RRV), and Sindbis virus (SINV). New world alphaviruses are generally found in the western hemisphere, cause encephalitis, and includes Venezuelan equine encephalitis virus (VEEV), eastern equine encephalitis virus (EEEV), and western equine encephalitis virus (WEEV). Not all alphaviruses are human pathogens. Although equine encephalitis viruses infect humans, the primary host of these viruses are equine species including horses and donkeys. Other alphaviruses specifically infect fish and seals such as rainbow trout sleeping disease virus and southern elephant seal virus (Weston *et al.*, 1999; Villoing *et al.*, 2000; La Linn *et al.*, 2001). Eilat virus is a unique alphavirus as it exclusively infects mosquitos (Nasar *et al.*, 2012).

Analysis of the E1 coding regions of all the alphaviruses revealed that alphaviruses evolved from a common, "New World" ancestor virus (Powers *et al.*, 2001). The same study also demonstrated that CHIKV falls into the "Semliki Forest Complex" alongside viruses including ONNV, MAYV and SFV. Due to the close evolutionary relationship between CHIKV and SFV, and the fact that SFV

is a biosafety level 2 (BSL2) pathogen, whereas CHIKV is BSL3, SFV is often used as a model virus for the study of CHIKV. Though evolutionarily less related, SINV is also used as a model for CHIKV as it is also a BSL2 pathogen (Sourisseau *et al.*, 2007).

1.1.2 Epidemiology and transmission

CHIKV is spread by the *Aedes* (*Ae.*) species of mosquito, primarily by *Ae. aegypti,* although the virus has been detected in many other species of the *Aedes* mosquitos as well as some *Anopheles* and *Culex* species (Diagne *et al.*, 2014). Humans become infected with CHIKV via mosquitos which bite when taking a blood meal. CHIKV can also be transmitted vertically from infected pregnant mothers to the unborn child (Gérardin *et al.*, 2008).

It is thought that CHIKV originated in African forests since the only non-human hosts to have been identified are wild primates in these areas (Brault *et al.*, 2000). These areas have been suggested to maintain a sylvatic cycle between primates and mosquito vectors which eventually spilled over into nearby human populations (Peyrefitte *et al.*, 2007). It is thought that, from this initial zoonotic event, the virus spread further in Africa and to Asia. Since the discovery of CHIKV in Tanzania in 1952, the virus has been isolated in many African and Asian countries and has repeatedly re-emerged, causing many outbreaks in these countries, a phenomenon that is difficult to predict (Brault *et al.*, 2000). There are now three distinct, both genetically and geographically, strains of CHIKV; the West African, the east/central/south African (ECSA) and the Asian genotypes (see Figure 1.1).

In recent years, CHIKV has re-emerged on a global scale, emerging in many countries where the virus had not previously been isolated. This global re-emergence is thought to have initiated through the large Kenyan and Indian Ocean outbreaks of 2004-6. Part of this re-emergence was the large outbreak on La Reunion island in 2005/6, where 33% of the population were infected and 213 deaths were recorded that were attributed to CHIKV infection (Josseran *et al.*, 2006). It is thought that CHIKV was introduced to the island from Kenya, transported by shipping of goods and the migration of people through the Indian Ocean (Staples *et al.,* 2009, Chretien and Linthicum, 2007). There are many

factors thought to contribute to this explosive outbreak including the fact that CHIKV had never before been detected in La Reunion, with the local population naïve to the virus (Borgherini *et al.*, 2007). It is well documented that CHIKV is capable of rapid transmission in populations with little or no pre-existing immunity (Johansson, 2015). Also, *Ae. albopictus*, the primary mosquito species attributed to this outbreak, was already fully established on the island. Finally, a mutation in the E1 glycoprotein E1-A226V, first identified in this particular epidemic, allowed adaptation to the *Ae. albopictus* mosquito. The E1 mutation that developed from the East Central South African strain (see Figure 1.1), was termed the Indian Ocean lineage (IOL) and was found to facilitate higher midgut infectivity and greater dissemination to the salivary glands of the mosquito, allowing for more efficient transmission to vertebrate hosts (Tsetsarkin *et al.*, 2007).
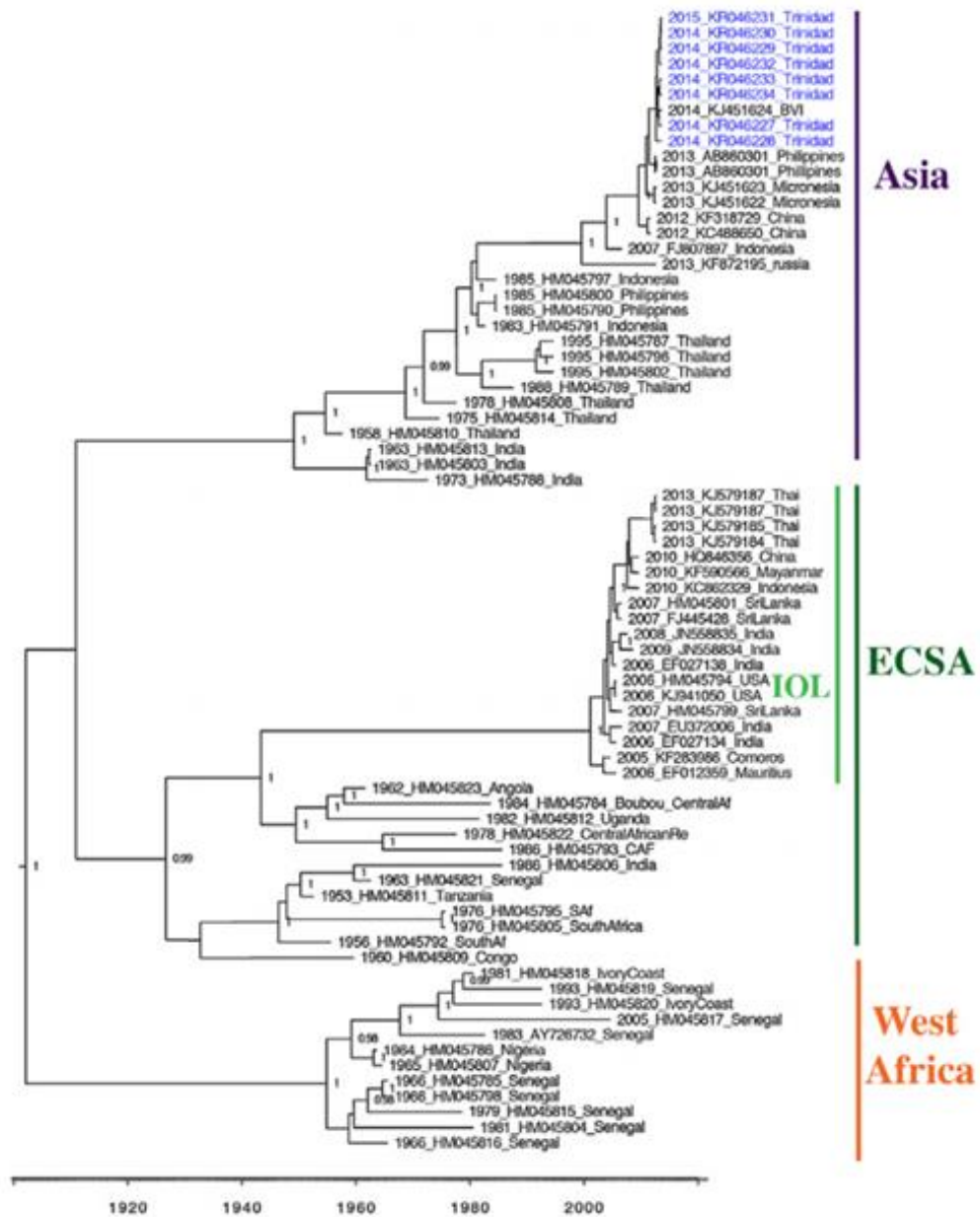
Figure 1.1 CHIKV phylogeny based on the complete coding region of clinical isolates. The east/central/southern African (ECSA) strain containing the E1-A226V mutation is represented as the Indian Ocean lineage (IOL) in light green. (Adapted from Wahid *et al.,* 2017).

The E1-A226V mutation has allowed CHIKV to thrive in areas where the previous, predominant vector; *Ae. aegypti* is absent, but where *Ae. albopictus* is established. There are many factors that contribute to the successful colonisation of *Aedes* mosquitos that differs greatly between the two sub-species. Generally,

the *Ae. aegypti* prefers much warmer and wetter climates, whereas the *Ae. albopictus* can tolerate much milder climates (Ducheyne *et al.*, 2018). There are many regions of the world where the *Ae. albopictus* has colonised but the *Ae. aegypti* has not, meaning that the E1-A226V mutation enables CHIKV to spread further than previously possible with the *Ae. aegypti* vector.

The *Ae. aegypti* mosquito is not common in Europe, however, over 30 European countries have established populations of the *Ae. albopictus* and are therefore susceptible to CHIKV outbreaks, as shown in Figure 1.2 (Wahid *et al.*, 2017). The first autochthonous CHIKV infection (transmission within the same country) in Europe was reported in Italy, 2007 and has been directly attributed to the E1-A226V mutation and the *Ae. albopictus* vector (Severini *et al.*, 2018). In France, multiple autochthonous infections have occurred in 2010, 2013 and 2014 which a small outbreak occurring in 2014. This outbreak originated by a traveller, returning from Cameroon, who introduced the virus to the local *Ae. albopictus* population resulting in the infection of 12 individuals. It is thought that the outbreak was limited due to the quick response of the French public health authorities, including the use of insecticide and the dissemination of information but also partly due to the onset of Autumn at the time, with cooler temperatures limiting the vector and therefore the spread of disease (Delisle *et al.*, 2015).
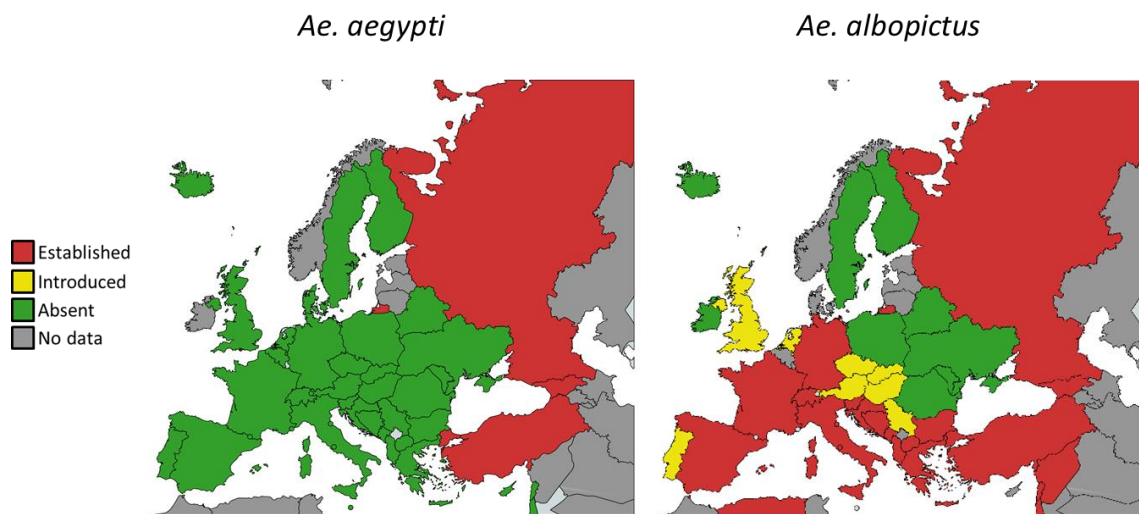
Figure 1.2 Distribution of the *Ae. aegypti* and *Ae. albopictus* in Europe. Correct as of Jan 2018. Red indicates countries with established populations of the mosquito (although not necessarily universally distributed within that country), yellow is where the mosquito has been detected but not established and green is where none have been detected. Adapted from the European Centre for Disease Prevention and Control (ECDC), map created using mapchart.net.

In contrast to Europe, the cases of CHIKV in the Americas are mostly due to the Asian strains of the virus. The first case of CHIKV in the Americas was on the island of Saint Martin in December 2013, with 50 cases confirmed in the same month (Leparc-Goffart *et al.*, 2014). By January 2014, many surrounding islands also reported autochthonous cases of CHIKV. In the Americas, there were existing, overlapping populations of both the *Ae. aegypti* and *Ae. albopictus* mosquito before CHIKV arrived into the region (Díaz *et al.*, 2015; Chin *et al.*, 2018; Honório *et al.*, 2018). Since 2013, autochthonous cases of CHIKV have been reported in 45 countries within the Americas. Genotypic analysis of CHIKV isolated from this outbreak have shown that the outbreak in the Americas was due to viruses that form a single clade within the Asian genotype of CHIKV, rather than the more recently-developed IOL clade (Lambert and Lanciotti, 2016). Early isolates from the initial St Martin outbreak were closely related to isolates from the Philippines taken at a similar time. Although the precise event that introduced CHIKV to the island is unknown, it is likely due to international travel that introduced the virus to the immunologically naïve populations of America

(Johansson, 2015). A summary of the global spread of CHIKV is show in Figure 1.3.
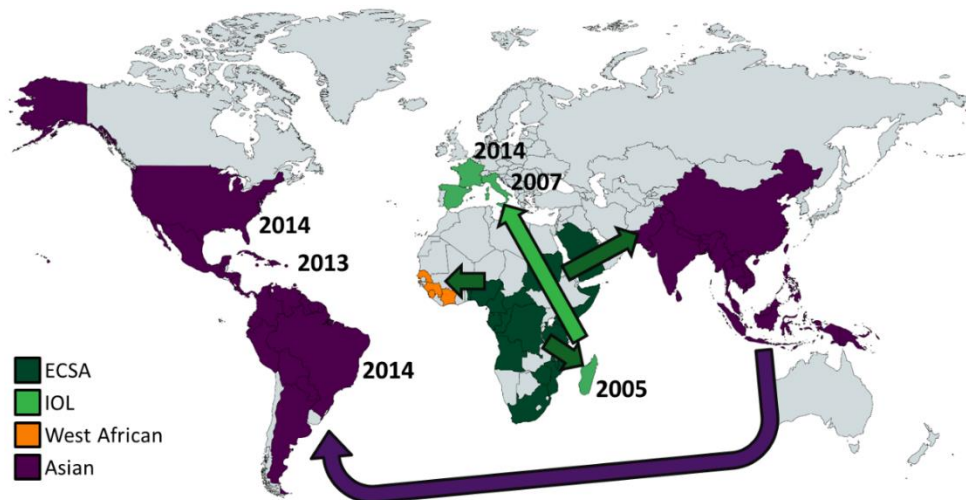
Figure 1.3 The global spread of CHIKV, with significant outbreaks denoted by the year. CHIKV is thought to have originated in central/eastern Africa (Brault *et al.,* 2000, with the ECSA strain depicted in dark green) and spread to west Africa and Asia which independently evolved to form distinct genotypes (shown in orange and purple respectively). The first major outbreak of recent years was in La Reunion and surrounding islands in 2005, which was the first detected instance of the E1-A226V mutation which has since been termed the Indian Ocean lineage (Tsetsarkin *et al.,* 2007, depicted in light green). The outbreaks in the Americas began in 2013 on the Caribbean island of Saint Martin, and were found to be from the Asian genotype (Johansson, 2015). This has since spread to all the American continents. Adapted from the Centre for Disease Control (CDC), correct as of May 2018. Map created using mapchart.net.

1.1.3 Pathology of Chikungunya fever

As shown in Figure 1.4, CHIKV is introduced into the body via a mosquito bite. The virus enters the skin and replicates to high levels in the local dermal fibroblasts. From the bite site, the virus is transported via the lymphatic and circulatory systems to disseminate throughout the body. It has been shown that the saliva from the mosquito, delivered alongside the virus, can enhance infection by inducing neutrophil-mediated inflammation which recruits myeloid cells (Pingen *et al.*, 2016). These myeloid cells become infected with CHIKV and transport the virus to the lymph nodes, where it is then disseminated systemically (Kam *et al.*, 2009). The virus favourably replicates in fibroblast, epithelial, neuronal, and endothelial cells in the tissues of the liver, muscles, joints and

brain (Thon-Hon *et al.*, 2012). After an incubation period of 2-4 days post-bite, symptoms occur such as high fever, myalgia, skin rash and arthralgia that can be debilitating (Tang, 2012). In this symptomatic period, viremia occurs with titres as high as 10^8 PFU/mL of blood (Simmons *et al.*, 2016), allowing mosquitos to acquire the virus from infected humans. It has been reported that titres of 10^7 PFU/mL of blood is sufficient for a mosquito to become infected through a blood meal (Hugo *et al.*, 2016).
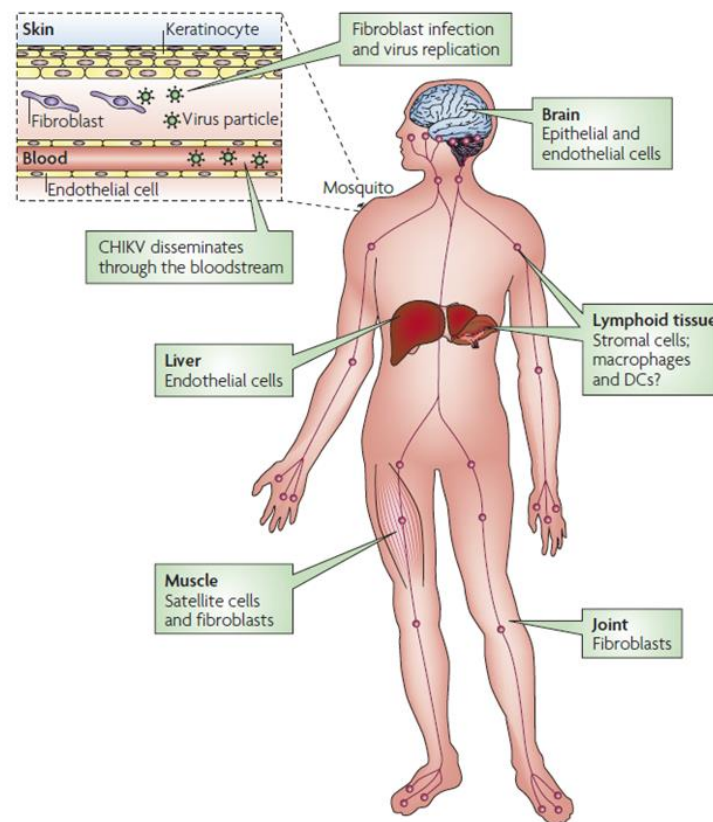
Figure 1.4 Infection and spread of CHIKV throughout the human body. The virus is introduced via mosquito bite where it infects and replicates in dermal fibroblasts and spreads through the circulatory and lymphatic systems to the lymphoid tissue, muscles, joints, liver and brain to replicate. Figure from Schwartz and Albert, 2010.

Although Chikungunya fever is rarely fatal, the joint pain resulting from infection can be incapacitating, thought to be mainly due to the direct infection of cells in musculoskeletal tissues (Haist *et al.*, 2017; Zaid *et al.*, 2018). After the acute phase of Chikungunya fever, the majority of patients recover within 2 weeks,

however, a sub-set of patients develop long term symptoms such as joint pain and swelling that can persist for months to years (Chang *et al.*, 2018; McHugh, 2018). Patients with long-term symptoms often report them occurring in a fluctuating manner. There were suggestions of these long-term symptoms being the result of CHIKV-induced autoimmunity, although there was no strong evidence to support this (Suhrbier *et al.,* 2012). More recently, chronic CHIKV-related symptoms have been attributed to viral persistence in joint tissues (Hawman *et al.*, 2013) and that a high viral load at the time of the acute infection is an indicator of persistence developing (Chow *et al.*, 2011).

1.1.3.1   Complications from CHIKV infection

In some cases of CHIKV infection, severe complications can develop. CHIKV can replicate in neuronal cells and, in rare cases, this can cause a range of neurological complications, the most common of which are encephalopathy and encephalitis. Encephalopathy is defined as "a clinical state of altered mental status, manifesting as confusion, disorientation, behavioural changes or other cognitive impairment" whereas encephalitis describes the pathological presentation of inflammation within the brain (Venkatesan *et al.*, 2013). In CHIKV-associated encephalitis, symptoms present between 0-13 days following onset of classical Chikungunya-fever symptoms. The pathology of CHIKV associated encephalitis varies between patients, with no district patterns on imaging by MRI, unlike other CNS pathogens such as cytomegalovirus (Boppana *et al.*, 1997). Encephalopathy is a particular problem with neonates and young children infected with CHIKV (Charlier *et al.*, 2017). Encephalitis is one of the most common presentation of atypical CHIKV infection and is a major cause of intensive care hospitalisation for CHIKV patients (Economopoulou *et al.*, 2009).

Another neurological complication caused by CHIKV is myelopathy (damage to the spinal cord) and myelitis (inflammation to the spinal cord). Patients with myelopathy present 0-3 weeks after classical CHIKV symptoms occur (Chandak *et al.*, 2009). The incident rate of spinal cord inflammation with CHIKV infection is unknown but is thought to be less common than encephalopathy, and no

deaths have been reported for CHIKV patients with myelopathy alone (Mehta *et al.*, 2018).

There have been reports that link Guillain-Barre syndrome (GBS) to CHIKV, with incidents of GBS increasing following outbreaks of CHIKV (Willison *et al.,* 2016). Individual case studies of CHIKV patients with GBS symptoms show that most made a full recovery within 3 months of infection (Mehta *et al.*, 2018).

Neurological complications of CHIKV are a particular issue for perinatal acquired infection with up to 50% of infected neonates developing encephalopathy, although this does vary by outbreak and causative genotype (Gérardin *et al.*, 2008). A significant number of children who acquire CHIKV perinatally develop issues later in life including reduced neurocognitive function, coordination and language issues with some cases of cerebral palsy and microcephaly (Gérardin *et al.*, 2014).

Another common complication of CHIKV infection is related to the cardiovascular system. In some outbreaks, up to 50% of patients infected with CHIKV report cardiovascular symptoms associated with the infection including myocarditis, heart failure and arrhythmia (Rajapakse, Rodrigo and Rajapakse, 2010). It has been shown that CHIKV is capable of infecting myocytes and this can result in damage of cardiac muscle fibres (Alvarez *et al.*, 2017). It has been noted however that these complications occur more regularly, although not exclusively, in patients with existing cardiac conditions (Economopoulou *et al.*, 2009).

Much rarer complications include hepatitis, which can be fatal (Torres *et al.*, 2015), as well as ocular inflammation, respiratory complications, pneumonia, renal failure and pancreatitis (Economopoulou *et al.*, 2009; Alvarez *et al.*, 2017).

1.1.4 Treatments and prevention strategies for CHIKV

Despite the pressing need for effective treatment and prevention of CHIKV there are currently no anti-viral agents or vaccines available (Abdelnabi *et al.,* Delang, 2016). Current treatment of CHIKV infection involves treating the symptoms rather than the virus with the predominant treatment of rest and hydration, alongside analgesics to treat the painful symptoms of the fever, with additional

medication to treat any specific complications that may occur (Cunha and Trinta, 2017).

1.1.4.1 Anti-viral agents for CHIKV

Although there are currently no licenced anti-viral agents available for the treatment of CHIKV infection, many agents have shown anti-viral effects *in vitro* and *in vivo*.

Some already licenced therapeutics such as ribavirin, which has been previously approved for use against Hepatitis C virus (HCV) and severe cases of respiratory syncytial virus (RSV), has also shown to have anti-CHIKV effects *in vitro*, which were enhanced when used in combination with IFN-α (Briolant *et al.*, 2004). Favipiravir (also referred to as T-705), was recently approved for use against Influenza in Japan, has broad-spectrum anti-viral activity. It has been shown to inhibit replication of both laboratory and clinical strains of CHIKV in cell culture and also reduced the mortality rate and limited neurological disease in experimentally infected mice (Delang *et al.*, 2014). It has shown to be effective against many RNA viruses *in vitro* and analysis of resistant mutants has implied its mechanism of action is against a highly conserved lysine residue (residue 291 in the case of CHIKV) in the RNA-dependent RNA-polymerase (RdRp).

Other treatments in development include monoclonal antibodies which has been demonstrated to protect mice lacking the IFN α/β receptor (IFNAR$^{-/-}$) mice from CHIKV induced mortality, both when given prophylactically or post-infection (Pal *et al.*, 2013). Another treatment strategy is to modulate cellular processes to combat CHIKV infection. This includes modulating the host immune response for example, treatment with IFN-α (Bordi *et al.*, 2011), polyinosinic acid:polycytidylic acid (poly(I:C)), (Li *et al.*, 2012) and RIG-I antagonists (Olagnier *et al.*, 2014) have all shown to reduce CHIKV replication *in vitro.*

Despite the recent advances in development of anti-viral agents for CHIKV in the pre-clinical stage, none have been approved for use in the clinic as of yet. Some therapeutics that demonstrated anti-viral activity *in vitro* were shown to not confer this activity *in vivo.* For example, chloroquine, originally used as an anti-malarial, was shown to have anti-viral activity against several viruses, including alphaviruses, where it has been shown to restrict CHIKV replication in cell

culture, possibly by disrupting the CHIKV entry process (Khan *et al.*, 2010). However, when used clinically on patients with acute CHIKV infection, chloroquine showed no significant efficacy (Chopra, Saluja and Venugopalan, 2014). This demonstrates that despite progress at the pre-clinical stage, there is still a lot more research and development required to produce an effective CHIKV anti-viral agent.

1.1.4.2 Vaccine development

Although there are currently no approved or licenced vaccines for use against CHIKV, there are many promising vaccine candidates in development that utilise a number of different strategies. Reverse genetics and biochemical studies of CHIKV have been utilised to better attenuate vaccines in order to increase safety, particularly to limit the possibility for reversion or to induce adverse reactions (Powers, 2018). It is therefore important to better understand the cellular and biochemical properties of the CHIKV proteins to rationally develop effective vaccines.

One of the first CHIKV vaccines to reach clinical trials was a virus-like particle (VLP) vaccine. These are non-infectious virus particles that lack genetic material so cannot replicate. These may be comprised of the structural proteins of a virus, or use a different, often more stable, virus 'scaffold' to which antigenic proteins can be presented to the immune system (Tagliamonte *et al.*, 2017). A particularly promising vaccine utilised a CMV expression vector, expressing the structural polyprotein of CHIKV in HEK293T cells, generating empty capsids of CHIKV. When tested *in vivo,* the vaccine conferred a strong neutralising antibody response in monkeys that protected them from infection, (Akahata *et al.*, 2010). When taken to human phase 1 trials, no adverse side effects were observed and all participants produced cross-genotype neutralizing antibodies, although the antibody titres were significantly reduced by the final point of the study (Chang *et al.*, 2014; Goo *et al.*, 2016).

Despite live attenuated vaccines requiring large scale production of virus in cell culture, recent developments of reverse genetics systems have allowed for genetic attenuation, increasing the safety profiles of vaccines and high expression of antigenic proteins (Stobart and Moore, 2014). One particular live

attenuated vaccine for CHIKV used reverse engineering to replace the subgenomic promotor with an IRES which restricted the host range so that, if the vaccine ever produced disease in individuals, it would not be able to replicate in mosquitos. This particular vaccine was able to produce a neutralizing antibody response and protect vaccinated mice when challenged.

Many of the CHIKV vaccines in development have adopted chimeric approaches. One of the most promising CHIKV chimeric vaccines is using alternate alphavirus systems. It has been shown previously that using alternate non-structural and structural open reading frames (ORFs) from different alphavirus can produce viruses that can replicate but are highly attenuated (Kim *et al.*, 2011). However, the resulting replicative phenotype can vary wildly with different combinations, not all of which being attenuated (Frolov, Frolova and Schlesinger, 1997). One particular alphavirus chimera, to protect from VEEV infection was formed using an attenuated strain of VEEV and SINV. This contained the SINV non-structural ORF and the VEEV structural ORF. This virus was further attenuated by mutating the sub-genomic promotor from the VEEV sequence to resemble the SINV sequence whilst still preserving the VEEV 5' RNA secondary structure in the subgenomic RNA. This vaccine produced strong immunogenic responses and inoculated mice survived and showed no symptoms when challenged with VEEV (Paessler *et al.*, 2003).

Subunit vaccines, such as those that contain the CHIKV structural proteins (Metz *et al.*, 2011) and DNA vaccines, which contain an attenuated CHIKV genome (Hallengard *et al.*, 2014) have both shown some effectivity against CHIKV, but as of yet, no vaccine is licenced for use against CHIKV.

1.1.4.3 Vector control

A different approach to reducing CHIKV and other arbovirus infections is to target the vector rather than the host. CHIKV cannot be transmitted horizontally between humans, mosquito vectors are essential for the spread of CHIKV, therefore effective control of the vector could reduce disease spread. A particular challenge for the control of alphavirus vectors; the *Aedes* mosquito, is that they have adapted to thrive in urban environments and bite during the day whereas other mosquito vectors, e.g. *Anopheles* species that transmit malaria, only bite

at night (Ferguson, 2018). Meaning that the simple measure of using mosquito nets to effectively reduce malaria infections is not an option for many arboviral infections (Fullman *et al.*, 2013). Many different measures have been attempted to control the *Aedes* alphavirus vector with varying levels of success.

Tackling environmental factors such as educating the local population about mosquitos and reducing potential breeding grounds has been shown to be effective although it requires willing community involvement that is sustained. This technique often reduces the risk of arboviral infections, but not significantly or for long periods of time (Andersson *et al.*, 2015).

Use of insecticides is the most prevalent approach to vector control, either by targeted deployment to destroy mosquito larvae, or by mass spraying. However this approach can be very costly and the success of application is highly dependent on the timing of the response which is often hampered by poor co-ordination (Esu *et al.*, 2010; Horstick *et al.*, 2010). Another recent issue with this approach is that many mosquitos have developed resistance to many insecticidal agents. There are multiple mechanisms of resistance including mutations to mosquito enzymes that process the insecticide. These include mutations to either the target protein of the insecticide, or to proteins that are able to process and excrete insecticides. Modification of behaviour allowing the mosquitos to actively avoid insecticide altogether has also been observed (as reviewed in Moyes *et al.*, 2017; Auteri *et al.*, 2018).

Some novel, biological approaches have been used to control *Aedes* mosquito populations and limit arboviral infections. *Wolbachia* bacteria have been previously characterised to inhibit multiple pathogens from replicating in infected mosquitos, including CHIKV and Dengue virus (Moreira *et al.*, 2009). *Wolbachia* are endosymbiotic intracellular bacteria, able to infect a wide range of insect species and is transmitted vertically. Although *Wolbachia* is not normally present in *Aedes aegypti* mosquitos (Zug and Hammerstein, 2012). The World Mosquito Program (formally 'Eliminate Dengue') aims to reduce arboviruses by releasing *Wolbachia*-infected mosquitoes into the wild, spreading *Wolbachia* to mosquito populations which produces a population that is less-able to transmit viruses to humans. It has been demonstrated that releasing infected mosquitos does

establish *Wolbachia* in wild, naïve mosquito populations which can be sustained (Jiggins, 2017). Data modelling has predicted that this technique will reduce arboviral infections however, in practice, this has yet to be determined (O'Neill *et al.*, 2018).

Another novel method of vector control is the use of genetically modified mosquitos to modify the wild population. One approach is to distort the sex-distribution of mosquitos, since only female mosquitoes bite humans, distorting the population to become predominantly male will reduce population number and restrict spread of disease. This can be achieved by introducing female-specific lethal genes, such as expression of X-chromosome endonucleases in sperm cells, so that male mosquitoes only produce sperm cells carrying Y-chromosomes so that all resulting offspring are male (Galizi *et al.*, 2014). Other methods such as use of transposons, engineering hyper-immune mosquitos, knock-out/knock-in systems, or introducing inducible lethal genes have all been demonstrated in laboratory mosquitos although it is unclear whether these systems could be established and maintained in wild populations (Gabrieli, Smidler and Catteruccia, 2014).

1.2 Molecular Biology of CHIKV

1.2.1 Genome organisation

CHIKV is a positive sense, single stranded RNA virus (+ssRNA). The 11.8 Kb genome comprises of two ORFs, the non-structural ORF at the 5' end and the structural ORF at the 3', separated by a junction region. The genome, as shown in Figure 1.5, has a 5' m7G cap and a poly(A) tail, resembling a cellular mRNA, as well as 5' and 3' untranslated regions (UTR) that are highly structured (Vasiljeva *et al.*, 2000; Solignat *et al.*, 2009).
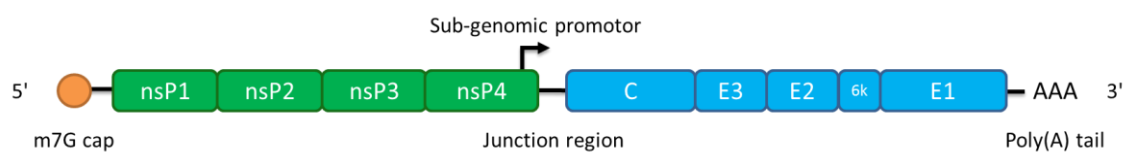
Figure 1.5 The genome organisation of CHIKV. The coding regions for the non-structural and structural proteins are shown in green and blue respectively. Black areas indicate untranslated regions of the genome. (Original figure).

The first ORF encodes for the four non-structural proteins (nsPs). The nsPs function to replicate viral RNA. RNA capping is performed by nsP1, nsP2 is a protease/helicase and nsP4 is the RdRp. The role of nsP3 is unclear but is required for RNA replication. Of the structural ORF, five proteins are expressed, three of which are components of the mature CHIKV virion: C, which forms the virus core, and E1 and E2 which form the viral glycoproteins. E3 acts as a chaperone protein to ensure correct glycoprotein folding and 6k is a proposed viroporin required for virus assembly.

Alphavirus genomes contain many RNA structures, both in coding and non-coding regions. In SINV, many of these structural elements have been shown to be important for virus production and/or replication. Some of these structures have been shown to be specific to either mammalian or mosquito cells whereas others have been shown critical for both species (Kutchko *et al.*, 2018). In CHIKV, there are many predicted secondary RNA structures across the genome, thought to be important for RNA replication and other functions (Parquet *et al.*,

17

2002). There is a high level of secondary structure in the 5' UTR and nsP1 coding regions. Multiple stem loops in this area have been shown to be crucial to viral replication in mammalian and mosquito cells – with some stem loops being mammalian or mosquito specific (Dr Andrew Tuplin, University of Leeds, personal communication). Interestingly, some of the secondary structures found in the 3' UTR of the CHIKV genome are genotype-specific, with unique structures found in the 3' UTR of the Asian genotype. These unique regions are thought to be due to adaptation to the mosquito vector (Chen *et al.*, 2013).

1.2.2 CHIKV virion organisation

All alphaviruses are spherical, enveloped viruses with a diameter of 70 nm (700 Å), as shown by Figure 1.6. At the centre of the virion is an icosahedral nucleocapsid core, comprising of 240 copies of C protein containing genomic RNA, closely surrounded by the membrane-derived envelope (Strauss and Strauss, 1994). Inserted in the envelope are the glycoprotein spikes formed of the E1, E2 and E3 proteins. The E1 and E2 proteins form a heterodimer where E1 is responsible for membrane fusion of the viral envelope with endosomal membranes whereas E2 binds cellular receptors as well as protecting the E1 fusion loop at a neutral pH (Yap *et al.*, 2017). E3 is responsible for the correct folding of the E2 precursor and the formation of the E1/E2 heterodimer. Unlike other alphaviruses, (R. Zhang *et al.*, 2011), E3 is not thought to be present on mature CHIKV particles (Sun *et al.*, 2013).
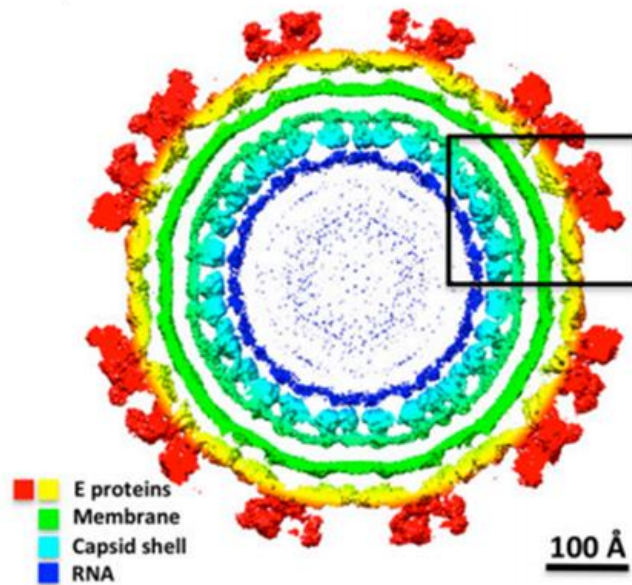
Figure 1.6 A cross section of CHIKV virion produced by cryo-electron microscopy reconstruction with envelope proteins shown in yellow/red, membrane in green, capsid in light blue and RNA in dark blue. Adapted from Yap *et al.,* 2017.

1.2.3 CHIKV life cycle

An overview of the CHIKV lifecycle is summarised in Figure 1.7. Few studies on alphavirus replication and lifecycle have been performed with CHIKV, instead much of the current literature have studied viruses such as SINV and SFV, presumably due to the lower containment requirement of these viruses. Due to the high level of sequence homology and protein structures, it is assumed that many of the processes in the alphavirus lifecycle are broadly similar across the alphaviruses. Hence, throughout this section, the virus used in each study has been explicitly stated to avoid confusion.
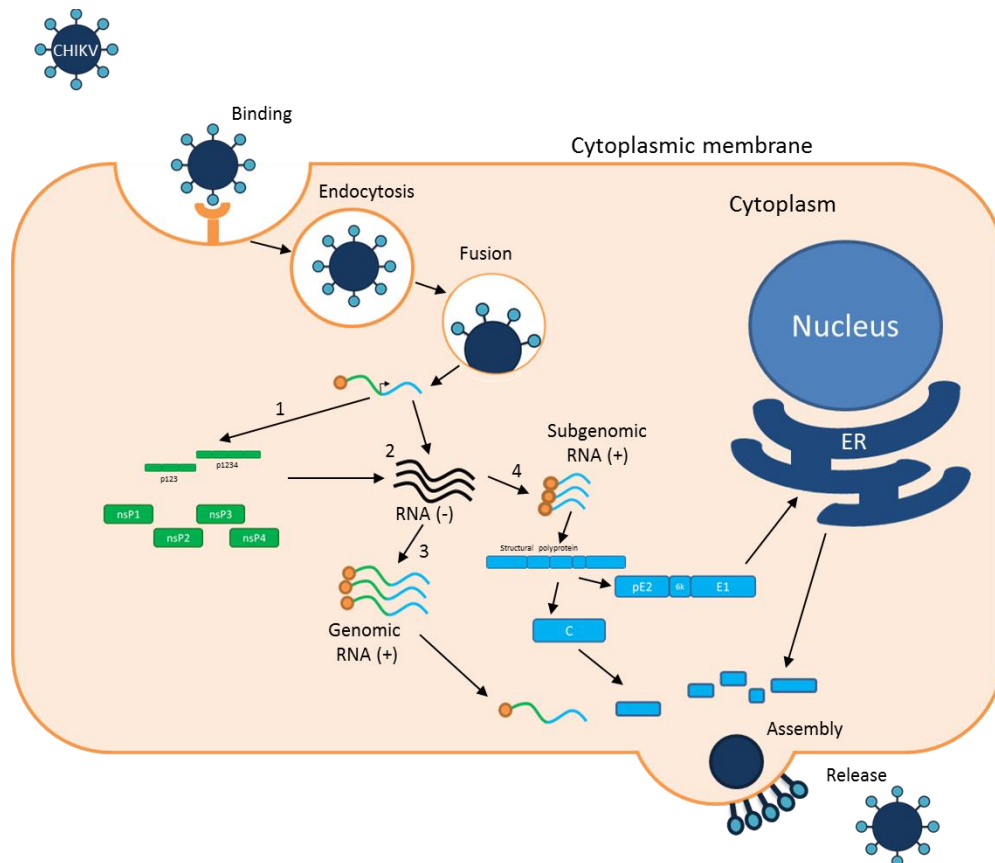
Figure 1.7 Overview of the CHIKV lifecycle. CHIKV enters cells through endocytosis and fuses with mature endosomes to release the genomic RNA into cells. (1) The non-structural proteins are directly translated from the genomic RNA which form replication complexes. (2) Replication complexes generate minus sense genomic RNA as a template to form genomic RNA for packaging (3) and for synthesis of the subgenomic RNA for translation of the structural proteins (4). The structural proteins are translated into a polyprotein which is subsequently cleaved in various areas of the infected cell. The structural proteins and the genomic RNA then co-ordinate at sites of assembly, thought to be at the plasma membrane, where they assemble to form virus particles and release from the cell. Original figure interpreted from references in section 1.2.3.

1.2.3.1 Cell entry

The first stage in CHIKV entry is the binding of a cellular receptor. It has been known for some time that the E2 glycoprotein is responsible for receptor binding, however, the cellular receptor for CHIKV is currently unclear (Smith *et al.*, 1995). CHIKV has a relatively wide cell tropism as it infects many cell types of the human body (Couderc *et al.*, 2008), as well as mosquito cells. This suggests that the cellular receptor for CHIKV must either be an ubiquitously expressed cellular

protein or, CHIKV utilises multiple receptors for cell entry. No single protein has been defined as the cell-entry receptor for CHIKV to date. Many cell surface proteins have been proposed to be the receptor or receptor binding factors for CHIKV entry in mammalian cells including (but not limited to): prohibitin (Wintachai *et al.*, 2012), T cell immunoglobulin mucin domain 1 (TIM-1), (Moller-Tank *et al.*, 2013), glycosaminoglycans (GAGs) (Silva *et al.*, 2014), and Mxra8 (Zhang *et al.*, 2018). In mosquito cells, ATP synthase beta subunit (ATPSβ) has been identified as a potential binding receptor. It was demonstrated via immunoprecipitation that ATPSβ binds CHIKV particles and co-localisation between CHIKV and the receptor was observed via immunofluorescence (Fongsaran *et al.*, 2014). It is likely that CHIKV uses multiple receptors for entry as few of these proposed receptor proteins are ubiquitously expressed and it has been shown for most of these proposed proteins, that CHIKV can still establish infection, albeit reduced, in the absence of these individual receptors.

Although there has been much conflicting data, the general consensus is that Alphaviruses enter host cells predominantly through clathrin-mediated endocytosis (CME), however there is also evidence for entry via clathrin-independent endocytosis (Bernard *et al.*, 2010; Hoornweg *et al.*, 2016). It has also been demonstrated that, under certain conditions, SINV particles can fuse directly with the plasma membrane (Vancini *et al.*, 2013). CME is a complex process involving many proteins. Many of the CME associated proteins have been shown to be essential for CHIKV cell entry including Esp15, Rab5, and dynamin (Sourisseau *et al.*, 2007; Bernard *et al.*, 2010), interestingly, all of these proteins play roles in both clathrin-mediated and clathrin-independent endocytosis. It is likely that CHIKV primarily utilises CME for entry into cells but is also able to exploit multiple entry mechanisms where required in order to achieve successful entry (Yat-Sing Leung *et al.,* 2011). In mosquito cells, CHIKV has only been shown to enter via CME although few studies have investigated this phenomenon in insect cells (Ching Hua Lee *et al.*, 2013).

In mammalian cells, it has been demonstrated that CHIKV predominantly fuses with early endosomes. Through both live-cell microscopy and the use of various inhibitors of endocytosis, it has been shown that CHIKV infection requires Eps15 and Rab5, both of which are involved in the early stages of endocytosis and are

present in early endosomes, but does not require Rab7, which is responsible for the maturation of endosomes to lysosomes (Bernard *et al.*, 2010; Hoornweg *et al.*, 2016). In contrast, despite CHIKV entering mosquito cells in a similar manner and is again reliant on Eps15 and Rab5, successful entry also requires Rab7, indicating that CHIKV fuses with late endosomes in mosquito cells, possibly due to variations in endosomal pH compared to mammalian cells (Ching Hua Lee *et al.*, 2013; Nuckols *et al.*, 2014). The E1 glycoprotein alone is responsible for fusion with the endosomal membrane. Work with SFV and SINV show that this process requires a conformational change of the E1/E2 heterodimer, induced by exposure a low pH, in order to expose the fusion loop of E1 (Bron *et al.*, 1993; Justman *et al.,* 1993; van Duijl-Richter *et al.*, 2015; Zeng *et al.*, 2015). Fusion of alphaviruses to endosomal membranes also requires cholesterol which is thought to facilitate hydrophobic interactions between E1 and the target membrane (White and Helenius, 1980; Smit *et al.*, 1999; Ahn *et al.*, 2002).

Once the virus envelope has fused with the endosomal membrane, the nucelocapsid is delivered into the cytoplasm. The nucleocapsids of SINV and SFV have shown to be destabilised due to an interaction of the 60S ribosomal RNA with the C protein (Ulmanen *et al.*, 1976; Wengler *et al.*, 1992). Once the nucleocapsid uncoats, the viral genomic RNA is released and becomes available for translation and the initiation of replication.

1.2.3.2   Genome replication

Once the genomic RNA is in the cytoplasm of the infected cell, the non-structural protein ORF is directly translated from the genome. The CHIKV non-structural proteins form replicases that are membrane associated. It is thought that nsP1 is responsible for the anchoring and the stability of the viral replicase as it has been shown to interact with membranes and is the only non-structural protein capable of binding all other non-structural proteins (Spuul *et al.*, 2007; Sreejith *et al.*, 2012). For SINV and SFV, replication sites have been reported to be in membrane invaginations, often referred to as spherules or cytopathic vacuoles (CPVs). Initially, it was thought that the CPVs were formed by modification of endosomal and lysosomal membranes at early stages of infection, as they are positive for endo/lysosomal markers (Froshauer *et al.,* 1988). Further study

demonstrated that the spherules are formed on the cytoplasmic side of the plasma membrane (shown in Figure 1.8), a process that does not require the presence of the non-structural proteins. The spherules are then internalised through endocytosis and develop into CPVs as previously described (Spuul *et al.*, 2010). Spuul *et al.* also demonstrate the dynamic nature of the CPVs which are eventually transported by microtubules to the perinuclear region of the infected cell.
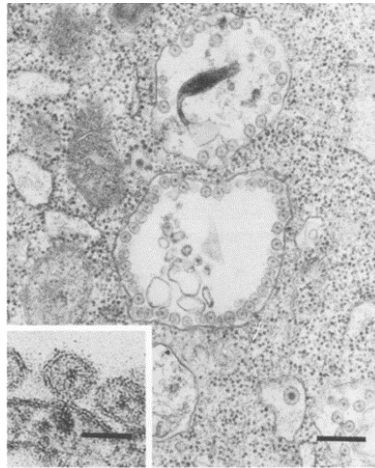
Figure 1.8 Electron microscopy of BHK cells transfected with SFV genomic RNA at 3 hpt. Spherules can be seen at the plasma membrane of the transfected cells. Scale bar for main image 0.3 µm, in the inset 60 nm. Figure from Peränen and Kääriäinen, 1991.

Due a conserved, leaky opal stop codon 6 residues from the end of nsP3, translation of the non-structural ORF results in either p123 or p1234 polyprotein (Chen *et al.*, 2013). This regulates the amount of nsP4 (the RNA-dependent-RNA-polymerase) that is produced in infection and the post-translation cleavage of nsP3/4 (Jones *et al.*, 2017). Some strains (e.g. Caribbean strains) have an arginine in place of the stop codon so only produce the p1234 polyprotein. The non-structural polyprotein is proteolytically cleaved by the nsP2 protein initially into p123 and nsP4 (Rausalu *et al.*, 2016). In SINV replication, it has been shown through the disruption of cleavage sites, that the p123 polyprotein alongside the nsP4 polymerase are predominantly required for minus-strand RNA production whereas the individual nsPs are required for positive-strand synthesis (Lemm *et al.*, 1994). This is proposed to increase replication efficiency as RNA replication

can be temporally segregated in two stages. As summarised in Figure 1.9, the first stage is the production of full length, minus-strand RNA. Then, upon polyprotein cleavage by nsP2, this switches to positive-strand production of the full length genomic RNA for further translation and packaging, and the 26S sub-genomic RNA, a small, positive-sense capped RNA that encodes for the structural proteins (Albulescu *et al.*, 2014).
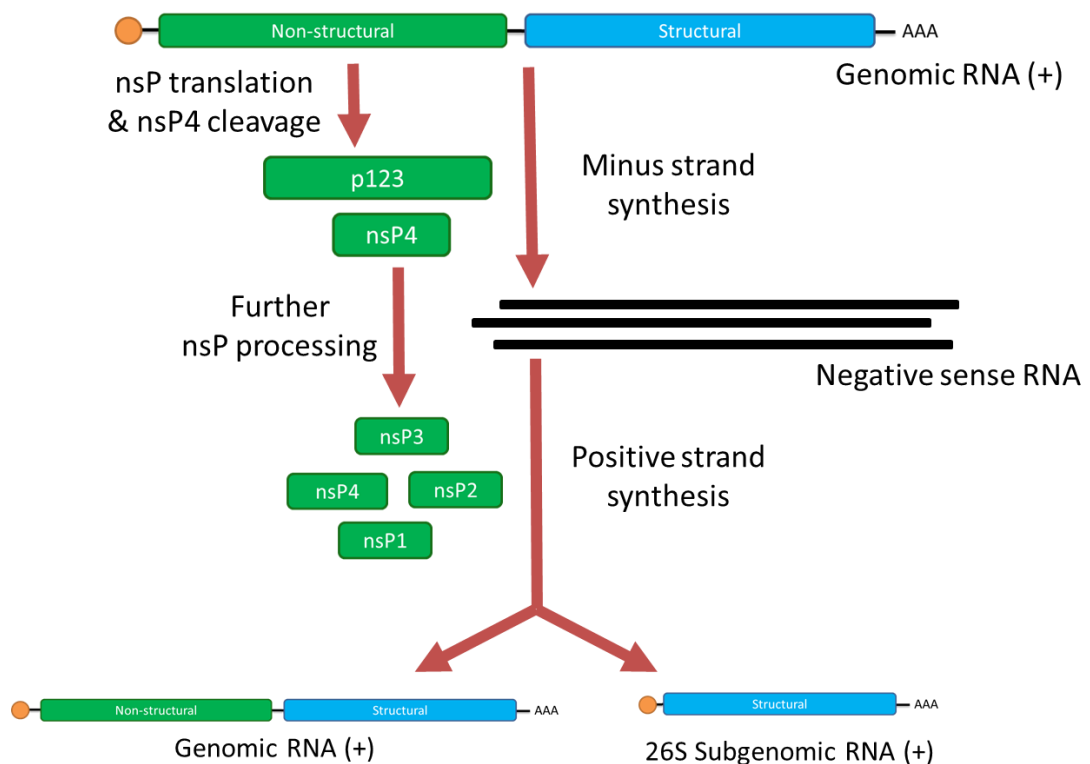
Figure 1.9 CHIKV RNA replication. Upon entry to the cell, the non-structural ORF is translated and produces polyprotein p123 and p1234, subsequently cleaved into p123 and nsP4. These proteins induce negative sense RNA production. Upon further polyprotein processing by the nsP2 protease to form the individual nsP1, nsP2, nsP3 and nsP4 proteins, positive sense RNA production is initiated, producing full genomic RNA for packaging or further transition, and the 26S subgenomic RNA for translation of the structural proteins. Original figure interpreted from Lemm *et al.,* 1994.

All four nsPs are required for RNA replication and have distinct roles. The nsP1 protein, as well as being the membrane-anchor of the replicase complex, also possesses methyltransferase (MTase) and guanylytransferase (GTase) activity,

that allow nsP1 to cap newly synthesised positive sense RNA (Ahola and Kääriäinen, 1995). The nsP2 protein has multiple functions. As discussed previously, it has protease activity and is responsible for polyprotein processing into individual proteins (Russo *et al.,* 2006). Another function of nsP2 is a helicase/NTPase, to unwind RNA secondary structure in order to facilitate replication (Rikkonen, 1996). Although known to be essential for RNA replication, it is unclear what specific role the nsP3 protein plays in this process. The alphavirus nsP3 contain a macro domain at the N terminus, an alphavirus unique domain (AUD) and a hyper-variable domain (HVD) at the C terminus. The functions of these domains in terms of viral replication are poorly understood although mutations in the AUD and HVD of nsP3 have been shown to be defective in synthesis of minus strand and subgenomic RNA (Rupp *et al.*, 2015). The nsP4 is the RdRp and its sole function is RNA synthesis. At the N-terminus of nsP4 is a disordered region which has been shown to interact with nsP1. Various mutations to this disordered region produced defects in either positive, or negative strand synthesis. This suggests that this region, and possibly its interaction with nsP1 is required for the switch from negative to positive strand synthesis (Shirako and Strauss, 1998; Rupp *et al.,* 2011).

1.2.3.3   Translation of structural proteins

Once RNA replication has occurred, the structural proteins can be translated from the newly synthesised 26s subgenomic RNA into the structural polyprotein. The polyprotein is then subsequently cleaved. The core protein (C) contains a serine protease allowing cleavage in cis to remove C from the N terminus of the polyprotein (Choi *et al.*, 1991). The cleavage of pE2 (the precursor to E3 and E2), 6k, and E1 occurs in the ER (Singh *et al.*, 2018). E1 then forms a heterodimer with the E2 portion of pE2 and is further cleaved by host cell furin to form E3 and the E1/E2 heterodimer (Firth *et al.*, 2008). The processing of the non-structural polyprotein is summarised in Figure 1.10.
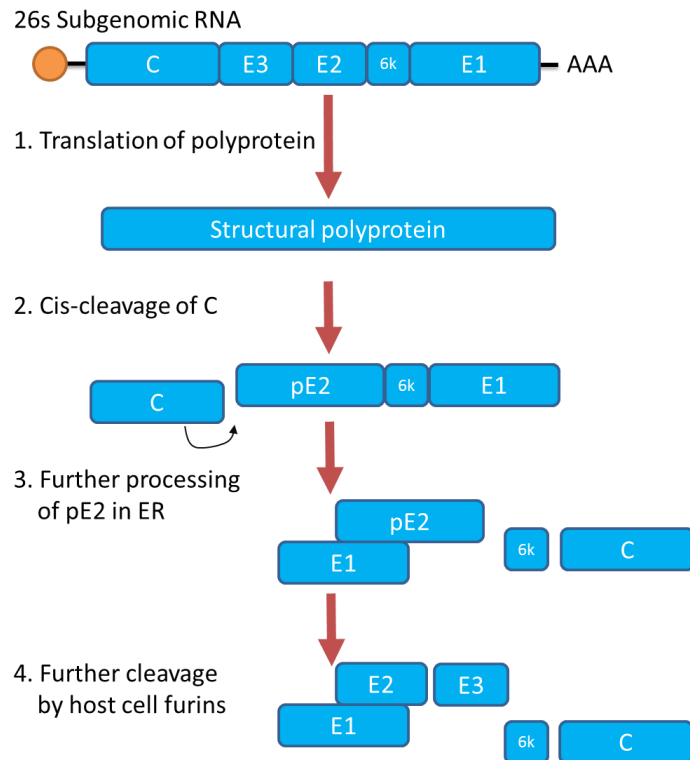
Figure 1.10 The processing of the structural polyprotein. The subgenomic 26s RNA is translated to form a single polyprotein. Core protein then auto-catalytically cleaves itself from the polyprotein. Processing in the ER allows correct cleavage and folding of the pE2, 6k and E1 proteins. E1 then forms a heterodimer with pE2 for stability, prior to E3 being cleaved by host cell proteases. Original figure interpreted from Choi *et al.,* 1991; Firth *et al.,* 2008; Singh *et al.,* 2018.

1.2.3.4 Assembly and release

Assembly of alphaviruses begins in the cytoplasm with the formation of the nucleocapsids with viral genomic RNA being encapsidated by C protein. In SINV, it has been shown that this process is facilitated and stabilised by a amphipathic coiled coil α-helix at the N-terminus of C that is highly conserved across the different alphaviruses, including CHIKV (Perera *et al.*, 2001). Once formed, it is thought that the nucleocapsid freely diffuses in the cytoplasm and binds to the E2 of the glycoprotein heterodimer in order to target the nucleocapsid to the cell membrane for assembly (Suomalainen *et al.,* 1992; Solignat *et al.*, 2009). The nucelocapsid is then thought to bud from the plasma membrane which contains E1/E2 heterodimers. Assembly requires the putative viroporin 6k, which although not believed to a virion component, is known to interact with E1 and has been

suggested to be involved in manipulation of the plasma membrane for efficient budding and release of the virus (Yao *et al.*, 1996; Sanz and Carrasco, 2001).

1.2.4 Immune response to CHIKV infection

Cells infected with CHIKV mount a profound inflammatory immune response, a time scale of which is shown in Figure 1.11. Much of this response is protective against CHIKV infection but some responses also contribute to the spread of the virus and the disease pathology.
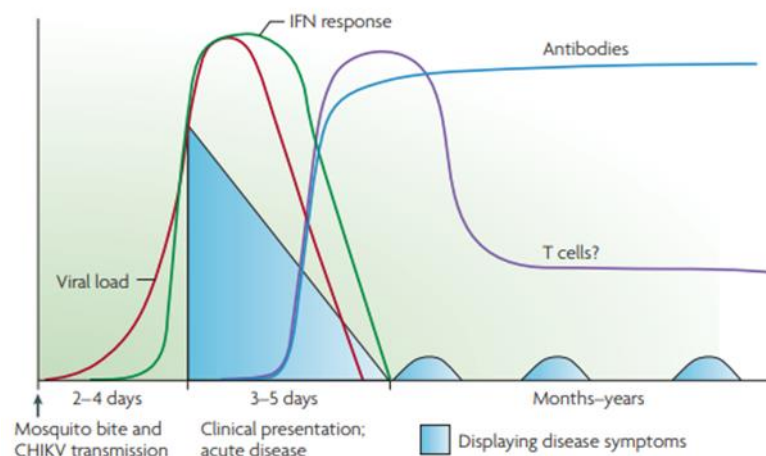
Figure 1.11 Time scale of cellular response to CHIKV infection. As viral load increases after initial infection, a substantial IFN response is formed that correlates with the acute disease symptoms. A protective antibody and protective T cell response is formed between 3-5 days post infection. Some infected individuals, after recovery of the acute infection, have long term, recurring symptoms. Image adapted from Schwartz and Albert, 2010.

1.2.4.1 IFN response

It has been well documented that CHIKV infected cells mount a profound type I interferon (IFN) response within 2-5 days of infection (reviewed by Schwartz and Albert, 2010). As shown in Figure 1.12, the type I IFN response is induced by virus-infected cells which release IFN-α and/or -β to alert surrounding naïve cells through the interferon-α/β receptor (IFNAR) to initiate an anti-viral state. The IFN pathway has been shown to be critical for survival in CHIKV infected mice, as

infected IFNAR^{-/-} mice develop a more severe disease with increased viral titres and neurological complications (Thérèse Couderc *et al.*, 2008).
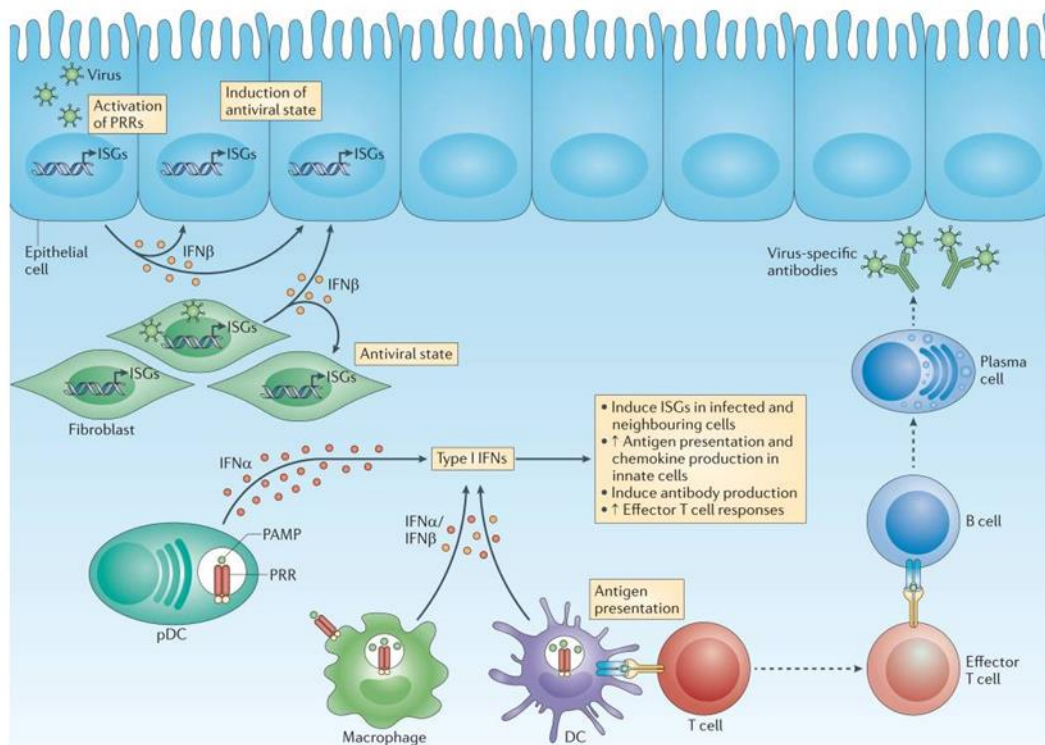
Figure 1.12 Type I IFN response. IFNα/β is produced by virus infected cells. This is released to the surrounding cells which is detected through the cell surface interferon-α/β receptor (IFNAR) to induce an IFN response in naïve cells, forming an anti-viral state prior to infection. IFNs also enhance the adaptive immune response through upregulation of antigen presentation and chemokine production to form a robust effector T cell response. The T cells further interact with B cells to form antibodies to the virus. Figure from Ivashkiv and Donlin, 2014.

CHIKV has been demonstrated to trigger the IFN pathway through sensing of the viral RNA. CHIKV RNA can be recognised in infected cells by both retinoic acid-inducible gene I (RIG-I) and toll like receptor 3 (TLR3). It has been shown that sensing through TLR3 is essential for the formation of a neutralising immune response to CHIKV infection (Her *et al.*, 2015). Upon the detection of CHIKV RNA, RIG-I is able to signal through mitochondrial anti-viral signalling protein (MAVS, also commonly referred to IFN promoter stimulator 1/IPS-1) to trigger the IFN pathway (Olagnier *et al.*, 2014). Cells with functional MAVS were more resilient to CHIKV infection than MAVS^{-/-} cells (Schilte *et al.*, 2010). Further work

has shown that interferon regulatory factor 3 (IRF3) is critical for the IFN response in CHIKV infected cells. IRF3 is activated via MAVS signalling and induces the transcription of many IFN stimulated genes (ISGs) (White *et al.*, 2011), as is summarised in Figure 1.13.
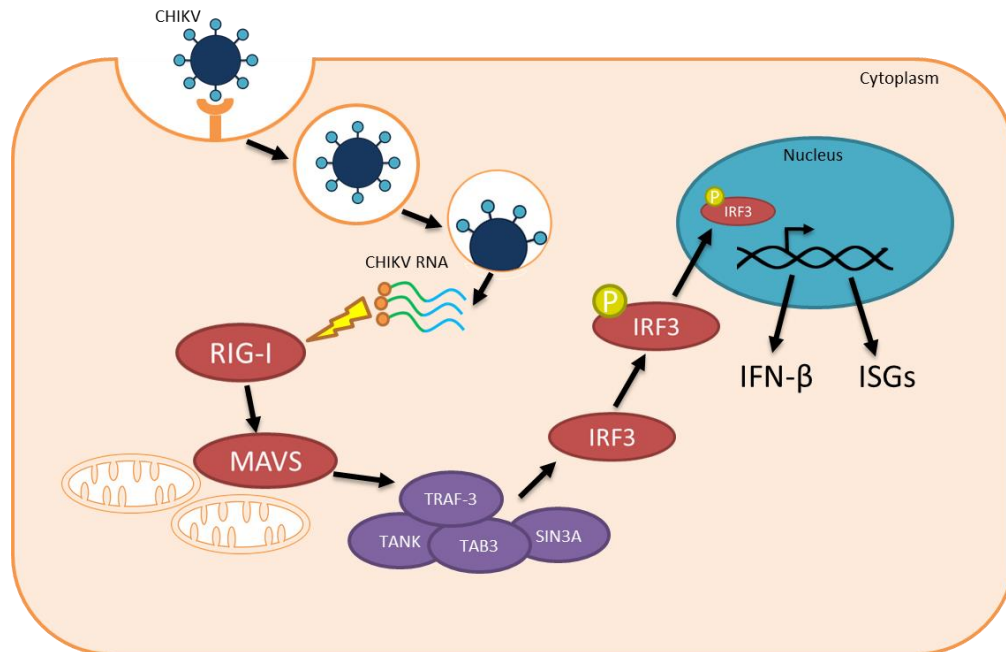
Figure 1.13 The IFN response to CHIKV infection. CHIKV RNA is detected in the cytoplasm by RIG-I (retinoic acid-inducible gene I) which signals through MAVS (mitochondrial anti-viral signalling protein) and many adaptor proteins to activate IRF3 (interferon regulatory factor 3) through phosphorylation. IRF3 then translocates to the nucleus to induce the transcription of IFN-β and many IFN stimulated genes (ISGs). Original figure, interpreted from White *et al.,* 2011; Olagnier *et al.,* 2014.

Many ISGs exhibit anti-viral effects against CHIKV. ISG15 has been shown to be critical for survival of CHIKV infection, as neonatal mice lacking ISG15 all died within 8 days of infection (Werneke *et al.*, 2011). Many other ISGs such as IFN regulatory factor 1 (IRF-1) and zinc anti-viral protein (ZAP) have been shown to be potently anti-viral against CHIKV (Bick *et al.*, 2003; Schoggins *et al.*, 2011). Interestingly, the ISG adenosine deaminase (ADAR) was found to be an enhancer of CHIKV infection (Schoggins *et al.*, 2011).

Although the IFN response is protective of cells infected with CHIKV, it does also contribute to disease pathology. IFNs have been well characterised as causing

generic disease symptoms such as fatigue and myalgia (Sleijfer *et al.*, 2005). In addition, CHIKV has been shown to induce the expression of cytokines CXCL9 and CXCL10, via the IFN response, which have been shown to contribute to joint inflammation in CHIKV infection. Both these cytokines are also implicated in the progression of rheumatoid arthritis (Kelvin *et al.*, 2011).

1.2.4.2 NFκB response

Despite CHIKV infection inducing a robust IFN response, it has been demonstrated that it does not trigger the NFκB pathway (Selvamani, *et al.,* 2014). An overview of the NFκB pathway is shown in Figure 1.14. The lack of activation of the pathway by CHIKV is particularly interesting as there are multiple points of cross-talk between the IFN and NFκB pathways with both pathways capable of activating the other (Wang *et al.*, 2010; Iwanaszko and Kimmel, 2011; Rubio *et al.*, 2013).
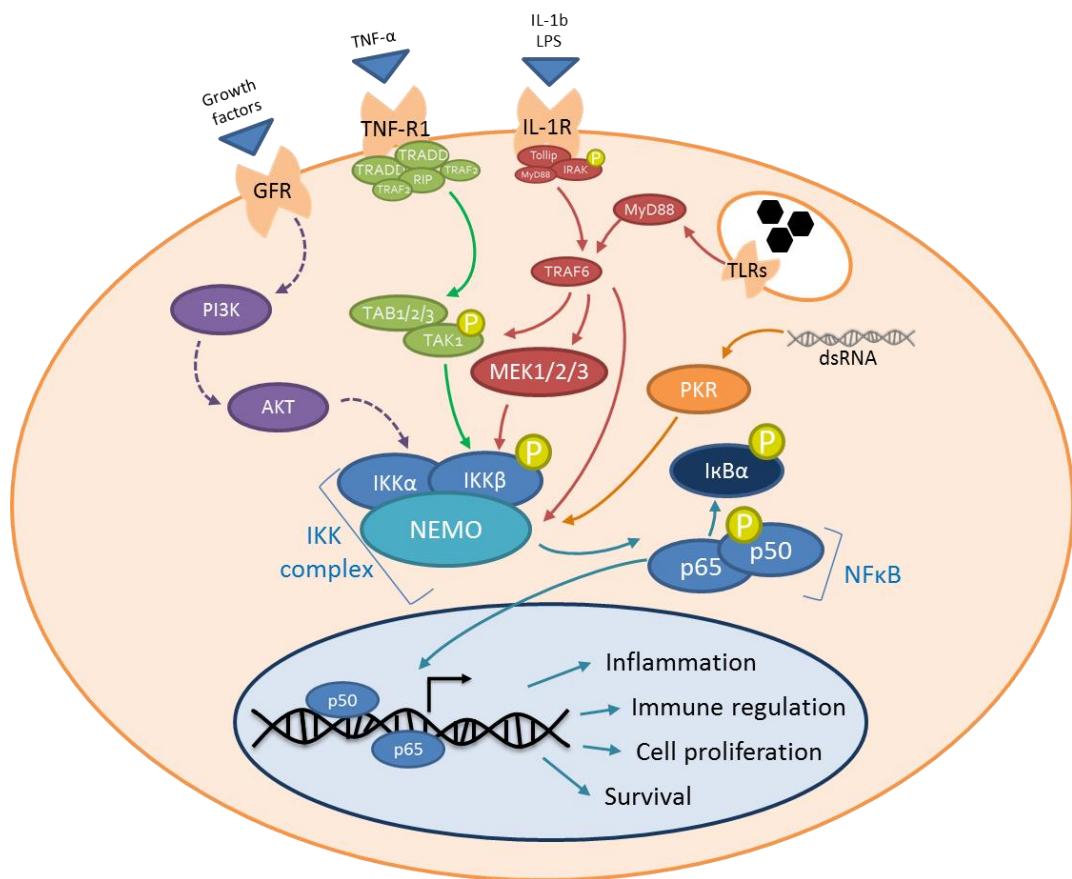
Figure 1.14 Overview of the NFκB pathway. The pathway can be triggered by multiple stimuli, both external such as TNF-α, or internal, for example dsRNA from infecting viruses. These stimuli activate the pathway through different mechanisms though, regardless of method of activation, the pathway converges on an active IKK complex that removes IκB (inhibitor of NFκB) from NFκB/p105. This activates the NFκB complex and allows translocation to the nucleus where it acts as a transcription factor for a range of inflammatory and antiviral genes. This results in an antiviral state of the cell and the secretion of molecules (e.g. IFN) to signal to surrounding cells.

1.2.4.3 Autophagy

In human cells, it has been shown that CHIKV induces autophagy which enhances the replication of the virus. In CHIKV infected cells, light chain 3 (LC3, a marker of autophagy) is redistributed to form punctate structures in the cytoplasm of CHIKV-infected HeLa and HEK293 cells, indicating the formation of autophagosomes. Activating autophagy in HeLa cells with rapamycin significantly increased CHIKV replication (Judith *et al.*, 2013). When autophagy

31

is inhibited in HEK293 cells, CHIKV replication is reduced, with fewer E1 positive cells and less viral RNA production (Krejbich-Trotot *et al.*, 2011). In mouse cells, CHIKV has also been shown to induce the formation of autophagosomes. However, in contrast to the human cells, these appear to have a protective effect from infection, as CHIKV caused higher rates of cell death in the absence of autophagy machinery (Joubert *et al.*, 2012). It was proposed that autophagy delays the onset of CHIKV-induced apoptosis, and therefore in the absence of autophagy , apoptosis occurs earlier in the virus lifecycle, therefore limiting production of infectious virus.

1.2.4.4 Apoptosis

Many viruses induce apoptosis in infected cells and this was widely considered to be a defence mechanism to reduce virus replication and further spread within the infected organism (Vaux and Häcker, 1995). Apoptosis rapidly occurs in CHIKV infected cells (Dhanwani *et al.*, 2012; Nayak *et al.*, 2017). Through recent studies, it is now considered that CHIKV and other alphaviruses induce apoptosis as a means to increase viral spread to neighbouring cells (Long and Heise, 2015). It has been shown that the apoptotic blebs left by dead CHIKV-infected cells can be engulfed by neighbouring cells and macrophages, the latter of which are normally refractory to CHIKV infection (Krejbich-Trotot *et al.*, 2011). The cellular regulation of apoptosis in response to infection can determine whether an alphaviral infection is acute (which normally occurs when apoptosis is rapid) or becomes persistent, the latter being commonly observed in older patients (Griffin and Hardwick, 1997).

1.2.5 Non-structural protein 3

The alphavirus nsP3 is known to be essential for viral RNA replication, yet, it is still unclear what specific functions nsP3 contributes to the virus lifecycle.

1.2.5.1 Structural features of nsP3

The alphavirus nsP3 has three distinct domains; the macro domain at the N-terminus, the alphavirus unique domain (AUD) in the centre, and the hyper variable domain (HVD) at the C-terminus, as shown in Figure 1.15.

N [Macro domain | AUD | HVD] C

Figure 1.15 Schematic of the CHIKV nsP3, highlighting the three domains of the protein: the macro domain, the alphavirus unique domain (AUD) and the hypervariable domain (HVD). (Original figure).

1.2.5.2 Macro domain

At the N-terminus of nsP3 there is a macro domain. Macro domain are found in the proteins of all species and are defined by their ability to bind ADP-ribose. The macro domain of CHIKV has been demonstrated to bind mono- and poly-ADP-ribose and RNA and possesses ADPR-hydrolase activity (Rupp *et al.*, 2015). As this is the focus of this project, the macro domain is discussed in more detail in section 1.3.2.3.

1.2.5.3 Alphavirus unique domain

The alphavirus unique domain (AUD) is, as the name implies, a domain only found in alphaviruses where it is highly conserved. The full protein structure of the AUD is currently unknown but structural analysis of the nsP2/3 interface revealed a zinc coordination site at the start of the AUD (Shin *et al.*, 2012). The function of the AUD is yet to be determined and there are currently very few publications that focus on this domain. Various mutagenic studies of the SINV and SFV AUDs have demonstrated it is required for minus strand-RNA synthesis, subgenomic RNA synthesis, and neurovirulence (Dé *et al.*, 2003; Tuittila and Hinkkanen, 2003). One study that focuses on the CHIKV AUD shows it has roles

in both RNA replication and virus assembly (Yanni Gao, University of Leeds, personal communication). Still the precise function of the AUD remains unclear.

1.2.5.4 Hypervariable domain

The hyper variable domain (HVD) also often referred to as the hyper variable region (HVR) or just variable region (VR), is an intrinsically disordered, unstructured domain that is highly phosphorylated. It is highly variable in both sequence and length between the alphavirus nsP3s. The HVD of various alphaviruses have been shown to have many interactions with various cellular proteins and processes, including the well characterised nsP3 interaction with G3BP (Foy *et al.*, 2013). Near the C-terminus of the HVD, there are two polyproline motifs (PxxP) that are known to bind SH3 domains. Many cellular proteins contain SH3 domains that are involved in a wide range of signalling pathways (Kaneko, Li and Li, 2008). The polyproline motifs of SFV, CHIKV and SINV have all been shown to bind amphiphysins 1 and 2 (Neuvonen *et al.*, 2011). Abrogation of this interaction by mutation or deletion of the PxxP motifs resulted in impaired RNA replication in both SFV and SINV. It is thought that since amphiphysins are able to induce curvature of membranes this interaction with nsP3 may contribute to spherule formation (Götte *et al.,* 2018). It is also proposed that the HVD is a hub of interactions with cellular proteins and these interactions are crucial to replication and the cellular distribution of nsP3 (Foy *et al.*, 2013). Deletion of the hypervariable domain results in a significant shift in cellular distribution. Unlike with deletions of the macro domain which resembles the cytoplasmic puncta of full length nsP3, deletion of the HVD resulted in distinctive filamentous-like structures as shown in Figure 1.16, postulated to be due to the loss of many interactions with cellular proteins (Fros *et al.*, 2012).
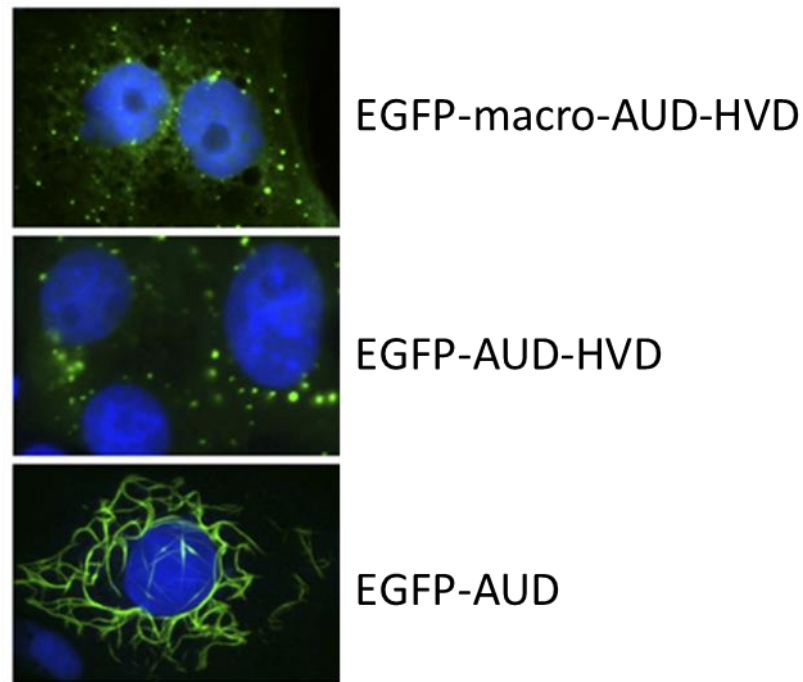
Figure 1.16 Deletions of nsP3 domains affect cellular distribution. EGFP-tagged forms of full nsP3 (top) and AUD-HVD (middle) show similar distribution however, the AUD alone (bottom) exhibits a drastic change in cellular distribution. Figure adapted from Fros *et al.,* 2012.

Seven codons N-terminal to the end of nsP3 is a 'leaky' stop codon. As discussed previously in section 1.2.3.2, this affects regulation of minus or positive strand synthesis, however it also has effects on nsP3 production and stability. The nsP3 stop codon, found in all CHIKV strains except the Caribbean strain (which instead encodes for an arginine at this site), results in two forms of nsP3; a 443 aa if terminated at the stop codon or 449 aa if read through to produce the full p1234 polyprotein (as shown in Figure 1.17). The additional amino acids in full length SFV nsP3 has been shown to act as a 'destability sequence' as their presence greatly reduces the stability of nsP3 in cells (Varjak, *et al,.* 2010). Although the precise functions of the short and full versions are still unclear, Varjak *et al.* demonstrated that both versions are required for efficient replication and suggested that the extra amino acids may alter nsP3 localisation, the result of which affects RNA synthesis.

UUA UGA CUA GAC AGG GCA GGU GGG
L X L D R A G G

Figure 1.17 RNA sequence (top) and protein translation (bottom) of the CHIKV nsP3 C-terminus. The leaky opal stop codon is shown in red. (Original figure).

1.2.5.5 Known interactions of nsP3

Although the structure and localisation of the non-structural proteins in replicase sites is currently unclear, it is known that nsP3 directly interacts with nsP1 which is required for functional replicases. The nsP1 then forms additional interactions with nsP2 and nsP4 (Sreejith *et al.*, 2012).

It has been demonstrated that nsP3 is able to bind RNA, a well-characterised property of the macro domain, but the AUD has also been shown to capable of RNA binding (Malet *et al.*, 2009, Yanni Gao, University of Leeds, personal communication) although it is yet unclear whether RNA binding is specific e.g. to viral RNA. It has been shown that the macro domain of nsP3 is capable of suppressing the RNA interference (RNAi) anti-viral pathway, although it is unclear what specific interaction is causing this effect (Mathur *et al.*, 2016).

One of the best characterised interactions of nsP3 is that with G3BP. G3BP is a marker of stress granules, which are pools of untranslated mRNAs and associated proteins that form in response to many cellular stresses such as viral infection (Protter and Parker, 2016). The interaction between G3BP and nsP3 is dependent on the SH3 domain binding motif in the HVD and is thought to actively inhibit stress granule assembly in CHIKV-infected cells (Fros *et al.*, 2012). It has been shown that G3BP is crucial for the RNA replication of the "old world" alphaviruses, of which CHIKV is a member of (Kim *et al.*, 2016). In mosquito cells, a similar interaction with rasputin (an insect homologue of G3BP), has been shown to play a very similar role in alphavirus replication to that of G3BP in mammalian cells (Gorchakov *et al.*, 2008).

Another interaction of nsP3 mediated by its SH3 domain binding motif is with amphiphysins. The nsP3 of SFV, SINV and CHIKV have all been shown to interact with amphiphysin 1 and amphiphysin 2. When these interactions were abolished by mutation of the SH3-binding motifs of nsP3, RNA replication was reduced (Neuvonen *et al.*, 2011). Amphiphysins are involved in many cellular pathways. Amphiphysin 1 is known to play a key role in clathrin mediated endocytosis, particularly in neuronal synapses and phagocytosis, and binds dynamin 1, an interaction facilitated by the SH3-binding domain of amphiphysin 1 (Yamada *et al.*, 2007). Amphiphysin 2 (also referred to as Bin1 in the literature) is an ubiquitously expressed protein, found in both the nucleus and cytoplasm of mammalian cells. It has a wide range of cellular functions including membrane trafficking and remodelling, regulation of the actin cytoskeleton, DNA repair, cell cycle regulation and apoptosis (Prokic *et al.*, 2014). It has been proposed that the alphavirus nsP3 utilises the membrane-regulation abilities of amphiphysins to rearrange host cell membranes to support viral replication (Neuvonen *et al.*, 2011).

The SINV nsP3 has been demonstrated to interact with Y-box-binding protein (YBX1), (Gorchakov *et al.*, 2008). YBX1 has many cellular roles including cell cycle progression, DNA repair, transcription, translation and is upregulated upon cellular stress (Prabhu *et al.*, 2015). YBX1 is also able to bind RNA and DNA, chaperone mRNAs and is a component of mRNPs (Eliseeva *et al.*, 2011). The function of the nsP3-YBX1 interaction and its effects on viral replication is unclear. YBX1 interacts with other viral proteins with contradictory outcomes. YBX1 is known to inhibit Dengue virus virion production and can suppress the translation of viral RNA (Paranjape and Harris, 2007). Conversely, in HCV, YBX1 association with viral proteins NS3 and NS4A is required for efficient RNA replication (Chatel-Chaix *et al.*, 2011). More research is required to determine the role of YBX1 in the alphavirus lifecycle.

The hyper-phosphorylated HVD of nsP3 of interacts with Akt, which activates the PI3K-Akt-mTOR pathway. This activation has been shown to be necessary for the internalisation of replicases at the plasma membrane for SFV but not for CHIKV, which activates the pathway to a much lesser degree (Spuul *et al.*, 2010; Thaa *et al.*, 2015).

Other interactions of nsP3 with cellular proteins includes the heat shock protein 70 (Hsp70) although the purpose of this interaction is currently unknown (Gorchakov *et al.*, 2008). The nsP3 of VEEV has been shown to interact with DEAD box domain proteins DDX1 and 3, which are thought to act as additional helicases to assist viral RNA replication (Amaya *et al.*, 2016). The VEEV nsP3 has also been shown to interact with IκB kinase-β (IKKβ) to activate the NFκB pathway. Inhibition of this interaction reduced production of infectious virus and genomic RNA copies (Amaya *et al.*, 2014).

1.3 Macro domains

At the N-terminus of the CHIKV nsP3 is a macro domain. A macro domain is a conserved protein fold that are found either singularly or, more commonly, as a component of larger proteins (Leung *et al.,* 2018). They are defined by their ability to bind ADP-ribose (ADPR), which exists either as a monomer: mono-ADP-ribose (MAR), or as a polymer: poly-ADP-ribose (PAR), as shown in Figure 1.18. Macro domains are capable of binding either free ADPR or that which is attached to proteins, as ADP-ribosylation is a common post-translational modification (Karras *et al.*, 2005; Dani *et al.*, 2009).
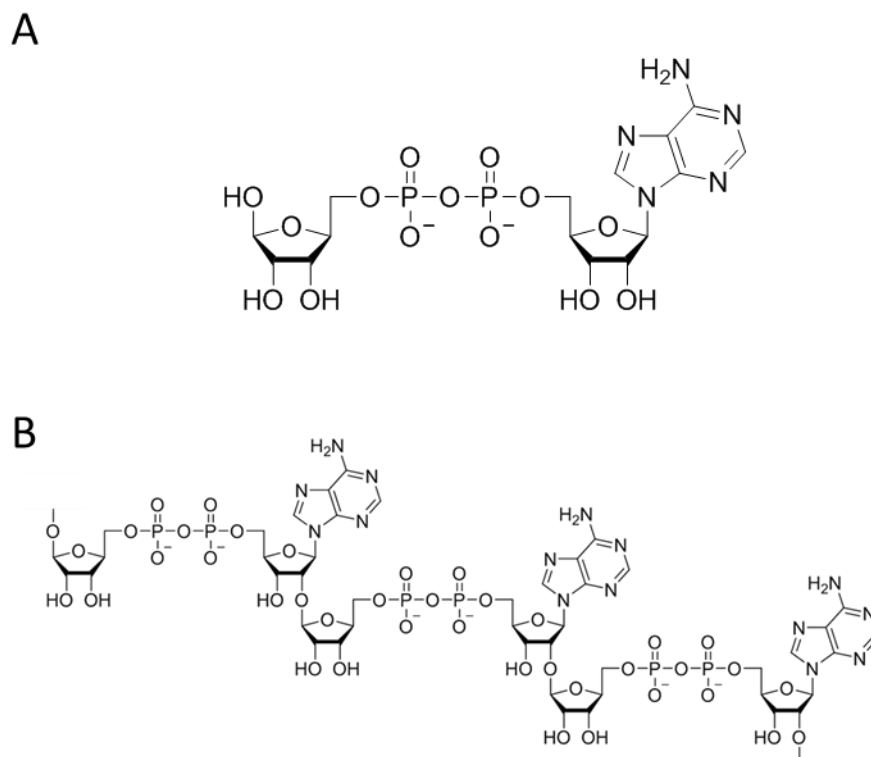
Figure 1.18 Chemical structures of the monomeric (A) and polymeric (B) forms of ADP-ribose. Original figure drawn using ChemDraw software.

Some macro domains have also been shown to have enzymatic activity such as ADP-ribose 1″-phosphate phosphatase activity, which catalyses the reaction shown in Figure 1.19, an activity required for tRNA splicing (Kumaran *et al.*, 2005; Shull *et al.*, 2005). More recently, it has been shown that some macro

domains possess hydrolase activity where they can remove ADPR from modified proteins (Gupte *et al.*, 2017).
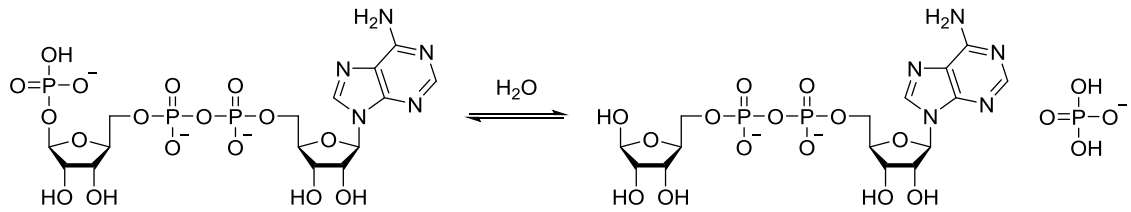
Figure 1.19 Reaction scheme showing the hydrolysis of ADP-ribose 1″-phosphate to form ADP-ribose, and inorganic phosphate, catalysed by enzymes that possess ADP-ribose 1″-phosphate phosphatase activity, such as the CHIKV macro domain. Original figure drawn using ChemDraw software.

The first macro domains discovered were in coronaviruses (Lee *et al.*, 1991). At the time, these highly conserved domains were termed "x-domains" to denote their unknown function. Since this initial discovery, similar domains were found in the proteins of mammals, birds, bacteria and viruses (Pehrson and Fuji, 1998). They were renamed 'macro domains' when high levels of homology were found with a histone protein called macroH2A, which is one of the most widely studied macro domains (Malet *et al.*, 2009; Pasque *et al.*, 2012). MacroH2A, is a histone protein in humans which has been shown to have roles in transcriptional repression, chromatin reorganisation, DNA replication and repair (Chakravarthy *et al.*, 2005; Buschbeck and Di Croce, 2010). Macro H2A functions to organise the nucleus and stabilise chromatin (Douet *et al.*, 2017). Further sequence alignments of the mammalian macroH2A with other proteins revealed similar domains in bacteria *Alicaligenes eutrophus* and *E. coli* as well as the RNA viruses Rubella and Sindbis (Pehrson and Fuji, 1998). In the same study, it was demonstrated that there was a high level of conservation of the amino acid sequence of the protein domain across species.

1.3.1 ADP-ribosylation in cell signalling

ADP-ribosylation is a common post-translational modification of many cellular proteins, discovered over 50 years ago (Chambon *et al.,* 1963). Relatively little study was done in this area until more recently, when it was shown that proteins

could be modified with either mono- or poly- ADPR. This modification is performed by a family of enzymes named poly-ADPR-ribose polymerases (PARPs) that are able to catalyse the transfer of ADPR onto proteins from nicotinamide adenine dinucleotide (NAD$^+$), (Leung, 2017). There are 17 known human PARPs which are implicated in a range of cellular functions as described in Table 1.1. Ironically most PARPs only exhibit mono-ADP-ribosylation activity, therefore a new nomenclature was proposed, terming 'PARPs' as 'ARTDs' (ADP-ribosyltransferase diphtheria toxin-like proteins) alongside the renumbering the PARPs due to function (Hottiger *et al.*, 2010). Despite this remaining addresses the accuracy of naming these proteins, it does cause confusion in the literature where many previous studies have referred to proteins as "PARPs" and others as "ARTDs" and, as shown in Table 1.1, the numbering of PARPs and ARTDs are not consistent (Gupte *et al.,* 2017).

PARP	ARTD / other names	ADP-ribosylation activity	Reported biological functions
PARP1	ARTD1	PAR	DNA maintenance and repair, cell cycle, transcription
PARP2	ARTD2	PAR	DNA maintenance and repair, cell cycle and transcription
PARP3	ARTD3	MAR	DNA repair and cell cycle regulation
PARP4	vPARP, ARTD4	MAR	Cancer biology
PARP5a	TNK1, ARTD5	PAR	Anti-viral, inflammation, RNA processing
PARP5b	TNK2, ARTD6	PAR	Inflammation
PARP6	ARTD17	MAR	Cell proliferation
PARP7	TiPARP, ARTD14	MAR	Anti-viral, RNA processing
PARP8	ARTD16	MAR	Unknown
PARP9	ARTD9, BAL1	None (inactive)	Cell migration
PARP10	ARTD10	MAR	Cell proliferation, RNA processing and inflammation
PARP11	ARTD11	MAR	Unknown
PARP12	ARTD12,	MAR	Anti-viral, RNA processing
PARP13	ARTD13, ZC3HAV1, ZAP	None (inactive)	RNA processing
PARP14	ARTD8, BAL2	MAR	Inflammation, transcription, RNA processing
PARP15	ARTD7, BAL3	MAR	RNA processing
PARP16	ARTD15	MAR	Unfolded protein response

Table 1.1 Human PARPs, their alternative names, enzymatic activity and known cellular functions. Adapted from Vyas *et al*. 2013, Vyas *et al*. 2014 and Bai 2015. PAR = poly-ADP-ribosylation, MAR = mono-ADP-ribosylation.

In much of the literature of ADP-ribosylation and signalling, ARTDs are termed the "writers," ADP-ribose binding domains being the "readers" and ADPR-hydrolases being "erasers" demonstrated by Figure 1.20 (Gupte *et al.*, 2017). All macro domains are considered "readers" but mainly also fall into the "eraser" category as some merely bind ADPR whilst others can both bind and hydrolase the moiety. This includes the human protein macroD2 which is able to both bind and hydrolyse ARPR (Chen *et al.*, 2011).
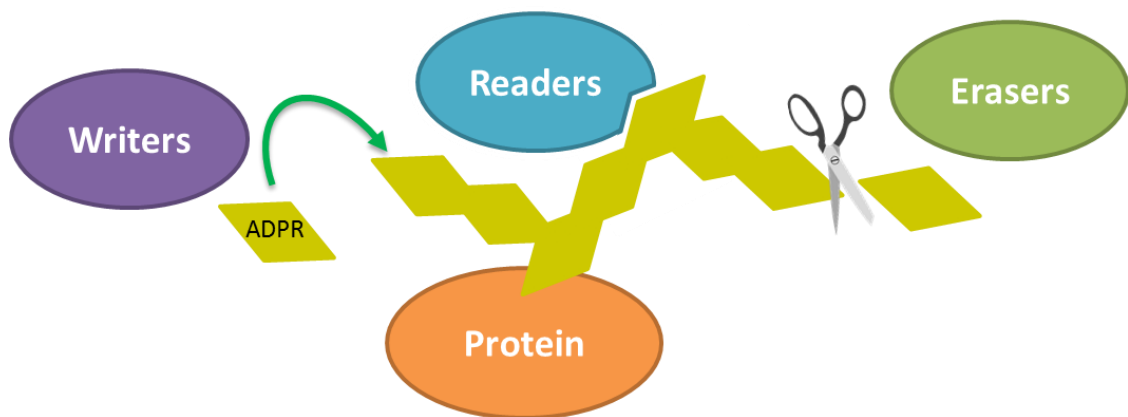
Figure 1.20 Overview of proteins involved in ADP-ribosylation. Writers, such as ARTDs, add ADPR to proteins. Readers such as macro domains and PBZ domains are able to bind ADPR. Erasers, such as PAR glycohydrolase (PARG), are able to remove ADPR from proteins by hydrolysis. Original figure adapted from Gupte, Liu and Kraus, 2017.

ADP-ribosylation of proteins has been shown to be a tool for cell signalling in many pathways including DNA repair, transcription, RNA processing and trafficking and innate immunity.

One of the best-studies ARTDs and ADP-ribose signalling pathways is PARP1, which is a true poly-ADP-ribose polymerase (Vyas *et al.*, 2014). PARP1 has been well characterised as a DNA repair protein. When DNA damage occurs by either single or double stranded breaks, PARP1 is activated and becomes heavily auto-ribosylated, forming extensive branches of PAR upon itself and nearby chromatin (Chaudhuri and Nussenzweig, 2017). This assists in the recruitment assembly of protein complexes in order to repair the damaged DNA. Proteins such as DNA repair scaffold proteins, and DNA damage checkpoint proteins are recruited (Ko

and Ren, 2012). Some of these proteins are ADP-ribosylated for recruitment whilst others contain ADPR-binding domains e.g. macroH2A which bind PARylated PARP1 through their macro domains (Timinszky *et al.*, 2009). When the DNA damage is minimal, PARP1 is able to quickly recruit the necessary proteins for successful repair. However, when there is excessive DNA damage, PARP1 performs extensive PARylation which drastically reduces NAD$^+$ levels of the cell (Yu *et al.*, 2002). This induces the translocation of apoptosis inducing factor (AIF) from the mitochondria to the nucleus, where it contributes to the degradation of chromatin (Candé *et al.*, 2002). Alongside AIF, mitochondria also release cytochrome C, which activates caspases and results in apoptosis (Chiarugi and Moskowitz, 2002). Caspases then cleave PARP1, presumably to cease pointless production of PAR by this stage in the process (Cohausz and Althaus, 2009). Cleaved PARP1 is considered a hallmark of apoptosis.

Many processes regulated by ribosylation involve interplay with other forms of signalling. It has been shown that poly-ADP-ribosylation can act as a signal for ubiquitination of proteins for eventual degradation by the proteasome. E3 ligase can bind PAR through its WWE domain, then ubiquitinate the ribosylated protein to target it for degradation (Zhang *et al.*, 2011). ADPR signalling has also been shown to interact with SUMOylation. In the DNA damage response, proteins are recruited to sites of DNA breakages by extensive PARylation of the damaged site by PARPs. Certain proteins such as tyrosyl-DNA phosphodiesterase 1 (TDP1), a crucial enzyme for DNA repair, have been shown to be both PARylated, for recruitment to the damage site, and SUMOylated for stability (Das *et al.*, 2014).

1.3.1.1   ADP-ribosylation in anti-viral immunity

Many ARTD proteins are IFN stimulated genes (ISGs). This includes ARTD10, ARTD12L (the long isoform of ARTD12), ARTD13 (aka ZAP) and ARTD14 (Guo *et al.*, 2004; Atasheva *et al.*, 2014).

ARTD12 has been shown to locate to stress granules to inhibit mRNA translation, which has been shown to be reliant on the catalytic activity and autoribosylation of the protein (Atasheva *et al.,* 2014; Welsby *et al.*, 2014). For alphaviruses, the anti-viral effect is thought to be due to this translational shutoff. However, in Zika

virus infection, ARTD12 has also been shown to exhibit strong anti-viral activity by targeting the viral proteins NS1 and NS3 for degradation (Atasheva *et al.*, 2014; Li *et al.*, 2018).

ARTD13, also referred to as Zinc-finger anti-viral protein (ZAP) is an anti-viral protein that has been widely studied. Curiously, this ARTD is catalytically inactive but has potent anti-viral effects. It is has an inhibitory effect on a range of viruses including retroviruses such as murine leukaemia virus, and alphaviruses such as SINV, the inhibition of which relied on the zinc finger motifs of ZAP (Guo *et al.*, 2004). Guo *et al.* demonstrated that ZAP inhibition varied dependent on the virus targeted. For retroviruses such as murine leukaemia virus (MLV), ZAP can bind viral mRNA and target it for degradation. It has also been shown that ZAP can prevent retrotransposition (Goodier *et al.*, 2015). Whereas for SINV, ZAP inhibited the translation of viral RNA. More recently, it has been shown that ZAP is able to selectively bind to RNA that has a higher GC content than host genomic RNA (Takata *et al.*, 2017). In vertebrate genomes, there is evidence for suppression of GC content as it is much lower than would be expected from a random distribution of nucleotides. In this publication, it was shown that ZAP selectively binds to GC-rich RNA. When the genome of HIV-1 was mutated to contain a higher GC content this resulted in a defective virus. However, when this GC-rich HIV-1 was used to infect ZAP$^{-/-}$ cells, replication of the virus was restored to wt levels. Together, this data indicates that ZAP is able to selectively bind GC-rich RNA and acts to remove this non-self RNA from cells.

ARTD10 has been shown to be a regulator of the inflammatory NFκB pathway. Upregulation of ARTD10 decreased NFκB activity, this was later shown to be due to an interaction with a key NFκB protein; NEMO (Verheugd *et al.*, 2013). ADP-ribosylation of NEMO by ARTD10 prevents the formation of the IKK complex, a kinase complex central to the pathway. The lack of an active IKK renders NFκB inactive in the cytoplasm, as it remains bound by IκBα, preventing it from translocating to the nucleus, so that it cannot enact its effects as a transcription factor for anti-viral and inflammatory genes.

ARTD12 has also been linked to activation of the NFκB pathway. Although the exact mechanism of this is unclear, it has been shown that it requires an active

catalytic domain, but not the zinc finger domain of the protein and possibly requires and interaction with the autophagy protein p62/SQSTM1 (Welsby *et al.*, 2014).

1.3.2 Viral macro domains

Macro domains are found in the proteins of several positive sense, single stranded RNA viruses. The first viral macro domains, termed x domains at the time of discovery, were identified in 1991 in coronaviruses (CoVs), specifically; mouse hepatitis virus (MHV) and infectious bronchitis virus (IBV) (Lee *et al.*, 1991). Since this discovery, macro domains have also been found in other coronaviruses such as severe acute respiratory syndrome (SARS) (Malet *et al.*, 2006), as well as hepatitis E virus (HEV) (Anang *et al.*, 2016), and alphaviruses (Götte, Liu and McInerney, 2018). Rubella virus, which is closely related to the alphaviruses, also possesses a macro domain (Neuvonen and Ahola, 2009) although to date, no studies have focussed on the Rubella macro domain.

The fact that macro domains are found in multiple positive sense, single-stranded RNA viruses with some degree of conservation at the amino acid level indicates there may be an evolutionarily conserved function of the domain across these viruses (Gorbalenya, Koonin and Lai, 1991).

1.3.2.1 Coronavirus macro domains

Macro domains were first discovered in the coronaviruses IBV and MHV. It has been since determined that all coronaviruses possess macro domains and they are important virulence factors (Eriksson *et al.*, 2008; Fehr *et al.*, 2016). The structure of the SARS-CoV macro domain was determined in 2006 and was demonstrated to readily bind ADP-ribose but have very poor ADPR 1"–phosphatase activity, providing evidence that this enzymatic activity is possibly not the primary function of viral macro domains (Egloff *et al.*, 2006). In terms of cellular function, there is mounting evidence that the CoV macro domain is involved in counteracting host defences. Fehr *et al* (2016) demonstrated that the SARS macro domain can suppress innate immunity but was not sufficient to block these pathways when triggered by various stimuli. Other have shown that various mutations in the SARS-CoV macro domain render the virus more sensitive to IFN treatment (Kuri *et al.*, 2011).

Most of studies of CoV macro domains focus on that of SARS however, studies have shown differences in the structure and binding capabilities between the SARS-CoV and the MERS-CoV macro domain (Cho *et al.*, 2016). This highlights the importance of studying individual viral macro domains as high conservation between macro domains of viruses within the same family does not ensure the same biochemical properties or cellular functions.

1.3.2.2 Hepatitis E virus macro domain

HEV is a small positive sense RNA virus in the *Hepeviridae* family (Doceul *et al.*, 2016). The HEV macro domain has shown to be essential for viral replication as certain deletions within macro domain completely abrogate virus replication (van Tong *et al.*, 2016). The HEV macro domain has been shown to interact with the viral methyltransferase and ORF3, a small viral phosphoprotein (Anang *et al.*, 2016). More recently, it has been shown that the HEV macro domain can interact with, and hydrolyse, MAR and PAR from ribosylated substrates *in vitro.* Further mutagenic studies showed that residues key to ADPR-binding and enzymatic activity are essential for HEV replication (Li *et al.*, 2016). Another study demonstrated that the HEV macro domain is able to inhibit the poly(I:C) mediated phosphorylation of IFN regulatory factor 3 (IRF3) (Nan *et al.*, 2014). The macro domain has also been associated with HEV persistence, attributed to its ability to modulate the host immune response (Lhomme *et al.*, 2014).

1.3.2.3 Alphavirus macro domains

In alphaviruses, the macro domain is found at the N-terminus of nsP3 (Leung *et al.*, 2018). Studies focussing on the SINV macro domain have shown that mutations that do not disrupt PAR-binding (N10A and N24A) can affect viral replication, although many of these mutations were shown to rapidly revert and/or produce compensatory mutations when in both cell culture and mice. These mutations were shown to disrupt interactions with nsP3 and other viral replicase proteins and reduced RNA replication, overall reducing virulence in mice (Park and Griffin, 2009). Other studies have shown that some insertion mutations in the macro domain affected plaque size and were defective in RNA synthesis (LaStarza *et al.*, 1994).

There have been multiple studies investigating the macro domain of CHIKV. The three-dimensional structure of the domain was determined by X-ray crystallography in 2009 (Malet *et al.,* 2009),. As shown in Figure 1.21, this study revealed the structure of both the native (apo) CHIKV macro domain but also the domain in complex with ADP-ribose and RNA. In the same publication, it was demonstrated that the CHIKV macro domain is capable of binding ADPR with a lower affinity than the VEEV macro domain, with both alphaviruses exhibiting far weaker affinity than the SARS-CoV macro domain. Conversely, the CHIKV macro domain, alongside VEEV, SFV and SINV, all bound PAR with far greater affinity than the SARS-CoV macro domain. The ADPR 1"-phosphatase activity was also detected in all alphavirus macro domains to varying levels except that of SFV, which was below the detection limit.
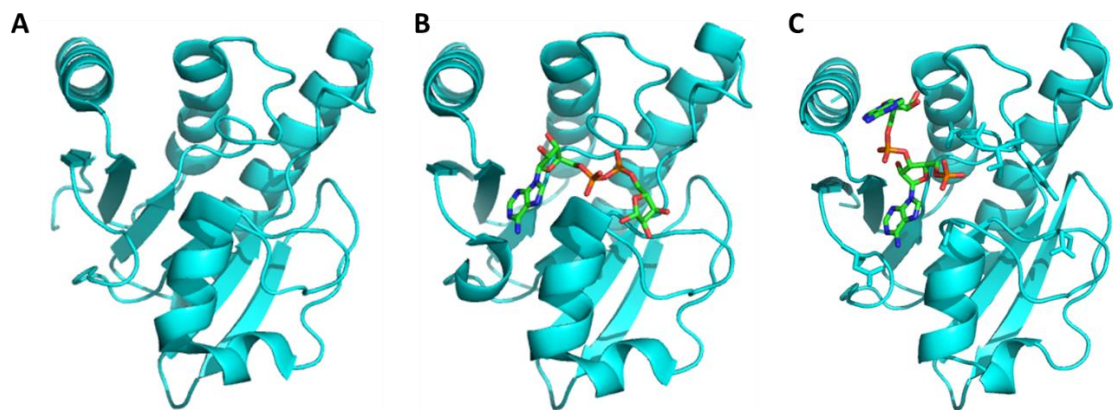
Figure 1.21 The 3-dimensional structure of the CHIKV nsP3 macro domain. (A) The native domain, (B) the domain in complex with mono-ADP-ribose, (C) the domain in complex with RNA. PDB numbers 3GPG, 3GPO and 3GPQ respectively (Malet *et al.,* 2009).

Surprisingly, the macro domain with the highest sequence and structural similarity to the CHIKV macro domain was that of *E. coli*, not coronaviruses. This may allude to the alphavirus macro domain having a different cellular function than the coronavirus equivalent and, interestingly, may also imply that there were two separate evolutionary events where +ssRNA viruses acquired macro domains (Malet *et al.,* 2009; Neuvonen and Ahola, 2009).

In common with the HEV macro domain, it was demonstrated that the CHIKV macro domain was able to function as a hydrolase (Li *et al.,* 2016). The CHIKV

macro domain was demonstrated to be able to efficiently remove MAR from ribosylated proteins *in vitro,* with evidence that this process also occurs *in vivo* (Eckei *et al.*, 2017). The same study demonstrated that hydrolysis of PAR from modified proteins was inefficient, which is curious as Malet *et al.* (2009) demonstrated that the CHIKV macro domain had a high affinity for PAR binding.

A separate study published very similar findings. It was demonstrated that the CHIKV macro domain could hydrolyse MAR from aspartate and glutamate residues, but not lysine (McPherson *et al.*, 2017). In the same publication, it was demonstrated through mutagenic studies, that binding and hydrolysis of MAR was essential for replication of the virus in cell culture and mutations to the domain reduced virulence in infected mice.

A more recent publication by the same group showed that upon CHIKV infection, there is an increase in general ADP-ribosylation within infected neurones and that MARylation activity of cellular ARTDs is required for optimal CHIKV infection (Abraham *et al.*, 2018). In agreement with previous results it was shown that when both hydrolase and ADPR-binding of the CHIKV macro domain were lost through mutation, the replication of the virus was significantly reduced from early stages of infection. However when binding capabilities are maintained but hydrolase activity reduced, early stages of infection proceeded as normal such as the translation of non-structural proteins and the formation of replicase complexes, however, translational shut-off occurs earlier than is observed for wt CHIKV, resulting in a delay in virus replication for these mutants.

All this information together forms a rather confusing picture. The CHIKV nsP3 macro domain is more similar to *E. coli* than coronaviruses, indicating that there may be little crossover between its function in alphaviruses and coronaviruses. It has also been shown to bind MAR and PAR with high affinity, yet possesses the ability to efficiently hydrolase MAR, but not PAR from ribosylated proteins. It has been shown that the CHIKV nsP3 macro domain requires binding and hydrolysis of MAR in order to establish replication, but when lacking hydrolase activity alone, early stages of replication resemble wt, only reducing due to the early onset of host translational shutoff. From this collective data, it is still unclear

as to what specific functions the CHIKV nsP3 macro domain provides in virus replication which forms the main aim of this project.

1.4   Aims

Previous studies have mostly focused on *in vitro* biochemical properties of the macro domain with few assessing its cellular function in detail. Therefore, the overall aim of this project was to determine the function of the CHIKV nsP3 macro domain in the context of the replication cycle of the virus. To achieve this, initially, replicon and infectious virus clones had to be optimised in a range of suitable and appropriate cell lines in order to study the molecular biology of CHIKV under optimal conditions. Following this, mutagenic studies were performed on the nsP3 macro domain to form a range of replicative phenotypes and investigate the cause(s) of these phenotypes. From this data, further study into the precise cellular function of the domain were conducted, leading to the investigation of whether the CHIKV nsP3 was able to interfere with cellular innate immunity pathways.

Chapter 2 Materials and Methods

2.1 Molecular Biology

2.1.1 Polymerase Chain Reaction (PCR)

PCRs were assembled at room temperature using as shown in Table 2.1 and were cycled as defined in Table 2.2. Details of plasmid maps and primers used for PCR and cloning are detailed in chapter 8.

Component	Per tube
Template DNA	100 ng
100 µM forward primer	0.5 µL
100 µM reverse primer	0.5 µL
Vent polymerase (NEB)	1 µL
ThermoPol buffer (NEB)	5 µL
100 mM dNTPs (BioLine)	0.4 µL
DMSO (ThermoFisher)	1 µL
ddH$_2$O	Up to 50 µL

Table 2.1 Assembly of PCRs

Temperature	Time (min)	Number of cycles
95 °C	2:00	X 1
95 °C	00:30	X 30
Annealing (see appendix?)	00:30	
72 °C	1:00 per 1 kb	
72 °C	2:00	X 1
4 °C	Infinite hold	X 1

Table 2.2 PCR cycle program generic template

2.1.2 Mutagenesis

Site-directed mutagenesis was performed using the NEB Q5 site directed mutagenesis kit, using primers in Table 7.2. Reactions were prepared as shown in Table 2.3 at room temperature, and cycled as specified in Table 2.4. The PCR

product was Kinase/ligase/DpnI (KLD) treated, assembling the reaction using: 1 µL PCR product, 5 µL KLD buffer, 1 µL KLD enzyme mix and 3 µL nuclease free ddH$_2$O. The reaction was incubated for 10 min at rt and 5 µL of the reaction was transforming into 50 µL competent cells (see 2.1.7).

Component	Per tube (µL)
Q5 master mix	12.5
10 µM forward primer	1.25
10 µM reverse primer	1.25
Template DNA (25 ng/µL)	1.0
Nuclease-free ddH$_2$O	9.0

Table 2.3 Assembly of Q5 mutagenesis reactions

Temperature	Time	Number of cycles
98 °C	0:30	X 1
98 °C	0:10	
Annealing temperature (see appendix for specific temperatures)	0:30	X 25
72 °C	0:30 per 1 kb	
72 °C	2:00	X 1
4 °C	Hold	X 1

Table 2.4 PCR cycle program for Q5 mutagenesis reactions

2.1.3   Restriction endonuclease digestions

All restriction digests were performed using NEB enzymes. Reactions were performed with the appropriate buffer and recommended temperature. For linearisation of the CHIKV replicon and virus DNA constructs for *in vitro* RNA transcription, 5 µg of DNA was digested for 5-16 h using NotI-HF. For general cloning, a minimum of 1 µg DNA was digested with 10 units of enzyme at a total reaction volume of 20 µL. After digestion, vector DNA for cloning was calf

intestinal phophatase (CIP, NEB) treated: 10 units of CIP was added directly to the digestion mix and incubated at 37 °C for a further hour. Resulting DNA was then extracted by phenol-chloroform extraction and ethanol precipitation (see sections 2.1.4 and 2.1.5).

2.1.4   Phenol-chloroform extraction DNA extraction

The total volume of DNA to be extracted was adjusted to 200 µL with ddH$_2$O. One volume phenol:chloroform:isoamyl (25:24:1) alcohol added, vortexed for 1 min and centrifuged at 16,000 xg for 5 min. The resulting upper phase was removed, transferred to a fresh tube and 1 volume of chloroform added, vortexed 1 min and centrifuged at 16,000 xg for 5 min. The upper phase was again removed and transferred to a new tube for ethanol precipitation (see 2.1.5)

2.1.5   Ethanol precipitation of DNA

Where possible, the total volume of the DNA sample for precipitation was adjusted to 200 µL, if the sample was in excess of 200 µL, the following volumes were adjusted accordingly. Three volumes of absolute ethanol and 0.1 volume of 3M sodium acetate added, briefly vortexed and incubated at -20 °C for a minimum of 3 h, preferably overnight. Samples were centrifuged at 20,000 xg at 4 °C for 30 min. Supernatant was discarded and replaced with 200 µL 70 % ethanol. Samples were centrifuged at 20,000 xg at 4 °C for 10 min. Ethanol was removed and samples left to air dry for 30 min before resuspending the DNA pellet in ddH$_2$O for most constructs (e.g. for cloning) or with RNase-free water for *in vitro* RNA synthesis.

2.1.6   Transformation of DNA into competent cells and culture

DNA was transformed into 5-alpha competent *E. coli* (NEB) that were prepared using the Mix and Go kit (Zymo), following manufacturer's protocol, to produce Z-competent cells. For intact DNA constructs, 20 µL of cells were mixed with 5 µL plasmid DNA and incubated on ice for 5 min. The total volume was made up to 200 µL with LB and plated out onto LB agar containing ampicillin (100 µg/mL), incubating at 37 °C overnight. For ligated or mutagenesis DNA products, a similar process was performed with an additional recovery step after LB was

added, with samples being incubated at 37 °C in a shaking incubator for 1-2 h prior to plating onto agar containing ampicillin.

2.1.7 DNA preparation

2.1.7.1 DNA constructs

2.1.7.1.1 Replicon constructs

All replicons used in this project were generated, and kindly provided by Andres Merits. All replicons were derived from the ECSA genotype RL2006OPY1 isolate virus and modified with various tags. The dual luciferase (dLuc) replicon contains a Renilla luciferase (RLuc) inserted into the VR of the nsP3 coding region via an engineered SpeI site, and contains a firefly luciferase (Fluc) in the subgenomic region of the genome, replacing the structural ORF (see appendix Figure 7.1).

An mCherry-tagged nsP3 replicon was generated using the same SpeI site as detailed for the dLuc replicon. The nsP3-mCherry replicon contains a subgenomic Gaussia luciferase and is referred to as nsP3-mCherry/SG-GLuc throughout.An untagged nsP3 replicon is also used in this project, referred to as wt-nsP3/SG-Fluc, which contains a Fluc in the subgenomic region of the replicon.

2.1.7.1.2 Virus constructs

Similarly to the replicon constructs, the virus construct used throughout this project, termed "ICRES," was derived from a patient isolate from the ECSA genotype RL2006OPY1 virus (see appendix Figure 7.3).

2.1.7.1.3 Expression constructs

For protein expression, constructs were formed using pcDNA3.1+ (see appendix Figure 7.1).

2.1.7.2 Small scale DNA preparation

To purify DNA on a small scale, a single colony containing the desired construct was used to inoculate a 5 mL LB culture containing 100 µg/mL ampicillin and grown overnight at 37 °C, shaking at 180 rpm. Plasmid DNA was then prepared by alkaline lysis using the Monarch Plasmid Miniprep kit (NEB) using the manufacturer's recommended protocol.

2.1.7.3   Large scale DNA preparation

For large DNA preparation, 1 mL from a 5 mL overnight culture (as described in 2.1.7.2) was used to inoculate a 50 mL LB culture containing 100 µg/mL ampicillin and incubated over night at 37 °C with shaking. DNA was prepared by alkaline lysis using the GeneJET Plasmid Midiprep kit (ThermoFisher Scientific) using the manufacturer's recommended protocol.

2.1.8   DNA agarose gel electrophoresis

Agarose gels at 1% were used for DNA gel electrophoresis (1% agarose in TAE buffer with SYBR safe 1:10000). DNA was prepared using purple gel loading dye (6x, NEB). Hyperladder 1kb (Bioline) was used for size markers. Gels were electrophoresed at 100 volts for 40 min.

2.1.9   Gel extraction of DNA

DNA bands were visualised via blue light (470 nm) with an orange filter, and relevant bands were excised from the gel. The DNA was extracted from the gel slices using the Monarch gel extraction kit (NEB) using the manufacturer's recommended protocol.

2.1.10 Ligation of DNA

Ligations were performed at a 5:1 molar ratio of insert to vector, with 50 ng of vector. DNA was mixed, incubated on ice for 5 min, then 50 °C for 5 min before adding 400 units of T4 ligase, ligation buffer and ddH$_2$O to 20 µL total volume. Ligation reactions were incubated at room temperature for 1 h then transformed into competent cells (see 2.1.6).

2.1.11 Verification and sequencing of DNA constructs

Generated DNA constructs were assessed for size and quality by an appropriate restriction digest and gel electrophoresis prior to DNA sequencing. All DNA sequencing was performed by Genewiz (formally Beckman Coulter Genomics) using primers shown in Table 7.5.

2.1.12 *In vitro* transcription of capped RNA

The mMessage mMachine kit (Ambion) was used to synthesise capped RNA transcripts using 1 µg of linearised template DNA, using the manufacturer's recommended protocol. Resulting RNA was assessed for size and quality by MOPS gel electrophoresis. For long term storage, RNA was aliquoted and stored at -80 °C.

2.1.13 RNA gel electrophoresis

RNA size and quality was determined by MOPS (3-(N-morpholino)propanesulfonic acid) gel electrophoresis. Samples were prepared using RNA loading dye (2x, NEB) and loaded on a 1% MOPS gel (1% agarose, 1X MOPS (40 mM 3-(N-morpholino)-propanesulfonic acid pH 7.0, 10 mM sodium acetate, 1 mM EDTA, 4.7% formaldehyde and 1:10,000 SYBR safe dye) at 80 V for 40 min, alongside ssRNA ladder (NEB).

2.2 Cell Culture

2.2.1 Mammalian cell lines and maintenance

Mammalian cell lines were maintained in media shown in Table 2.5

Cell line	Origin	Media
Huh7	Human, hepatocellular carcinoma (HCC)	Dulbecco's modified eagle medium (DMEM) + 10% foetal calf serum (FCS) + non-essential amino acids (NEAA)
HepG2	Human, HCC	DMEM + 10% FCS + NEAA
C2C12	Mouse, myoblast	DMEM + 20% FCS
RD	Human, rhabdomyosarcoma	DMEM + 10% FCS
SVG-A	Human, astroglia	DMEM + 10% FCS + NEAA
Dermal fibroblasts	Human, dermal fibroblasts	DMEM + 10% FCS + NEAA
BHK-21	Hamster, kidney fibroblast	DMEM + 10% FCS
HeLa	Human, cervical adenocarcinoma	DMEM + 10% FCS
Vero	African green monkey, kidney epithelia	DMEM + 10% FCS
A549	Human, lung carcinoma	DMEM + 10% FCS

Table 2.5 Mammalian cell lines used, their origin and culture media

All mammalian cell lines were maintained in their full media in T175 flasks at 37 °C with 5% CO_2. Cells were passaged by washing in PBS, 2 mL trypsin added and incubated at 37 °C until cells detached from the flask, resuspended in complete media and the required amount transferred to a new T175 flask and the total volume made up to 20 mL with media.

2.2.2 Mosquito cell lines and maintenance

All mosquito cells were maintained in media shown in Table 2.6.

Cell line	Origin	Media
Aag2	*Aedes aegypti*	Leibovitz's L-15 media, 10% FCS and 10% Tryptose phosphate broth
A20	*Aedes aegypti*	Leibovitz's L-15 media, 10% FCS and 10% Tryptose phosphate broth
U4.4	*Aedes albopictus*	Leibovitz's L-15 media, 10% FCS and 10% Tryptose phosphate broth
C6/36	*Aedes albopictus*	Leibovitz's L-15 media, 10% FCS and 10% Tryptose phosphate broth

Table 2.6 Mosquito cell lines used, their origin and culture media

All mosquito cell lines were maintained in full media in T175 flasks at 28 °C (no additional CO_2). Cells were passaged by washing in PBS, scraping the cells into 10 mL media, the required amount was then transferred to a new T175 flask and the total volume made up to 20 mL with media.

2.2.3 Transfection of cells

Transfection mixes were generated by mixing the desired amount of lipofectamine (Invitrogen) in Optimem (50 µL/well, Gibco) and, separately, the required amount of RNA/DNA in Optimem (50 µL/well), incubating each for 5 min at rt then mixing together and incubating for a further 20 min. Cells were washed and media changed to Optimem prior to adding 100 µL of the transfection mix to each well and mixed by gentle swirling. Cells were incubated for 4 h in the transfection mixture prior to washing with PBS and media replaced with complete media.

For RNA transfection, number of cells, amount of lipofectamine and RNA was dictated by plate size (see table 2.2.3).

For DNA transfections, cell number and amount of lipofectamine used was the same as RNA shown in Table 2.7, though the amount of DNA used varied by specific construct.

DNA constructs transfected into cells were pcDNA3.1+ expression constructs (see appendix figure 7.1), expressing various tagged forms of nsP3. For assessing activation of the NFkB pathway, two plasmids were used in combination; the NFkB-Fluc plamsid, that encodes a firefly luciferase under the control of a NFKB-sensitive promotor, and the pRL-TK plasmid, which encodes a Renilla luciferase under the control of a thymidine kinase promoter, therefore acting as a transfection control.

Plate size	Number of cells plated	Lipofectamine (per well)	RNA (per well)
24-well	1×10^5	1 µL	250 ng
12-well	2×10^5	2 µL	500 ng
6-well	4×10^5	3 µL	1 µg

Table 2.7 Numbers for lipofectamine transfection of cells

2.2.4 Luciferase assay

Transfected cells were lysed in 1x passive lysis buffer (PLB, Promega, 100 µL/well in 24 well plates) and frozen at -20 °C until dual luciferase assays were performed using the Promega dual luciferase reporter assay system. Cell lysates were defrosted and aliquoted at 30 µL per well in a white, flat-bottomed 96 well plate. Manually, 40 µL of LarII (FLuc detection reagent) was pipetted per well then luciferase signal read. Then, 40 µL of Stop and Glo (RLuc detection reagent, which also quenches the firefly reaction) was added to the wells and luciferase signal read again for *Renilla*. Luciferase activity was detected using the FLUOStar optima microplate reader (BMG Labtech).

2.2.5 Electroporation for virus propagation

Electroporations for virus propagation were performed in BHK cells. Cells were trypsinised, resuspended in complete media, centrifuged at 1000 xg for 3 min, resuspended in pre-cooled DePC (Diethyl pyrocarbonate) PBS, centrifuged again and resuspended in 5 mL DePC PBS. Cells were counted and resuspended to achieve a concentration of 3×10^6 cells/mL. In a pre-cooled electroporation cuvette, 1 µg of virus RNA was added to the bottom, 400 µL (approx. 1.2×10^6 cells) were added, gently mixed then electroporated with a

single pulse at 250 volts for 25 ms. Two electroporations were pooled in 10 mL of complete media in a T75 flask and transferred to the BSL3 facility. Media was removed at 24 h post electroporation, aliquoted and frozen at -80 °C and titred by plaque assay.

2.2.6 Plaque assay

Plaque assays were performed on BHK cells. Number of cells/media used was dependent on plate size as shown by Table 2.8.

Plate size	Number of cells	Volume of virus	Volume of MC
6-well	4×10^5	200 µL	2 mL
12-well	1.5×10^5	150 µL	1 mL

Table 2.8 Numbers for plaque assays

Cells were plated 16 h prior to plaque assay. Virus to be titred was serially diluted in serum-free media (number of dilutions was dependent on expected titres). Dilutions of virus was then placed on pre-plated cells (150 µL for 12 well plates and 180 µL for 6 well plates), rocked for 5 min at rt then incubated at 37 °C for 1 h. Virus was then removed and cells overlaid with 1.6 % methyl cellulose (MC) mixed 1:1 with complete media. Cells were incubated at 37 °C for 48-72 h, then fixed in 10 % formaldehyde for 30 min and stained using 0.5% crystal violet for 1 h. Stain was then removed and plates washed in water until plaques become visible. Virus titres were calculated using the equation shown in equation 2.1.

$$PFUmL = \frac{Number\ of\ plaques\ observed}{dilution\ factor\ (10^{-x})\times volume\ of\ virus\ added\ (mL)}$$

Equation 2.1 Calculation of virus titres (plaque forming units/mL) from plaque assay

2.2.7 Infection of cells with CHIKV

Virus stocks were diluted in serum-free media to the desired MOI. Cells were washed in PBS, virus added, plates were rocked for 5 min then incubated at 28 °C (mosquito cells) or 37 °C (mammalian cells) for 1 h. Virus was removed

and cells were washed thoroughly in PBS twice before replacing complete media. Cells were then incubated at 28/37 °C for the required amount of time.

2.2.8 Infectious centre assay (ICA)

BHK cells were plated in 6 well plates, 4×10^5 cells/well, 16 h prior to the assay, and a minimum of two T175 flasks prepared to achieve confluency overnight. Confluent BHK cells were then electroporated with virus RNA (see section 2.2.5), two separate electroporations per RNA were pooled and total volume made to 1.2 mL with serum-free media. Suspensions of electroporated cells were serially diluted from 10^{-1} to 10^{-6} in complete media. Pre-plated BHK cells were washed in PBS and 1 mL of cell dilution added to each well. Plates were gently rocked by hand briefly, transferred to BSL3 and incubated at 37 °C for 1 h, cell suspension removed from wells and replaced with 2 mL of 1.6% MC mixed in complete media (1:1). Plates were incubated for 72 h prior to fixation and stain as described in 2.2.6. Resulting plaques were used to calculate PFU/µg of input RNA via the equation shown in Equation 2.2.

$$ PFU/_{\mu g\ RNA} = \frac{\left(Number\ of\ plaques \middle/ dilution\ factor\ (10^{-x}) \right)}{Input\ RNA\ (\mu g)} $$

Equation 2.2 Calculation of virus production per µg of input RNA (PFU/µg RNA) from an infectious centre assay

2.2.9 Trizol Extractions

RNA was extracted from infected cells using TRIzol (Life Technologies). Media was removed, cells were washed in PBS then 500 µL/well of TRIzol added (for 12 well plates, or used at 1 mL/10 cm^2 for other dishes), plates were rocked to ensure coverage and mixed by pipetting in the well before transferring to microcentrifuge tubes. The TRIzol samples were incubated for 5 min at rt and then stored at -80 C before continuing. Once thawed, 100 µL chloroform was added, samples were vortexed briefly and incubated at rt for 3 min. Tubes were then centrifuged at 12,000 xg for 15 min at 4 °C. The resulting upper layer was transferred to a new tube, 250 µL isopropanol added, mixed by inversion and incubated for 10 min at rt. Tubes were centrifuged at 12,000 xg for 10 min at 4 °C

resulting in a visible RNA pellet. Supernatant was removed (without disturbing the pellet) and 500 µL of ice cold 75% ethanol added. Samples were centrifuged at 7500 xg for 5 min at 4 °C, ethanol removed and sample briefly air dried at rt before resuspending in 20-50 µL nuclease-free water. Resulting RNA was electrophoresed on a MOPs gel to ensure successful extraction where ribosomal RNA can be visualised.

2.2.10 qRT-PCR

All qRT-PCR was performed using the 'one step MESA GREEN qRT-PCR MasterMix for SYBR assay' (EuroGenTec). Following manufacturer's protocol with reaction mix being assembled as described in Table 2.9, with primers used described in Table 7.3.

Component	Per Tube (µL)
2x buffer	12.5
Foward Primer (10 µm)	2.0
Reverse primer (10 µm)	2.0
Enzyme mix and RNase inhibitor	0.125
RNA (50 ng/µL) or standards	2.0
RNase-free ddH2O	6.375

Table 2.9 Reaction assembly for qRT-PCR using MESA green qRT-PCR mastermix kit

For each qRT-PCR, a set of DNA standards of known concentrations as well as a no template control were assembled alongside extracted RNA samples. Reactions were cycled using the Stratagene Mx3005P (Agilent technologies) as shown in Table 2.10.

Temperature	Time (min)	Cycles
48 °C	30:00	X1
95 °C	5:00	X1
95 °C	0:15	X40
56 °C	1:00	
95 °C	1:00	X1
55 °C	0:30	
95 °C	0:30	

Table 2.10 qRT-PCR cycle template

2.2.11 Reverse transcription and sequencing of extracted virus RNA

In order to sequence TRIzol extracted RNA, reverse transcription was performed using the SuperScript II Reverse Transcriptase kit (Life technologies) using manufacturer's recommended protocol and random hexamer primers (Themo Scientific). Resulting cDNA was then used as input for PCR to amplify the nsP3 region (see section 2.1.1) using primers described in Table 7.4, and the resulting PCR product was sequenced as detailed in section 2.1.11.

2.3   SDS-PAGE and Western blotting

2.3.1   Bradford assay

Protein samples were quantified by Bradford assay. Protein samples and bovine serum albumin (BSA) standards were plated on flat bottom, clear 96 well plate (5 µL/well), 250 µL of Bradford reagent (8.5% H_3PO_4, 5% methanol, 0.005% Coomassie Brilliant Blue G-250) added, incubated at rt in the dark for 10 min, absorbance read on a plate reader at 570 nm and protein concentrations calculated from the standard curve formed by the BSA protein standards.

2.3.2   SDS-PAGE

Protein samples were quantified by Bradford assay and prepared with Laemmli loading dye (250 mM Tris-HCl, 40% (v/v) glycerol, 8% SDS, 0.2% bromophenol blue, 20% ? β-mercaptoethanol). SDS-polyacrylamide gels were prepared with either 7.5%, 10% or 15% acrylamide with 375 mM Tris-HCl/Cl, pH 8.8; 0.1% SDS, 0.1% APS, 0.01% TEMED; with stacking gel: 5% Acrylamide, 125 mM Tris-HCl, pH 6.8; 0.1% SDS, 0.1% APS, 0.01% TEMED. Gels were assembled in a gel tank, filled with Tris-glycine buffer (0.25 M glycine, 25 mM Tris-HCl and 0.1% SDS), and electrophoresed at 180 v until required protein resolution was achieved.

2.3.3   Western blot

SDS-PAGE gels were transferred onto Immobilon PVDF membranes (Sigma) using a semi dry trans-blotter at 15 A for 1 h in transfer buffer (25 nM Tris base, 192 mM glycine, 20% methanol, 0.1% SDS). Membranes were blocked in LICOR-TBS blocking buffer for a minimum of 20 min, rocking at rt. Primary antibodies (see Table 2.11) were diluted in TBS and added to membranes overnight, rocking at 4 °C. Membranes were washed in TBS 5 times, then appropriate LICOR secondary antibody was applied (diluted 1:10,000 in TBS) for 1 h rocking at rt in the dark. Blots were washed a further 5 times in TBS, then rinsed in water and left to dry in the dark. Membranes were imaged using the LICOR Odyssey.

Antibody	Species	Origin	Working dilution
Anti-nsP3 (full)	Rabbit	Andres Merits	1:1000
Anti-β actin	Mouse	Sigma A1978	1:10,000
Anti-p65	Mouse	Santa Cruz SC-8008	1:200
Anti-phospho-p105	Rabbit	NEB 4806	1:1000
Anti-flag	Mouse	Sigma F3165	1:500

Table 2.11 Primary antibodies used for western blotting

2.4   Immunofluorescence

Cells for immunofluorescence (IF) were plated out into 12-well plates onto glass coverslips. Cells were fixed using 4% para-formaldehyde (PFA) for 10 min and washed with PBS three times. Cells expressing fluorescent proteins that did not require antibody staining were washed and mounted in Prolong Diamond with DAPI (Life Technologies). For cells requiring antibody staining, after fixation, cells were permeabilised with 0.5% Triton-x for 10 min, washed with PBS and blocked in 2% BSA for 1 h. Three more PBS washes were performed and cells were subjected to primary antibody (see Table 2.12) , diluted in PBS, for 1 h at rt. Coverslips were again washed and then incubated with appropriate secondary antibody, (diluted 1:1000) in PBS for another h. Coverslips were washed in PBS three times, dipped in ddH$_2$O then mounted onto slides using Prolong Gold with DAPI (Life Technologies) and left to dry overnight.

Antibody	Species	Origin	Working dilution
Anti-nsP3 (full)	Rabbit	Andres Merits	1:1000
ARTD10/PARP10	Rat	Santa Cruz 5H11	1:50
p65	Mouse	Santa Cruz SC-8008	1:50

Table 2.12 Primary antibodies used for immunofluorescence

Chapter 3 Establishing a panel of suitable and relevant cell lines for CHIKV research

3.1 Introduction

CHIKV was discovered in 1952, but little research has been conducted on the virus until recently, within the last 10 years. In publications on the molecular biology of CHIKV, the cell lines most commonly used are BHK (baby hamster kidney cells), Vero (African green monkey cells), HeLa (human cervical carcinoma) and HEK293T (human embryonic kidney, expressing SV40 T antigen) cells. These cells are often used in virological research and are regarded as the 'workhorse' cell lines for the production of many viruses, however, none of these are particularly physiologically relevant to CHIKV infection *in vivo*.

CHIKV is introduced to the human host via mosquito bite. From the bite site, CHIKV infects and replicates in the dermal fibroblasts. The virus then spreads throughout the lymphatic and circulatory systems throughout the body to the 'target organs;' the liver, muscles, joints and the brain (Thérèse Couderc *et al.*, 2008).

There have been multiple studies on CHIKV infection of the myeloid and lymphoid cells as little is known on how CHIKV disseminates through the lymphatic and cardiovascular systems (Sourisseau *et al.*, 2007). There have also been some studies on cell tropism, particularly in neuronal cell types due to the severe symptoms CHIKV can induce if the brain becomes infected (Dhanwani *et al.*, 2012). However, there is currently no consensus on 'model' cell lines for molecular CHIKV research.

Choice of cell line can be critical for experiments. Many cell lines, because of transformation or their origins, may have different expression profiles than their tissue of origin which may have a profound effect on experiments. Many malignant cell lines have mutations typical of cancers. For instance, cells from the malignant mammary cell line, MCF-7 do not express caspase-3 (Kagawa *et al.*, 2001) and A549 cells have a mutated Ras gene that affects cell motility (Okudela *et al.*, 2004). HeLa cells are the most widely used cell line in many areas of research but are severely mutated, contain various numbers of chromosomes per cell (aneuploidy) and possess a range of chromosome abnormalities that vary between lineages. Some studies have shown that as

many as 2000 proteins are over-expressed in HeLa cells when compared to human tissue (Landry *et al.*, 2013). HeLa cells also contain integrated human papilloma virus DNA and express the viral oncogenic proteins E6 and E7 (DeFilippis *et al.*, 2003) which make them a poor model for most areas of cellular and molecular study. Despite this, HeLa cells have proved useful for many purposes including the production of the first polio vaccine (Turner, 2012) and for early-stage drug testing for cancer (Shi *et al.,* 2015; Y. Zhang *et al.*, 2018).

Some cell lines, despite not being malignant, can possess expression profiles which can make them irrelevant for certain areas of study. For instance Vero cells, a non-malignant cell line commonly used for virus studies, cannot produce endogenous IFN in response to infection (Desmyter *et al.*, 1968). These cell lines are therefore not suitable for the study of pathways that involve these proteins that are absent or mutated. However, defective cell lines such as these can also prove useful in experiments looking at these particular pathways.

Primary cell lines are often regarded as more representative of cellular processes *in vivo,* however, the use of primary cells has many issues. Firstly, they are slow growing with a limited life-span, meaning that it may take weeks to months to grow sufficient cells for a single experiment that then must be done in a timely manner. This often makes experimental replicates difficult as the cells may not survive long enough for all required repeats and different primary cells must be used. Secondly, most individual primary cells come directly from the donor and are therefore not well characterised in terms of their expression profile, and cells from different donors introduce the issue of heterogeneity. Thirdly, many cell types quickly de-differentiate in cell culture so become less representative of their progenitor cell type after a few days in culture, this is a particular issue with primary hepatocytes (Hengstler *et al.*, 2005). However, it is possible to immortalise primary cells *in vitro* in order to produce physiologically relevant cells that are easier to work with, as shown here with the dermal fibroblast cells.

Established cell lines are more commonly used in laboratory work as they are immortal, quick-growing and many are well characterised from previous studies. They are also more widely available so that different research groups can

successfully replicate data produced by others. This makes them relatively simple to work with and convenient for experimental work.

3.1.1 Aims

The aim of this part of the project was to screen a wide range of cells and cell lines. With particular attention to those that are physiologically relevant to CHIKV infection *in vivo*, but also cells commonly used in the literature as a comparison, in order to determine a set of appropriate cell lines that are useful for CHIKV research. Mosquito cell lines were also evaluated as CHIKV is an arbovirus and it is important to study the virus lifecycle in the mosquito vector as well as the human host.

An ideal cell line for CHIKV research would be one that is physiologically relevant (i.e. derived from a tissue that CHIKV would infect in an *in vivo* infection) and can be easily propagated in culture (exhibit a reasonable growth rate, no requirement for complex or unusual growth media, maintain viability during passage and trypsinisation). In practical terms, in order to study CHIKV, cells would also need to be capable of being transfected with replicon RNA, support replication of the replicon, be able to be successfully infected with CHIKV and support viral replication. Since this project is focussed on nsP3, cells were also evaluated for nsP3 expression and detection of the protein by western blot and immunofluorescence.

3.2 Results

3.2.1 Mammalian cell lines

Humans are the main host for CHIKV. The virus is introduced to the body via a mosquito bite, where the virus replicates in the dermal fibroblast cells before spreading through the lymphatic and cardiovascular systems to the "target" organs; the liver, muscles, joints/connective tissues and the brain.

There is some evidence that CHIKV is able to infect and replicate in non-human primates but this is not essential for the infectious cycle between mosquitos and humans (Haese *et al.*, 2016).

In contrast to its cell tropism *in vivo,* in cell culture, CHIKV has been shown to be capable of replication in a vast range of cell types with a few exceptions. For example, A549 cells, a lung epithelial cell line have been shown not to support virus replication despite CHIKV being able to bind to the cell surface (Sourisseau *et al.*, 2007).

As of yet, there is little consensus in the literature as to which cell lines are appropriate for their use in CHIKV research. Here, multiple cell lines were evaluated for their use in CHIKV research, from this four 'model' mammalian cell lines were selected for their use with CHIKV, particularly for investigating nsP3.

3.2.1.1 Replicon

Initially, ten cell lines were selected for transfection with CHIKV replicon RNA to determine whether each cell line could support CHIKV RNA replication. The ten cell lines (shown in Table 2.5) represent lines that are representative of that 'target organs' that CHIKV favourably replicates *in vivo* (e.g. Huh7, dermal fibroblasts) but also cell lines commonly used in virus work including CHIKV (e.g. BHK, Vero). For initial experiments, the dual luciferase (dLuc) CHIKV replicon was used, a schematic of which is shown in Figure 3.1 A. This replicon expresses all four non-structural proteins, with nsP3 containing a Renilla luciferase in the variable region as an indirect indicator of translation of the non-structural ORF. In the subgenomic region, a firefly luciferase (Fluc) gene replaces the structural ORF previously described by McFarlane *et al.*, 2014. When Fluc signal is detected, it indicates that RNA replication has occurred as CHIKV generates a

sub-genomic RNA (26S RNA) from this region in order for the structural proteins to be expressed. All ten cell lines were transfected with the dLuc replicon, using lipofectamine2000, cell lysates taken over a 48 h time period and luciferase assayed and resulting signals shown in Figure 3.1.
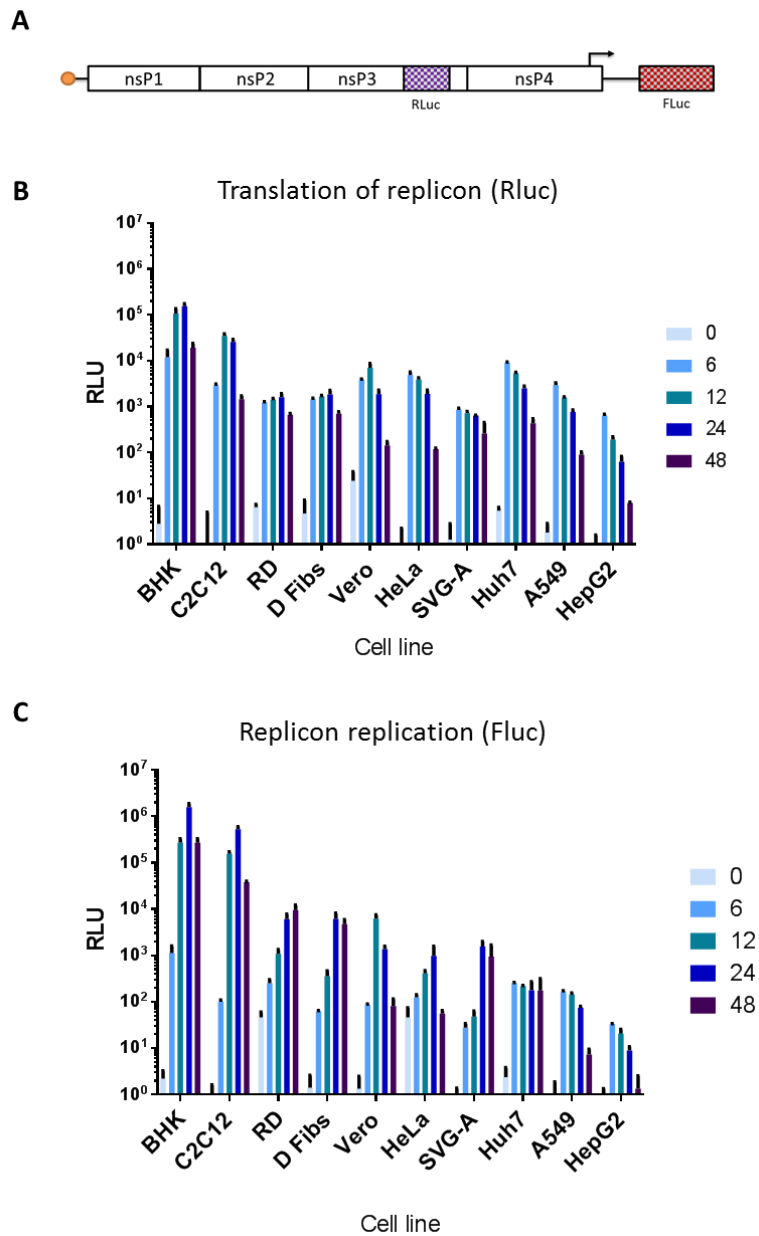
Figure 3.1 Transfection of mammalian cell lines with the dual luciferase CHIKV replicon. (A) Schematic of the dual luciferase CHIKV replicon. Mammalian cell lines transfected with the CHIKV replicon. Liver (Huh7, HepG2), muscle (C2C12, RD), brain (SVG-A), fibroblasts (Dermal fibs, BHKs), as well as Vero, HeLa and A549 cells were transfected with dLuc CHIKV replicon RNA. Cell lysates were taken at indicated time points over a 48 h period and luciferase assayed (n=3). The Renilla luciferase is present in the VR of nsP3, indicating levels of nsP3 present in the cell (B). The Firefly luciferase is in the sub-genomic region of the replicon, indicating that RNA replication has occurred (C).

The increase in Renilla luciferase values between 0 and 6 hpt indicates that the replicon RNA was translationally-competent in all 10 cell lines. The replication of the replicon RNA, however, was quite diverse between the cell lines in both signal levels and pattern of RNA replication. Half of the lines exhibited peak replication at 24 hpt. The exceptions to this were RD, Vero, Huh7, A549 and HepG2 cells. Both A549 and HepG2 cells produced quite low signal throughout the time course with the highest at 6 hpt. RD cells produced higher levels of replication at 48 hpt. Vero cells were the only line to produce the highest Fluc signal at 12 hpt. Of the physiologically relevant cell lines, C2C12, RD, dermal fibroblasts and SVG-A cells performed well. Both liver-derived cell lines supported low levels of CHIKV RNA replication with HepG2 cells performing far worse than the Huh7 cells.

To ensure these results were due to the ability of the cells to replicate the replicon, rather than their transfection efficiency, all 10 cell lines were transfected with pRL-TK plasmid DNA, which constitutively expresses Renilla luciferase under control of a thymidine kinase promoter, with lipofectamine2000 for 24 h and luciferase signal assayed (Figure 3.2).
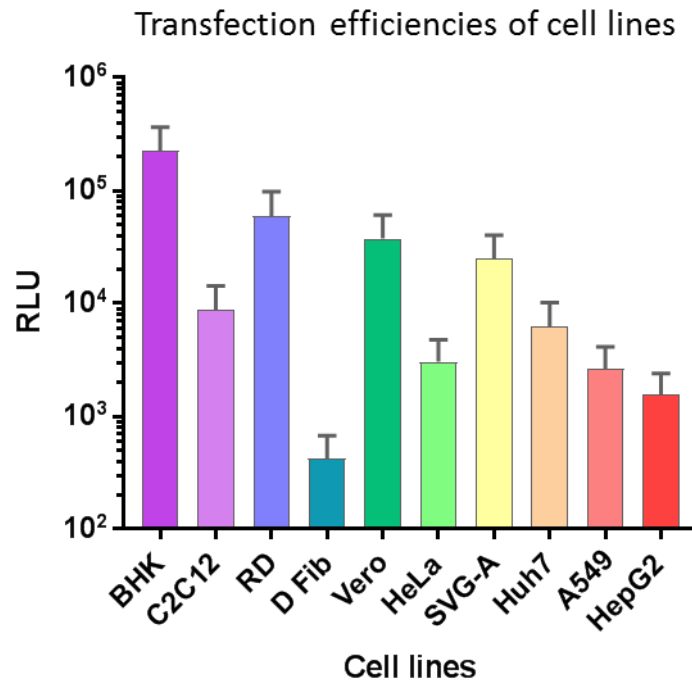
Figure 3.2 Transfection efficiencies of screened cell lines. Cells were transfected with 100 ng pRL-TK using lipofectamine2000, harvested at 24 hpt and luciferase signal assayed.

Although there were some marked differences in transfection efficiencies, this did not directly relate to replicon translation/replication. For instance, the dermal fibroblasts had the lowest transfection efficiency, which was expected due to their primary-like origins, but with the dLuc replicon, exhibited high replication levels. RD and BHK cells had some of the highest transfection efficiencies as well as very high replication levels, this may suggest that the luciferase produced in the dLuc CHIKV replicon experiment (Figure 3.1) may be partly due to high transfection efficiency.

As this project is based around understanding the role of nsP3, the ten cell lines were assessed for their use in western blotting for the detection of this particular protein (Figure 3.3).
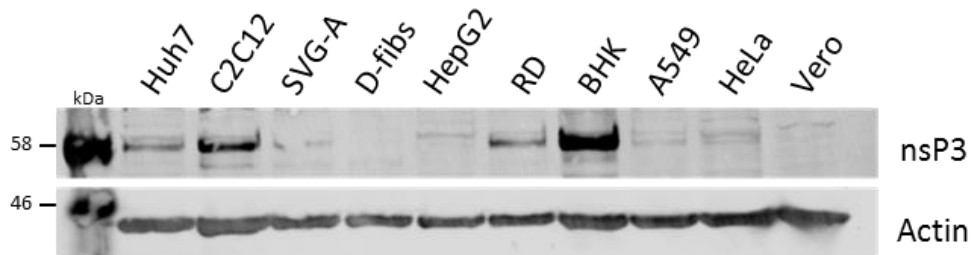
Figure 3.3 Western blot for nsP3 in mammalian cell lines transfected with CHIKV replicon.   Cells were transfected with wt (untagged) nsP3/SG-Fluc replicon, lysed at 24 hpt and blotted for nsP3.

On the western blot, nsP3 was clearly detectable in lysates from Huh7, C2C12, SVG-A, RD and BHK cells. Faint bands were observed in the lysates of HepG2, A549, HeLa and Vero cells. In contrast to the luciferase data, nsP3 was practically undetectable in dermal fibroblasts.

Next, all cell lines were transfected with a CHIKV replicon that contained a mCherry-tagged nsP3 in order to visualise the intracellular distribution of nsP3 via confocal microscopy (Figure 3.4 A and B). Three different organisations of nsP3 were observed: puncta, rings and rods. Although not all cells contained all these organisations. All lines contained puncta of nsP3. Only C2C12 and Huh7 cells produced ring organisations – though these were a small sub set of the nsP3-expressing cell populations. All cell lines contained rods except RD and HeLa cells. There was no apparent link between replication levels and type of nsP3 organisation in cells. At present, it is unclear what determines these different structures of nsP3 and what significance they represent in terms of CHIKV replication.

From the collective data, four physiologically relevant cell lines were selected as 'model' cell lines for their use in CHIKV research. C2C12 (myoblast) cells were overall, the physiologically relevant cell line that produced the highest levels of RNA replication, and high levels of nsP3, both on a western blot and via IF. Dermal fibroblasts also performed well, producing high levels of RNA replication and good expression of nsP3-mCherry but unfortunately, produced very low nsP3 signal on western blot, this could potentially be due to their significantly slower growth compared to the other cell lines used here. SVG-A (astroglia) cells

produced moderate levels of replication, and detectable nsP3 via western blot and IF. The liver cell lines Huh7 and HepG2 cells both were among the worst replicators of CHIKV RNA but overall, Huh7 cells had higher replication levels, higher nsP3 expression as shown by western blot and IF. Huh7 cells are also more practical to culture than HepG2 cells, which grow in large aggregates instead of monolayers. Huh7 cells were therefore chosen as the liver model cell line.
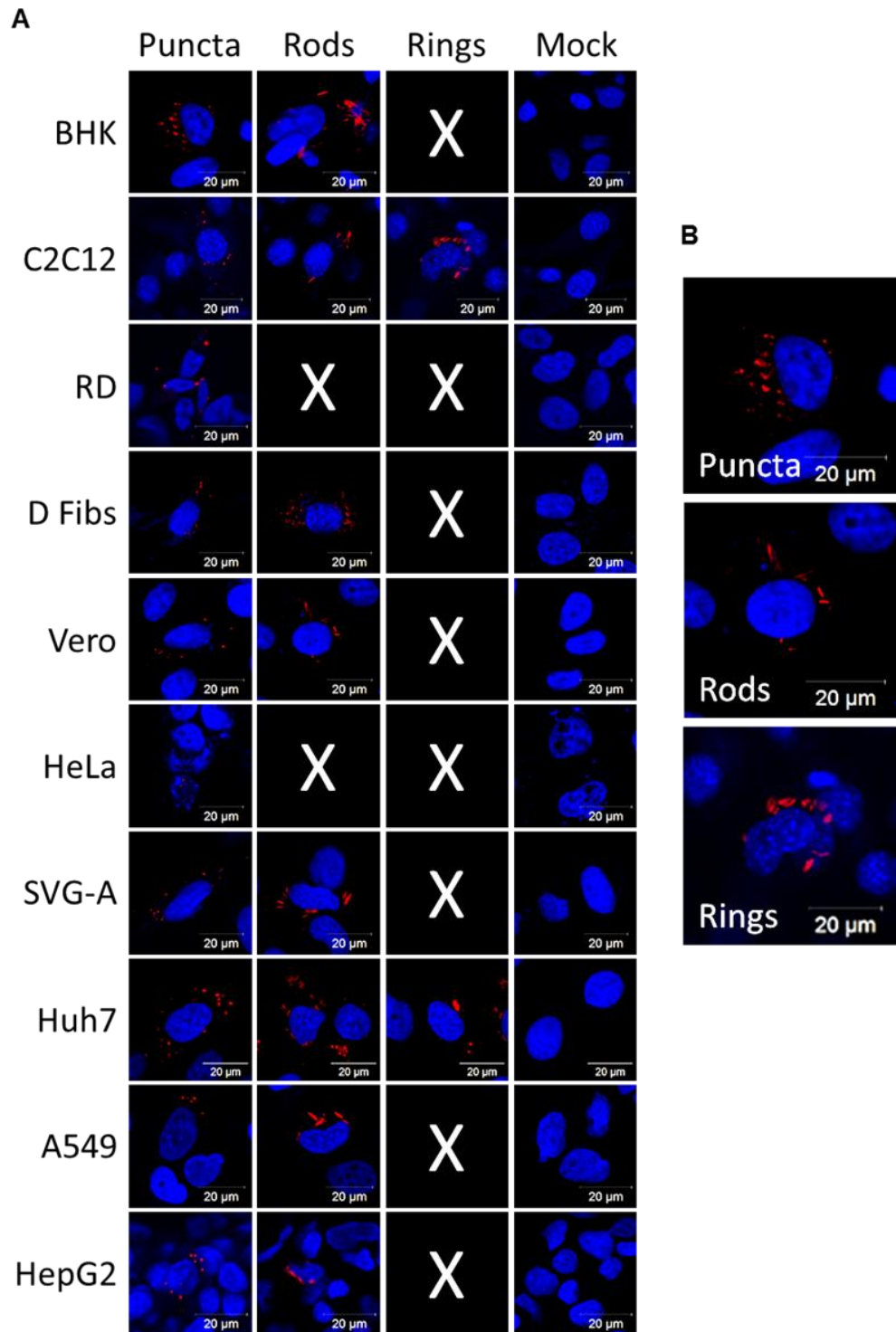
Figure 3.4 IF of nsP3-mCherry in mammalian cell lines. (A) All 10 mammalian cell lines were transfected with CHIKV replicon RNA containing an mCherry tagged-nsP3. Cells were fixed, DAPI stained and imaged using the LSM700 confocal microscope. Three cytoplasmic organisations of nsP3 were observed; puncta, rods and rings. An "X" indicates that the type of organisation was not observed for that particular cell line. (B) Large representative examples of the three types on organisation observed for nsP3.

3.2.1.2 Infectious virus

Before work could be initiated using infectious virus with the selected cell lines, optimisation of the production and titration of infectious CHIKV was required.

3.2.1.2.1 Production of virus stocks and titration by plaque assay

CHIKV has been routinely propagated and titrated using BHK cells (Gardner *et al.*, 2012; Lani *et al.*, 2015). It was therefore decided to use these cells for production of virus stocks. Using these cells, high titres of virus could be produced allowing for a wide range of MOIs to be utilised in experiments. Using this method, virus could be detected as early as 6 hpe, though at very low titres (data not shown). It was established through observations in the laboratory and personal communications from others (Prof Andres Merits) that, for production of virus stocks, virus should be collected at 24 hpe rather than 48 h. By 48 h, high levels of cell death has occurred due to CHIKV replication so for an additional day of incubation, there is little gain in virus titres but more cell debris is produced. Therefore all virus stocks were produced by electroporation of CHIKV RNA into BHK cells, and supernatant collected and titred at 24 hpe. Supernatant was briefly centrifuged to pellet cell debris, resulting virus-containing supernatant was removed, mixed, aliquoted and stored at -80 °C.

Throughout this project, virus titration was performed using plaque assay with BHK cells. Other have shown that CHIKV can be titred on Vero cells (Her *et al.*, 2015), however, since no issues were experienced using BHK cells for plaque assays in this project, there was no need for further optimisation using Vero cells. Initially, titration of CHIKV was performed in 6 well plates as shown in the example plaque assay in Figure 3.5.
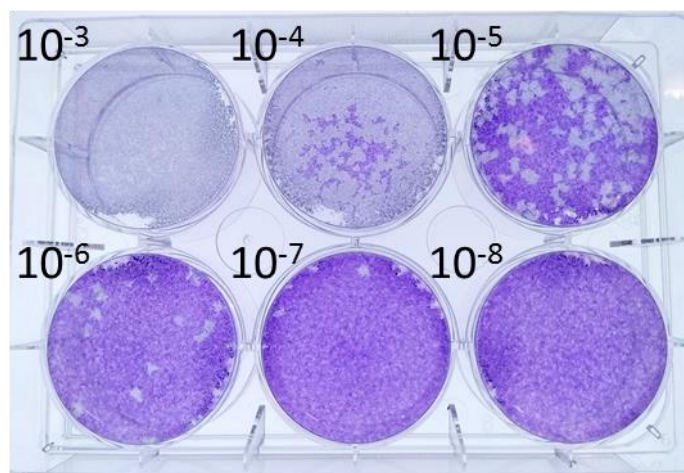
Figure 3.5 Example plaque assay of wt CHIKV. Plaque assay was performed by standard protocol, using dilutions of 10^{-3} to 10^{-8} to calculate wt CHIKV titres.

In an effort to increase productivity and reduce waste and reagents, plaque assays using 12 well plates were optimised (as described in methods section – 2.2.6). To ensure that results obtained using 12-well plaque assays did not differ from those using 6-well, a direct comparison of the two methods was performed using wt CHIKV. As shown by Figure 3.6, there was no significant difference between the resulting virus titres obtained using the two different methods.
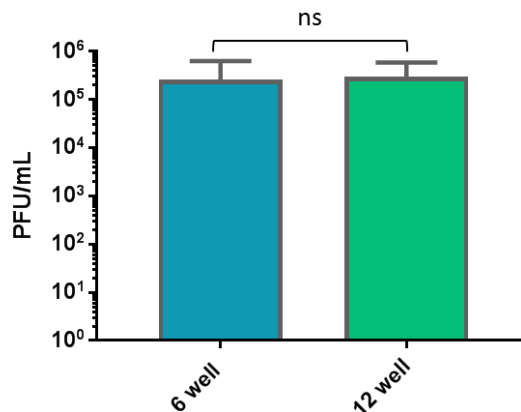
Figure 3.6 Direct comparison of CHIKV titres obtained using either 12 well or 6 well plate plaque assays. CHIKV was serially diluted in serum free media, of which 200 µL (for 6-well) or 150 µL (12 well) from the same dilution series were placed onto pre-plated, sub-confluent BHK cells. Normal plaque assay protocol was adhered to as described previously (n=2 for each condition, data analysed by paired T test).

As there were no significant differences between the results obtained using either 12 well or 6 well plaque assays, hereafter all plaque assays were performed in 12 well plates.

3.2.1.2.2 Mammalian cell lines for use with infectious CHIKV

To confirm the findings of the replicon-based assays using the selected cell lines, similar experiments were conducted using infectious virus. The virus construct used was derived from the East Central and South African (ECSA) strain that all the replicons used in this project were derived from (all kindly provided by Andres Merits). A virus stock was produced by electroporation of BHK cells with CHIKV genomic RNA and subsequently titrated on BHK-21 cells by plaque assay.

The four selected mammalian cell lines were infected at an MOI of 1 and 5 for 24 h. Virus production was quantified by plaque assay of the cell supernatant, and intracellular genomic RNA was quantified by qRT-PCR (Figure 3.7 A and B). Western blots for nsP3 was performed on these samples to confirm expression (Figure 3.7 C).
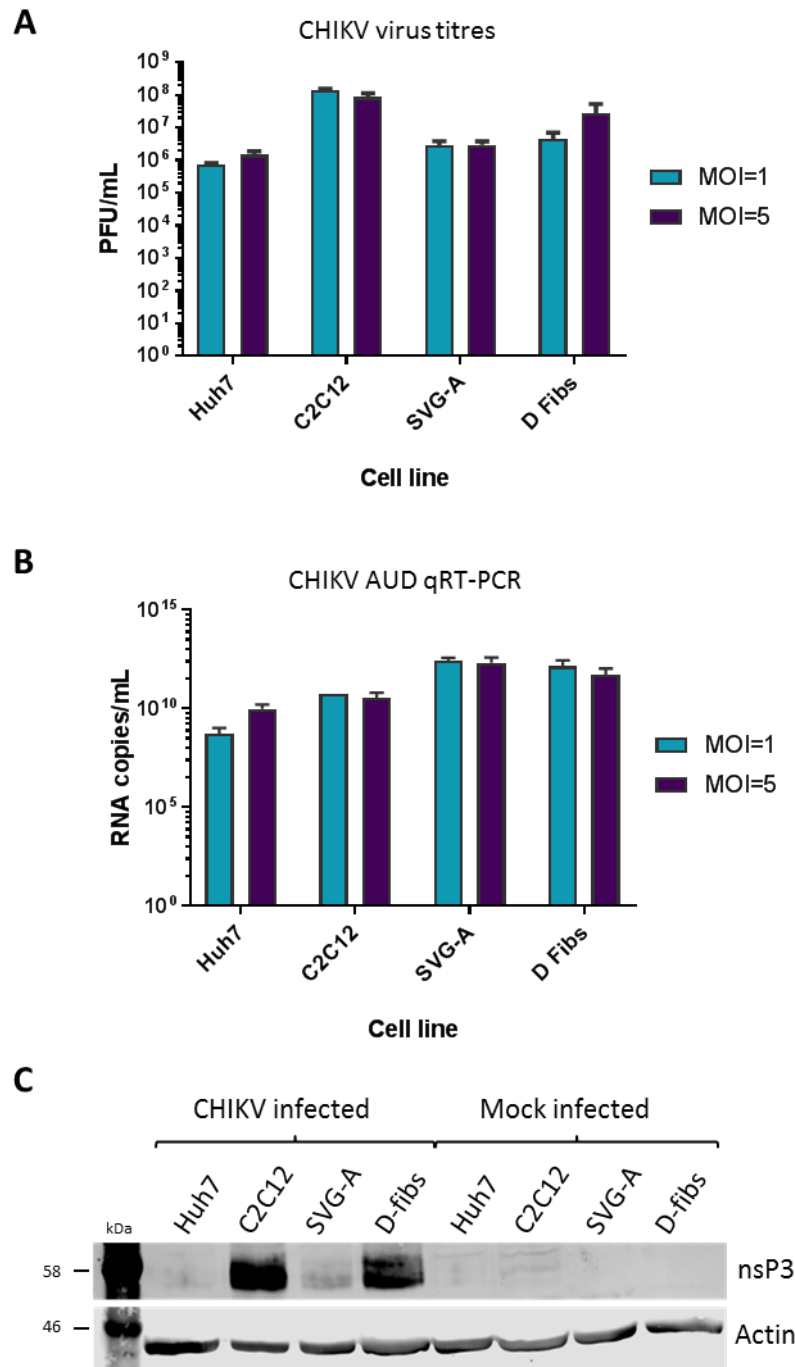
Figure 3.7 CHIKV infection of mammalian model cell lines. (A) Huh7, C2C12, SVG-A, and dermal fibroblasts (D Fibs) cells were infected, in triplicate, at MOIs of both 1 and 5. Cell supernatant was collected at 24 hpi and virus titred by plaque assay (n=3). **(B)** Corresponding qRT-PCR quantification of genomic CHIKV RNA in infected cells. Intracellular RNA was extracted using TRIzol reagent and RNA quantified using CHIKV nsP3-specific primers (n=3). **(C)** Western blots for nsP3 in infected cells lysed at 24 hpi.

Resulting virus titres of infected mammalian cells broadly reflect the replicon replication levels, with C2C12 producing the highest titres and Huh7 cells the lowest. However, all cell lines produced workable levels of virus over a 24 h period, with little difference between the different two MOIs. The RNA quantification broadly reflects the virus titres for each cell line. SVG-A cells appear to contain more intracellular genomic RNA copies relative to the virus titre, and C2C12 cells appear to have slightly less genomic copies compared to their high virus production. With virus infection, the nsP3 expression levels in C2C12, and for dermal fibroblasts in particular, were much higher than with the replicon (Figure 3.3), indicating the suitability of these cells for virus replication. This also highlighting the difference between using replicon and infectious virus, and indicates that caution is needed when interpreting data from replicon experiments when using them as a model for infection virus.

Similarly to the replicon experiments, cells were infected with CHIKV for 24 h then fixed, stained for nsP3 and DAPI and imaged by confocal microscopy (Figure 3.8). Unlike in the replicon cells, only two cytoplasmic forms of nsP3 were observed; puncta and rods. No ring like structures were found. Similarly to replicon, the vast majority of cells contained exclusively either rods or puncta, very few cells contained both forms of nsP3. The two cell lines that produced the highest titres; C2C12 and dermal fibroblasts, appeared to contain more rods per cell and more cells in the population that contained rods.
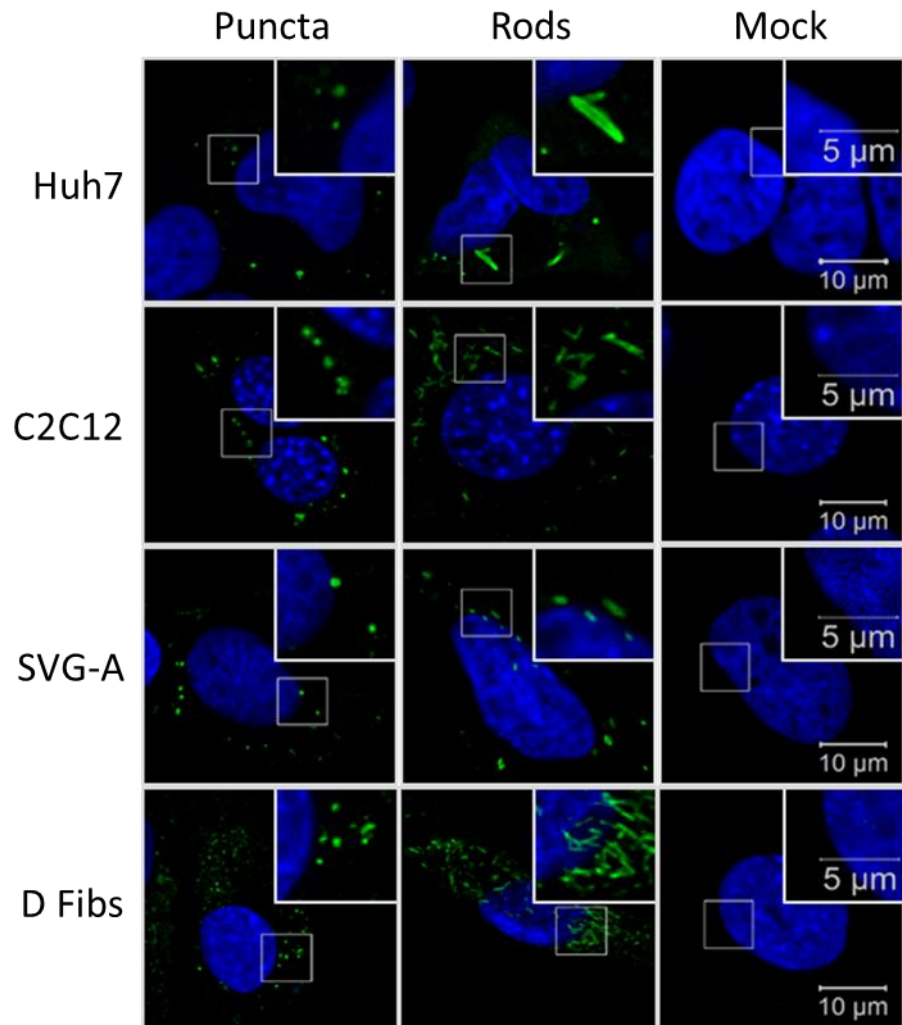
Figure 3.8 Confocal images of nsP3 in wt CHIKV infected mammalian cells.
Mammalian cell lines (Huh7, C2C12, SVG-A and Dermal fibroblasts)
were infected with an CHIKV , fixed at 24 hpi, stained for nsP3 and
DAPI, then imaged using the LSM700 confocal microscope. Two
different cytoplasmic structures of nsP3 were observed; puncta and
rods.

3.2.1.3 Differentiated cells

Both Huh7 (liver) and C2C12 (myoblast) cells can be differentiated to cells that
more resemble *in vivo* liver and muscle tissue respectively. To assess whether
these differentiated states would support higher levels of replication, both cell
lines were differentiated then transfected with the dLuc CHIKV replicon.

3.2.1.3.1 Differentiation of Huh7 Cells

Adding 2% DMSO to the culture medium of Huh7 cells arrests their growth, keeping cells in G_0 phase of the cell cycle. It also upregulates liver-specific genes such as albumin and cytochrome p450 (Choi et al. 2009). This model is considered more representative of liver tissue in vivo and is often used in early stage pharmaceutical testing. Huh7 cells have also been demonstrated to differentiate using human serum, which led to increased titres of hepatitis C virus (Steenbergen *et al.*, 2013).

To assess whether the differentiation status of Huh7 cells affected CHIKV replication, cells were differentiated by the addition of 2% DMSO to complete media for 7 days (replacing the media when necessary), then transfecting the differentiated cells with the dLuc CHIKV replicon over a 48 h time period, alongside non-differentiated Huh7 cells. For the Huh7 cells, there is a clear morphological difference between undifferentiated and differentiated cells. Differentiated hepatocytes form large rafts of confluent epithelial-like cells that have higher levels of albumin and CYP3A4 (a cytochrome p450 enzyme), as shown by Figure 3.9 A and B respectively indicating that these differentiated cells more closely represent liver tissue *in vivo* than Huh7 cells.
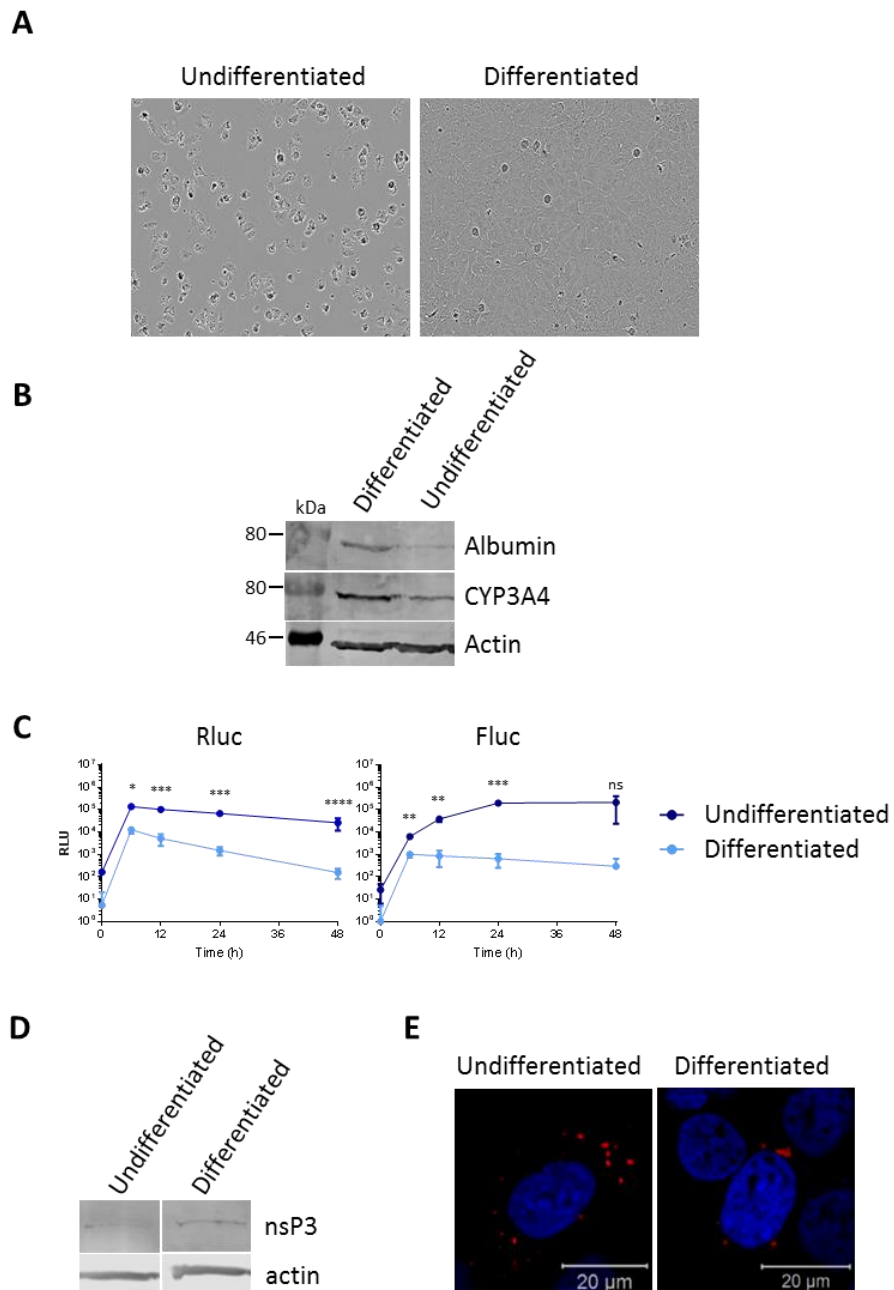
Figure 3.9 Differentiation of Huh7 cells and transfection with the CHIKV replicon. Huh7 cells were differentiated via addition of DMSO to complete media. (A) Bright field image demonstrating the morphology of differentiated cells compared to Huh7 cells maintained in complete culture medium. (B) Western blot for albumin and Cytochrome P450 3A4 (CYP3A4), is more highly expressed in differentiated cells compared to undifferentiated cells. (C) Both Huh7 cells and differentiated hepatocytes were transfected with CHIKV dLuc replicon RNA, cells were lysed at indicated time points and luciferase assayed. Data analysed by parametric T-test. (D) Western blot of nsP3 in transfected differentiated and undifferentiated cells, 24 hpt. (E) Confocal images of Huh7 and differentiated cells transfected with CHIKV replicon expressing an mCherry-tagged nsP3.

When transfected with the dLuc-CHIKV-SGR, the differentiated cells have greatly reduced translation and replication throughout the time course, when compared to undifferentiated Huh7 cells (Figure 3.9 C and D). The cytoplasmic distribution of nsP3 differs between the undifferentiated and differentiated cells (Figure 3.9 E). In the majority of undifferentiated Huh7 cells, nsP3 is arranged in small puncta found throughout the cytoplasm, whereas in the differentiated cells, nsP3 tends to form fewer, larger puncta that are mostly perinuclear. Though, again, it unclear what these differences in nsP3 distribution represent in terms of CHIKV replication.

3.2.1.3.2 Differentiation of C2C12 Cells

For C2C12 cells, reducing the serum in the media to 2% FBS (rather than 20%) induces the myoblasts to form myotubes, forming a similar organisation to muscle tissue in vivo (Lawson and Purslow, 2000; Burattini *et al.*, 2004). This serum depletion has been shown to induce the expression of insulin-like growth factors, suppresses proliferation and promotes differentiation (Yoshiko *et al.*, 2002).
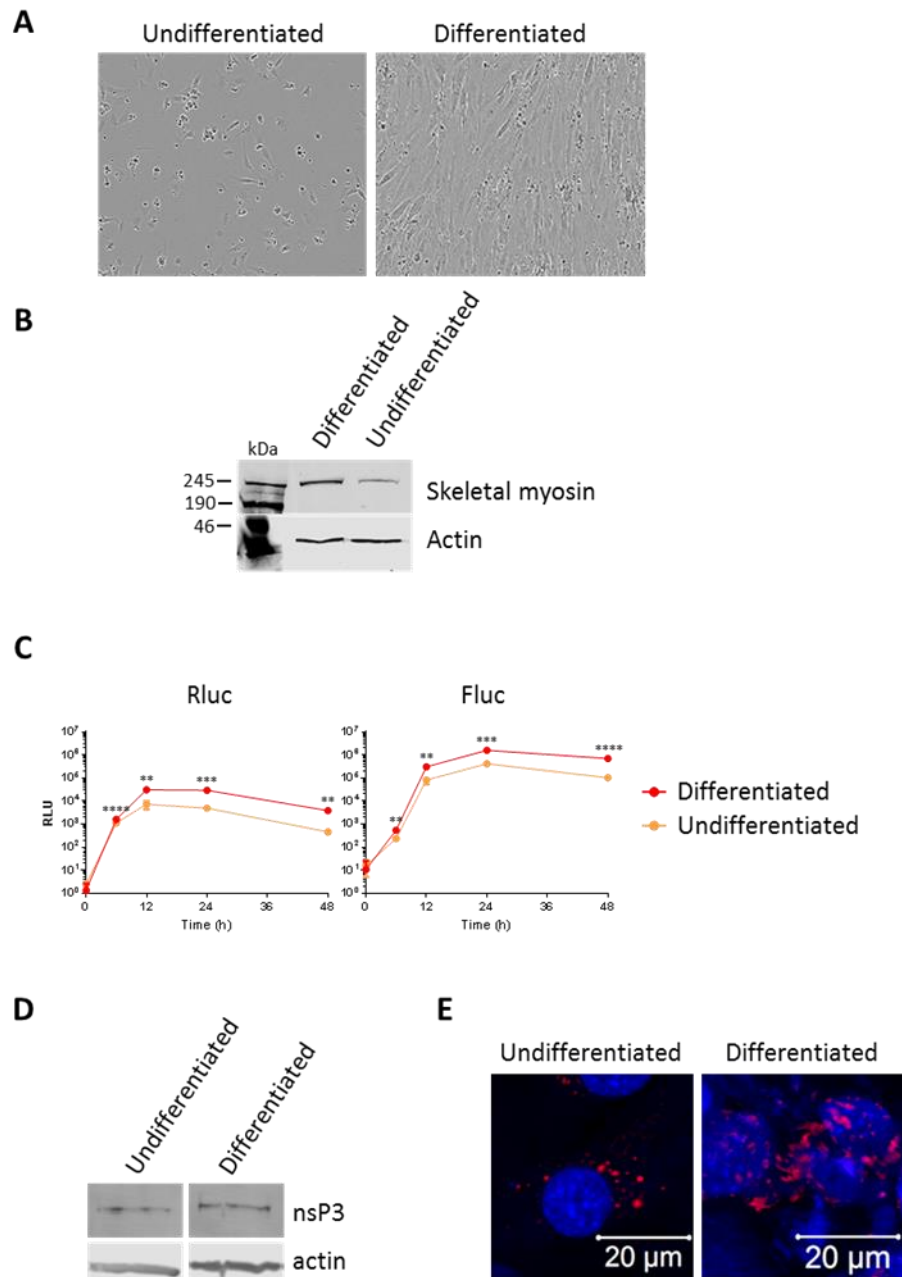
Figure 3.10 Differentiation of C2C12 cells and transfection with the CHIKV replicon. C2C12 cells were differentiated via serum starvation. (A) Bright field image showing the different morphology of differentiated cells compared to C2C12 cells maintained in complete culture medium (undifferentiated cells). (B) Western blot for skeletal myosin, a marker of skeletal muscle tissue, is highly expressed in differentiated cells (D) compared to undifferentiated (U). (C) Both differentiated and undifferentiated C2C12 cells were transfected with dLuc replicon RNA. Cells were lysed at indicated time points and luciferase assayed. Data analysed by parametric T-test. (D) Western blot of nsP3 in undifferentiated (U) and differentiated (D) transfected cells at 24 hpt. (E) Confocal images of C2C12 and differentiated cells transfected with CHIKV replicon RNA containing an mCherry-tagged nsP3.

Differentiated C2C12 cells form very distinct, multinucleated myotubes, demonstrated in the bright field images in Figure 3.10 A, with upregulated skeletal myosin, a marker of muscle tissue (Figure 3.10 B) both indicate that these differentiated cells are more representative of muscle tissue in vivo compared to C2C12 cells. In the differentiated myotubes, the CHIKV replicon exhibits significantly higher levels of RNA replication (Fluc), approximately 7 fold higher than undifferentiated cells by the 48 h time point, despite little detectable difference in nsP3 by western blot (Figure 3.10 C and D respectively). The cellular localisation of nsP3 also varies between transfected differentiated and undifferentiated cells (Figure 3.10 E). In undifferentiated C2C12 cells, nsP3 forms distinct puncta or rod-like organisations throughout the cytoplasm. In contrast, nsP3 in differentiated cells appears less organised with less distinction between the clusters of nsP3 which have no clear shape or organisation. However, the IF data is inherently unclear as differentiated C2C12 form large multi-nucleated cells which lack their own structure which can make it difficult to determine cellular components such as the nucleus or the cytoplasmic membrane.

3.2.2 Mosquito cell lines

As CHIKV is an arbovirus, it is important not only to study the virus in the human host but also in the mosquito vector. CHIKV is transmitted by the *Aedes* species of mosquito – primarily the *Aedes aegypti* but more recently, the *Aedes albopictus.* The virus is acquired by mosquitoes through a blood meal from a viremic host. CHIKV initially replicates in the cells of mid-gut before disseminating to all organs of the insect, including the salivary glands where it then goes on to infect upon future blood meals upon naïve human hosts (Vega-Rua *et al.*, 2014).

A popular strategy of controlling the spread of arboviruses is to target the vectors (Alphey, 2014). If achieved, this would mitigate the need for vaccines or antivirals as, since CHIKV cannot be transmitted from human to human, successful control of the vector would prevent human disease. Therefore it is crucial to understand the pathology of CHIKV in mosquito cells.

Here we were able to evaluate four mosquito cell lines for their use with CHIKV, and specifically nsP3. A20 and Aag2 cells are derived from *Aedes aegypti* and U4.4 and C6/36 cells are derived from *Aedes albopictus.* All four lines are derived from embryonic cells of the stated species. C6/36 cells have been commonly used in viral research for many years as they are permissible to a wide range of arboviruses. However, these cells have recently been shown to have an ineffective RNAi system, a key anti-viral pathway of insects, resulting from a single nucleotide deletion in the coding region of Dicer2 producing a frame shift and a premature stop codon, rendering the resulting protein non-functional (Brackney *et al.*, 2010; Miller *et al.*, 2018). Dicer2 is active in U4.4 cells however, and its activity has been shown to restrict viral replication of Bunyamwera virus (Szemiel *et al.,* 2012). Aag2 cells been shown to be persistently infected with cell fusing agent virus (CFAV), an insect specific flavivirus (Zhang *et al.*, 2017), this infection was detected in the original cell line and is known to be able to transmit vertically, so it is assumed that CFAV was present in the larval cells used to form the cell line and therefore is present in all resulting Aag2 lineages (Stollar and Thomas, 1975).

3.2.2.1 Replicon

Much like with the mammalian cell lines, initially the four mosquito cell lines were transfected with the dual luciferase CHIKV replicon to assess their ability to translate and replicate the replicon (Figure 3.11).
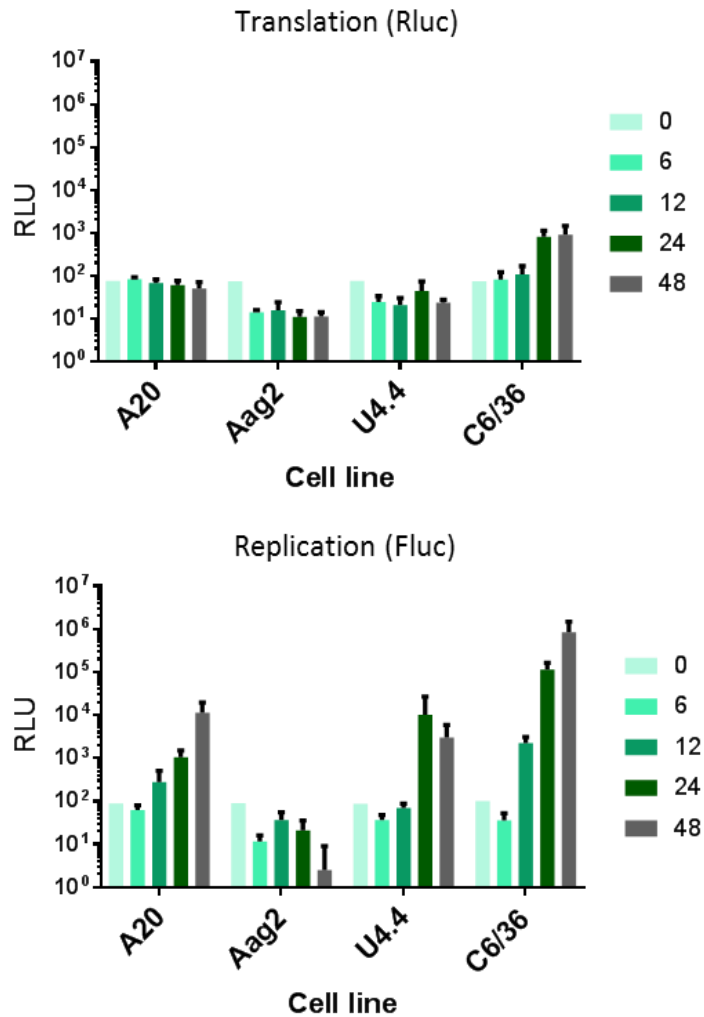
Figure 3.11 Transfection of mosquito cell lines with CHIKV dLuc replicon RNA. Aag2, A20 (both *Aedes aegypti*), U4.4 and C6/36 (both *Aedes albopictus*) cells were transfected with CHIKV dLuc replicon RNA. Cells were lysed over a 48 h period and luciferase assayed. Rluc is present in the VR of nsP3 and indicates translation of the non-structural proteins. Fluc is present in the subgenomic region of the replicon, indicating that RNA replication has occurred.

Renilla luciferase was detected in three of the four cell lines, indicating that the replicon was translationally- competent in all cells except in Aag2 cells, which exhibited luciferase signal below the detectable level ($<5 \times 10^2$ RLU) throughout the time course. Despite their different origins, A20 and U4.4 cells exhibited similar levels of translation and RNA replication of the replicon over the time course, though U4.4 cells had peak firefly luciferase signal at 24 h whereas A20 cells peaked at 48 hpt. C6/36 cells had much higher translation and replication, which was as expected due to their dysfunctional RNAi system.

Western blots for nsP3 with mosquito cell lysates proved to be problematic due to high levels of cross reactivity with the antibodies to many mosquito proteins (Figure 3.12). Initially, all four mosquito cell lines were transfected with an untagged-nsP3 replicon, but the nsP3 antibody was cross reactive with proteins of many sizes, but particularly with one ~58 kDa, the same size as nsP3, – which is present in roughly equal intensities in both the transfected and mock samples. Many alterations to the method were tried e.g. different blocking buffers, different/longer wash steps, but the contaminating 58 kDa band was always present. The blot shown in Figure 3.12 A is representative of the various attempts of blotting using nsP3 for mosquito cell lysates. The nsP3 antibody used here is a polyclonal antibody, produced in-house so it was not surprising that it was highly cross reactive. In order to rectify this, a flag-tagged nsP3 replicon was utilised so that a commercial, monoclonal flag-tag antibody could be used to detect nsP3. Though this did produce blots with far fewer non-specific bands, it still cross reacted with a protein around 58 kDa, so nsP3 was undetectable using this method.
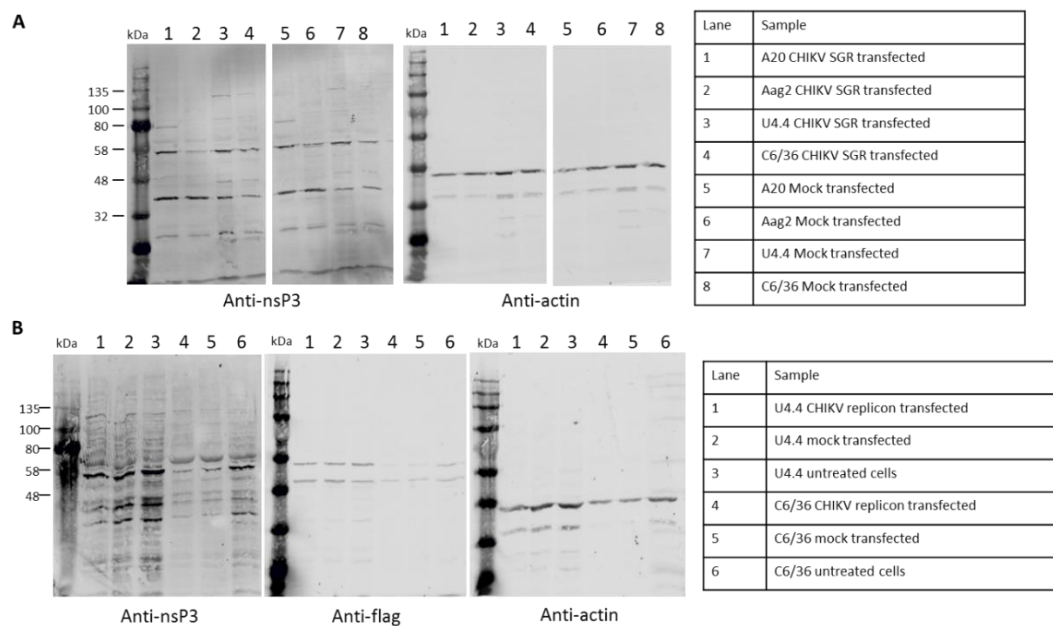
Figure 3.12 Western blots for various proteins in mosquito cells. **A. Mosquito cell lines were transfected using the CHIKV Fluc SGR (with untagged nsP3), cells were lysed at 24 hpt and western blot performed for nsP3 (58 kDa) and actin (42 kDa). B. U4.4 and C6/36 cells were transfected with nsP3-Flag replicon and cells were lysed at 24 hpt. Western blots were performed using both anti -nsP3 and -Flag antibodies to detect nsP3 as well as anti-actin as a loading control.**

The mosquito cell lines were then transfected with the nsP3-mCherry replicon for 24 h then fixed, DAPI stained and imaged by confocal microscopy (Figure 3.13).
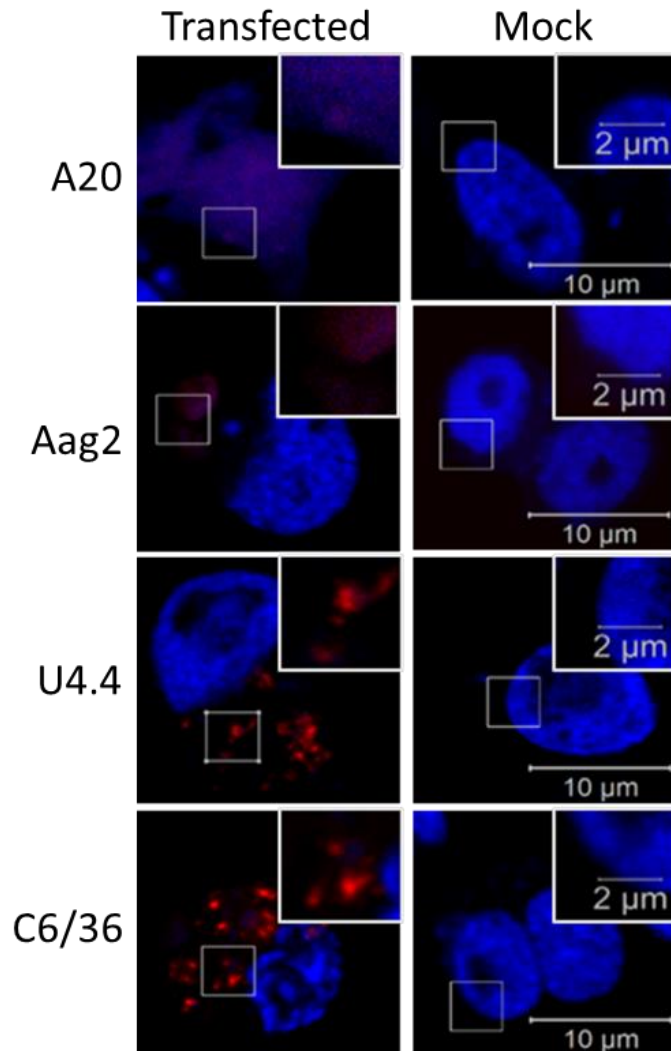
Figure 3.13 Confocal images of mosquito cell lines transfected with nsP3-mCherry replicon. A20, Aag2, U4.4 and C6/36 cells were transfected with nsP3-mCherry/SG-Gluc-SGR RNA.

In the transfected U4.4 and C6.36 cells, nsP3 formed distinct puncta in the cytoplasm. However, both A20 and Aag2 cells exhibited very different organisations of nsP3. In Aag2 cells, nsP3 was very diffuse in the cytoplasm with no apparent organisation. All nsP3-positive A20 cells observed had diffuse and

blebbing nuclei with diffuse nsP3, indicating that the replicon, or perhaps the transfection reagent, was toxic to the cells.

From the collective replicon data, the use of A20 and Aag2 cells was abandoned due to the inability of the Aag2 cells to support replication of the replicon and the difficulty experienced imaging nsP3 in both Aag2 and A20 cells.

3.2.2.2 Infectious Virus

To confirm the results from the replicon work and assess the ability of the mosquito cells to produce virus, the U4.4 and C6/36 cells were infected with the ECSA virus at MOIs of both 1 and 5 for 24 h, the supernatant was collected and titred by plaque assay (performed on BHK cells, Figure 3.14).

The titres produced by both cell lines was reflective of the replicon experiments with C6/36 cells producing more virus than U4.4 for both MOIs. However both cell lines exhibited similar levels of intracellular genomic CHIKV RNA as indicated by the qRT-PCR.
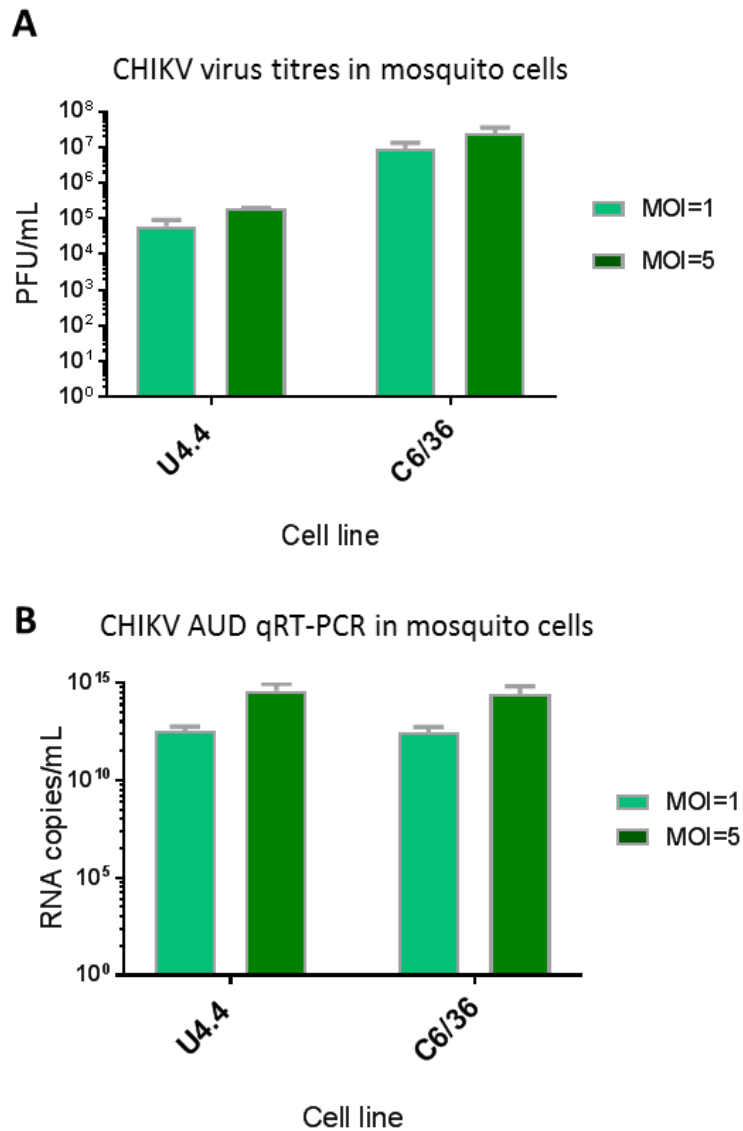
Figure 3.14 CHIKV infections of model mosquito cell lines. U4.4 and C6/36 cells were infected at an MOI of 1 or 5 for 24 h. (A) Supernatant was collected and titred by plaque assay (n=3). (B) Intracellular RNA was extracted from the infected cells using TRIzol and CHIKV genomic RNA was quantified by qRT-PCR using primers specific for nsP3 (n=3).

Since the nsP3 antibody proved to be unreliable on western blots with mosquito cells, to image nsP3 in infected cells we opted to use virus expressing ZsGreen tagged nsP3. Cells were infected for 24 h, fixed, DAPI stained and imaged via confocal microscopy (Figure 3.15).
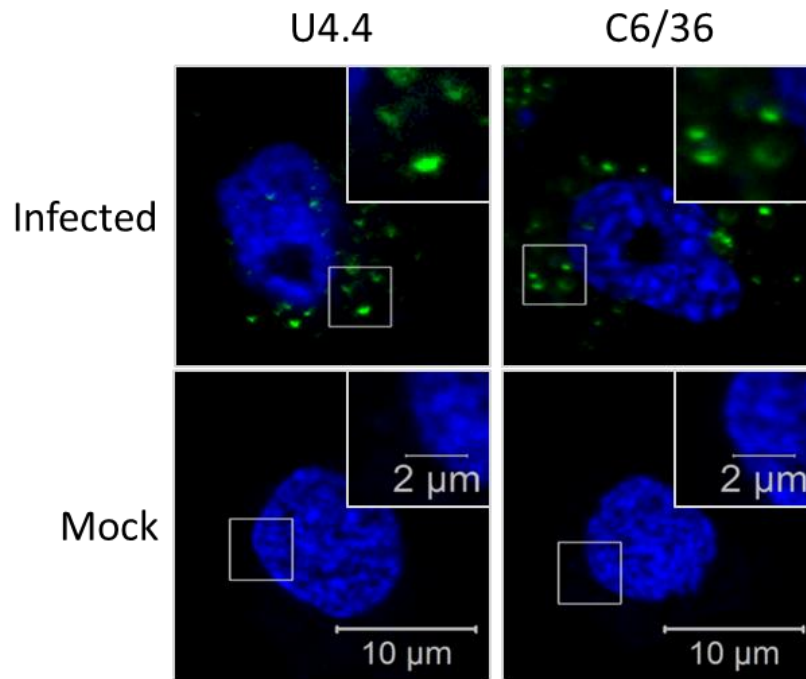
Figure 3.15 Confocal images of mosquito cell lines infected with nsP3-ZsGreen virus. Cells were infected for 24 h, fixed, DAPI stained and imaged using the LSM700 confocal microscope.

Infected mosquito cells had similar nsP3 expression to the cells transfected with the replicon. Both mosquito cell lines exhibited cytoplasmic puncta of nsP3 with a slightly less distinct appearance than the puncta observed in mammalian cells. For both cell lines, nsP3 positive cells contained many puncta with a range of puncta sizes observed throughout the cytoplasm.

3.3   Discussion

3.3.1   Mammalian cells

At the start of this project, it was unclear which cell lines should be utilised in order to study the molecular virology of CHIKV. In the literature, a range of cells have been used,, such as Vero, BHK and HeLa cells, though none of these are physiologically relevant to CHIKV infection *in vivo*. Therefore, a range of cell lines, both physiologically relevant ones and ones previously used in the literature were evaluated for their ability to replicate the CHIKV replicon and assayed for their expression of nsP3 via IF and western blot.

From the replicon data, multiple cell lines fulfilled the role of being physiologically relevant whilst also supporting replication of the CHIKV replicon. Both muscle cell lines (C2C12 and RD) exhibited high levels of replicon replication and nsP3 expression. C2C12 cells were selected over RD as they exhibited higher replicon replication, can be differentiated to a state closely resembling muscle tissue and are widely used in the field of muscle biology as a model for muscle development and differentiation (Burattini *et al.*, 2004). RD cells, derived from a rhabdomyosarcoma are considered the model cell line for the study of the disease (Hinson *et al.*, 2013) as well as for the study of enteroviruses (Perez-Ruiz, 2003). For the liver cell lines, Huh7 and HepG2 cells were assessed. Though neither of these cell lines produced particular high luciferase signal when compared to the full panel, Huh7 cells were selected as the model liver cell line as they had the higher replicon replication of the two liver cell lines and had detectable nsP3 via western blot and IF. Huh7 cells can also be differentiated to better mimic liver tissue *in vivo*. Both dermal fibroblasts and SVG-A (astroglia) cells were selected as model cell lines as they were the only cells of their respective tissue type tested. Both cell lines did support replicon replication and expressed nsP3 well. These four cell lines were then further assessed using infectious virus, and all four produced high titre virus with good expression of nsP3 as shown by western blot and IF. C2C12 and dermal fibroblasts both produced the highest titres and nsP3 expression levels. Huh7 and SVG-A cells performing similarly, both producing moderate virus titres. This reflects the signals seen in the replicon luciferase assays.

The ability to differentiate both C2C12 and Huh7 cells may be useful in future CHIKV experiments. Differentiation of these cells are commonly used; differentiated hepatocytes are commonly used in early-stage pharmaceutical testing (Guo *et al.*, 2011), and differentiated C2C12 cells are used to study muscle development (Erbay and Chen, 2001). Other studies have shown that differentiated Huh7 cells were more permissive to infection and produced higher titres of hepatitis C virus, which is thought to be due to the more cells mimicking liver tissue more closely than undifferentiated Huh7 cells (Sainz and Chisari, 2006). To see whether this was the same of CHIKV, both cell lines were differentiated for seven days prior to transfection with the dual luciferase CHIKV replicon. Both cell lines demonstrated they were more representative of their corresponding i*n vivo* tissue both by cell morphology and the upregulation of certain markers that are highly abundant in the *in vivo* tissue (albumin and CYP3A4 for liver, and skeletal myosin for muscle tissue). Differentiated C2C12 cells supported higher levels of replicon replication than undifferentiated cells which was as expected. Surprisingly, however, differentiated Huh7 cells produced a lower luciferase signal than the undifferentiated cells. Though there was little detectable difference in nsP3 expression by western blot, the IF shows that there were far fewer puncta of nsP3 per cell though these tended to be larger. This was surprising as we hypothesised that a more physiological-like model of the liver, an organ that CHIKV preferentially replicates in, would support higher levels of CHIKV replication. However, it may be that since the cells are in growth arrest, this may slow down the replication cycle of CHIKV. Though there has been little research into CHIKV replication and the cell cycle, studies have shown that CHIKV is able to replicate in serum-starved non-dividing cells (Sourisseau *et al.*, 2007) and, in early infection, CHIKV downregulates cell cycle proteins such as CDK1 (Thio *et al.*, 2013). It may also be that despite differentiated cells being more representative of liver tissue, it may still be lacking certain factors that CHIKV requires to efficiently replicate. It is possible since differentiated Huh7 cells produce 'rafts' of cells with tight cell-cell junctions, it may be limiting the transfection process, reducing the amount of RNA that enters the cells. Alternatively, it may just be that the slower replication of the replicon in these differentiated cells is more representative of the *in vivo* infection. Ideally,

infectious virus could be used to infect the differentiated cells which would be more representative of *in vivo* infection and would remove the issue of transfection efficiency.

Other cell lines that have been previously used for CHIKV research in the literature had surprising results. In the replicon luciferase assay, both Vero and HeLa cells supported replication to only moderate levels, with dramatically reduced signal at 48 hpt. The IF data for both these cell lines showed blebbing nuclei in nsP3-positive cells indicating that the replicon is very toxic to these cells, which would explain why both cell lines had low luciferase signal at later time points. There would appear to be no apparent advantage to using these cell lines in CHIKV research, particularly in comparison to the others tested here. In contrast, BHK cells, which have been used extensively in virological research, including for CHIKV, produced the highest luciferase signals throughout the luciferase assay and expressed nsP3 to high levels as shown by IF and western blot. It was therefore sensible to use these cells for virus production and plaque assay as others have previously (Gardner *et al.*, 2012; Lani *et al.*, 2015). Though many other groups have used Vero E6 cells for virus propagation and titre (Gokhale *et al.*, 2015; Her *et al.*, 2015), BHK cells were used initially in this project and had no issue with these cells for these purposes so felt no need to try alternative methods.

The data obtained for A549 cells is in agreement with the literature where studies have shown that CHIKV is able to bind and enter A549 cells but is unable to effectively replicate in these cells (Solignat *et al.*, 2009). The mechanism of inhibition and the stage in the virus lifecycle at which inhibition occurs is currently unknown, but the replicon and IF data shows that the replicon can be successfully translated in A549 cells to produce non-structural proteins, and a limited amount of RNA replication can occur, as indicated by signal at the 6 and 12 hpt time points, but this signal reduces at 24 and 48 h. The reduction in signal at later time points could suggest that the inhibition is due to an innate immune response, as A549 cells are known to elicit a comprehensive innate immune response upon viral infect (Hartman *et al.,* 2007; Devhare *et al.*, 2013), though this was not further investigated in this project.

It is worth noting that in this project although it would have been ideal to trial a much wider range of physiologically relevant cell lines, there were limitations to the cell lines that were available. The limitations of the cell lines used are also noteworthy. For instance, C2C12 cells are mouse derived and mice are not natural hosts of CHIKV. Though mice can be successfully infected in the lab environment and are frequently used as models for the disease (Teo *et al.*, 2013). SVG-A cells are astroglia-derived cells. Experimentally, infected mice have demonstrated glial infection which results in an illness similar to that shown in CHIKV infected humans with neurological-complications (Das *et al.*, 2015). However, there is evidence that the neuronal cells are also infected and unfortunately we were unable to obtain a neurone-derived cell line for this project. Immortalised liver cell lines are widely known to be problematic as most do not express similar proteomic profiles when compared to hepatocytes *in vivo.* However, immortalised liver cell lines are much easier to culture and more widely available than primary liver cells (Choi *et al.*, 2009). Primary liver cells are particularly problematic as they rapidly de-differentiate in culture, therefore Huh7 cells are commonly used in hepatitis research despite their drawbacks. The dermal fibroblasts used here were a primary cell line from a healthy donor that were transformed in-house. They are physiologically ideal due to their origin however, since they are not a well-used established cell line, it is unclear what their expression profile is like and whether the process of transformation had any unintended consequences such as disrupting a gene or promotor region.

3.3.2 Mosquito cells

As CHIKV is an arbovirus, transmitted by the *Aedes* species of mosquito, it is important to study the virus in mosquito cells as well as mammalian cells. Four mosquito cell lines were available to us; A20, Aag2 (both are derived from the *Aedes aegypti*), and U4.4 and C6/36 cells (both *Aedes albopictus*). Again, all cells were transfected with the CHIKV replicon to assess their ability to replicate CHIKV RNA. All cell lines were able to translate and replicate the replicon except Aag2 cells where signal was below detectable levels throughout the time course. This may be due to their persistent infection with CFAV – potentially activating the cells' anti-viral response which could restrict CHIKV replication from the initial

transfection (Zhang *et al.*, 2017). From this data, Aag2 cells were dismissed as a usable cell line for CHIKV research.

U4.4 and A20 cells exhibited very similar levels of replication from the luciferase assay but behaved very differently when looking at nsP3 via IF. U4.4 cells exhibited defined puncta of nsP3 whereas the only nsP3 positive A20 cells had very diffuse nsP3 with no intact nuclei. This implies that either the replicon or transfection process is toxic to these cells. Due to this, A20 cells were also discarded for the study of CHIKV.

C6/36 cells have been extensively used in virological research, probably due to their inactive RNAi system allowing them to produce high titres of virus (Brackney *et al.*, 2010; Miller *et al.*, 2018). In the replicon experiment, the C6/36 cells produced the highest signal, which reflects the literature. These cells also produced defined puncta of nsP3, as shown by IF, making them a useful cell line for CHIKV research.

U4.4 and C6/36 cells were further evaluated with infectious virus. Both produced high titres of virus, again with C6/36 cells producing approximately 2-log higher titres than U4.4 cells. However, both cell lines appear to have similar levels of genomic RNA as shown by the qRT-PCR. This implies that RNA replication may not be the limiting factor in the production of virus in these cell lines.

3.3.3 Chapter summary

Here, a range of physiologically relevant cell lines have been demonstrated for their usefulness in the study of CHIKV, and particularly for nsP3. These provide a range of appropriate cell lines to choose from when undertaking experiments, using both replicon and infectious virus, to investigate the function of the CHIKV nsP3 macro domain. These experiments are described in the following chapters where initially mutations were generated in the RNA/ADPR binding pocket of the nsP3 macro domain, in both replicon and infectious virus. The phenotypes of these mutants were assessed in several cell types to have a more comprehensive understanding of the function of the macro domain in different mammalian tissue types as well as mosquito cells. This data has been published in an open-access journal, available for other researches to access and use for their own work (Roberts *et al.*, 2017).

Chapter 4 Macro domain mutants

4.1 Introduction

Now that appropriate cell lines had been optimised for use with the CHIKV replicon and infectious system, attention could be turned to the specific focus of this project: determining the function of the CHIKV nsP3 macro domain.

The three-dimensional structure of the CHIKV macro domain in complex with either ADP-ribose or RNA had been previously solved (Malet *et al.*, 2009, see Figure 4.1). This study highlighted the binding pocket, similar to that of other macro domains, which is only partially shared by ADP-ribose and RNA nucleotides.
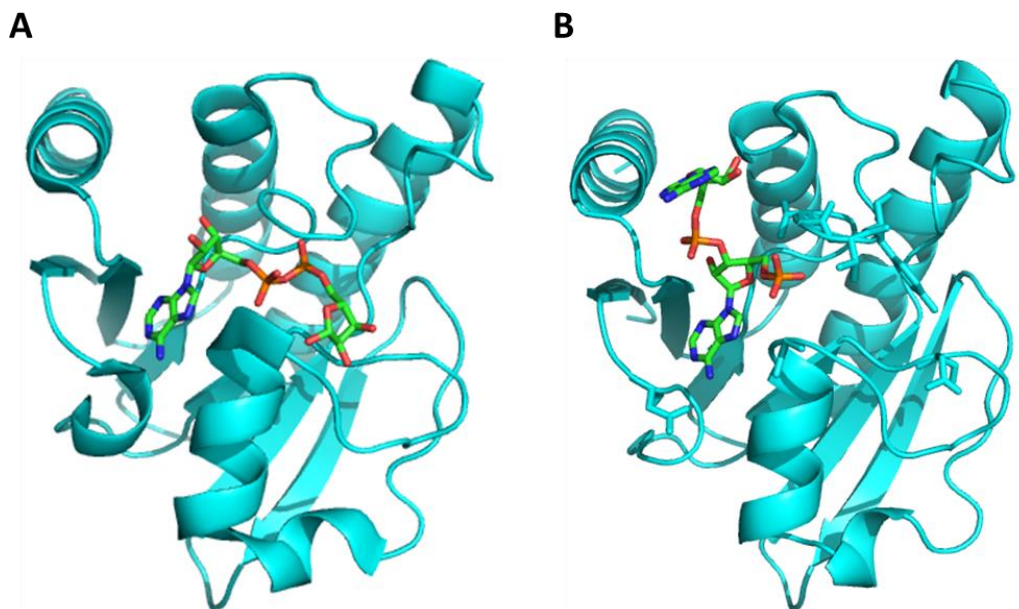
Figure 4.1 The CHIKV nsP3 macro domain in complex with ADP-ribose (A) and RNA (two adenosine bases) (B) adapted from PBD 3GPO and 3GPQ respectively (Malet *et al.* 2009).

The biochemical function and capabilities of the CHIKV macro domain have been assessed previously. The CHIKV macro domain has been shown to be capable of binding poly-ADP-ribose (PAR) and mono-ADP-ribose (MAR). Mutagenic analysis of the CHIKV macro domain has revealed that the aspartic acid residue at position 10 is crucial for ADPR binding, as substitution for alanine obliterates ADPR binding (Malet *et al.*, 2009).

It has also been demonstrated that the CHIKV nsP3 macro domain possesses ADP-ribose 1"-phosphate phosphatase activity, to similar levels as the VEEV nsP3 macro domain, although the macro domain of SFV does not possess this activity as it was below the limit of detection (Egloff *et al.*, 2006; Malet *et al.*, 2009). Egloff *et al.* suggest that ADP-ribose 1" phosphatase activity may have little relevance *in vivo* as macro domains (both cellular and viral) are not closely related to any other known phosphatases. Furthermore, viruses such as SFV replicate with a macro domain that does not exhibit this activity, suggesting that ADP-ribose 1"-phosphate phosphatase activity is a dispensable function that contributes little to virus replication.

More recently, the CHIKV macro domain has been shown to possess hydrolase activity where MAR is removed from aspartate and glutamate residues *in vitro* (McPherson *et al.*, 2017). In the same publication, McPherson *et al.* generated a panel of macro domain mutants and assessed their ability to bind and hydrolyse MAR *in vitro* and their ability to produce virus in cell culture and mice. From these experiments, it was concluded that binding and hydrolysis of MAR is essential for CHIKV replication in cell culture and for virulence in mice.

Further investigation from the same research group revealed that CHIKV infection increases the general level of ADP-ribosylation in cells and that the ability of cells to MARylate proteins was required for optimal CHIKV replication (Abraham *et al.*, 2018). In addition, this publication demonstrated that defects in both the hydrolase and ADPR-binding capabilities of the CHIKV macro domain resulted in diminished virus replication but when only the hydrolase function was reduced, initial stages of replication occur much like wt, such as expression of the nsPs and the formation of replicases. However, with the hydrolase-defective macro domain, protein synthesis was more rapidly shut off, replication complexes become inefficient and virus production was delayed.

Despite these recent advances in the biochemical properties of the domain, the precise function of the macro domain in CHIKV replication and lifecycle are still unclear.

4.1.1 Aims

In this chapter, the aim was to define the function of the CHIKV nsP3 macro domain in the virus lifecycle. To achieve this, a range of mutations were generated in the binding pocket of the CHIKV macro domain, based on the data available in the literature, and these mutants were assessed for their ability to replicate in a range of biologically-relevant cell lines.

4.2 Results

4.2.1 Generation of macro domain mutants

To determine the function of the macro domain, firstly a panel of substitutions were made individually in the ADPR binding pocket. To determine which residues to mutate, sequence alignments were performed on the nsP3 macro domain of CHIKV compared to other alphaviruses, and of the CHIKV macro domain compared to other viral macro domains such Rubella virus, SARS and HEV (Figure 4.2).

A

```
SINV    APSYRTKRENIADCQEEAVVNAANPLGRPGEGVCRAIYKRWPTSFTDSATETGTARMTVC    60
VEEV    APSYHVVRGDIATATEGVIINAANSKGQPGGGVCGALYKKFPESFDLQPIEVGKARLVKG    60
MAYV    APAYAVKRADIATAIEDAVVNAANHRGQVGDGVCRAVARKWPQAFRNAATPVGTAKTVKC    60
CHIKV   APSYRVKRMDIAKNDEECVVNAANPRGLPGDGVCKAVYKKWPESFKNSATPVGTAKTVMC    60
SFV     APSYRVKRADVATCTEAAVVNAANARGTVGDGVCRAVAKKWPSAFKGAATPVGTIKTVMC    60
        **:*  . *  ::*    *   ::****  *   * *** *: :::* :*       .*. : .

SINV    LGKKVIHAVGPDFRKHPEAEALKLLQNAYHAVADLVNEHNIKSVAIPLLSTGIYAAGKDR   120
VEEV    AAKHIIHAVGPNFNKVSEVEGDKQLAEAYESIAKIVNDNNYKSVAIPLLSTGIFSGNKDR   120
MAYV    DETYIIHAVGPNFNNTSEAEGDRDLAAAYRAVAAEINRLSISSVAIPLLSTGIFSAGKDR   120
CHIKV   GTYPVIHAVGPNFSNYSESEGDRELAAAYREVAKEVTRLGVNSVAIPLLSTGVYSGGKDR   120
SFV     GSYPVIHAVGPNFSATTEAEGDRELAAVYRAVAAEVNRLSLSSVAIPLLSTGVFSGGRDR   120
         :******:*    * *.: *  .*. :*  :.  . .***********::..:**

SINV    LEVSLNCLTTALDRTDADVTIYCLDKKWKERIDAALQLKE              160
VEEV    LTQSLNHLLTALDTTDADVAIYCRDKKWEMTLKEAVARRE              160
MAYV    VHQSLSHLLAAMDTTEARVTIYCRDKTWEQKIKTVLQNRS              160
CHIKV   LTQSLNHLFTAMDSTDADVVIYCRDKEWEKKISEAIQMRT              160
SFV     LQQSLNHLFTAMDATDADVTIYCRDKSWEKKIQEAIDMRT              160
        :  **. * :*:* *:* *.*** ** *:  :. .:  :
```

B

```
CHIKV   --------------------APSYRVKRM--DIAKNDEECVVNAANPRGLPGGGVCKA    36
SARS    ------EEPV-NQFTGYLKLTDNVAIKCVDIVKEAQSANPMVIVNAANIHLKHGGGVAGA    59
HEV     -------GPRRRLLHTYPDGS-----KVYAG--SLFESECTWLVNASNPGHRPGGGLCHA    46
Rubella ----------SDIVESYARAAGPVHLRVRNI--MDPPPGCKVVVNAANEGLLAGSGVCGA    48
                            :                 :***:*     *.*:. *

CHIKV   VYKKWPESFKNSATP----VGT--------AKTVMCGTYPVIHAVGPNFSNYSE--SEGD    82
SARS    LNKATNGAMQKESDDYIKLNGPLTVGGSCLLSGHNL-AKKCLHVVGPNLNA-----GEDI   113
HEV     FYQRFPESFDPAEFI----MSD---GF----AAYTLTPRPIIHAVAPDYRV-----EHNP    90
Rubella IFASAAASLAEDCRR----LAPCPTGEAVATPGHGCGYAHIIHAVAPRRPQDPAALEQSE   104
        .    ::         .                     :*.*.*         ..

CHIKV   RELAAAYREVAKEVTRLGVNSVAIPLLSTGVYSGGKDRLTQSLNHLFTAMDSTDA---DV   139
SARS    QLLKAAYENFN------SQDILLAPLLSAGIFGAKPLQS---LQVCVQTV------RTQV   158
HEV     KRLEAAYRETC-----SRRGTAAYPLLGAGIYKVPVGLS---FDAWERNH--RPGDEL--   138
Rubella ALLERAYRSIVALAAARRWTCVACPLLGAGIYGWSAAES---LRAALAAARTEPAERVSL   161
         *   **..              ***.:*::            :

CHIKV   VIYCRDKEWEKKISEAIQMRT-              160
SARS    YIAVNDKALYEQVVMDYLDNLK             180
HEV     YLTEPAIAWFE-----------             149
Rubella HICHPDRATLMHASVLVGA---             180
         :
```

C

```
Asian     APSYRVKRMDIAKNDEECVVNAANPRGLPGDGVCKAVYKKWPESFKNSATPVGTAKTVM     60
ECSA      APSYRVKRMDIAKNDEECVVNAANPRGLPGGGVCKAVYKKWPESFKNSATPVGTAKTVMC    60
W/African  APSYRVKRMDIAKNDEECVVNAANPRGLPGDGVCKAVYKKWPESFKNSATPVGTAKTVMC    60
          ******************************. ***************************

Asian     GTYPVIHAVGPNFSNYTESEGDRELAAAYREVAKEVTRLGVNSVAIPLLSTGVYSGGKDR   120
ECSA      GTYPVIHAVGPNFSNYSESEGDRELAAAYREVAKEVTRLGVNSVAIPLLSTGVYSGGKDR   120
W/African  GTYPVIHAVGPNFSNYSESEGDRELAAAYREVAKEVTRLGVNSVAIPLLSTGVYSGGKDR   120
          ***************.********************************************

Asian     LTQSLNHLFTAMDSTDADVVIYCRDKEWEKKISEAIQMRT                       160
ECSA      LTQSLNHLFTAMDSTDADVVIYCRDKEWEKKISEAIQMRT                       160
W/African  LTQSLNHLFTAMDSTDADVVIYCRDKEWEKKISEAIQMRT                       160
          ****************************************
```

Figure 4.2 Macro domain sequence alignments. (A) Amino acid sequence alignment of alphavirus macro domains. (B) Amino acid sequence alignment of CHIKV macro domain compared to other non-alphavirus viral macro domains. (C) Amino acid sequence alignment of CHIKV macro domain from the three major strains, with differences highlighted in blue. Produced using Clustal Omega (McWilliam *et al.*, 2013). (* = absolute alignment, : = residues with strongly similar properties, . = residues with weakly similar properties).

As shown by Figure 4.2, in the alphavirus sequence alignment, there were 57 absolutely conserved residues. When comparing CHIKV to other viruses, there were 17 absolutely conserved residues. Figure 4.2 C demonstrates the high level of conservation at the amino acid level of the macro domain between the three major CHIKV strains. These conserved residues were then compared to the three-dimensional structure of the CHIKV macro domain. Conserved residues that were also exposed in the ADPR/RNA binding pocket were selected for mutagenesis as indicated by Figure 4.3.
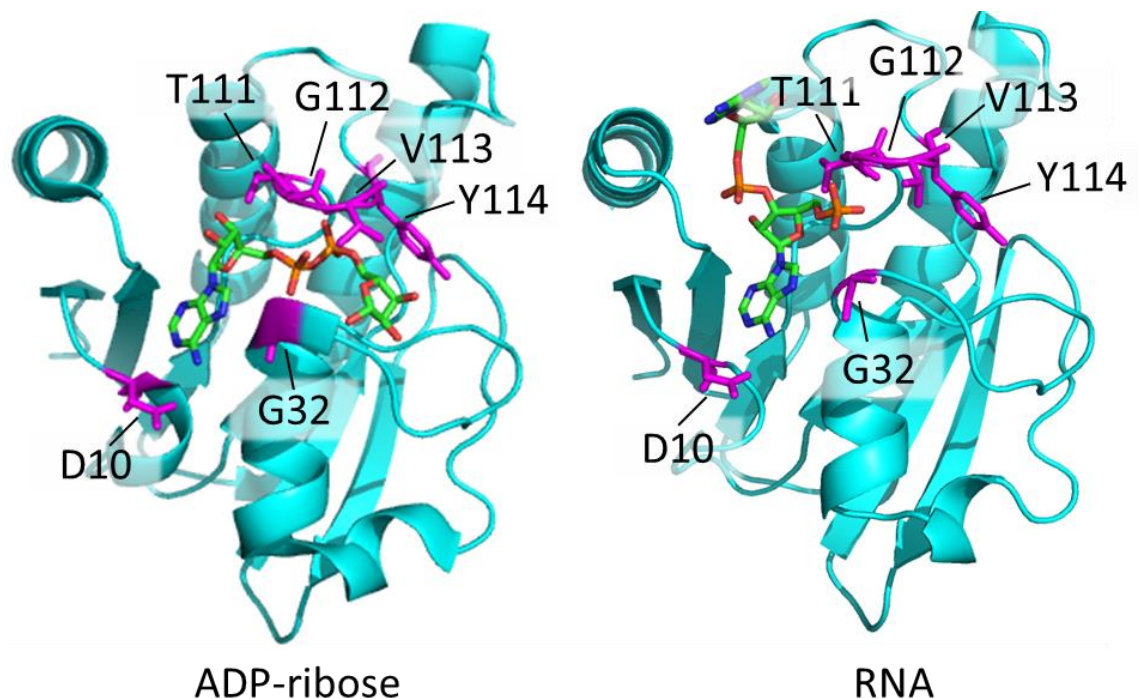
Figure 4.3 Selection of residues for mutagenesis. The three-dimensional structures of the CHIKV macro domain bound to ADP-ribose (left) and RNA (right) with indicated residues for mutagenesis shown in pink. Adapted from Malet *et al.,* 2009, PBD 3GPO and 3GPQ respectively.

Residues G32 and G112 were completely conserved across all viral macro domains and were highly conserved in mammalian, yeast and bacterial macro domains (Li *et al.,* 2013). Although not completely conserved throughout viruses, the D10 and T111 residues are highly conserved in the macro domains across several species including yeast and mammals. Residues V113 and Y114,

although not particularly highly conserved, were selected for mutagenesis due to their proximity to the ADP-ribose molecule within the CHIKV macro domain binding pocket as shown by the three-dimensional structure in Figure 4.3.

Alanine scanning was performed on the residues selected for mutagenesis. These mutations were engineered into the infectious CHIKV clone. Mutagenesis was performed using Q5 site directed mutagenesis on the CHIKV virus construct. Specific nucleotide changes are noted in appendix Figure 7.4.

4.2.2 Phenotypic analysis of CHIKV macro domain mutants in mammalian cell lines

4.2.2.1 BHK cells

As BHK cells were frequently used to generate wt CHIKV at high titres, they were initially used here to assess the replicative phenotypes of the macro domain mutants in the infectious CHIKV clone. Capped CHIKV RNA was produced for wt, each macro domain mutant. Alongside these, an nsP4 active site GDD>GAA polymerase mutant was generated to act as a negative control, as this mutation has been shown to completely inactivate polymerase activity. An infectious centre assay (ICA) and corresponding time course and titres were performed together. ICAs have been used in virological research in multiple contexts, such as assessing the number of infected cells in a patient sample (Dutta and Myrup, 1983). Here, it is used to assess the ability of an RNA genome to form an infectious virus whilst preventing any reversion to wt from overwhelming the population due to the presence of the overlay, using the method previously described by Gorchakov *et al.*, 2004.

BHK cells were electroporated with wt or mutant CHIKV RNA, and either serially diluted and plated onto a monolayer of prepared BHK cells for the ICA. These were then overlaid with MC and incubated for 72 h prior to staining and quantification. From the same electroporated BHK cells, 1 mL of each suspension was plated into 12 well plates, harvested at 24 and 48h and titred by standard plaque assay.

As shown by Figure 4.4 A, three mutants, G32A, T111A and Y114A were able to produce infectious virus with titres similar to, or higher than wt. V113A

produced very few plaques and D10A and G112A produced no plaques at all. When comparing this to the 24 and 48 hpe titres as shown in Figure 4.4 B, the three mutants that produced ~wt levels for the ICA also produced similar to wt levels over the time course. For both D10A and V113A titres increased between at 48 hpe, indicating possible reversion to wt. In contrast, much like the GAA polymerase negative control, G112A did not produce any infectious virus as measured by either ICA or plaques assay at 24 or 48 hpe.

To detect nsP3 in cells electroporated with mutant virus RNA, lysates were probed by western blot. As indicated by Figure 4.4 C, nsP3 was easily detectable for wt, G32A, T111A and Y114A at 24 hpe, attributable to their high titres. Despite some virus production by V113A, nsP3 was not detectable in these cells by this method. No nsP3 was detected for D10A nor G112A due to extremely low virus production, by these mutants. Despite the high titres at 48 hpe, levels of nsP3 as detected by western blot were much lower at this time point. In addition, it was not possible to extract RNA from these cells for further experiments such as qRT-PCR and RT for sequencing. This was most likely due to high levels of cytotoxicity and cell death in CHIKV infected BHK cells. Therefore, other cell lines were utilised for further study of the mutants.
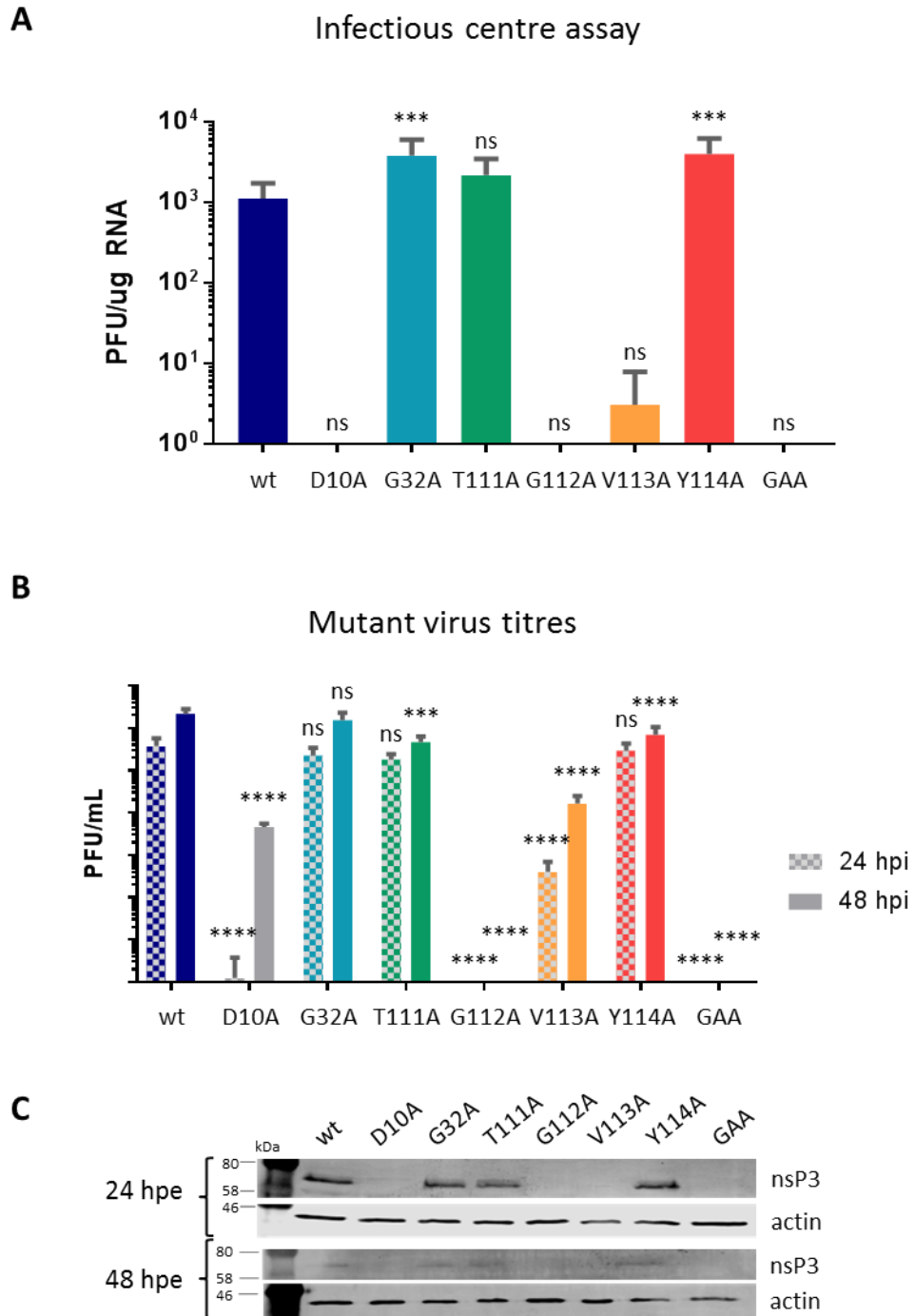
Figure 4.4 Phenotype of CHIKV nsP3 macro domain mutants in BHK cells.
(A) ICA of the macro domain mutants. RNA was produced for wt, each macro domain mutant and nsP4-GAA. An ICA was performed for each RNA. (Data analysed by One-way ANOVA with Bonferroni correction compared to wt, ns = P > 0.05, * = P ≤ 0.05, ** = P ≤ 0.01, *** = P ≤ 0.001, **** = P ≤ 0.0001). (B) Electroporated cells from A were plated separately and supernatant collected at 24 and 48 hpe. Virus was titred via plaque assay. Data analysed as described in part A. (C) Western blot for nsP3 and actin loading control in electroporated BHK cells at 24 and 48 hpe.

4.2.2.2   Huh7 cells

Due to the issues experienced with BHK cells, Huh7 cells were selected to analyse the replicative phenotypes of the macro domain mutants, as it had been shown in Chapter 3 that they are suitable and relevant to CHIKV research. We have observed in the laboratory that Huh7 cells were less sensitive to the cytotoxic effects of CHIKV infection when compared to other cell lines such as BHK cells. They were therefore proposed as a more suitable cell line for experiments such as RNA and protein extraction or immunofluorescence.

Prior to experiments using the infectious virus, the dLuc CHIKV replicon (as described previous in 3.2.1.1) was utilised to assess the levels of RNA replication of the macro domain mutants in Huh7 cells. As shown in Figure 4.5, all macro domain mutants were able to replicate CHIKV RNA, as all produced signal above that of the nsP4-GAA mutant. Both V113A and Y114A exhibited a significant increase in RNA replication compared to wt. Though none of the other mutants exhibited a statically significant difference to wt replication, D10A, G32A, G112A, and, to a lesser extent, T111A were all reduced from wt.
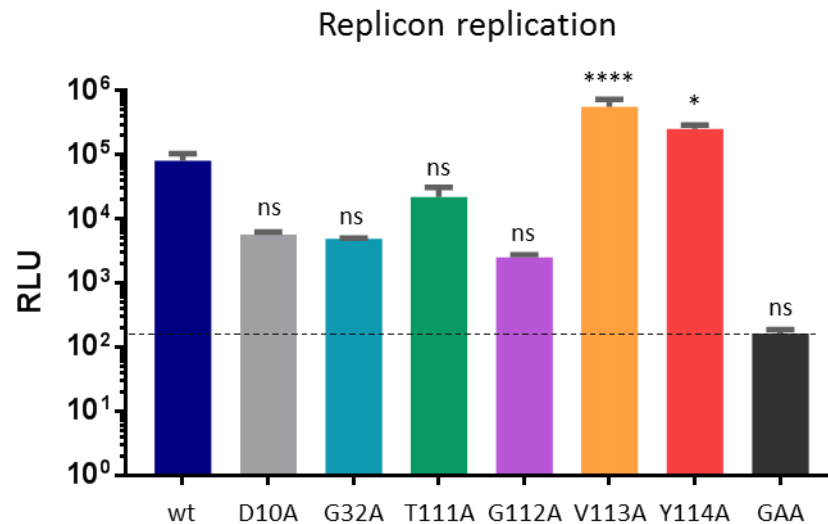
Figure 4.5 All macro domain mutants are capable of RNA replication in Huh7 cells. Huh7 cells were transfected with the dual luciferase replicon and lysed over at 2 and 24 hpt. Data shown is the 24 h Fluc signal, normalised to the 2 h Rluc signal for each individual mutant. The dotted line indicates signal from the GAA polymerase mutant. (Data analysed by One-way ANOVA with Bonferroni correction compared to wt, ns = P > 0.05, * = P ≤ 0.05, ** = P ≤ 0.01, *** = P ≤ 0.001, **** = P ≤ 0.0001).

Despite attempts to optimise the process, it was not possible to perform quantitative ICAs using electroporated Huh7 cells, nor did these cells respond well to electroporation with CHIKV RNA. Therefore, cells were transfected with CHIKV wt or mutant RNA, plated into 12 well plates and resulting virus was harvested and titred by plaque assay at 24 and 48 hpt. As shown by Figure 4.6, Huh7 cells did not support virus replication of most mutants. Only one mutant, Y114A, was capable of producing detectable virus at both 24 and 48 h time points. At 48 h, infectious virus was also detected for T111A. However, as shown by Figure 4.6 B, western blot analysis revealed that nsP3 was only robustly expressed in cells containing wt RNA at 24 and 48 hpe.

To complement the western blot analysis, IF for nsP3 was performed for Huh7 cells transfected with wt or mutant CHIKV RNA. Cells were transfected with wt or mutant CHIKV RNA, fixed at 12 and 24 hpt, and stained for nsP3, and DAPI stained to highlight nuclei. These time points were selected as previous work (data not shown) indicated that 12 hpt was the earliest time point at which nsP3

was detectable by IF. No 48 h time point was taken as, for most cell lines, by 48 h there is a high level of cell death making imaging of cells problematic. As shown by Figure 4.7, at 12 hpt, wt-electroporated cells contain many defined puncta of nsP3, with many localised to the perinuclear region of the cells. In contrast, all of the mutants either contained no puncta or few puncta per cell. These few puncta may be indicative of input translation or the attempt to form replication complexes that are defective. Interestingly, with cells that contained few, small puncta, few were localised to the perinuclear region indicating a possible transport/trafficking issue for nsP3 macro domain mutants. At 24 hpt, wt appears very similar to that shown for 12 h with cells containing more nsP3 puncta. Again, most cells electroporated with mutant RNA contained one or two puncta of nsP3. Cells transfected with T111A RNA exhibited multiple puncta, although fewer and far less intense than wt. Many of these puncta were perinuclear and may indicate low levels of replication which is in agreement with the virus titre data shown in Figure 4.6. Similarly in agreement to the previous data, Y1114A at 48 hpt exhibited many bright puncta, with some in the perinuclear region, much resembling the wt cells at earlier time points.
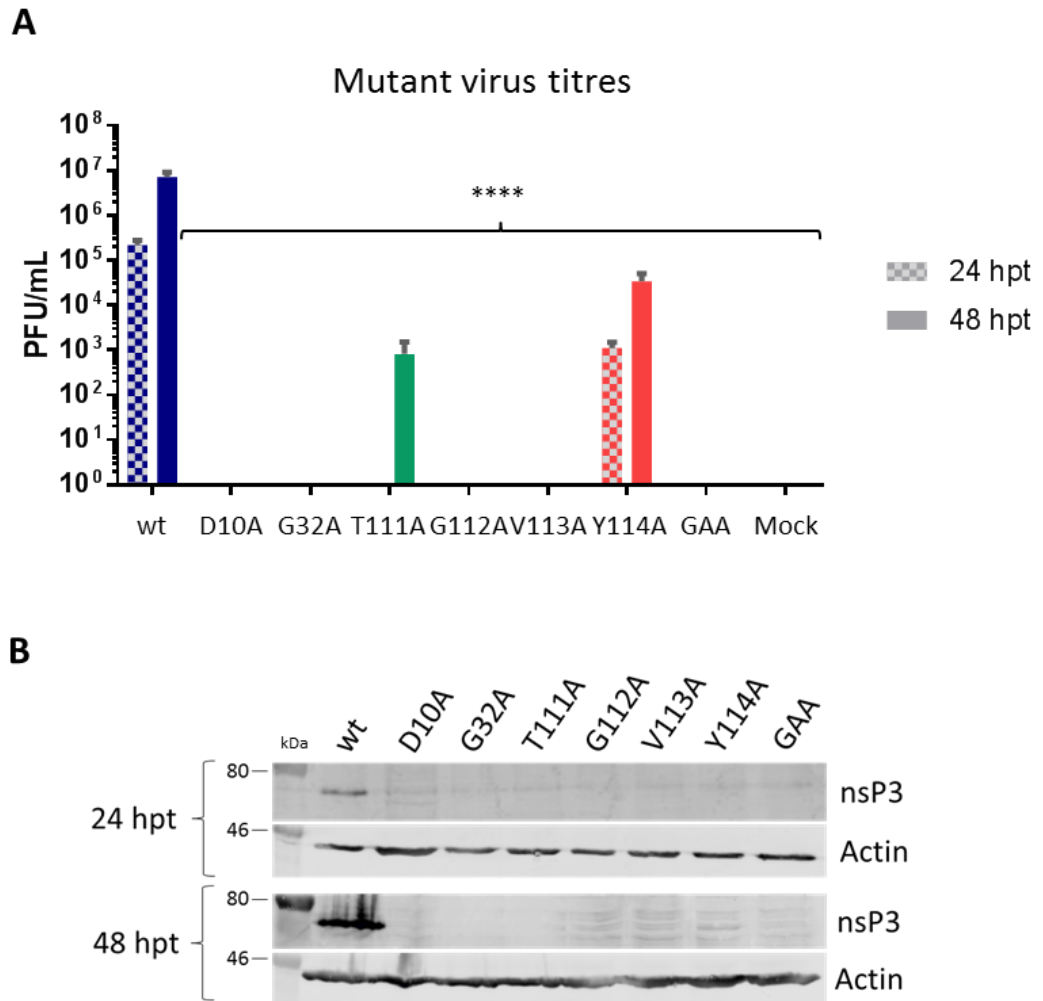
Figure 4.6 Phenotype of CHIKV nsP3 macro domain mutants in Huh7 cells.
(A) Huh7 cells were transfected with wt or mutant CHIKV RNA. Cells
were plated out into 12 well plates and supernatant harvested and
titred by plaque assay on BHK cells at 24 and 48 hpt. Mock cells were
electroporated without RNA present. (Data analysed by One-way
ANOVA with Bonferroni correction compared to wt, **** = P ≤ 0.0001).
(B) Western blot for nsP3 and actin loading control in corresponding
cell lysates at 24 and 48 hpt.
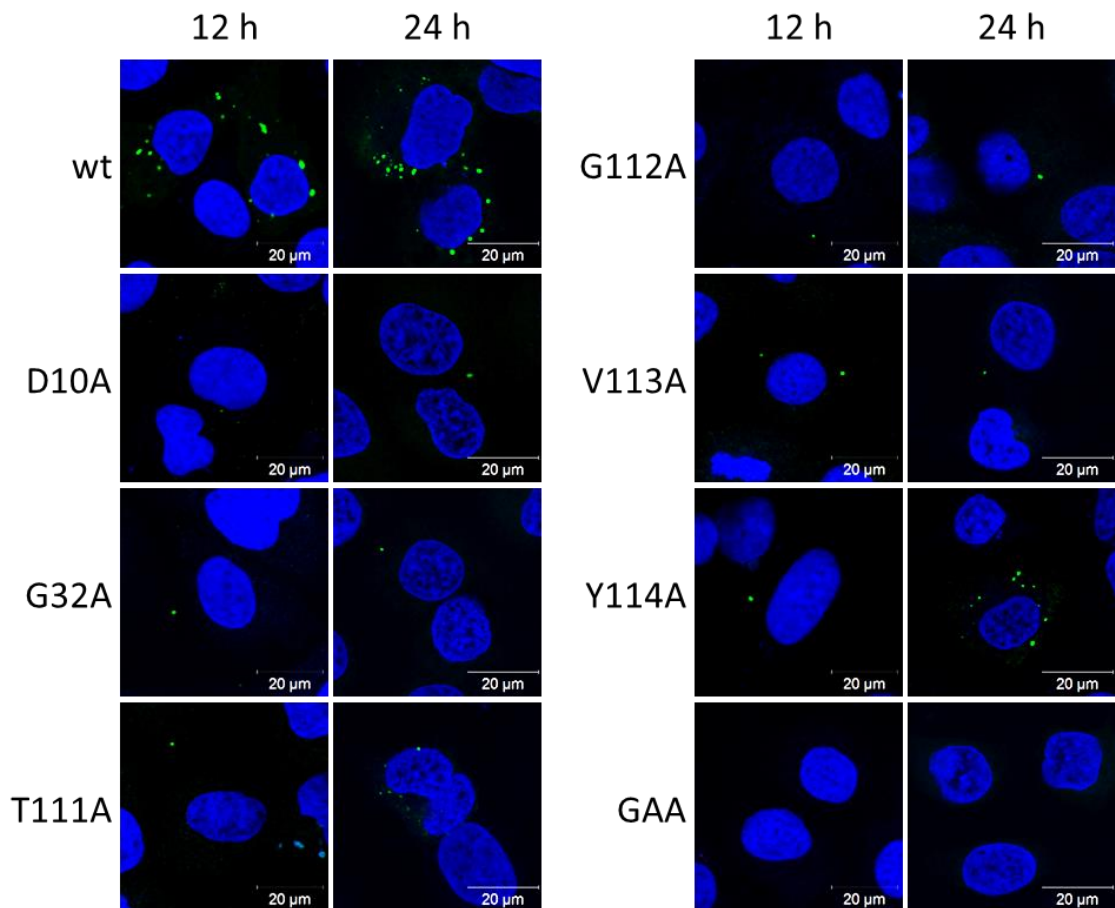
Figure 4.7 Cytoplasmic distribution of mutant nsP3 Huh7 cells. IF was performed for nsP3 in Huh7 cells electroporated with macro domain mutant RNA, fixed at 12 and 24 hpt. Images taken using an LSM700 confocal microscope.

Corresponding transfected cells were used to extract whole cell RNA by TRIzol extraction at 24 hpt. Unfortunately, it was not possible to extract RNA from cells at 48 h due to cytotoxicity, this was particularly true for cells transfected with wt CHIKV. Extracted RNA was then used to quantify viral RNA in transfected cells via qRT-PCR. Unlike in chapter 3, qRT-PCR shown here was performed using primers specific for the E1 coding region of the genome. These were found to be more consistent than the primers for the AUD which were previously used. However, unlike the previous primers used, as these primers are specific for the E1 region of the genome, they will be detecting both genomic and subgenomic 26s RNA.

As shown by the dotted line in Figure 4.8, the levels of RNA detected for GAA is considered to be the level of input RNA remaining from transfection. All mutants

were above this level to some degree except G112A which reiterates the inability of this mutant to replicate. It is surprising however to observe that T111A and Y114A, which were both able to produce infectious virus as shown in Figure 4.6, exhibited genomic RNA levels not substantially above the GAA negative control. The mutant with the highest genomic RNA levels; V113A, was unable to produce detectable virus when electroporated into Huh7 cells. This may indicate an ability to replicate RNA but not form infectious virus.
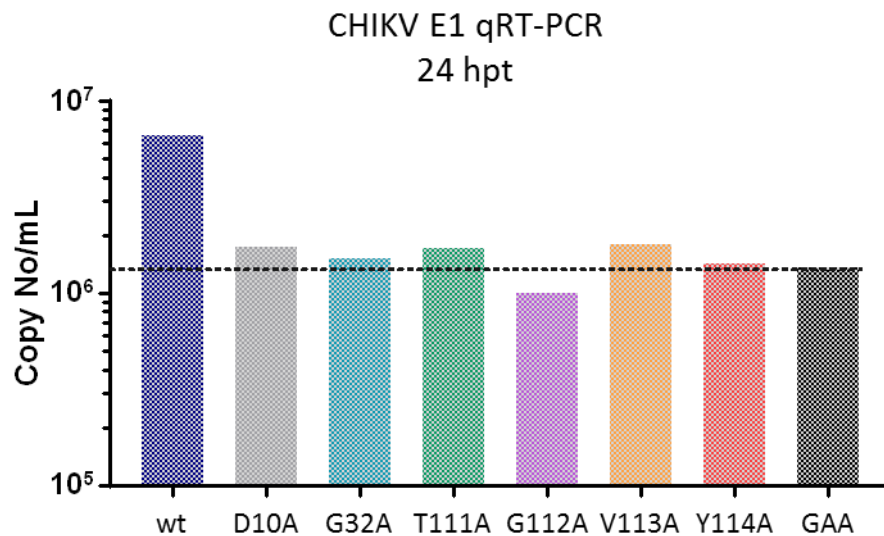
Figure 4.8 qRT-PCR of viral RNA from electroporated Huh7 cells. Corresponding cells from Figure 4.6 were TRIzol extracted at 24 hpt. Resulting RNA was adjusted to 50 ng/µL and 100 ng per RNA was used per qRT-PCR reaction using the MESA green qRT-PCR MasterMix (EuroGenTec) with primers specific for the E1 region of the CHIKV genome. Data normalised to cell only control (1.36×10^3 copy No/mL). Dotted line indicates input RNA levels as indicated from the GAA negative control.

It was attempted to reverse transcribe the RNA from wt, T111A and Y114A samples in order to amplify the macro domain coding region for consensus sequencing. However, despite multiple attempts with various methods, it was only possible to successfully amplify a fragment by PCR from the wt cDNA, when using 30 cycles of the PCR program (Figure 4.9). Ideally, when screening PCR products for the presence of mutations, the cycle number should be kept to a minimum to reduce the possibility of introducing mutations, or selecting for mutations within the PCR. For other amplifications from cDNA shown in this

work, a maximum of 25 cycles was used. Therefore, since it was not possible to amplify fragments for either the T111A or Y114A cDNA within 30 PCR cycles, this line of inquiry was abandoned.
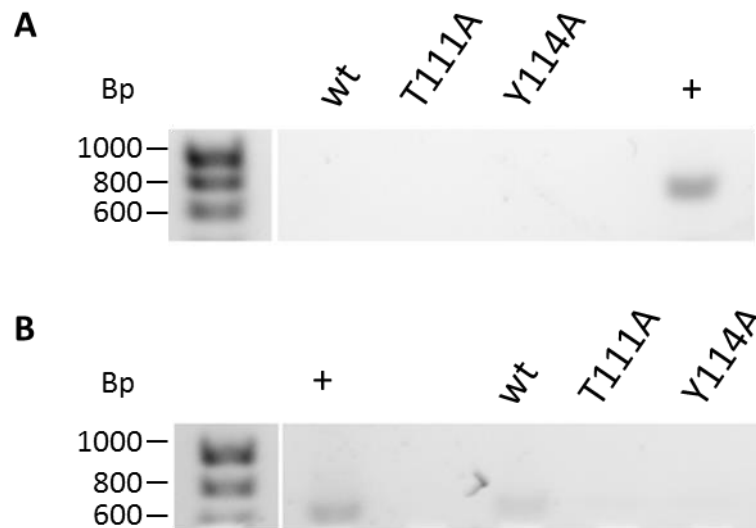
Figure 4.9 PCR amplification of a macro domain containing fragment from cDNA formed from total RNA of Huh7 cells transfected with macro domain mutant CHIKV RNA. Huh7 cells were transfected with wt and macro domain mutant CHIKV RNA. Total cell RNA was extracted at 24 hpe using TRIzol. Resulting RNA was used to generate cDNA which was used as input for PCR to amplify a macro domain containing fragment for sequencing. Resulting PCR products from 25 cycles (A), and 30 cycles (B) were ran on agarose gels. The positive control ('+') contained CHIKV plasmid DNA as template.

4.2.2.3 C2C12 cells

Due to the issues that occurred with the macro domain mutants in Huh7 cells another physiologically relevant cell line, C2C12 cells, were used to assess the replicative phenotypes of the CHIKV macro domain mutants .

As for Huh7 cells, initially C2C12 cells were transfected with wt and mutant virus RNA, supernatant was collected at 24 and 48 hpt and titred via plaque assay. As shown by Figure 4.10, in contrast to the Huh7 cells, every mutant was able to produce some level of detectable, infectious virus by 48 hpt. Although none of the mutants, including the GAA negative control, were significantly different at the 48 h time point, presumably due to higher variation in the wt data caused by cytotoxicity at this later time point. Mutants G32A, T111A, and Y114A all resembled wt levels at 24 h however, unlike the wt, this was reduced at 48 h, possibly due to higher cytotoxicity for these particular mutants. Both D10A and V113A were reduced compared to wt. G112A which, although in both BHK and Huh7 cells was unable to produce any infectious virus, produced a low level of infectious virus in C2C12 cells by 48 hpe ($4.7x10^2$ PFU/mL).

As the western blot indicates in Figure 4.10 B, nsP3 was detectable for wt, G32A, T111A, V113A and Y114A at both 24 and 48 hpt. By 48 h nsP3 was also detectable for D10A. Due to technical issues the 48 h samples for western blot were not equally loaded . Therefore the actin loading control must be taken into consideration when comparing the quantities of nsP3 for each mutant at 48 hpt.
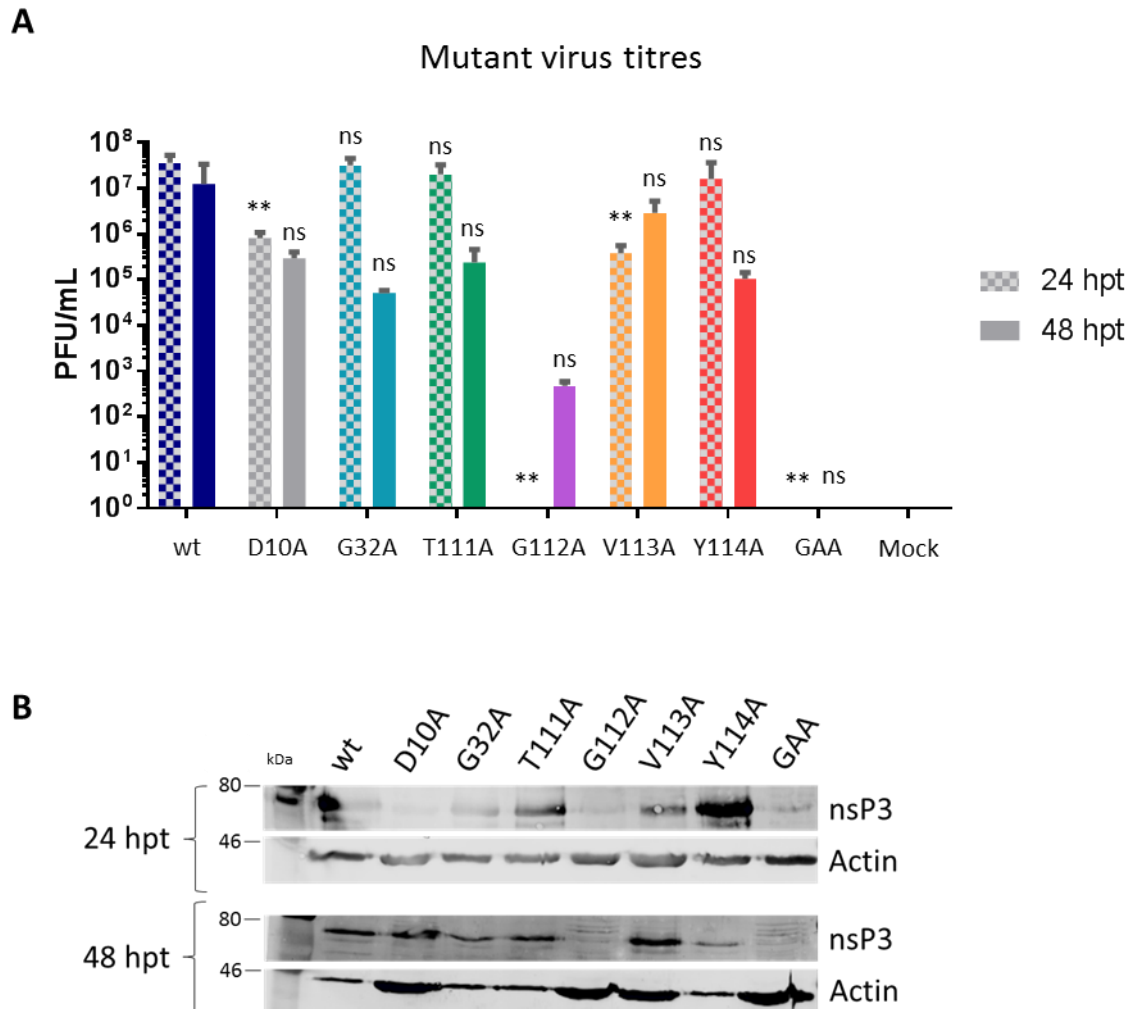
Figure 4.10 Macro domain mutants within the infectious CHIKV system in C2C12 cells. (A) C2C12 cells were transfected with wt or mutant CHIKV RNA. Cells were plated out into 12 well plates and supernatant harvested and titred by plaque assay on BHK cells at 24 and 48 hpt. (Data analysed by One-way ANOVA with Bonferroni correction compared to wt, ns = P > 0.05, * = P ≤ 0.05, ** = P ≤ 0.01,). (B) Western blot for nsP3 and actin loading control in corresponding transfected C2C12 cells at 24 and 48 hpt.

IF was again performed on C2C12 cells that were transfected with wt or mutant CHIKV RNA to visualise nsP3. Transfected cells were fixed at 12 and 24 hpt and stained for nsP3, and nuclei using DAPI. As shown by Figure 4.11, at 12 hpt, the IF data is much in agreement to the viral titres produced (see Figure 4.10) with wt, G32A, T111A and Y114A all exhibiting similar, high levels of expression of nsP3 localised throughout the cytoplasm, with several perinuclear puncta. At 24 h the nsP3 expressed in G32A-, and Y114A- electroporated cells still much

resembled the wt. However, cells infected with T111A CHIKV had a very different appearance with many nsP3-positive cells containing abnormal nuclei that were smaller in size, and appeared to be hollow. As shown by the inset image for T111A at 24 h, some nsP3 expressing cells did resemble those of wt, with intact nuclei, but these were a minority in the sample. For mutants D10A and V113A, no cells were found at 12 hpt that expressed nsP3, however, by 24 h both mutants exhibited nsP3 expression. Cells expressing D10A or V113A nsP3 at 24 hpt contained fewer puncta of nsP3 that were less intense when compared to wt. In cells with G112A RNA, a small number of cells appeared to contain single puncta of nsP3 which did not increase by 24 hpt. In this experiment, no cells were detected for G112A that contained more than one puncta.
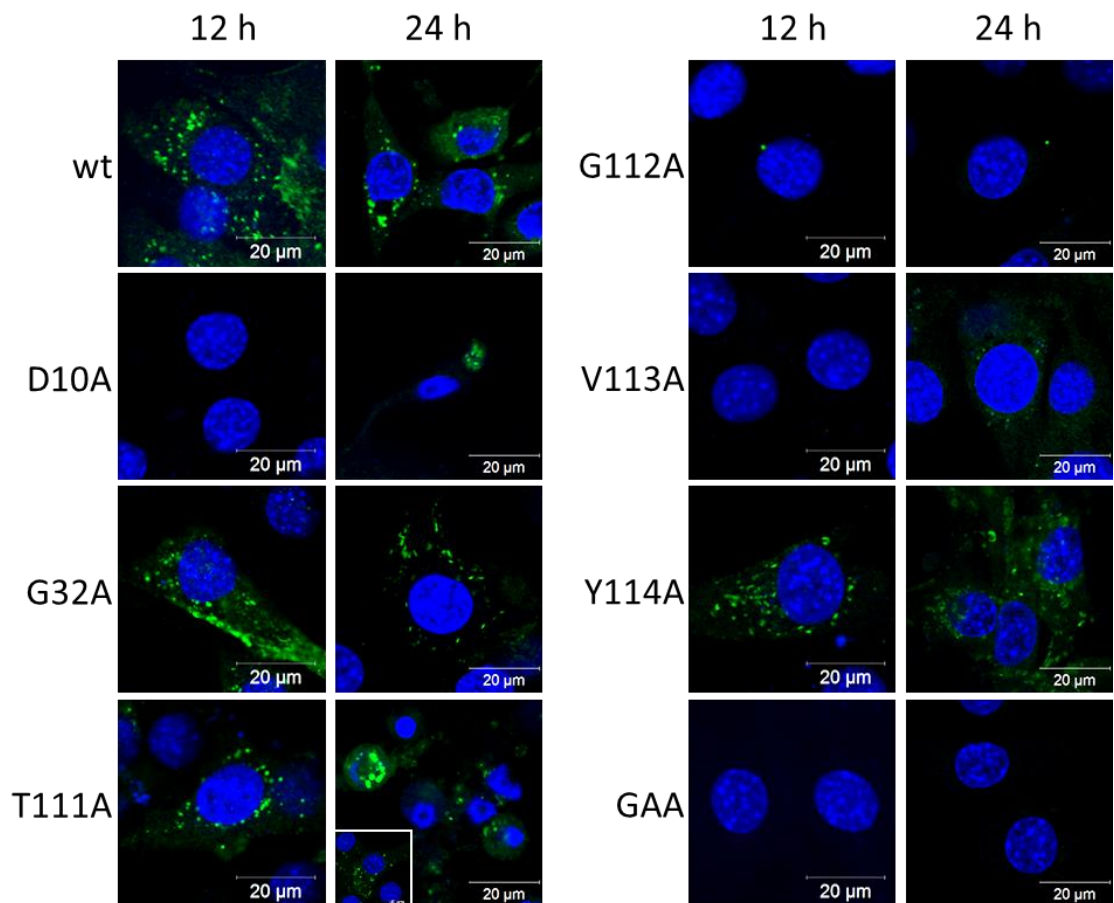
Figure 4.11 Distribution of nsP3 in C2C12 cells transfected with mutant CHIKV RNA. IF was performed for nsP3 in C2C12 cells electroporated with macro domain mutant RNA, fixed at 12 and 24 hpt. Images taken using an LSM700 confocal microscope.

Total cell RNA was extracted from transfected cells at 24 hpe by TRIzol extraction. Resulting RNA was then used for qRT-PCR. As shown in Figure 4.12, all mutants except G112A had copy numbers above the nsP4-GAA negative control. Mutants G32A, T111A and Y114A were all approximately wt levels, which reflects the virus titre data shown in Figure 4.10. Both D10A and V113A were drastically reduced from wt, indicating their poor ability to replicate RNA. At 24 hpt, G112A is exhibiting no RNA replication as it is below GAA levels, again reflecting the data shown in Figure 4.10 however, this mutant was capable of producing virus at 48 hpt which would suggest it should be capable of some level of RNA replication.
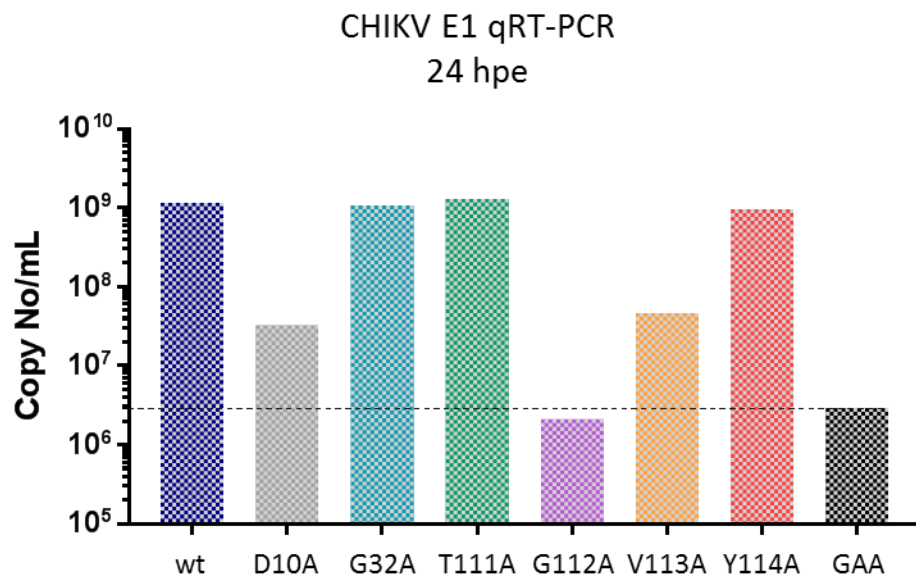
Figure 4.12 qRT-PCR of viral RNA from transfected C2C12 cells. Corresponding cells from Figure 4.6 were TRIzol extracted at 24 hpt. Resulting RNA was adjusted to 50 ng/µL and 100 ng per RNA was used per qRT-PCR reaction using the MESA green qRT-PCR MasterMix (EuroGenTec) using primers specific for the E1 region of the CHIKV genome. Data normalised to cell only control (1.31x10^3 copy No/mL). The dotted line indicates the level of input RNA which is that of the GAA polymerase negative control.

To assess whether any replicative phenotype observed was due to reversion, corresponding RNA was reverse transcribed and a macro domain containing fragment was amplified via PCR for sequencing. As shown in Figure 4.13, it was only possible to amplify the macro domain PCR fragment from wt, G32A, T111A

and Y114A transfected cells. Therefore it was only possible to obtain the coding sequences for these mutants.

As shown by the highlighted nucleotides in Figure 4.13 B, for all of the mutants that were successfully amplified by PCR, all original mutations were maintained. No additional mutations were detected, at least not within the macro domain coding region. Although it may have been interesting to determine whether mutants with lower titres were a result of reversion or compensatory mutations, it was not possible to amplify the macro domain PCR product from D10A or V113A infected cells.

Figure 4.13 Consensus sequencing of cDNA generated from C2C12 cells 24 h post transfection with macro domain mutant CHIKV RNA. TRIzol extracted RNA from Figure 4.12 was used to form cDNA and used as input for PCR to amplify the macro domain coding region. (A) PCR products were electrophoresed on a 1% agarose gel. (B) Successful PCR fragments (G32A, T111A and Y114A) were then sequenced via sanger consensus sequencing by GeneWiz. Resulting sequences were aligned with wt using Clustal omega with mutant nucleotides highlighted in blue.

4.2.3 Phenotypic analysis of CHIKV macro domain mutants in mosquito cell lines

As CHIKV is an arbovirus, it would be prudent to assess the role of the macro domain, not only in the human host but also in the mosquito vector. Therefore the phenotypes of the macro domain mutant viruses were assessed in the two *Ae albopictus* cell lines previously demonstrated to replicate CHIKV: C6/36 and U4.4 (chapter 3). However, as the optimisation in chapter 3 was performed by infection of cells with virus produced in BHK cells, further optimisation was required to determine both the transfection method and the appropriate time points to harvest virus.

Transfection with lipofectamine was trialled as this had been used successfully with these cell lines with CHIKV replicon RNA (see section 3.2.2) and it had been reported that electroporation of mosquito cells was both inconsistent and requires specific reagents (Boylan *et al.*, 2017, M Müller and A Merits personal communication). U4.4 and C6/36 cells were therefore transfected using lipofectamine with wt CHIKV RNA and supernatant collected over a three day period. Virus was then titred by plaque assay. As shown by Figure 4.14, C6/36 cells produced low titres of infectious virus by 24 h, increasing to 10^7 PFU/mL at 48 and 72 hpt . Conversely, U4.4 cells only produced detectable infectious virus at 72 hpt with the lower titres in the range of 10^5 PFU/mL, demonstrating the effect of an intact RNAi system on virus replication. It was therefore decided that the transfection protocol was successful and suitable for use in transfecting mutant RNA into mosquito cells and that virus would be harvested at 72 hpt.
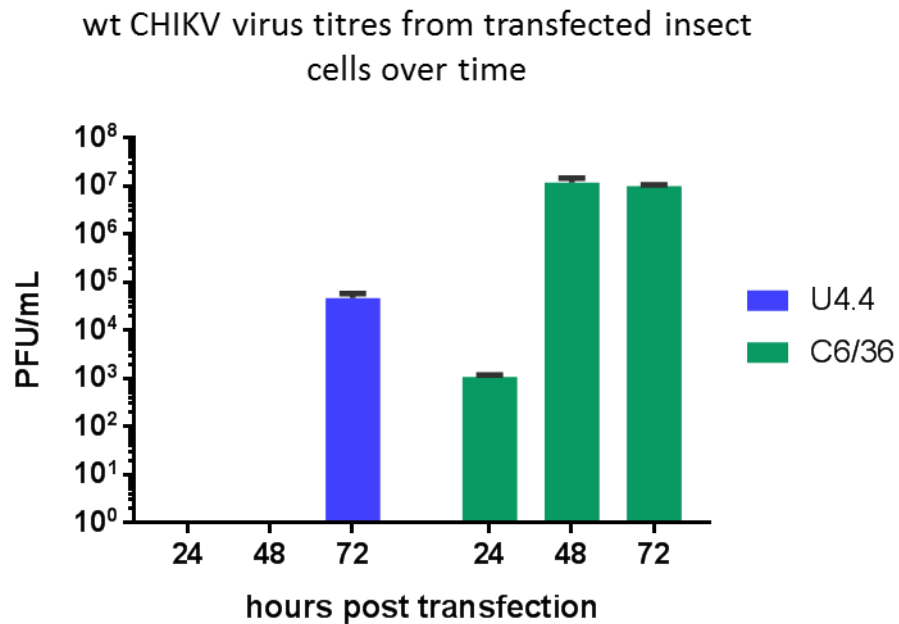
Figure 4.14 CHIKV titres from transfected mosquito cells over time. U4.4 and C6/36 cells were transfected with wt CHIKV RNA, supernatant collected at 24, 48 and 72 hpt and resulting virus titred by plaque assay.

U4.4 and C6/36 cells were then transfected with wt and mutant CHIKV RNA, incubated for 72 h prior to collection of supernatant and titration by plaque assay. As shown in Figure 4.15, there were some stark differences of the ability of the mutants to replicate in the two cell lines. For both cell lines, T111A resembled wt, with no significant different between T111A from wt titres. G32A resembled wt in C6/36 cells but demonstrated a significant increase in titre, compared to wt, in U4.4 cells. In both cell lines, G112A did not produce any detectable virus. In U4.4 cells, Y114A also resembled wt but in C6/36 cells, replication of this mutant was significantly reduced. For V1113A, there was no detectable virus in U4.4 cells, yet this mutant produced titres of 2.1×10^6 PFU/mL in C6/36 cells, although this was still significantly reduced from wt. Similarly, D10A did not replicate at all in U4.4 cells but did replicate to a reduced level in C6/36 cells.
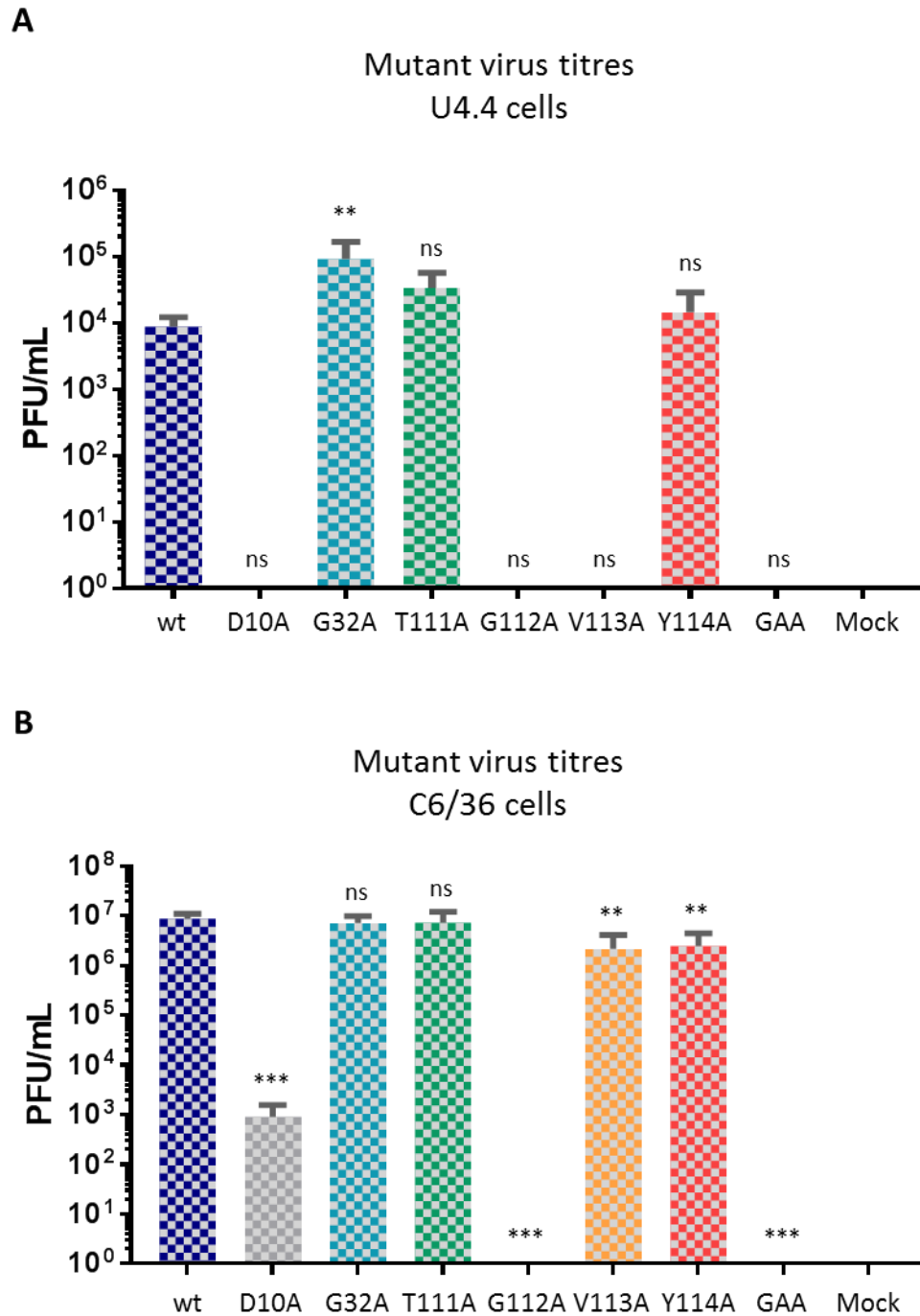
Figure 4.15 Mutant virus titres from transfected mosquito cell lines. U4.4 (A) and C6/36 cells (B) were transfected with wt or mutant CHIKV RNA as previously described (or mock transfected with no RNA present). Supernatant was collected at 72 hpt and titred by plaque assay on BHK cells. (Data analysed by One-way ANOVA with Bonferroni correction compared to wt, ns = P > 0.05, * = P ≤ 0.05, ** = P ≤ 0.01, *** = P ≤ 0.001).

In parallel, transfected mosquito cells were TRIzol extracted and resulting RNA used for qRT-PCR. As shown in Figure 4.16, for the U4.4 cells, the qRT-PCR data is reflective of the virus titres shown in Figure 4.14. It is interesting that the three mutants that produced no detectable virus, D10A, G112A and V113A, were also below the level of the GAA polymerase negative control. This implies that these three mutants were completely unable to replicate RNA in U4.4 cells. In contrast, all mutants had copy number higher than the GAA control in C6/36 cells. Again, the qRT-PCR data broadly reflected the virus titres produced in these cells. However, it is curious that both D10A, that produced low levels of virus, had a very similar copy number to that of G112A which was unable to produce virus in these cells. This could imply that the macro domain has an alternative function (other than RNA replication), in the virus lifecycle.

A

CHIKV E1 qRT-PCR of macro domain
mutants in U4.4 cells, 72 hpt
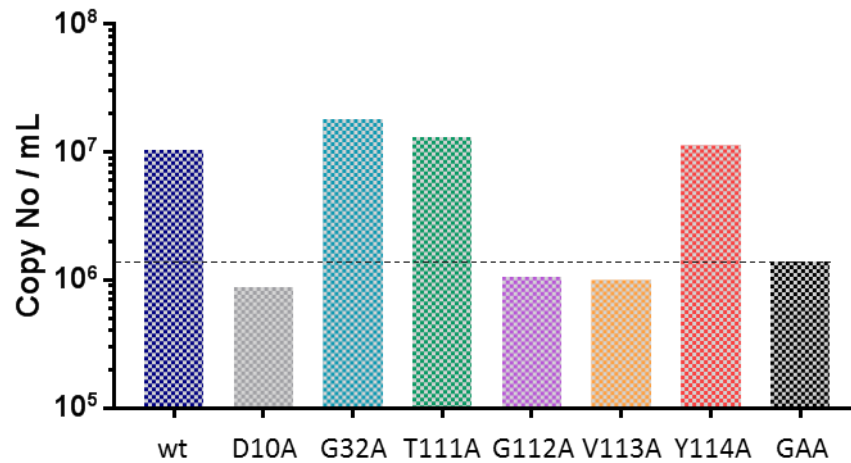
B

CHIKV E1 qRT-PCR of macro domain
mutants in C6/36 cells, 72 hpt
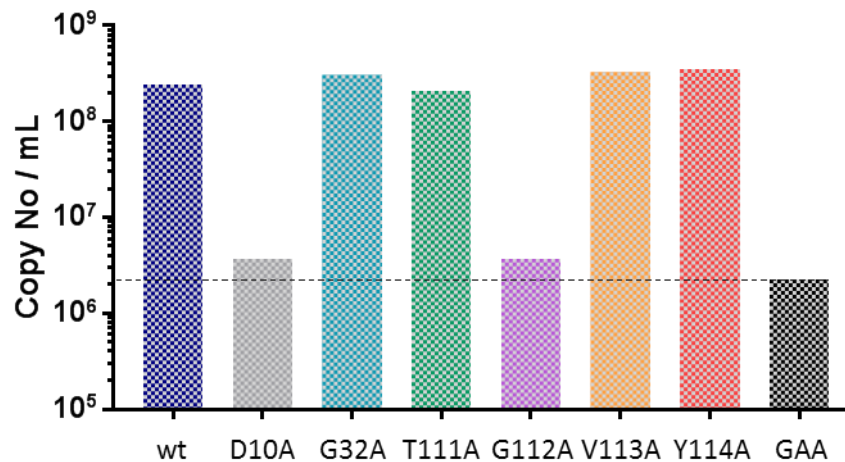
Figure 4.16 qRT-PCR in mosquito cells transfected with wt or mutant RNA (72 hpt). U4.4 and C6/36 cells were transfected with wt or mutant CHIKV RNA (or mock transfected with no RNA present). RNA was extracted via TRIzol at 72 hpt. Resulting RNA was adjusted to 50 ng/µL, and 100 ng per RNA was used per qRT-PCR reaction using the MESA green qRT-PCR MasterMix (EuroGenTec) using primers specific for the E1 region of the CHIKV genome. Data normalised to mock transfected control (4.78x10^3 and 8.27x10^3 copy No/mL respectively). The dotted line indicates the level of input RNA which is that of the GAA polymerase negative control.

145

To assess whether any of the replicative phenotypes observed in mosquito cells was due to reversion, corresponding RNA from the qRT-PCR experiments was reverse transcribed into cDNA and a macro domain containing fragment was amplified via PCR and sequenced via consensus Sanger sequencing (Figure 4.17).
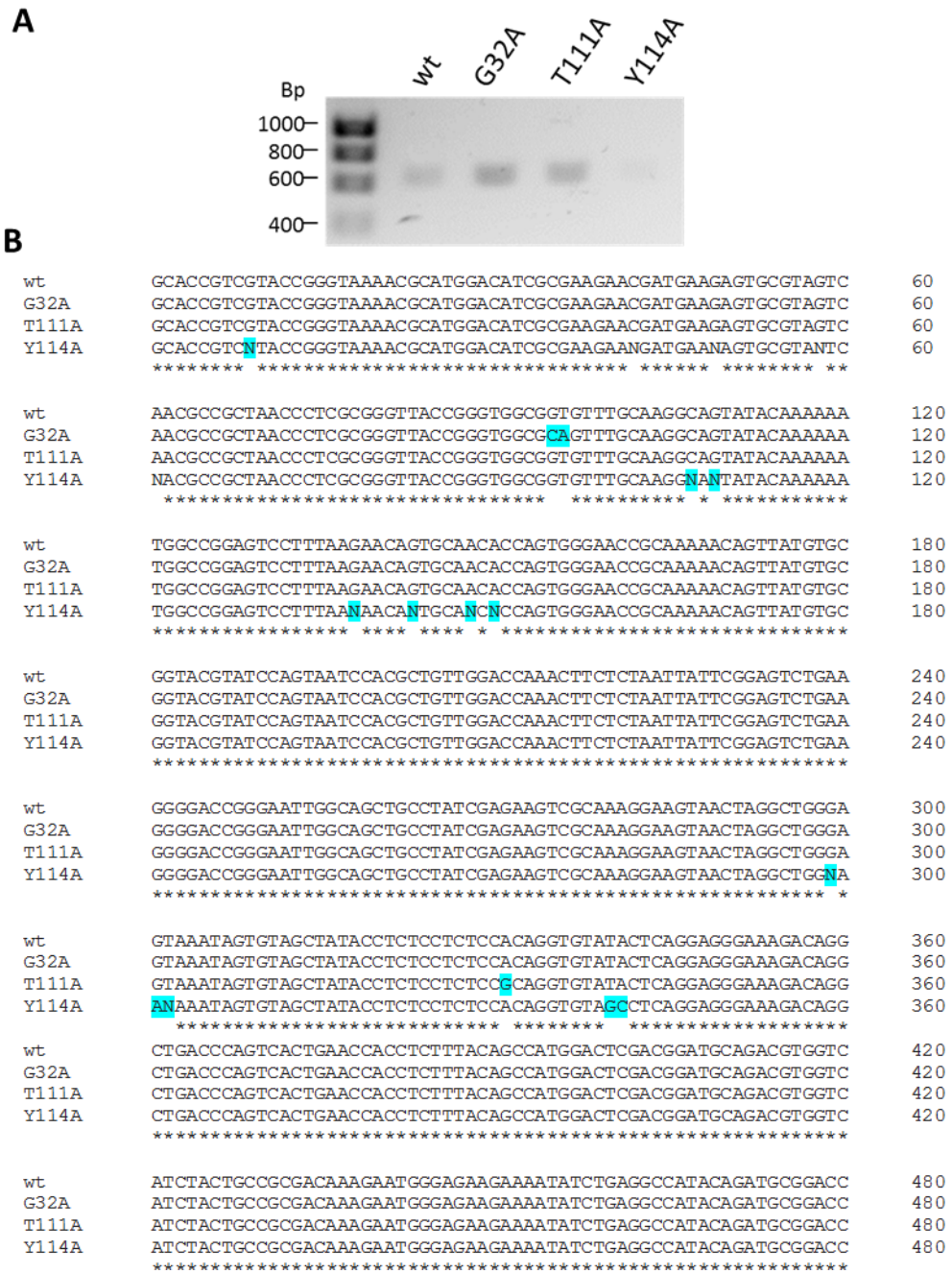
Figure 4.17 Sequencing of the macro domain mutant genomes from infected U4.4 cells. Corresponding RNA to Figure 4.16 was reverse transcribed to form cDNA which was used the template to amplify a macro domain containing fragment via PCR. (A) Resulting PCR fragments were electrophoresed on a 1% agarose gel. (B) Samples containing the correct PCR fragment were sequenced via consensus Sanger sequencing by GeneWiz. Resulting sequences were aligned with wt using Clustal Omega. Mutant nucleotides highlighted in blue.

As seen previously in the C2C12 cells, all mutations present at time of transfection into the U4.4 cells, were retained by 72 h. Although the sequencing data received for the Y114A sample was of poor quality with several undefined bases present (termed 'N' in the sequence alignment), the original Y114A mutation (TAC>GCC) was clearly retained.

This process was also performed for the C6/36 cells,. As shown by Figure 4.18 A, it was only possible to amplify the macro domain DNA fragment from G32A, T111A, V113A and Y114A samples. Again, as seen in all other cells lines, for all the mutants that it was possible to obtain sequencing data, the original mutation present in the transfected RNA was retained for the 72 h, when the total cell RNA was extracted (Figure 4.18 B).

A

```
                    wt  D10A G32A T111A V113A Y114A
Bp
1000—
 800—
 600—
 400—
```

B

```
wt      GCACCGTCGTACCGGGTAAAACGCATGGACATCGCGAAGAACGATGAAGAGTGCGTAGTC   60
G32A    GCACCGTCGTACCGGGTAAAACGCATGGACATCGCGAAGAACGATGAAGAGTGCGTAGTC   60
T111A   GCACCGTCGTACCGGGTAAAACGCATGGACATCGCGAAGAACGATGAAGAGTGCGTAGTC   60
V113A   GCACCGTCGTACCGGGTAAAACGCATGGACATCGCGAAGAACGATGAAGAGTGCGTAGTC   60
Y114A   GCACCGTCGTACCGGGTAAAACGCATGGACATCGCGAAGAACGATGAAGAGTGCGTAGTC   60
        ************************************************************

wt      AACGCCGCTAACCCTCGCGGGTTACCGGGTGGCGGTGTTTGCAAGGCAGTATACAAAAAA  120
G32A    AACGCCGCTAACCCTCGCGGGTTACCGGGTGGCGCAGTTTGCAAGGCAGTATACAAAAAA  120
T111A   AACGCCGCTAACCCTCGCGGGTTACCGGGTGGCGGTGTTTGCAAGGCAGTATACAAAAAA  120
V113A   AACGCCGCTAACCCTCGCGGGTTACCGGGTGGCGGTGTTTGCAAGGCAGTATACAAAAAA  120
Y114A   AACGCCGCTAACCCTCGCGGGTTACCGGGTGGCGGTGTTTGCAAGGCAGTATACAAAAAA  120
        *********************************  *************************

wt      TGGCCGGAGTCCTTTAAGAACAGTGCAACACCAGTGGGAACCGCAAAAACAGTTATGTGC  180
G32A    TGGCCGGAGTCCTTTAAGAACAGTGCAACACCAGTGGGAACCGCAAAAACAGTTATGTGC  180
T111A   TGGCCGGAGTCCTTTAAGAACAGTGCAACACCAGTGGGAACCGCAAAAACAGTTATGTGC  180
V113A   TGGCCGGAGTCCTTTAAGAACAGTGCAACACCAGTGGGAACCGCAAAAACAGTTATGTGC  180
Y114A   TGGCCGGAGTCCTTTAAGAACAGTGCAACACCAGTGGGAACCGCAAAAACAGTTATGTGC  180
        ************************************************************

wt      GGTACGTATCCAGTAATCCACGCTGTTGGACCAAACTTCTCTAATTATTCGGAGTCTGAA  240
G32A    GGTACGTATCCAGTAATCCACGCTGTTGGACCAAACTTCTCTAATTATTCGGAGTCTGAA  240
T111A   GGTACGTATCCAGTAATCCACGCTGTTGGACCAAACTTCTCTAATTATTCGGAGTCTGAA  240
V113A   GGTACGTATCCAGTAATCCACGCTGTTGGACCAAACTTCTCTAATTATTCGGAGTCTGAA  240
Y114A   GGTACGTATCCAGTAATCCACGCTGTTGGACCAAACTTCTCTAATTATTCGGAGTCTGAA  240
        ************************************************************

wt      GGGGACCGGGAATTGGCAGCTGCCTATCGAGAAGTCGCAAAGGAAGTAACTAGGCTGGGA  300
G32A    GGGGACCGGGAATTGGCAGCTGCCTATCGAGAAGTCGCAAAGGAAGTAACTAGGCTGGGA  300
T111A   GGGGACCGGGAATTGGCAGCTGCCTATCGAGAAGTCGCAAAGGAAGTAACTAGGCTGGGA  300
V113A   GGGGACCGGGAATTGGCAGCTGCCTATCGAGAAGTCGCAAAGGAAGTAACTAGGCTGGGA  300
Y114A   GGGGACCGGGAATTGGCAGCTGCCTATCGAGAAGTCGCAAAGGAAGTAACTAGGCTGGGA  300
        ************************************************************

wt      GTAAATAGTGTAGCTATACCTCTCCTCTCCACAGGTGTATACTCAGGAGGGGAAAGACAGG  360
G32A    GTAAATAGTGTAGCTATACCTCTCCTCTCCACAGGTGTATACTCAGGAGGGGAAAGACAGG  360
T111A   GTAAATAGTGTAGCTATACCTCTCCTCTCCGCAGGTGTATACTCAGGAGGGGAAAGACAGG  360
V113A   GTAAATAGTGTAGCTATACCTCTCCTCTCCACAGGTGCATACTCAGGAGGGGAAAGACAGG  360
Y114A   GTAAATAGTGTAGCTATACCTCTCCTCTCCACAGGTGTAGCCTCAGGAGGGGAAAGACAGG  360
        ******************************* ****** *  *******************

wt      CTGACCCAGTCACTGAACCACCTCTTTACAGCCATGGACTCGACGGATGCAGACGTGGTC  420
G32A    CTGACCCAGTCACTGAACCACCTCTTTACAGCCATGGACTCGACGGATGCAGACGTGGTC  420
T111A   CTGACCCAGTCACTGAACCACCTCTTTACAGCCATGGACTCGACGGATGCAGACGTGGTC  420
V113A   CTGACCCAGTCACTGAACCACCTCTTTACAGCCATGGACTCGACGGATGCAGACGTGGTC  420
Y114A   CTGACCCAGTCACTGAACCACCTCTTTACAGCCATGGACTCGACGGATGCAGACGTGGTC  420
        ************************************************************

wt      ATCTACTGCCGCGACAAAGAATGGGAGAAGAAAATATCTGAGGCCATACAGATGCGGACC  480
G32A    ATCTACTGCCGCGACAAAGAATGGGAGAAGAAAATATCTGAGGCCATACAGATGCGGACC  480
T111A   ATCTACTGCCGCGACAAAGAATGGGAGAAGAAAATATCTGAGGCCATACAGATGCGGACC  480
V113A   ATCTACTGCCGCGACAAAGAATGGGAGAAGAAAATATCTGAGGCCATACAGATGCGGACC  480
Y114A   ATCTACTGCCGCGACAAAGAATGGGAGAAGAAAATATCTGAGGCCATACAGATGCGGACC  480
        ************************************************************
```

Figure 4.18 Sequencing of the macro domain mutant genomes from infected C6/36 cells. Corresponding RNA to Figure 4.16 was reverse transcribed to form cDNA and used as the template to amplify a macro domain containing DNA fragment via PCR. (A) Resulting PCR fragments were electrophoresed on a 1% agarose gel to ensure correct size and quality. (B) Samples containing the correct PCR fragment were sequenced via consensus Sanger sequencing by GeneWiz. Resulting sequences were aligned with wt using Clustal Omega. Mutant nucleotides highlighted in blue.

4.3 Discussion

4.3.1 The macro domain is essential for CHIKV replication

In this research, it has been demonstrated that the CHIKV nsP3 macro domain is essential for viral replication. In all cell lines, including both mammalian and mosquito, a single point mutation of G112A abrogated CHIKV replication, except in C2C12 cells at 48 h where it was capable of replicating to extremely low levels. Other mutants such as D10A and V113A exhibited low or no replication in all cell lines. This highlights that a functional macro domain is essential for efficient replication of CHIKV in both mammalian and mosquito cells.

4.3.2 The different macro domain mutants produced a range of replicative phenotypes

Here, the replicative phenotypes of a panel of mutations within the CHIKV nsP3 macro domain were assessed in a range of cell lines. In the literature, several publications have made a similar panel of mutants and assessed the biochemical properties of these mutants. A summary of this data is shown in Table 4.1. Results from the infectious virus in Huh7 cells have been omitted from this table as, despite some replication from T111A and Y114A, all mutants were reduced at all time points to the same significance.

It is of note that, regardless of cell line the mutant CHIKV RNA was transfected into, all virus samples were ultimately titred by plaque assay on BHK cells. Therefore these results may be affected by the ability of the mutant to replicate in BHK cells. However, in most cases, the qRT-PCR and western blot data largely corresponded with the virus titres indicating that the limitation of cell line for virus quantification was not significantly altering the results.

		wt	D10A	G32A	T111A	G112A	V113A	Y114A
Replicon replication (Huh7)		wt	<wt	<wt	<wt	<wt	>wt	>wt
Replication in mammalian cells	BHK	wt	<wt	~wt	~wt	ND	<wt	~wt
	C2C12	wt	<wt	~wt	~wt	>wt	<wt	~wt
Replication in insect cells	U4.4	wt	ND	~wt	~wt	ND	ND	~wt
	C6/36	wt	<wt	~wt	~wt	ND	<wt	<wt
Mutation maintained?*		-	NT	Yes	Yes	NT	Yes	Yes
ADPR binding (k_D)		22.9	ND	21.0	71.4	ND[+]	6.46[^]	4.84
Hydrolase activity (% wt)		100	16.1	75.3	64.1	3.7[+]	15.0[^]	40.6
Phosphatase activity		wt	<wt	NT	NT	NT	NT	ND
RNA binding		wt	~wt	NT	NT	NT	NT	<wt

Table 4.1 Summary of the replicative phenotypes and known biochemical properties of the macro domain mutants. ND= none detected. NT = not tested / unable to test. ADPR binding and hydrolase activity data taken from McPherson *et al.,* 2017. Phosphatase activity and RNA binding data taken from Malet *et al.,* 2009, where, instead of G112A and V113A, mutations of [+]G112E and [^]V113R were assessed.

The D10A mutation in the CHIKV nsP3 macro domain was first assessed by Malet *et al.*, 2009, where it was demonstrated that this mutation had a significantly reduced ability to bind ADP-ribose, though only a small reduction in phosphatase activity, and RNA binding capabilities similar to the wt macro domain. It has also been shown that the D10A mutation decreases the hydrolase capability of the CHIKV macro domain (McPherson *et al.*, 2017). In this study, this mutant consistently replicated at a lower level than wt in replicon and virus in most cell lines and was did not produce any infectious virus in either Huh7 or

U4.4 cells. This implies that RNA binding and phosphatase activity are less important for the role of the macro domain in virus replication than ADPR binding and hydrolase activity. It was not possible to sequence the RNA resulting from D10A-transfected cells to assess whether the production of infectious virus by D10A mutant was due to reversion, most likely due to low levels of virus RNA. However, the differences in replication in BHK cells between the ICA and the 24 and 48 h titres indicates that it is probable that reversion or a compensatory mutation did occur. In addition, other studies have shown that virus produced with D10A mutant RNA had reverted to wt (McPherson *et al.*, 2017).

The G32 residue is highly conserved across the macro domains of many species. It was therefore unsurprising that, the replicon system, G32A exhibited poor RNA replication. However, in infectious virus, the G32A mutant was able to replicate at approximately wt levels in all cells except Huh7 cells. In C2C12, U4.4. and C6/36 cells, it was shown that this mutation was maintained in infection. This discord between the results from the replicon and infectious virus experiments indicates that the nsP3 macro domain may have roles required for virus production other than in RNA replication. Other studies have shown that the biochemical properties of the G32A mutant are not dissimilar to wt, with similar affinity for ADPR and only a slightly decreased level of hydrolase activity as shown in Table 4.1. As alanine and glycine are both hydrophobic residues with very little difference in structure, it is likely that this substitution mutation had very little effect on the structure or function of the macro domain. Other studies have shown that G32A and G32S were both able to replicate and maintain the mutation however, mutation of G32E reverted to wt, possibly due to the domain not tolerating the larger side chain of glutamate compared to the smaller residues of glycine, alanine or serine as indicated by Figure 4.19 (McPherson *et al.*, 2017).
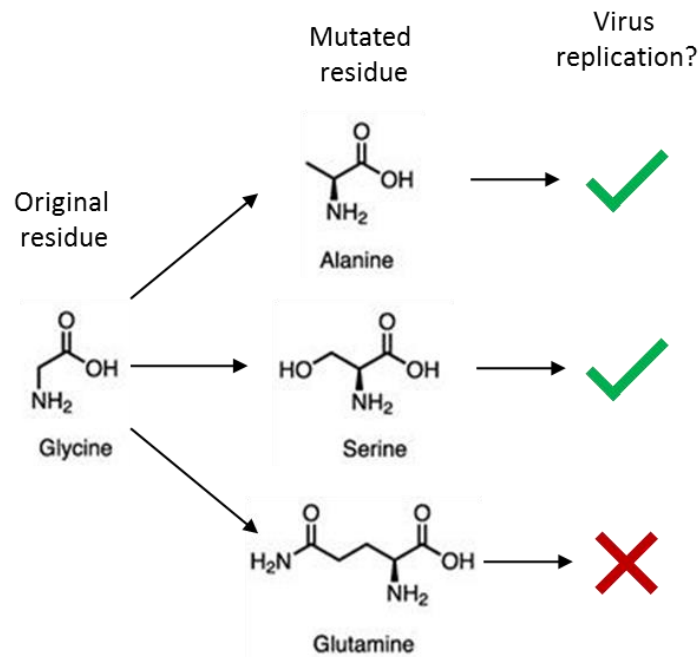
Figure 4.19 Amino acid substitutions at position 32 of the CHIKV nsP3 macro domain. Substitutions with small residues such as with alanine or serine are tolerated, able to produce virus and, in the case of G32A, are maintained, but larger residues such as glutamine are not tolerated.

Both the T111A and Y114A mutations behaved similarly to wt across all cell lines. These were the only mutants capable of producing infectious virus in Huh7 cells, although both were significantly reduced from wt titres. Despite their similarities in virus production, other studies have shown the two mutants to possess very different biochemical properties. Y114A had reduced RNA binding to wt when assessed via slot blot, although this study did not assess the properties of the T111A mutant (Malet *et al.*, 2009). It has been shown that T111A possesses weaker ADPR binding than wt, and hydrolase function of 64.1% of wt (see Table 4.1). Conversely, Y114A was shown in this study to have a much higher affinity for ADPR compared to wt and a hydrolase activity of 40.6% of wt. It is surprisingly therefore that these two mutants have a similar replicative phenotype across a variety of cell lines given the differences in their biochemical properties. Particularly when it has been shown that these mutations are maintained in infected cells with no detected reversion or compensatory mutations within the macro domain. The T111A mutant became of particular interest from the IF data as, for all other cell lines and mutants, nsP3 was consistently observed as distinct

cytoplasmic puncta. In contrast, T111A nsP3 puncta were larger, less defined with some diffuse cytoplasmic nsP3. The nuclei of T111A-infected cells became highly distorted, appearing condensed and hollow. It has been shown that nuclei condense and become hollow due to apoptosis (Toné *et al.*, 2007). This may indicate that, in this particular cell line, the T111A nsP3 is enhancing apoptosis, possibly due to an inability to inhibit a cellular process, as no other mutant or wt infected cells exhibited any indicators of apoptosis via IF at the 24 h time point.

The glycine residue at position 112 was selected for mutagenesis as, similar to G32, it was highly conserved across the macro domains of many species. Both G32A and G112A behaved similarly in the replicon system, both replicating RNA to significantly reduced levels. However, in contrast to G32A, the G112A substitution had a detrimental effect on viral replication in the infectious system. The G112A mutant was unable to produce virus in any cell line with the exception of C2C12 cells where, at the 48 h time point, titres of approximately 4.7×10^2 PFU/mL were detected. Unfortunately, it was not possible to determine through sequencing whether this was due to reversion. Other groups have shown that a mutation to glutamine at this position completely obliterated ADPR binding and had extremely low hydrolase activity (3.7% of wt, as shown in Table 4.1) indicating that this residue is important for both ADPR binding and hydrolysis, and therefore unsurprising that this mutant consistently produced no, or very little virus in all cell lines assayed. The G112E mutant also readily reverted to wt (McPherson *et al.*, 2017). It is interesting that a glutamine at this position allowed for enough initial replication to facilitate a reversion event, whereas in this study, a substitution for alanine prevented replication entirely in the majority of cell lines.

Mutant V113A varied the most between cell lines implying that there are some cell-line specific roles of the nsP3 macro domain. In the replicon system in Huh7 cells, V113A exhibited RNA replication that was significantly higher than wt. In the infectious system, V113A produced virus at both 24 and 48 h in BHK and C2C12 cells, although the titres produced by this mutant were much reduced from wt. In Huh7 cells, no virus was produced by the V113A mutant, despite having the highest level of genomic RNA detected via qRT-PCR of all the mutants. This data combined again indicates an additional role for the macro

domain, separate to RNA replication, which is required to produce infectious virus. In mosquito cell lines, the V113A mutant is interesting as it did not produce any detectable virus in U4.4 cells but was only slightly reduced from wt in C6/36 cells, again implying cell-line specific functions. This could again indicate that the macro domain may be involved in RNAi suppression as U4.4 cells, where this mutant was unable to replicate, have an intact RNAi pathway yet C6/36 cells do not.

4.3.3 Elucidating the function of the macro domain in CHIKV replication

4.3.3.1 ADP-ribose binding of the macro domain is required for efficient virus replication

Comparing the replicative phenotypes of the macro domain mutants determined in this project to the biochemical data from the literature (summarised in Table 4.1), implies that ADPR binding is the most important aspect of the CHIKV macro domain to facilitate virus replication. The two mutants with no detectable ADPR binding, D10A and G112A, were the two mutants that consistently produced either significantly reduced virus titres or no virus at all. It is unfortunate that it was not possible to determine whether the virus produced by these two mutants was a result of a reversion. Data from other groups implies that this may have been the case as McPherson *et al.*, 2017 demonstrated that virus produced by D10A and G112E RNA was a result of reversion to the wt sequence.

Hydrolase activity also appears important for the function of the macro domain as those with the lowest activity were again, poor at producing virus, including D10A, G112A and V113A. However, there appears to be less correlation between replication and hydrolase activity than there was for replication and ADPR affinity. V113A was able to replicate to wt levels in BHK cells, was reduced in C2C12 and C6/36 cells and was unable to produce any virus in U4.4 cells. This implies that either the hydrolase activity is less important for virus replication or it is required but in a cell-specific manner. However it is important to highlight that hydrolase activity was only assayed for a V113R mutant (McPherson *et al.*, 2017) , although it is likely that the V113A mutant also abrogates this enzymatic activity. The Y114A mutant has been shown to possess a hydrolase activity of

just over 40% of wt yet, in most cell lines used here, was shown to have replication comparable to wt, indicating that CHIKV can tolerate reduced hydrolase activity to produce infectious virus.

It has been suggested in the literature that the ADPR 1"–phosphatase activity is unlikely to be the primary function of viral macro domains. Other viral macro domains such as the wt SARS-CoV and SFV macro domains possess no phosphatase activity indicating that this enzymatic activity is not required for viral replication (Egloff *et al.*, 2006; Malet *et al.*, 2009). The data shown here is in agreement with the literature as the Y114A mutant, which was shown to have poor ADPR 1"–phosphatase activity by Malet *et al.*, 2009, replicated to wt levels in almost every cell line tested. Conversely, the D10A mutant, with only slightly decreased phosphatase activity from wt, consistently replicated to either significantly reduced levels or was unable to produce any virus.

4.3.3.2   The macro domain does not affect cellular distribution of nsP3

From the IF data, staining for nsP3 for all the macro domain mutants in both Huh7 and C2C12 cells, it would appear that none of the macro domain mutants induce any significant relocalisation of nsP3 as nsP3 remained cytoplasmic and punctate. This indicates that, for the replicative phenotypes observed, it is not the result of re-localisation of nsP3. This is in agreement with the literature where it has been shown that the HVD is responsible for nsP3 cellular localisation, not the macro domain or the AUD (Fros *et al.*, 2012). However, for the majority of mutants that were unable to replicate, unlike wt nsP3, very few mutant puncta were observed in the perinuclear region of the cell. This may indicate that perinuclear nsP3 puncta only occur in established, or late-stage replication.

4.3.3.3   Possible roles for the macro domain in countering cellular innate immunity

Although the majority of the macro domain mutants exhibited consistent replication between the two different mosquito cells lines, both D10A and V113A differed, implying cell-specific functions of the CHIKV macro domain. Both the D10A and V113A mutants were able to produce virus, to a reduced level, in C6/36 cells but not in U4.4 cells. C6/36 cells have been shown to have an inactive RNAi pathway, due to a frame shift mutation in Dicer2 (Brackney *et al.*,

2010). Therefore, since D10A and V113A virus cannot replicate in U4.4 cells but can produce virus in C6/36 cells, this indicates that the nsP3 macro domain may play a role in RNAi inhibition to allow viral replication. It has been shown that the RNAi pathway is activated in mosquitos upon CHIKV infection (Morazzani *et al.*, 2012) and that an inhibition of the RNAi pathway in infected mosquito cells enhanced CHIKV replication and virus production (McFarlane *et al.*, 2014). The expression of the nsP3 macro domain was found to inhibit the RNAi pathway in Sf21 cells, a cell line derived from *Spodoptera frugiperda* (the fall armyworm), and that certain mutations (though none that correspond with the mutants shown here) can disrupt the ability of the nsP3 macro domain to exert this inhibition (Mathur *et al.*, 2016). The specific mechanism of this function was not elucidated, however this study suggested that it is the RNA binding capability of the macro domain that facilitated this inhibition. However, no studies to date have confirmed this macro domain mediated inhibition in an infectious virus system or in a mosquito cell line.

It has been shown previously that nsP3 macro domain mutants possessing wt ADPR affinity but reduced hydrolase activity were able to form replication complexes and support early stage virus replication in CHIKV-infected neuronal cells. However, host translational shut off occurred earlier than for wt CHIKV (Abraham *et al.*, 2018). In this publication Y114A is used as an example mutant, and here our data is somewhat in agreement with this as in C2C12 cells, Y114A produces high titres, comparable to wt but is reduced at 48 h, possibly due to the early onset of apoptosis. However, Y114A exhibited very different levels of replication across time points in other cell lines, again highlighting that cell specific functions may be occurring. The early onset of host translational shutoff in cells transfected with Y114A CHIKV RNA may suggest a role for the macro domain in inhibition or subversion of the innate immune response in mammalian cells.

4.3.4 Chapter summary

In this study, six residues were selected for mutagenesis in the ADPR-binding pocket of the CHIKV nsP3 macro domain. These mutants were individually engineered into the infectious CHIKV system and their replicative phenotypes assessed in a range of mammalian and mosquito cell lines.

From the six mutations assessed, a range of phenotypes were observed, some mutants were unable to produce virus, or able virus to levels significantly lower than wt, indicating the importance of the CHIKV nsP3 macro domain for efficient viral replication.

Some mutations highlighted there may be cell-specific roles for the macro domain, such as V113A which replicated to a reduced level in BHK and C2C12 cells but did not replicate in Huh7 cells. In addition, this mutant replicated to levels slightly reduced from wt in C6/36 cells, which have an inactive RNAi pathway, but was unable to produce virus in U4.4 cells. This, in agreement with the literature, highlights a possible role for the nsP3 macro domain in inhibition of the insect innate immunity RNAi pathway.

When comparing the replicative phenotypes of the macro domain mutants to the biochemical analysis published by others, it appears that the ADPR-binding ability of the nsP3 macro domain is most important for replication. Mutants that had no detectable ADPR binding corresponded to low or undetectable levels of replication.

In agreement with the literature, it appears that the ADPR 1"–phosphatase activity is not important for CHIKV replication as mutant Y114A, shown in the literature to have no detectable phosphatase activity consistently replicated to approximate wt levels in most cell lines assessed here.

Chapter 5 Inhibition of the NFκB pathway by CHIKV nsP3

5.1   Introduction

In response to viral infections, the first line of defence of cells are the innate immunity pathways. Many of these pathways have been shown to be crucial to limiting damage caused by viral infections and prevent spread of viruses to surrounding cells (Haller *et al.* 2006).   However, many viruses have developed strategies to combat and subvert these pathways in order to continue replicating in cells.

In the case of CHIKV, it is known that infection of cells induces a robust interferon (IFN) response in humans, which has also been shown to be crucial to survival of mice infected with CHIKV (Schilte *et al.*, 2010). However, little has been reported on other antiviral pathways in the context of CHIKV infection.

Like most viruses, Alphaviruses have developed multiple strategies to counteract the innate immune response. CHIKV nsP2 has been shown to inhibit JAK-STAT signalling, an early stage in the exogenous IFN signalling pathway (Fros *et al.*, 2010). In addition, nsP2 has also been shown to induce host-translational shutoff in infected cells, shown to be a result of the degradation of Rpb1 – a catalytic subunit of the cellular RNA polymerase II (Akhrymuk *et al.*, 2012; Fros *et al.*, 2013). In the case of VEEV, the 5' UTR has been shown to be capable of altering the binding and function of IFIT-1 (interferon induced protein with tetratricopeptide repeats 1), a protein normally capable of binding viral capped RNAs and preventing their translation (Hyde *et al.*, 2014). There is much evidence that the 5' UTRs of other alphaviruses, including CHIKV, have similarly important antiviral activity (Hyde *et al.*, 2015; Reynaud *et al.*, 2015).

The only anti-immune function reported to date for nsP3 is the interaction with G3BP. This interaction, as previous discussed in section 1.2.5.5 is thought to sequester G3BP and prevent it from forming functional cytoplasmic stress granules (Fros and Pijlman, 2016). When this interaction was lost through deletion of 30 aa of the HVD of nsP3 in SINV, virus replication was greatly reduced (Varjak *et al.*, 2010). Though it is debateable whether this interaction is purely to prevent the formation of stress granules as it has been shown that the interaction with G3BP is critical for the formation of replication complexes and for RNA replication (Kim *et al.*, 2016). Therefore this interaction may be more to

exploit G3BP for replication, rather than the prevention of stress granule formation.

From the results of the mutagenesis studies in chapter 4, many of the defective macro domain mutants seemed to exhibit their defective phenotype at or after 6 hpt. This indicated that there may be some part played by the innate immune system, which can take up to 4 h for pathways to become fully activated in order to exhibit their effects (Janeway, 2001). Looking specifically at what role the macro domain may play in antagonising the innate immune response, attention was drawn to the NFκB pathway as it has recently been demonstrated that ADP-ribosylation plays a regulatory role in this pathway. It was therefore hypothesised that nsP3 may be able to interact with these ribosylated proteins and therefore interfere with the NFκB pathway.

A mono-ribosyltransferase; ARTD10 (ADP-ribosyltransferase diphtheria toxin-like 10, also known as PARP10) has been shown to be capable of regulating the NFκB pathway as over expression of ARTD10 prevented the nuclear translocation of NFκB, which is required in order for the expression of NFκB dependent genes (Verheugd et al., 2013). Further investigation demonstrated that this inhibition was a result of ARTD10 mono-ADP-ribosylating NEMO (NFκB essential modulator) also referred to as IKK-γ, a component of the IKK complex central to the NFκB pathway.

The IKK complex is comprised of three proteins; IKKα, IKKβ, and IKKγ/NEMO. An active IKK complex is required for two key phosphorylation steps in the NFκB pathway. As indicated by Figure 5.1, the IKK complex phosphorylates IκB. IκB is normally bound to NFκB/p105 to keep it inactive in the cytoplasm. When phosphorylated by the IKK complex, it is removed and targeted for degradation, freeing NFκB in the cytoplasm (Solt and May, 2008). The second, essential phosphorylation step is that of NFκB. The IKK complex phosphorylates the NFκB protein complex in the cytoplasm which is required for protein interactions to facilitate the nuclear translocation of NFκB (Dong et al., 2010).

As summarised in Figure 5.2, ARTD10, prevents the formation of an active IKK complex by ADP-ribosylating NEMO, which prevents NEMO from being poly-ubiquitinated, keeping NEMO in an inactive state. When inflammation is

required, the cellular protein MacroD2 (macro domain containing protein 2) antagonises ARTD10 by the removal of the ADPR from NEMO, allowing poly-ubiquitination and the formation of an active IKK complex. This results in the downstream signalling of the NFκB pathway and activation of an antiviral state (Chen, 2012; Feijs *et al.*, 2013). Mutations in both ARTD10 and MacroD2 results in dysregulation of inflammation and chronic diseases such as cancer and autoimmune related conditions (Khong *et al.*, 2016; Sakthianandeswaren *et al.*, 2018).
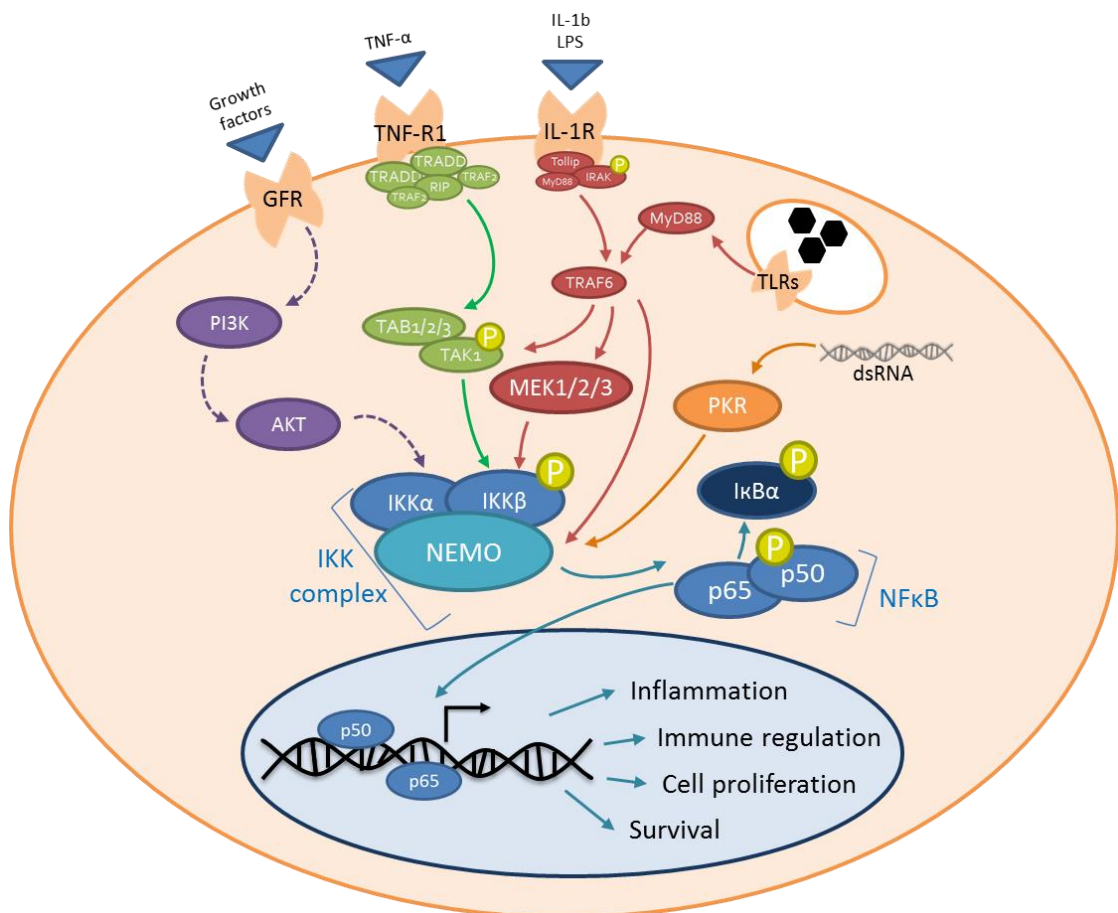
Figure 5.1 Overview of the NFκB pathway. There are multiple stimuli that trigger the NFκB pathway through various sensors and receptors. Regardless of activation, the pathway converges on the central IKK complex that is required to phosphorylate, and therefore remove, IκB from NFκB (p105), revealing the nuclear localisation signal of p105. The IKK complex also phosphorylates NFκB to allow translocation to the nucleus where it acts as a transcription factor for various inflammatory and antiviral genes. Original figure interpreted from Perkins, 2006; Hayden and Ghosh, 2008; Napetschnig and Wu, 2013.
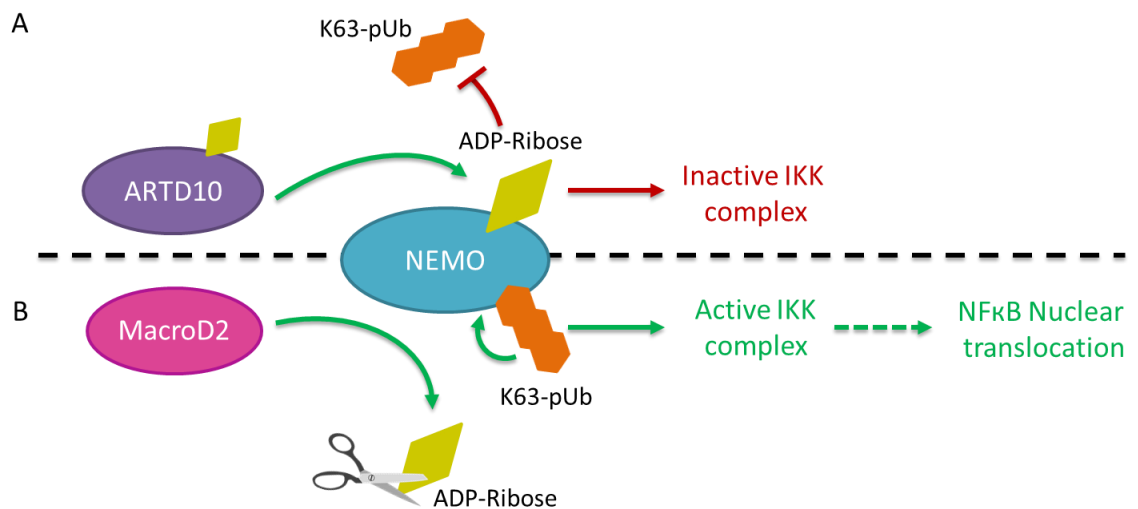
Figure 5.2 Regulation of NEMO by ADP-ribosylation. (A) ARTD10 mono-ribosylates NEMO, which prevents it being poly-k63 ubiquitinated. This prevents an active IKK complex from forming therefore the NFκB pathway does not continue. (B) When the pathway is triggered, the cellular protein MacroD2 is able to hydrolyse the ADP-ribose from NEMO, allowing poly-K63 ubiquinitination, allowing formation of an active IKK complex, allowing downstream effects of the NFκB pathway Original figure interpreted from Verheugd *et al.*, 2013.

More recently it has been shown that, *in vitro*, the CHIKV nsP3 macro domain can remove mono-ADP-ribose from ARTD10 and NEMO as well as multiple other MARlysated substrates tested (Eckei *et al.*, 2017). Though it is yet unclear whether nsP3 hydrolyses these proteins *in vivo.*

To date, the only paper that investigates the NFκB pathway in CHIKV infection showed that CHIKV decreased NFκB activation through increased expression of miR-146a, though the precise mechanism of the upregulation of this particular miRNA by CHIKV is unknown (Selvamani *et al.*, 2014). MicroRNA-146a is known to inhibit the NFκB pathway though a negative feedback loop. This miRNA is associated with many autoimmune diseases, including rheumatoid arthritis where it has also been detected in the synovial fluid patients (Xu *et al.*, 2012). Though it is unclear how miRNA-146a contributes to inflammation in these diseases.

Studies have shown that CHIKV infection can be detected by toll-like receptor 3 (TLR3) in endosomes and that this sensing was crucial to forming an effective

neutralising antibody response (Her *et al.*, 2015). TLR3 is capable inducing both the NFκB and IFN pathways upon detection of dsRNA (Jiang *et al.*, 2004; Uematsu and Akira, 2007).

VEEV has been shown to activate the NFκB pathway, and that IKKβ, a component of the IKK complex, enhances the replication of the virus, though the precise mechanism of this is unknown (Amaya *et al.*, 2014). In RVFV, the IKK complex has also been shown to enhance viral replication and it is thought that the complex is modified in order to phosphorylate the non-structural proteins of the virus (Narayanan *et al.*, 2012).

5.1.1 Aims

This chapter address two main aims. Firstly, due to the limited information in the literature, to further investigate the role of the NFκB pathway in CHIKV infection. Following this, we aimed to investigate whether the CHIKV nsP3 was able to disrupt or affect the NFκB pathway. Additionally, to determine whether interactions between the nsP3 macro domain and ADP-ribosylated components of the pathway were the cause of any observed disruption to the NFκB pathway.

5.2 Results

5.2.1 Part 1 – CHIKV infection and the NFκB pathway

5.2.1.1 Optimisation of the NFκB dual-luciferase reporter system

Initially, it was sought to confirm previous findings by Selvamani *et al.,* 2014 that CHIKV did not activate the NFκB pathway using our infectious system. Therefore a two-plasmid reporter system was utilised, similar to that used by Selvamani *et al.,* As shown in Figure 5.1 A: firstly, a Firefly luciferase under control of a NFκB-sensitive promoter (referred herein by NFκB-Fluc) and a Renilla luciferase (RLuc) under control of a herpesvirus TK promoter as a transfection control (referred herein as pRL-TK), as described by Abdul-Sada *et al.*, 2017.

Initially, optimisation was required of the dual reporter system. A range of cell lines were selected for their suitability with this system but also, ideally, these cells would be relevant to the study of CHIKV. From chapter 3, BHK, C2C12 and Huh7 cells have all been shown to be suitable for their use with CHIKV infectious and replicon systems. In addition, A549 cells were selected as they have been used in previous studies on virus interactions with the innate immune system and are known to have an intact and robust immune response (Hartman, Black and Amalfitano, 2007; Devhare *et al.*, 2013). These four cell lines were transfected with the two reporter plasmids for 16 h prior to activation with TNFα treatment, a well-defined activator of the NFκB pathway (Schütze *et al.*, 1995), or mock treated, for 6 h then lysed and luciferase quantified using a dual-luciferase system. The Firefly signal, induced by activation of the NFκB pathway, was normalised to the Renilla signal from pRL-TK, which is constitutively expressed upon successful transfection.

As shown by Figure 5.3, only the human cell lines; A549 and Huh7, responded to TNFα treatment. The remaining two cell lines, BHK and C2C12 (hamster and mouse cells respectively), failed to respond to treatment, producing very little Fluc signal, at the detection limit of the assay. These cell lines were therefore not considered for further experiments investigating the NFκB pathway.

Others have shown that A549 cells were refractory to CHIKV infection and these cells were also poor replicators of the CHIKV replicon as demonstrated in chapter

3 (Sourisseau *et al.*, 2007; Roberts *et al.*, 2017). Therefore these cells were not used for experiments involving infectious CHIKV. Huh7 cells which have previous been determined to facilitate productive infection (chapter 3, Roberts *et al.*, 2017) and supported the NFκB dual-reporter system, as shown in Figure 5.3, were selected for use in experiments to determine the relationship between CHIKV and the NFκB pathway.
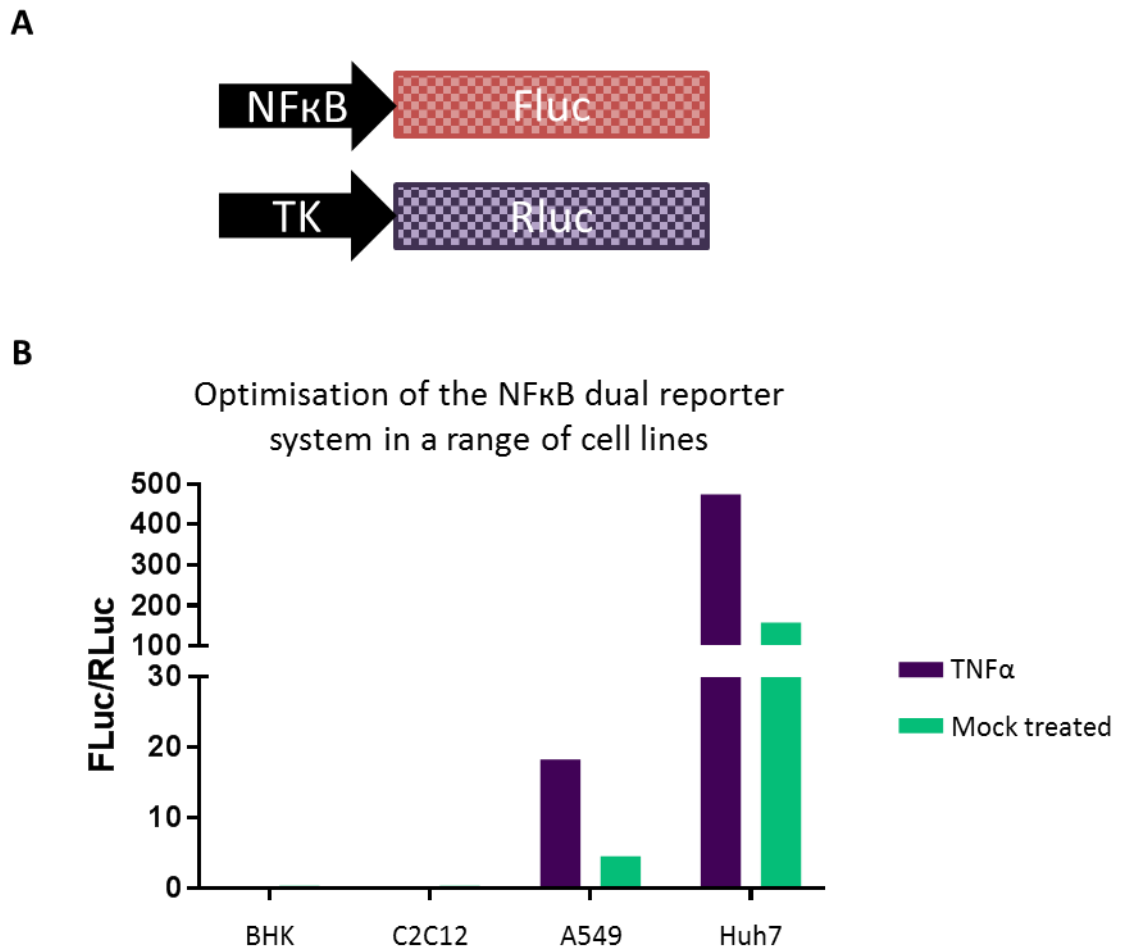
Figure 5.3 Optimisation of the NFκB-Fluc and pRL-TK reporter system. (A) Schematic of the NFκB-Fluc and pRL-TK plasmids. NFκB-Fluc contains a Firefly luciferase under the control of a NFκB sensitive promoter. The pRL-TK plasmid contains a Renilla luciferase under the control of the constitutive human thymidine kinase promoter. (B) A range of cell lines were transfected with the NFκB-Fluc and pRL-TK plasmids at a ratio of 9:1, incubated for 16 h then treated with TNFα (50 ng/mL) or mock treated for 6 h. Cells were lysed and luciferase signal quantified by dual luciferase assay. Data is presented as the Fluc signal (indicating NFκB activation) normalised to the Rluc signal (transfection control).

5.2.1.2 CHIKV infection does not activate the NFκB pathway

To assess whether CHIKV infection activates the NFκB pathway, Huh7 cells were transfected with the NFκB dual reporter plasmids 16 h prior to infection with CHIKV at an MOI of 5 or mock infection. As positive and negative controls, separate populations of cells were TNFα or mock treated. Cells were then lysed over at different times over a 24 h period and luciferase levels assayed using the dual-luciferase system.

As shown in Figure 5.4 B, CHIKV infected cells did not show any increase in the levels of Fluc when compared to mock infected or mock treated cells. TNFα infected cells however, induced high levels of Fluc expression that was detectable by 6 hpt and continued to increase over the 24 h period. To confirm that the CHIKV infected cells were indeed infected, the corresponding cell lysates were used to perform a western blot for nsP3. As shown by Figure 5.4 part C, CHIKV infected cells express nsP3 detectable from 8 hpi, and strongest at 24 hpi with no nsP3 detected in mock infected, TNFα treated, or mock treated cells.
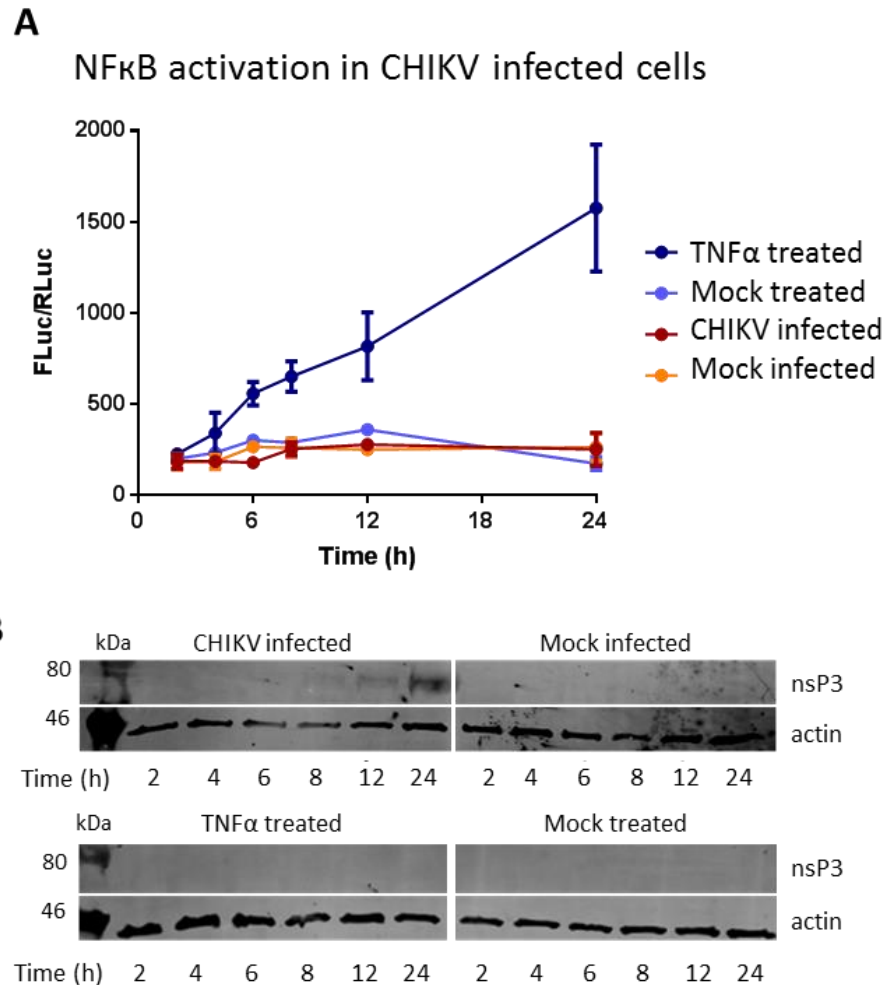
Figure 5.4 CHIKV infection does not activate the NFκB pathway in Huh7 cells. (A) Huh7 cells were transfected with the reporter plasmids 16 h prior to infection (MOI=5), mock infection, TNFα treatment (50 ng/mL) or mock treatment. Cells were lysed at indicated time points and luciferase signal assayed. Fluc signal is normalised to Rluc signal (n=3). (B) Western blot for nsP3 in indicated cells, showing that nsP3 (~58 kDa) was only present in CHIKV infected cells.

To further confirm these results in a more physiological system, the subcellular localisation of NFκB was assessed in infected cells. When the pathway is active, NFκB translocates to the nucleus, a phenomenon that is easily detectable by immunofluorescence. Huh7 cells were therefore infected with CHIKV at an MOI of 5, or mock infected or TNFα treated as a positive control. Cells were fixed at 24 hpi and stained for nsP3 and the NFκB subunit; p65. As shown in Figure 5.5, in agreement with the previous data, CHIKV infected cells (confirmed by positive nsP3 staining), did not show nuclear translocation of p65 to the nucleus, with a

similar appearance to that of mock infected cells. In contrast, TNFα treated cells showed a marked difference with a clear increase in nuclear p65, more so than either the infected or mock infected cells.
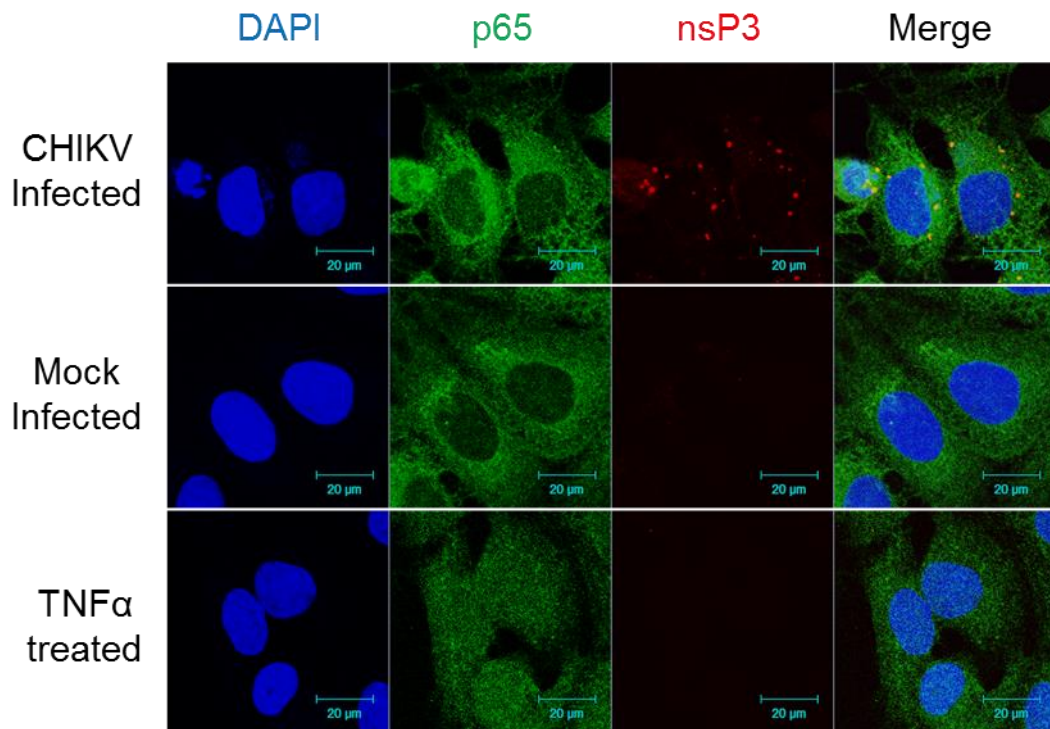
Figure 5.5 NFκB does not translocate to the nucleus in CHIKV infected cells. Huh7 cells were infected with CHIKV (MOI=5), mock infected or TNFα treated (50 ng/mL), fixed at 24 hpi and stained for the NFκB subunit; p65 (green), and nsP3 (red). Nuclear p65 indicates activation of the NFκB pathway.

It is clear from Figure 5.4 and Figure 5.5 that nuclear translocation of NFκB, one of the final stages of the NFκB pathway, does not occur in CHIKV infected cells. It was therefore investigated whether the IKK complex was active in CHIKV infected cells, as the complex has been implicated in VEEV and RVFV replication. Huh7 cells were infected, mock infected or TNFα treated, and cells were lysed over a 6 h time course. IKK complex activation was assessed by western blotting for phosphorylated NFκB (p105), one of the targets of the kinase complex when activated. As shown by Figure 5.6, upon TNFα treatment, phosphorylated p105 appears between 0-15 min post treatment and persists for approximately 60 min. In contrast, CHIKV infected cells exhibited virtually no

phosphorylated p105 throughout the entire 6 h time course, much resembling the mock infected cells. It could be argued that there are extremely faint bands in the CHIKV-infected cells around 30 min post infection. This shows that the IKK complex is either not active (or extremely weakly active) in CHIKV infected cells.
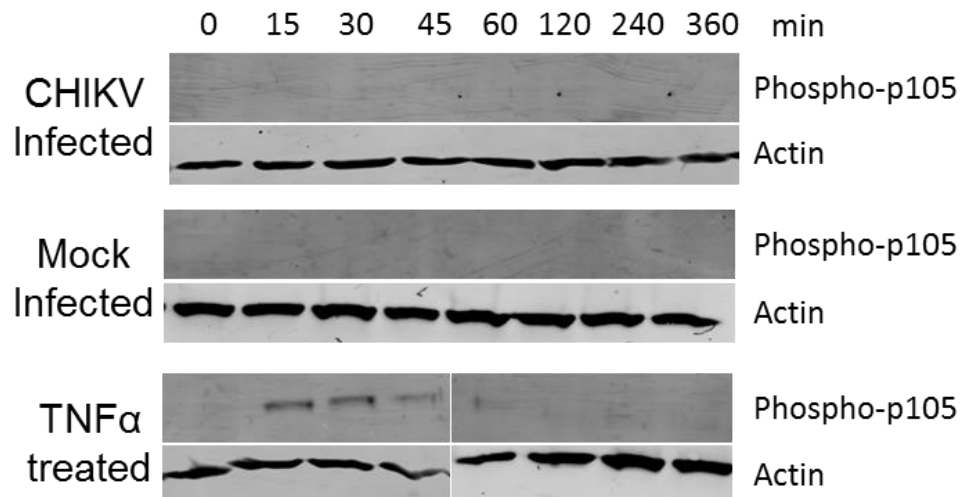
Figure 5.6 The IKK Complex is not active in CHIKV infected cells. Cells were either infected, mock infected or TNFα treated, then lysed over a 6 h time course. Western blotting was then performed for phospho-p105 (~105 kDa, 30 µg lysate/well). The presence of phospho-p105 indicates an active IKK complex.

5.2.1.3   CHIKV infection cannot suppress an activated NFκB pathway

It has been clearly demonstrated that CHIKV does not activate the NFκB pathway but it was unclear to what extent the virus could inhibit the pathway. Therefore, similar experiments to those shown in section 5.2.1.2 were performed but using TNFα treatment and CHIKV infection in combination to assess the ability of CHIKV to inhibit or reduce activation of the NFκB pathway.

Huh7 cells were transfected with the same reporter plasmids as described in Figure 5.4 A, then at 16 hpt were infected or mock infected with CHIKV for 1 h prior to replacing the media with either complete media or media containing TNFα. Cells were lysed over a time course and luciferase assayed using the dual luciferase system. As shown in Figure 5.7 A, there was no significant difference in NFκB activation between cells that were TNFα treated regardless of whether they were infected or mock infected. Similarly, cells that were mock treated

171

exhibited similar levels of NFκB activation regardless of infection. To confirm CHIKV infection, western blots for nsP3 were performed to demonstrate expression in infected cells and not in any other conditions, as shown in Figure 5.7 B.
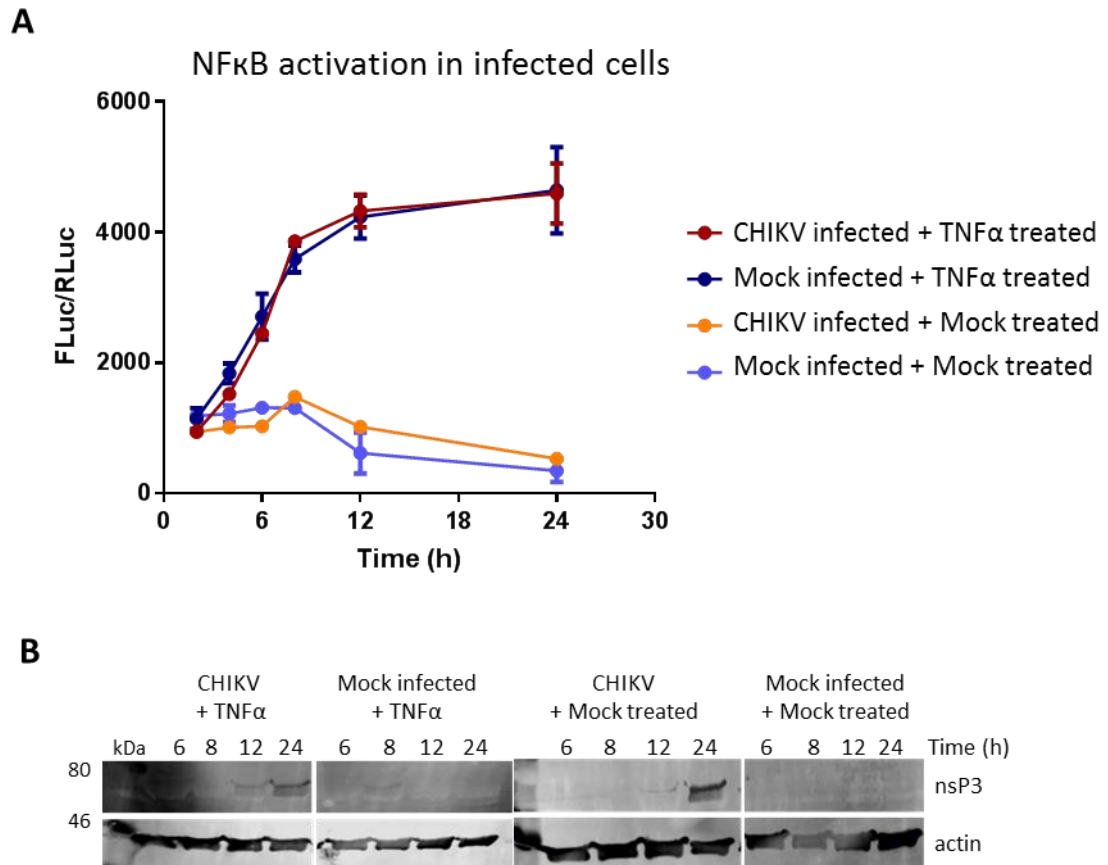
Figure 5.7 CHIKV cannot inhibit TNFα-induced NFκB activation. (A) Cells were transfected with the NFκB-Fluc and pRL-TK plasmids, incubated for 16 h then either infected with CHIKV (MOI=5) or mock infected for 1 h then either TNFα treated (50 ng/mL) or mock treated. Cells were lysed over a 24 h period and luciferase assayed. Data shown as Fluc signal normalised to Rluc (n=3). (B) Western blot for nsP3 on corresponding cell lysates.

These findings were then further confirmed by immunofluorescence. Cells were infected or mock infected with CHIKV at an MOI of 5 for 1 h then media was replaced with either media containing TNFα or normal media, cells were incubated for a further 12 h before fixation and staining for both nsP3 and p65.

As shown by Figure 5.8, for mock treated cells, both infected and mock infected show exclusion of p65 from the nucleus. In the TNFα treated cells, regardless of infection, p65 was shown to have translocated to the nucleus, indicating that CHIKV infection was not able to inhibit the NFκB pathway when activated exogenously.
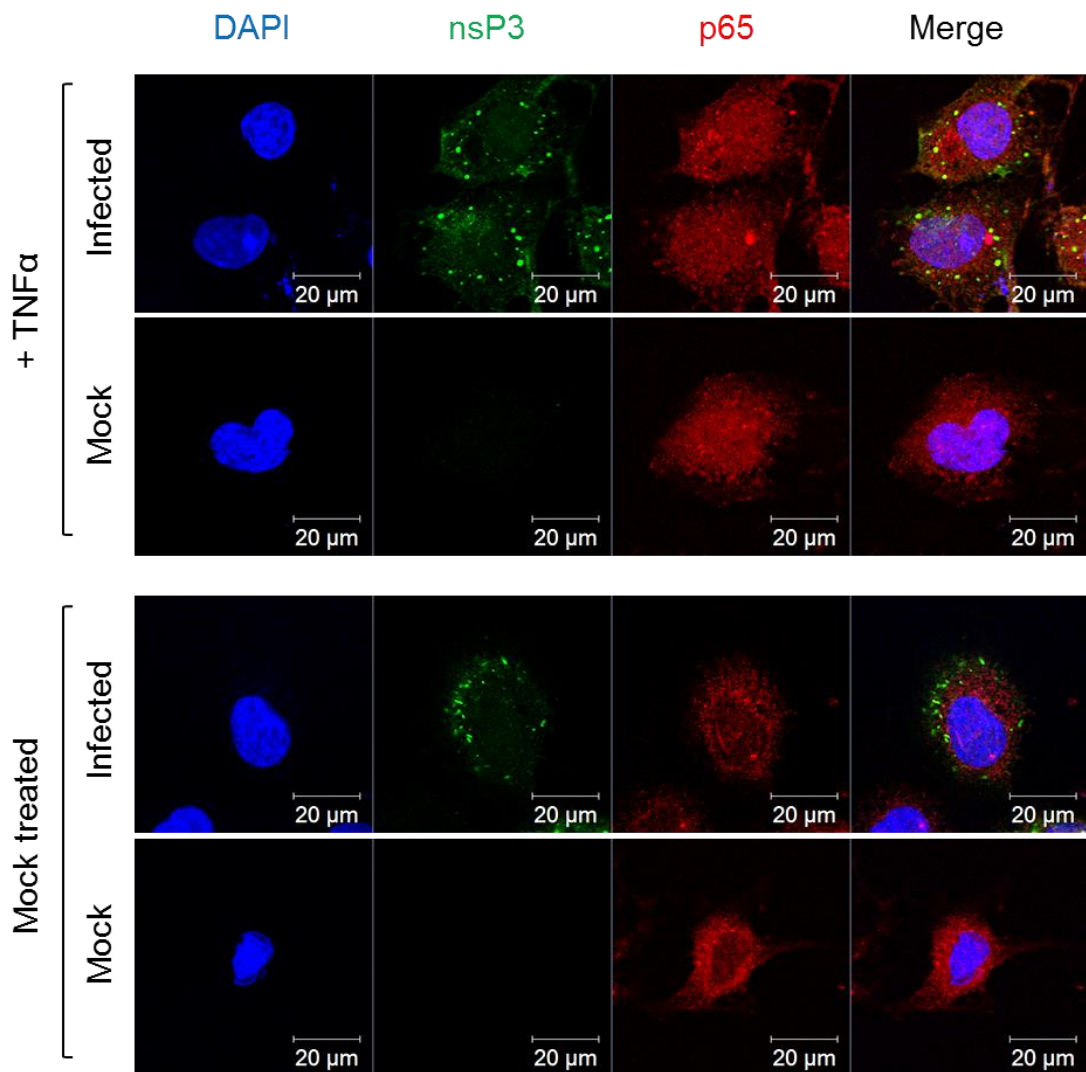
Figure 5.8 CHIKV cannot inhibit TNFα-induced NFκB activation (IF). Cells were infected or mock infected with CHIKV MOI=5 for 1 h, then media replaced with TNFα (50 ng/µL) or normal media. Cells were fixed at 12 hpi and stained for nsP3 (green) and p65 (red). Nuclear localisation of the NFκB subunit p65 indicates an active NFκB pathway.

5.2.1.4   NFκB activation reduces production of CHIKV in infected cells

As it has been shown that CHIKV does not induce the NFκB pathway upon infection and that infection is not able to suppress the pathway if exogenously activated, we sought to determine the effects of an activated NFκB pathway upon production of CHIKV in infected cells. It was hypothesised that, if CHIKV is actively inhibiting the NFκB pathway it must be advantageous to do so, therefore activating the pathway in CHIKV infected cells may reduce virus production.

To determine whether activation of NFκB would affect production of infectious CHIKV, cells were treated with TNFα at either 6 h prior to infection, at the time of infection, or 1 h post infection (as shown in the schematic Figure 5.9 A). Infections were performed at an MOI of 5. Supernatant was harvested at 24 hpi and titred by plaque assay.

As shown in Figure 5.9, TNFα treatment of cells, regardless of time of application, reduced CHIKV titres at 24 hpi. However, this reduction was only significant when TNFα was applied at time of infection, or 1 h post infection. This indicates that CHIKV suppression of the NFκB pathway is required for efficient viral replication. It was confirmed that the pathway was activated at indicated times via IF of p65 on cells treated with TNFα parallel to the infection experiment. Activation of the NFκB pathway was identified via nuclear translocation of p65 as shown in Figure 5.9 C.
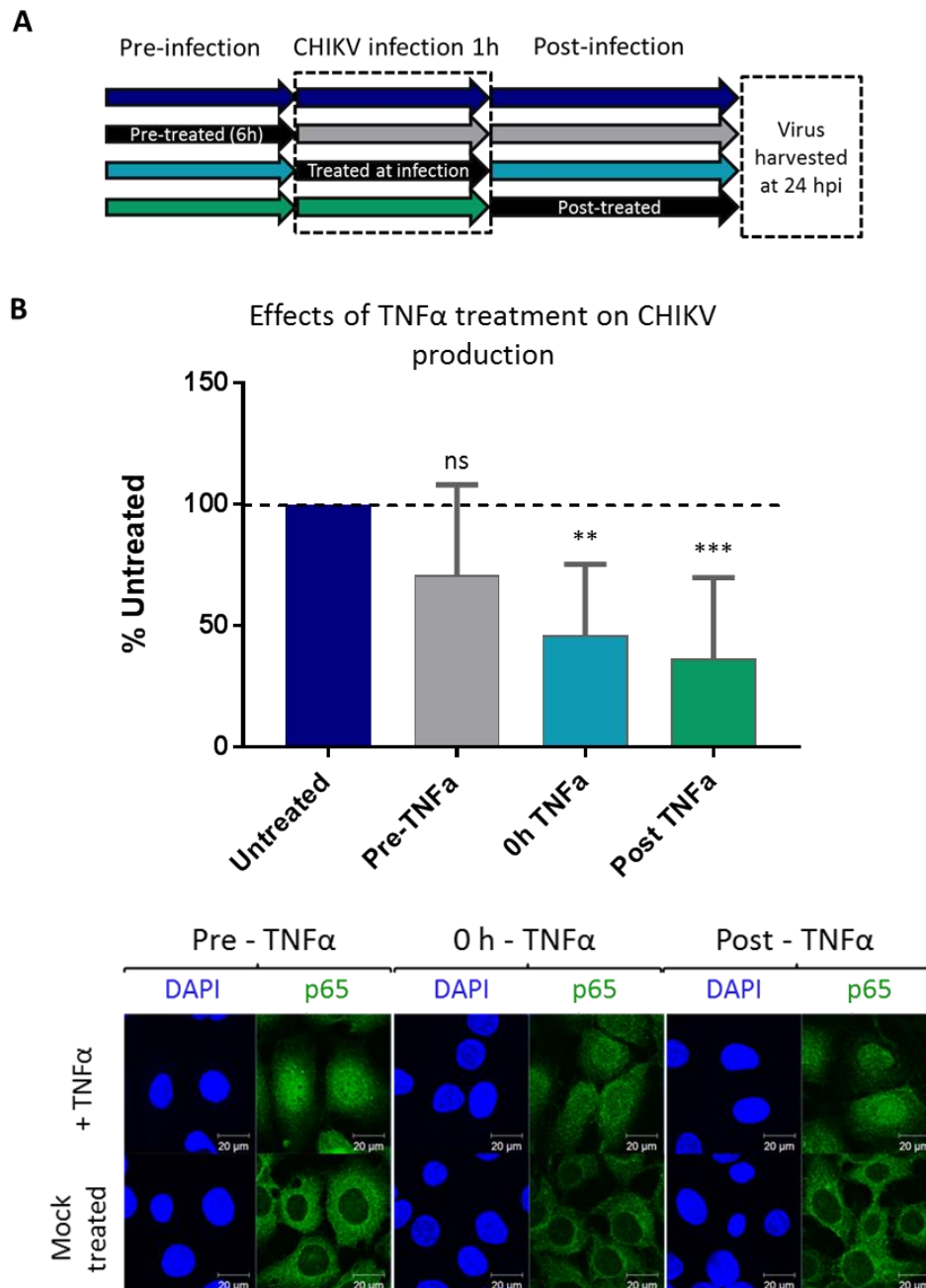
Figure 5.9 Activating the NFκB pathway reduces CHIKV titres. (A) A schematic representing the time scale of the experiment: Huh7 Cells were treated with TNFα either 6 h prior to infection, at the time of infection, or at 1 h post-infection. (B) Cells were infected with CHIKV at MOI=5. Supernatant was harvested at 1 h and 24 h for each sample and titred by plaque assay. Titres for 24 h were normalised to that of the 1 h samples. Data is presented as % of untreated cells (two separate experiments combined, each at n=2 data analysed by One-way ANOVA with Bonferroni correction compared to wt, ns = P > 0.05, * = P ≤ 0.05, ** = P ≤ 0.01, *** = P ≤ 0.001). (C) Cells were TNFα treated in parallel, fixed at 6 hpt and stained for p65 to confirm activation of the NFκB pathway by TNFα treatment.

5.2.2   Part 2 – CHIKV nsP3 inhibits the NFκB pathway

5.2.2.1   Optimisation of nsP3 expression

Now it has been confirmed that CHIKV infection does not activate the NFκB pathway, it was investigated whether nsP3 was specifically involved in inhibition of the pathway. To determine this, an expression construct of nsP3 was generated. As shown in Figure 5.10 part A, wt, untagged nsP3 was cloned into pcDNA3.1+. This was achieved by generating the coding sequence for nsP3 flanked by a start and stop codons, and *BamHI* and *NotI* restriction sites via amplification by PCR. Resulting PCR fragments were then purified via ethanol precipitation and, along with the empty pcDNA3.1+ vector, subjected to restriction digest. Resulting DNA was then separated by agarose gel electrophoresis, the relevant bands extracted and ligated together.
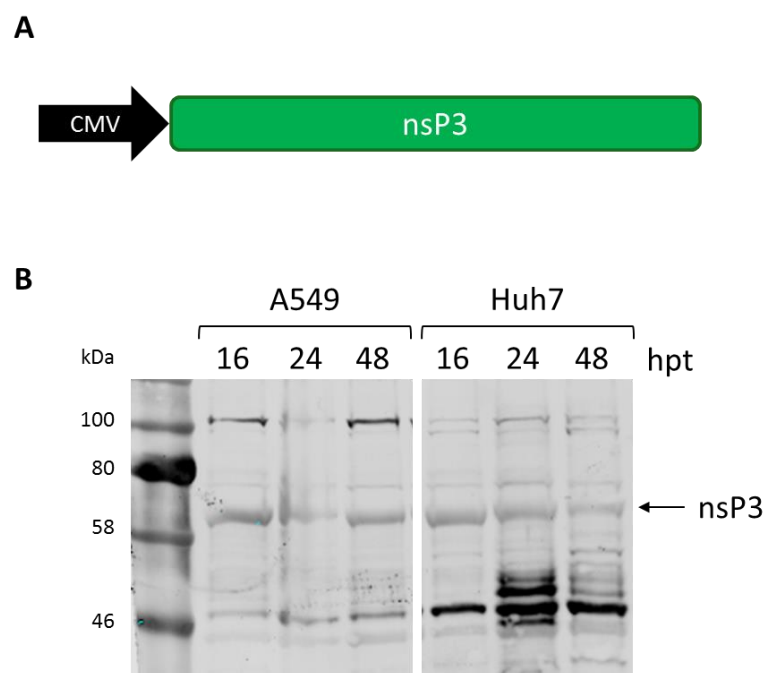
Figure 5.10 Optimisation of nsP3 expression in mammalian cells. (A) A schematic of the nsP3 expression vector with wt, untagged nsP3 in pcDNA3.1+, under the control of a CMV promoter. Herein referred to as pcDNA3.1+ nsP3 (B) A549 and Huh7 Cells were transfected with 1 µg of pcDNA3.1+ nsP3 and cells were lysed at 16, 24 and 48 hpt and western blot performed for detection of nsP3.

To assess the optimal cell line and transfection protocol to use for experiments involving nsP3 expression, in addition to the NFκB dual luciferase reporter

plasmids as shown in Figure 5.3 in section 5.2.1.1, A549 and Huh7 cells were assessed for their expression levels of nsP3 when transfected with pcDNA3.1+ nsP3. Whilst both cell lines exhibited similar levels of nsP3 expression, as shown by the western blot in

Figure 5.10 B, Huh7 cells appeared to have significant degradation of nsP3 whereas A549 cells had very little degradation. Therefore, for the following experiments assessing the effects of nsP3 expression on the NFκB pathway, A549 cells were used. For A549 cells, the optimal time for nsP3 expression was at 16 hpt, therefore for following experiments, cells were transfected and incubated for 16 h prior to downstream applications.

5.2.2.2 nsP3 expression inhibits NFκB activation

To assess whether nsP3 could inhibit the NFκB pathway, A549 cells were transfected with the NFκB reporter plasmids and co-transfected with an expression vector with either wt or D10A mutant nsP3 (a construct generated using the same protocol as wt as described in 5.2.2.1) or empty vector as a negative control. At 16 hpt, cells were treated with TNFα or mock treated. Cells were lysed at 6 h post-TNFα treatment and luciferase assayed via the dual luciferase system. As shown by Figure 5.11 A, expression of wt nsP3 significantly reduced NFκB activation in activated cells. Reduction was also seen at a basal level (in mock treated cells) though this was not statistically significant. In contrast, mutant D10A nsP3 behaved similarly to the empty vector control with no significant difference in NFκB activation between the two.

Despite this assay providing highly reproducible results (Figure 5.11 A is a result of three separate experiments), detection of protein expression in these experiments was difficult and inconsistent. As shown by Figure 5.11 B, when attempting to confirm nsP3 expression in these cell lysates by western blotting, often none, or very little could be detected when compared to a positive nsP3 control (in this case, an infected cell lysate). It has been previously shown that nsP3 is an unstable protein with high turnover, possibly the extended time of the experiment or the presence of additional plasmids was limiting expression or increasing degradation of nsP3. It was therefore decided to tag nsP3 to increase stability of the protein.

A

NFκB activation in nsP3 expressing cells
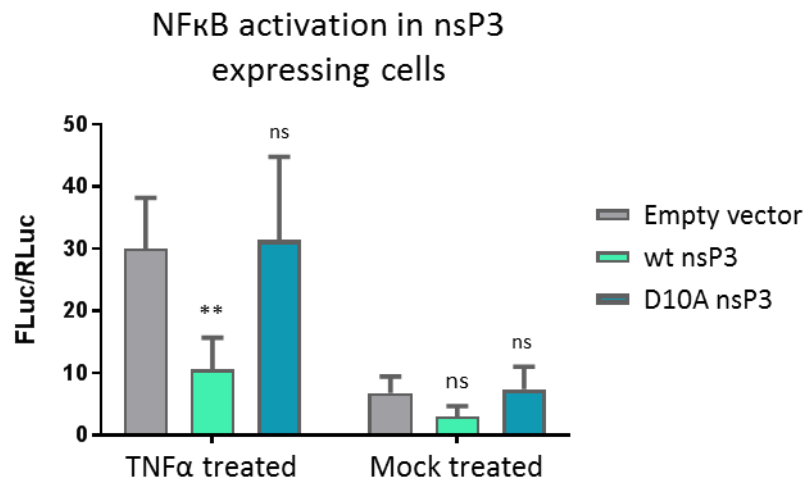
B
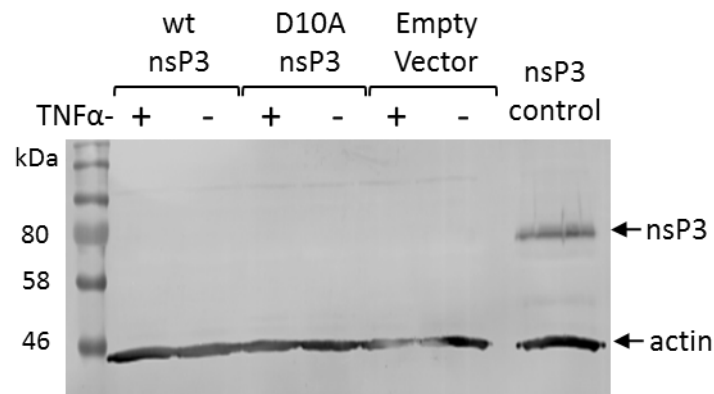
Figure 5.11 wt nsP3 reduces NFκB activation but expression is unstable. (A) A549 cells were transfected with the NFκB-Fluc and pRL-TK plasmids and co-transfected with either pcDNA3.1+ nsP3 wt or D10A or empty pcDNA3.1+ vector. Cells were then TNFα treated (50 ng/mL, activated) or mock treated, prior to lysis at 6 hpt and luciferase levels assayed (two separate repeats combined, each repeat n=3, data analysed by One-way ANOVA with Kruskal-Wallis test and Dunns' correction compared to wt, ns = P > 0.05, * = P ≤ 0.05, ** = P ≤ 0.01). (B) Western blot for nsP3 in transfected cells (30 µg/well). In these experiments, it was challenging to demonstrate consistent nsP3 expression for each replicate.

The first tag used in an attempt to stabilise and better detect nsP3 was ZsGreen. This tag has been used previously in both the CHIKV replicon, and infectious virus with ZsGreen cloned into the engineered *SpeI* site within the HVD of nsP3 (Pohjala *et al.*, 2011) and is well tolerated in both replicon and virus as shown by Remenyi *et al.*, 2018. An expression construct was generated using the same method as described in 5.2.2.1 but with the nsP3-ZsGreen virus template in order to generate a coding sequence of nsP3-ZsGreen that was digested and ligated into the pcDNA3.1+ vector, a schematic of which is shown in Figure 5.12 A. Previous work demonstrated that the presence of the ZsGreen tag within nsP3 had little effect on virus replication (Remenyi *et al.*, 2018). To ensure that the ZsGreen tag did not exhibit any significant differences in the behaviour of nsP3 when expressed in isolation, the newly formed nsP3-ZsGreen construct was transfected into cells, alongside expression constructs of ZsGreen alone and the empty vector as controls and the subcellular localisation assessed by confocal microscopy. As shown by Figure 5.12 B, the cellular localisation of the nsP3-ZsGreen resembled the defined, cytoplasmic punctate appearance of the nsP3 shown previously in both replicon and virus (chapter 3). It was therefore concluded that the addition of the ZsGreen tag in nsP3 did not significantly alter the behaviour of the protein.
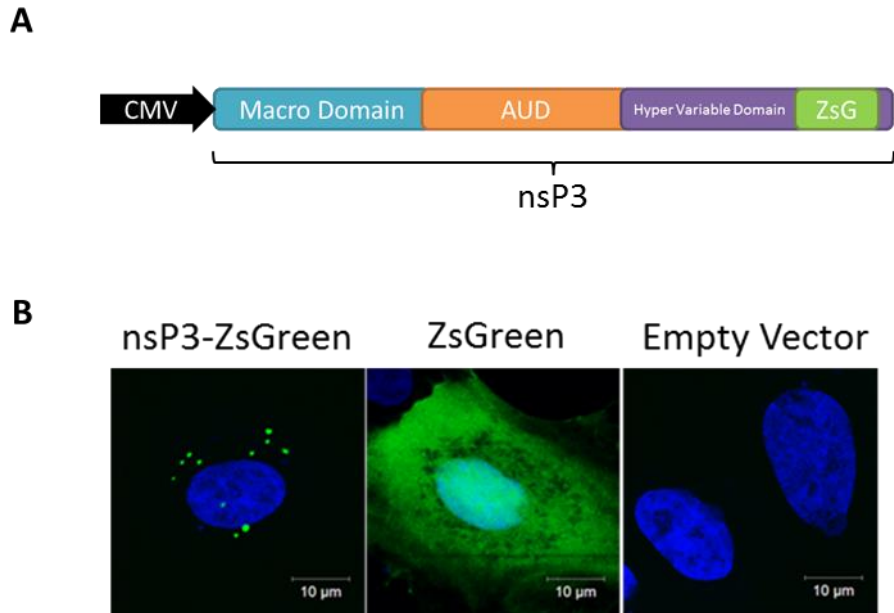
Figure 5.12 An addition of the ZsGreen tag does not affect the cellular localisation of nsP3. (A) A schematic of the ZsGreen tagged nsP3, where ZsGreen is present within the C-terminal HVD of nsP3. (B) Confocal images of A549 cells transfected with an expression vector of either nsP3-ZsGreen, ZsGreen alone or empty vector, cells were fixed and DAPI-stained 16 hpt and imaged via the LSM700 confocal microscope.

This construct was therefore used in further experiments. As shown in Figure 5.13 A and C, successful expression of the nsP3-ZsGreen constructs was easily detectable by wide field fluorescence microscopy and western blot. However, when used in the NFκB reporter plasmid system, the levels of activation had changed from the previous experiment using the untagged nsP3 expression constructs in Figure 5.11. As shown by Figure 5.13 B, the mutant D10A nsP3 exhibited some reduction in NFκB activation in activated cells, and significant reduction of activation at the basal level in mock treated cells.

When performing IF to assess the sub-cellular localisation of p65 it became apparent why the results for the ZsGreen tagged nsP3 constructs (shown in Figure 5.13) differed from those seen previously. As shown in Figure 5.14, when activating cells with TNFα, in the ZsGreen-transfected cells (which should be acting as the negative control), p65 remains cytoplasmic when it should resemble the nuclear appearance of the empty vector-transfected control.

Indicating that ZsGreen alone is capable of inhibiting p65 nuclear translocation and is therefore not a suitable tag for use in these experiments.
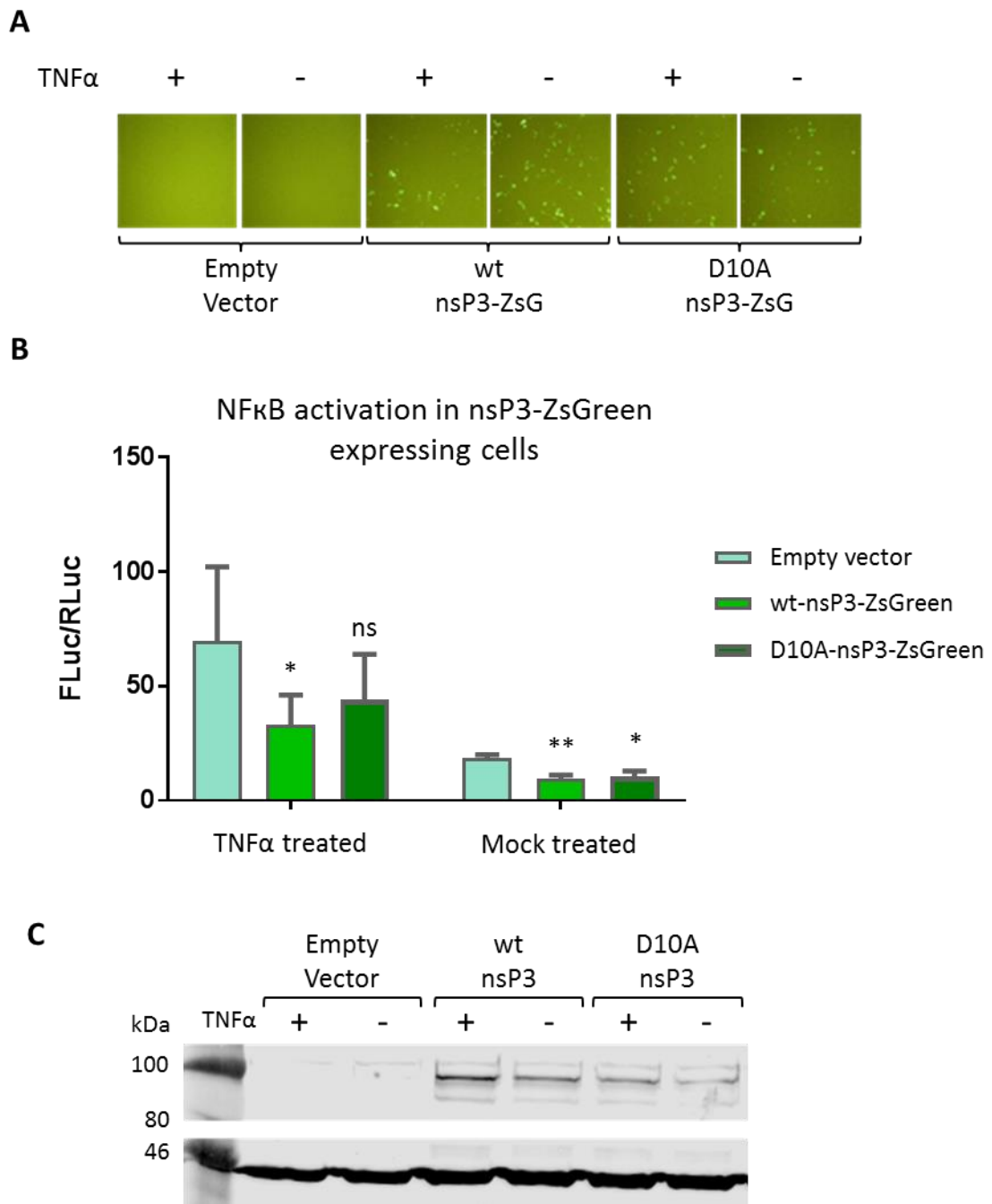
Figure 5.13 Tagging of nsP3 with ZsGreen improved stability, and the detection of the protein. (A) Wide-field fluorescence microscopy of A549 cells transfected with pcDNA3.1+ nsP3 wt, D10A or empty vector, alongside the NFκB reporter plasmids, imaged 16 hpt, prior to activation. (B) Cells were then TNFα treated (50 ng/mL, activated) or mock treated, prior to lysis at 6 hpt and luciferase levels assayed (2 separate repeats combined, each repeat n=3, data analysed by One-way ANOVA with Kruskal-Wallis test and Dunns' correction compared to wt, ns = P > 0.05, * = P ≤ 0.05, ** = P ≤ 0.01). (C) Western blot for nsP3-ZsGreen (~ 85 kDa) for corresponding cell lysates.
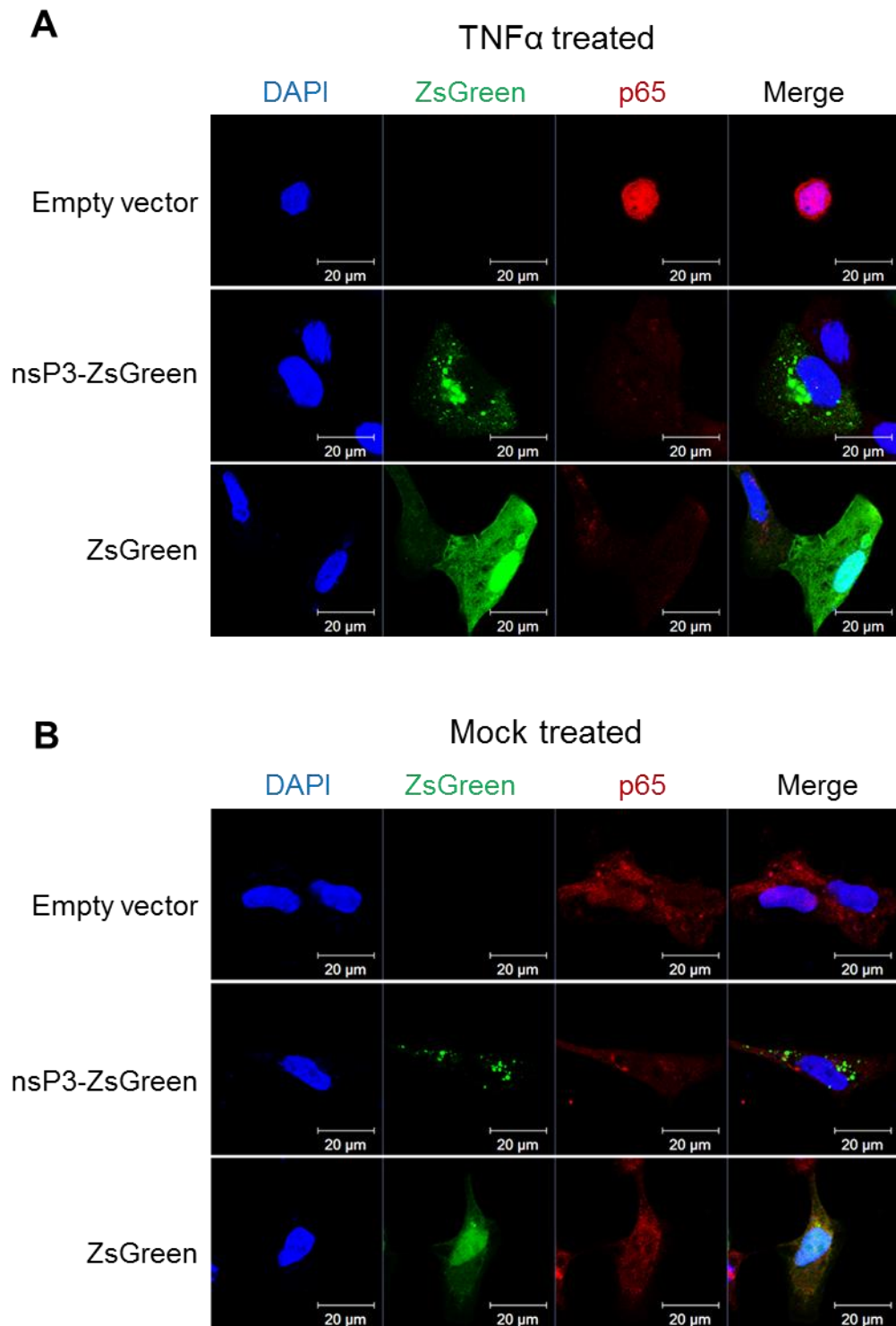
Figure 5.14 Immunofluorescence of p65 with ZsGreen-tagged constructs. Cells were transfected with pcDNA3.1+ either empty vector, nsP3-ZsGreen or ZsGreen alone. At 16 hpt, cells were TNFα treated (A) or mock treated (B) for 6 h prior to fixation and immunofluorescence for p65 performed.

Due to the unsuitability of the ZsGreen tag, it was then considered to use a Flag tag at the C terminal end of nsP3. A Flag tag was suggested due to its short size (8 aa and ~1 kDa) so would be unlikely to affect the function of nsP3 or interfere with cellular pathways.

Prior to using the nsP3-Flag (referred to herein as nsP3-F) construct in experiments, firstly it was important to check that the properties of nsP3-F did not differ to untagged, wt nsP3. Therefore, the nsP3-F and untagged nsP3 expression constructs were transfected into cells alongside the NFκB reporter plasmids, and cells were activated or mock activated as before. As shown in Figure 5.15 A, the behaviour of the Flag-tagged nsP3 protein was similar to that of the untagged nsP3 (when compared to cells transfected with empty vector) and there was no significant difference between nsP3 and nsP3-F. It was also confirmed that the nsP3-F was detectable via western blotting. Figure 5.15 B demonstrates that cells transfected with nsP3-F expressed the protein which was detectable on a western blot using both anti-Flag and anti-nsP3 primary antibodies.
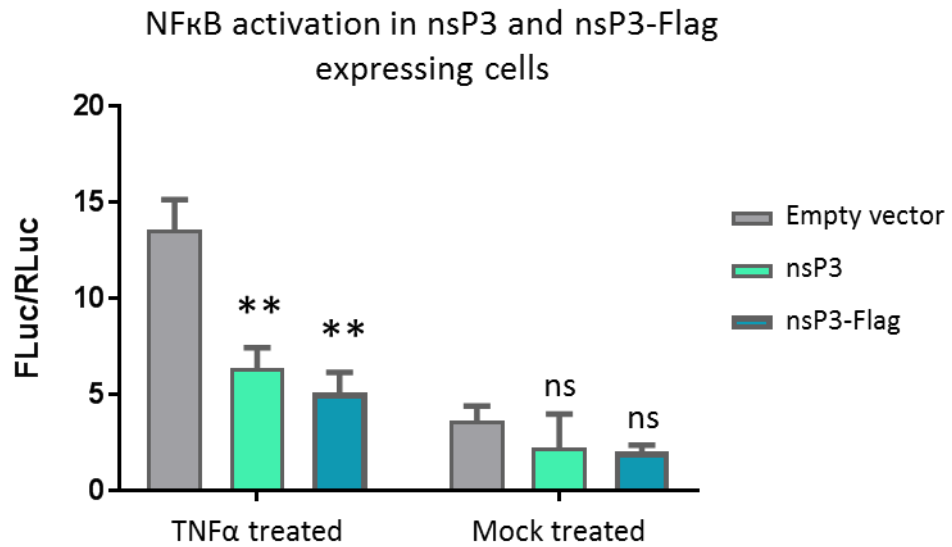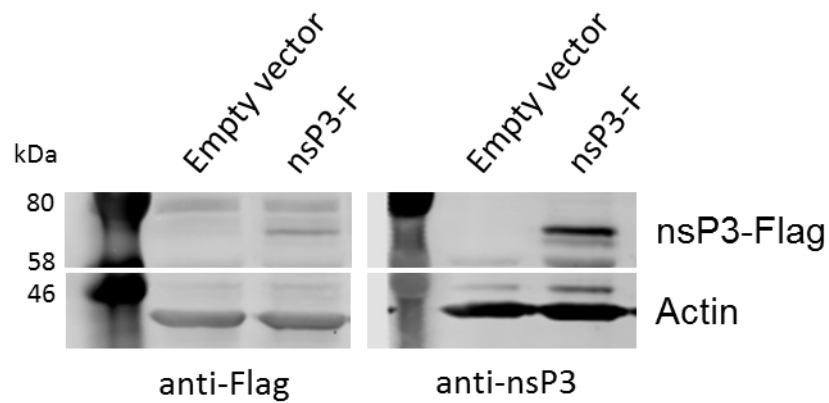
Figure 5.15 Optimisation of the nsP3-F construct for use in NFκB experiments. (A) Cells were transfected with the NFκB-Fluc and pRL-TK plasmids and co-transfected with either empty pcDNA3.1+ vector or the vector expressing nsP3 (untagged) or nsP3-F. Cells were then TNFα or mock treated for 6 h prior to lysis and luciferase quantified. (n=3, data analysed by One-way ANOVA with Kruskal-Wallis test and Dunns' correction compared to wt, ns = P > 0.05, * = P ≤ 0.05, ** = P ≤ 0.01). (B) Western blot for nsP3-F (59 kDa) using both anti-Flag and anti-nsP3 antibodies.

Now that a suitable tagged expression construct had been generated and validated, it was then put into the experimental system. Additionally, two controls, alongside the empty vector control, were used as indicated in Figure 5.16 A. Firstly, a pcDNA3.1+ GFP construct as a negative control to ensure that excess protein expression was not inducing the observed results. GFP expression has been successfully used as a negative control in experiments assessing inhibition of the NFκB in the literature (Ember *et al.*, 2012). Secondly, a pcDNA4 construct expressing B14, a vaccina virus protein that is a well characterised inhibitor of the NFκB pathway where it has been shown to bind to IKKβ and inhibit the formation of a functional IKK complex (Chen *et al.*, 2008). In this expression construct, B14 was tagged at the N-terminus with a Flag tag (herein referred to as F-B14) and was used as a positive control.

As in the previous experiments, empty vector, nsP3-F, GFP and F-B14 expression constructs were transfected into cells, alongside the NFκB dual reporter plasmids. Cells were incubated for 16h then treated or mock treated with TNFα and lysed at 6 h post treatment. As shown in Figure 5.16 B, when cells are activated by TNFα, nsP3-F inhibits the NFκB pathway to the same extent as the known inhibitor F-B14. For the inhibition of basal levels, (as indicated by the mock treated cells), nsP3-F does significantly reduce activation when compared to empty vector but not quite to the same level of inhibition that F-B14 is capable of. The expression of GFP did not induce any significant differences in NFκB activation, when compared to empty vector, for the treated or mock treated cells. Protein expression for nsP3-F and F-B14 were confirmed by western blotting as shown in Figure 5.16. Unfortunately, it was not possible to detect GFP on a western blot so wide-field fluorescent images were taken to confirm GFP expression (Figure 5.16 D).

IF was then utilised to determine the sub-cellular localisation of p65 in nsP3-F expressing cells. Cells were again transfected with the relevant constructs, incubated for 16 h prior to treatment with TNFα or mock treated. Cells were fixed at 6 hpt and stained for p65. Additionally, all cells, except GFP-expressing cells, were additionally stained for nsP3. As is expected, Figure 5.17 B shows that, for all cells, when mock treated, p65 is predominantly cytoplasmic. When treated with TNFα however (Figure 5.17 A), in the case of cells transfected with empty

vector or GFP-expressing cells, p65 becomes nuclear indicating an active NFκB pathway. In cells that are clearly expressing nsP3-F, p65 is restricted from the nucleus, remaining mostly cytoplasmic. This indicates that the expression of nsP3-F in cells prevents nuclear translocation of NFκB therefore inhibiting the NFκB pathway.
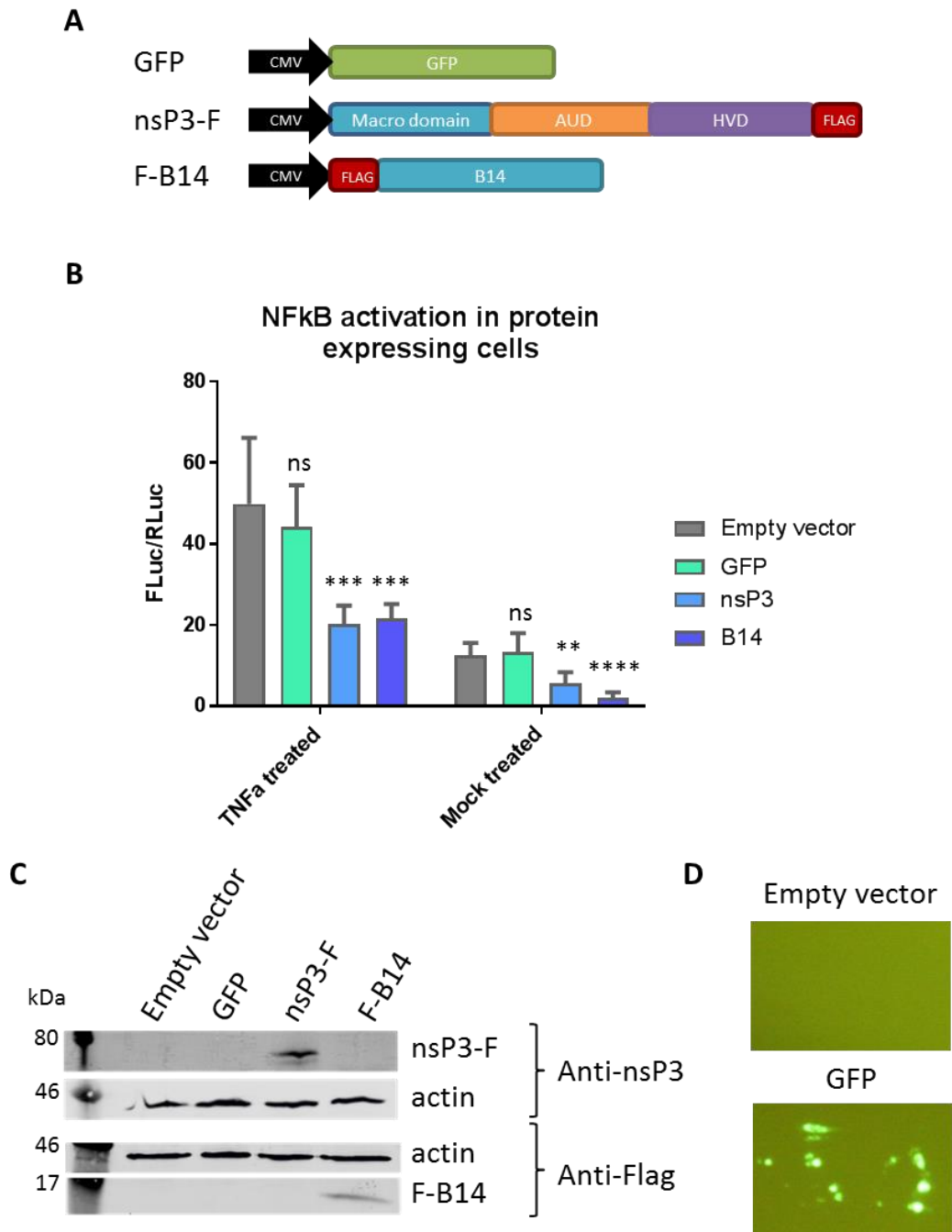
Figure 5.16 nsP3-F inhibits the NFκB pathway. (A) A schematic of the expression constructs used in this experiment. **(B)** Cells were transfected with the NFκB-Fluc and pRL-TK plasmids and co-transfected with expression constructs for GFP, nsP3-F, F-B14 or empty vector. At 16 hpt cells were TNFα or mock treated for 6 h prior to lysis and luciferase quantified. (Two experiments combined, each n=3, data analysed by One-way ANOVA with Bonferroni correction compared to wt, ns = P > 0.05, * = P ≤ 0.05, ** = P ≤ 0.01, *** = P ≤ 0.001, **** = P ≤ 0.0001). **(C)** Western blot for nsP3-F (59 kDa) and F-B14 (15 kDa). **(D)** Wide field fluorescent microscopy images of GFP-expressing cells compared to cells transfected with the empty vector.
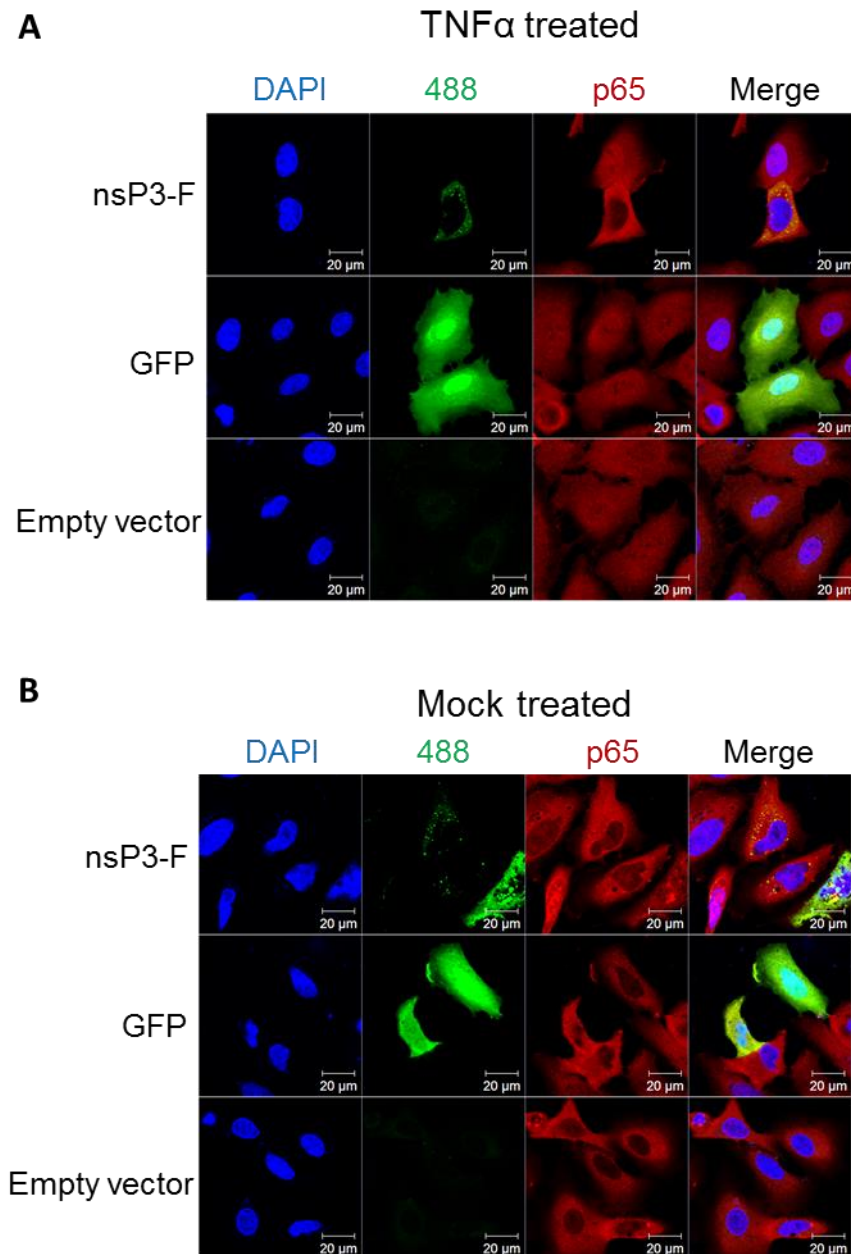
Figure 5.17 The expression of nsP3-F inhibits nuclear translocation of p65. A549 cells were transfected with either nsP3-F, GFP or empty vector expression constructs. At 16 hpt, cells were TNFα (A) or mock treated (B) for 6 h prior to fixation and staining for p65 (red). Cells were co-stained for nsP3 (shown in green/488), except GFP expressing cells.

Quantification was performed on the TNFα samples shown in Figure 5.17 by imaging via tile scans (see Figure 5.18 A) and manually counting nsP3 or GFP positive and negative cells with nuclear p65. As shown by Figure 5.18 B, of the cells expressing GFP, approximately 75% had nuclear p65, only a slight reduction from nuclear p65 observed in the GFP negative cells. In contrast,

approximately 20% of the nsP3 expressing cells contained nuclear p65, a reduction of approximately 50% from the nsP3-negative cells.

A

B
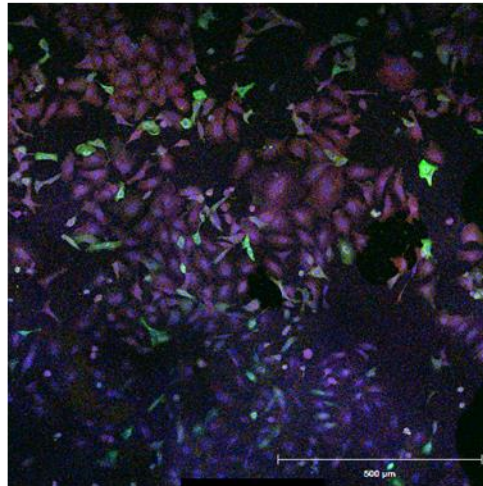
Figure 5.18 Quantification of nuclear p65 in TNFα treated, nsP3-F and GFP expressing cells. (A) An example tile scan of cells stained for nsP3 and p65. (B) The number of cells with nuclear p65 was quantified manually for both cells that were positively expressing nsP3/GFP, or that were negative for protein expression from the same sample. Data shown is percentage of cells with nuclear p65 from total cells counted for each condition. Cells counted for each conditions were 51, 55, 26 and 46 respectively.

5.2.2.3 The macro domain is partly responsible for the anti-NFκB activity of nsP3

To determine whether inhibition of the NFκB pathway by nsP3 involved the macro domain, initially it was attempted to generate an expression construct for the macro domain and a Flag-tagged macro domain. As shown in Figure 5.19, neither the macro domain or Flag tagged macro domain expression constructs produced detectable expression of the macro domain.
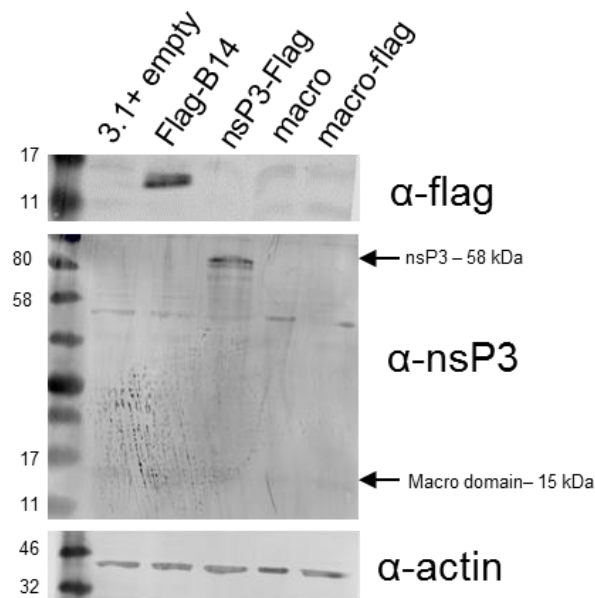
Figure 5.19 Western blot to test macro domain expression. A549 cells were transfected with either empty vector, or expression constructs of F-B14, nsP3-F, macro domain or macro domain-Flag (both approx. 15 kDa) for 16 h prior to lysis and western blot performed in order to detect macro domain expression. Both anti-Flag and anti-nsP3 primary antibodies were used.

As it was not feasible to express the macro domain to determine whether it was capable of inhibiting the NFκB pathway, the macro domain mutants (as defined in chapter 4), were employed instead. Flag-tagged nsP3 constructs with each individual mutation were generated as described previously in 5.2.2.1, and used, alongside the wt nsP3-F construct, with the NFκB reporter plasmid system as before. As shown in Figure 5.20, all the mutants were successfully expressed in transfected cells and produced a range of NFκB inhibition phenotypes. Upon activation with TNFα (Figure 5.20 A), both the V113A and Y114A mutants

significantly reduced NFκB activation when compared to the empty vector negative control. In the mock transfected cells, representing basal levels of NFκB activation (Figure 5.20 B), all mutants were capable of significantly reducing the activation levels except D10A, G112A and Y114A. These results indicate that the macro domain does have a role in the inhibition of the NFκB pathway.
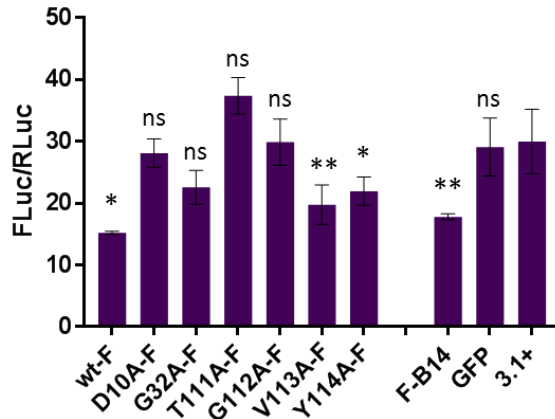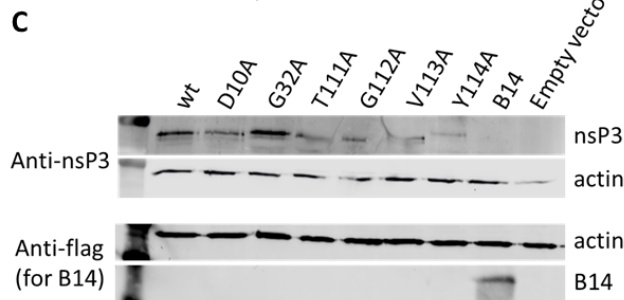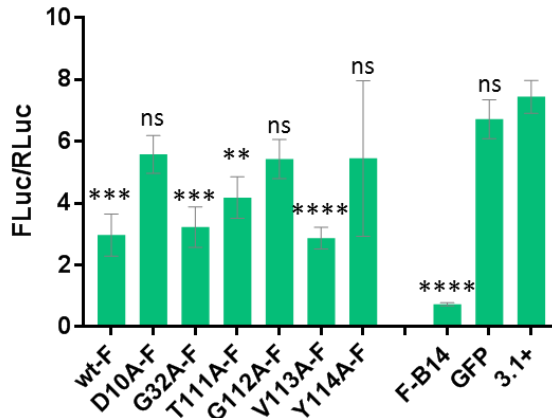
Figure 5.20 nsP3 macro domain mutants exhibit a wide range of inhibitory effects on the NFκB pathway. A549 cells were transfected with the nsP3-F wt and mutant expression constructs alongside F-B14, GFP and empty vector controls. At 16 hpt, cells were TNFα activated (A) or mock treated (B) then lysed at 6 h post treatment and luciferase assayed. (n=3, data analysed by One-way ANOVA with Bonferroni correction compared to empty vector, ns = P > 0.05, * = P ≤ 0.05, ** = P ≤ 0.01, *** = P ≤ 0.001, **** = P ≤ 0.0001) (C) Confirmation of protein expression by western blotting for nsP3 and Flag tag (for F-B14) on the corresponding cell lysates.

When comparing this data to the known biochemical properties of the CHIKV nsP3 macro domain (McPherson *et al.*, 2017), as shown in Table 5.1, there is a correlation between the ability of the mutant nsP3s to inhibit the NFκB pathway and the ability to bind ADPR. Specifically, D10A, T111A and G112A exhibited the least inhibition of the pathway and are the three mutants with the lowest affinity for ADPR, with D10A and G112A having no detectable binding and T111A demonstrating far less affinity to ADPR than the wt or any other mutant. There is little correlation between NFκB inhibition and the hydrolase activity of the mutants. For example, V113A, the only mutant able to significantly inhibit the NFκB pathway when activated, has stronger ADPR binding than wt but only 15% hydrolase activity of wt. This data indicates that ADPR affinity, and not hydrolase activity, may be crucial for the role of the nsP3 macro domain in its ability to inhibit the NFκB pathway.

	nsP3 mutants							Controls		
	wt	D10A	G32A	T111A	G112A	V113A	Y114A	B14	Empty vector	GFP
Inhibition of NFκB pathway (%)	49.2	6.3	24.7	-24.7	0.4	34.1	26.8	40.6	0	3
ADPR k_D (µM)*	22.9	NDB	21.0	71.4	NDB	6.46**	4.84	N/A	N/A	N/A
Hydrolase activity (% wt)*	100	16.1	75.3	64.1	3.7	15.0**	40.6	N/A	N/A	N/A

Table 5.1 Comparison of the macro domain mutants inhibition of the NFκB pathway to their biochemical properties. *Data from McPherson *et al.* 2017, **V113R was used in this study instead of V113A. Colours denote comparison to wt. (Light green = approximately wt, dark green = above wt, yellow = below wt, and red = less than 30% wt).

Again, IF was performed to corroborate the luciferase data. The wt and mutant nsP3-F expression constructs and the empty vector control were transfected into cells, incubated 16 h then treated with TNFα. After 6 h, cells were fixed and stained for p65 and nsP3. The IF data (Figure 5.21) generally agrees with the luciferase data. Both wt and V113A nsP3 are shown to exclude p65 from the nucleus of cells. For T111A and Y114A nsP3 the distribution of p65 resembles the highly nuclear distribution shown by the empty vector control. For all other mutants; D10A, G32A and G112A, there is some reduction in p65 in the nucleus

when comparing to the empty vector control, though it is not as distinct as the nuclear exclusion exhibited in the wt nsP3-expressing cells. Interestingly for many of these three mutants, there appears to be a concentration of p65 in the perinuclear region which may indicate translocation is being inhibited at, or near the nuclear membrane.
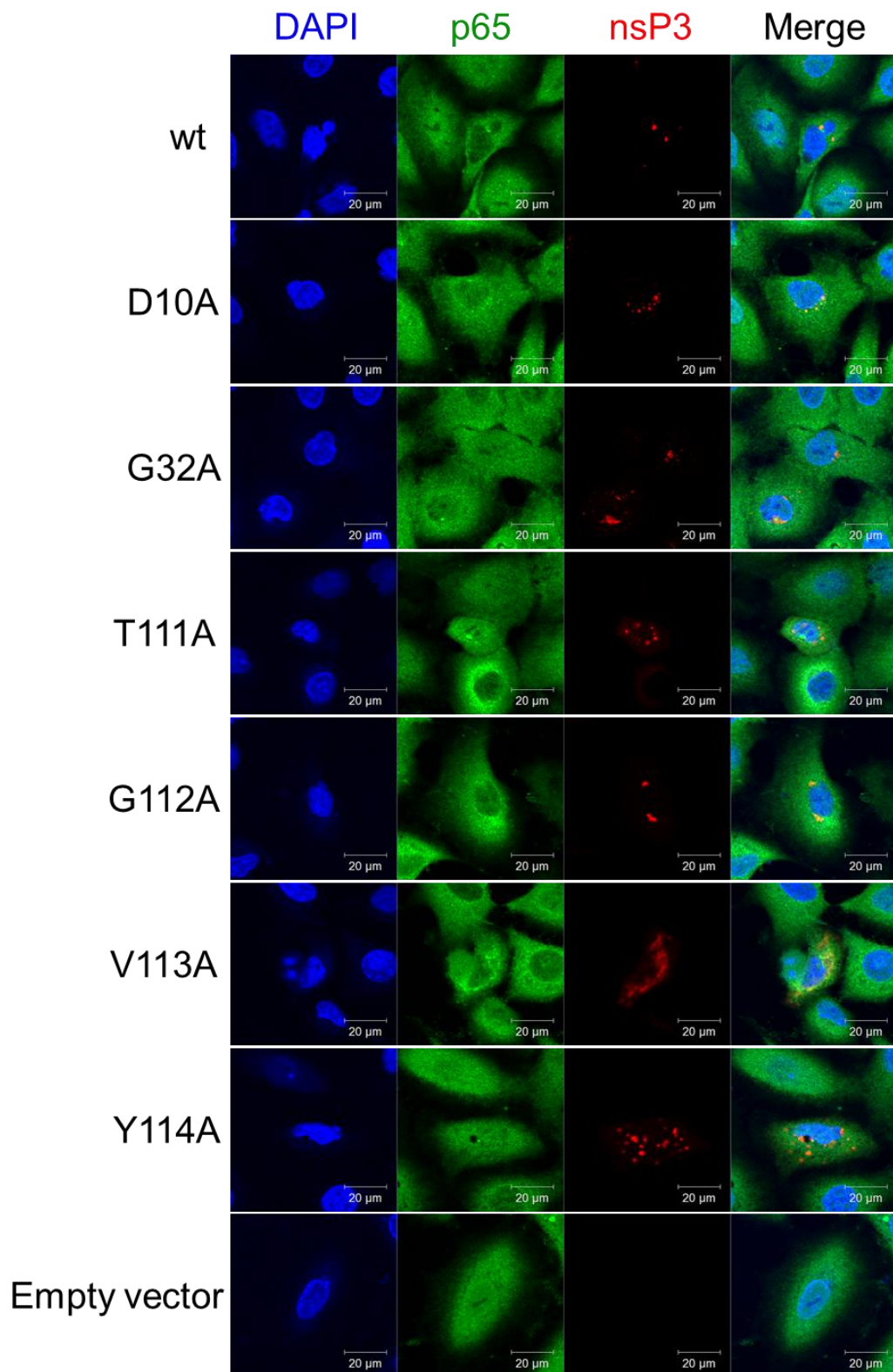
Figure 5.21 IF of p65 in nsP3 wt and mutant expressing cells. A549 cells were transfected with nsP3-F expression vector for wt or mutant nsP3 or empty vector as a negative control. At 16 hpt, cells were TNFα treated for 6 h prior to fixation and staining for p65 (shown in green) and nsP3 (shown in red).

5.2.2.4 Elucidating the stage of nsP3-mediated inhibition of the NFκB pathway

Here, it has been shown that the macro domain of nsP3 is capable of inhibiting the NFκB pathway and that nsP3 expression prevents the nuclear translocation of NFκB to the nucleus. However, it is still unclear at which stage of the NFκB pathway CHIKV nsP3 functions. Therefore it was investigated whether the IKK complex, central to the NFκB pathway, was active in nsP3 expressing cells. This would determine whether the inhibition was occurring before/at or after the IKK complex in the pathway. Again, cells were transfected with the nsP3-F, F-B14 and GFP expressing constructs as well as empty vector. Cells were then activated with TNFα and lysed over a short time course. Western blots were then performed to detect phosphorylated p105, the presence of which indicates that the IKK complex is active. Once the IKK complex is active, the phosphorylation of p105 occurs rapidly but is short lived as p105 then translocates to the nucleus to act as a transcription factor. As shown in Figure 5.22, cells transfected with empty vector, once activated, exhibit phospho-p105 at 5 min-post activation which persists for 25-30 min. This is mirrored by the GFP negative control. In the presence of B14 however, there is a delay in the phosphorylation of p105, with first detection being at 15 min post-treatment, and with weaker signal than either the empty vector or GFP negative controls. This is as expected as B14 directly inhibits the IKK complex through an interaction with IKKβ (Chen *et al.*, 2008). Cells expressing nsP3 appeared to exhibit similar levels of expression with phospho-p105 appearing at similar time points and both the GFP and empty vector controls. This implies that nsP3 inhibition of the NFκB pathway occurs after the formation of an active IKK complex but before nuclear translocation of NFκB.
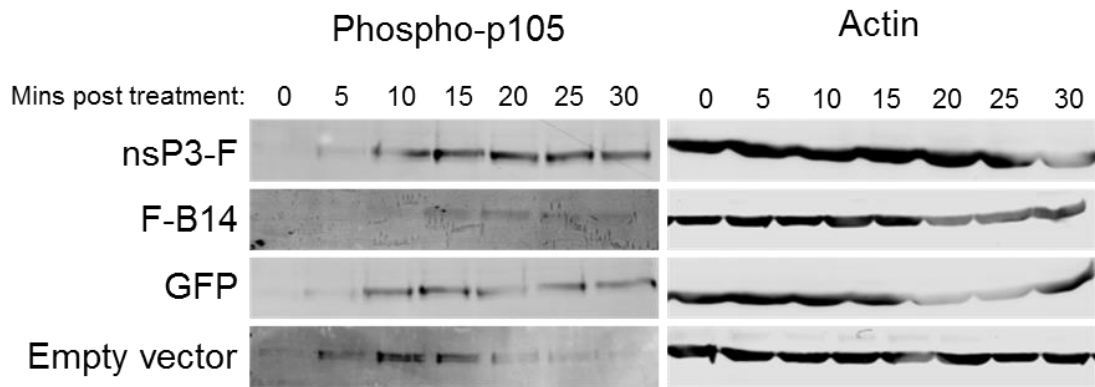
Figure 5.22 The IKK complex is active in nsP3-F expressing cells. A549 cells were transfected with an expression construct for nsP3-F, F-B14, GFP or empty vector. Cells were incubated for 16 h then activated with TNFα. Cells were lysed at 5 minute intervals over a 30 min period and western blotting was performed for the detection of phosphor-p105. The presence of phospho-p105 indicates an active IKK complex.

It was also investigated whether CHIKV nsP3 co-localised with either NEMO or ARTD10. Unfortunately, through various different methods and attempts at optimisation, it was not possible to visualise NEMO through immunofluorescence. However it was possible to detect ARTD10 though this method. Cells were therefore infected with CHIKV and fixed over a 24 h time course and stained for both nsP3 and ARTD10. As shown by Figure 5.23, nsP3 was only detected after 8 hpi. At this point, and at the later time of 24 hpi, co-localisation of nsP3 with ARTD10 was observed. Though many cells within the sample exhibited co-localisation, it must be noted that it was not observed in all infected cells. Also, in cells that did exhibit co-localisation of ARTD10 with nsP3, not all nsP3 puncta were associated with ARTD10.
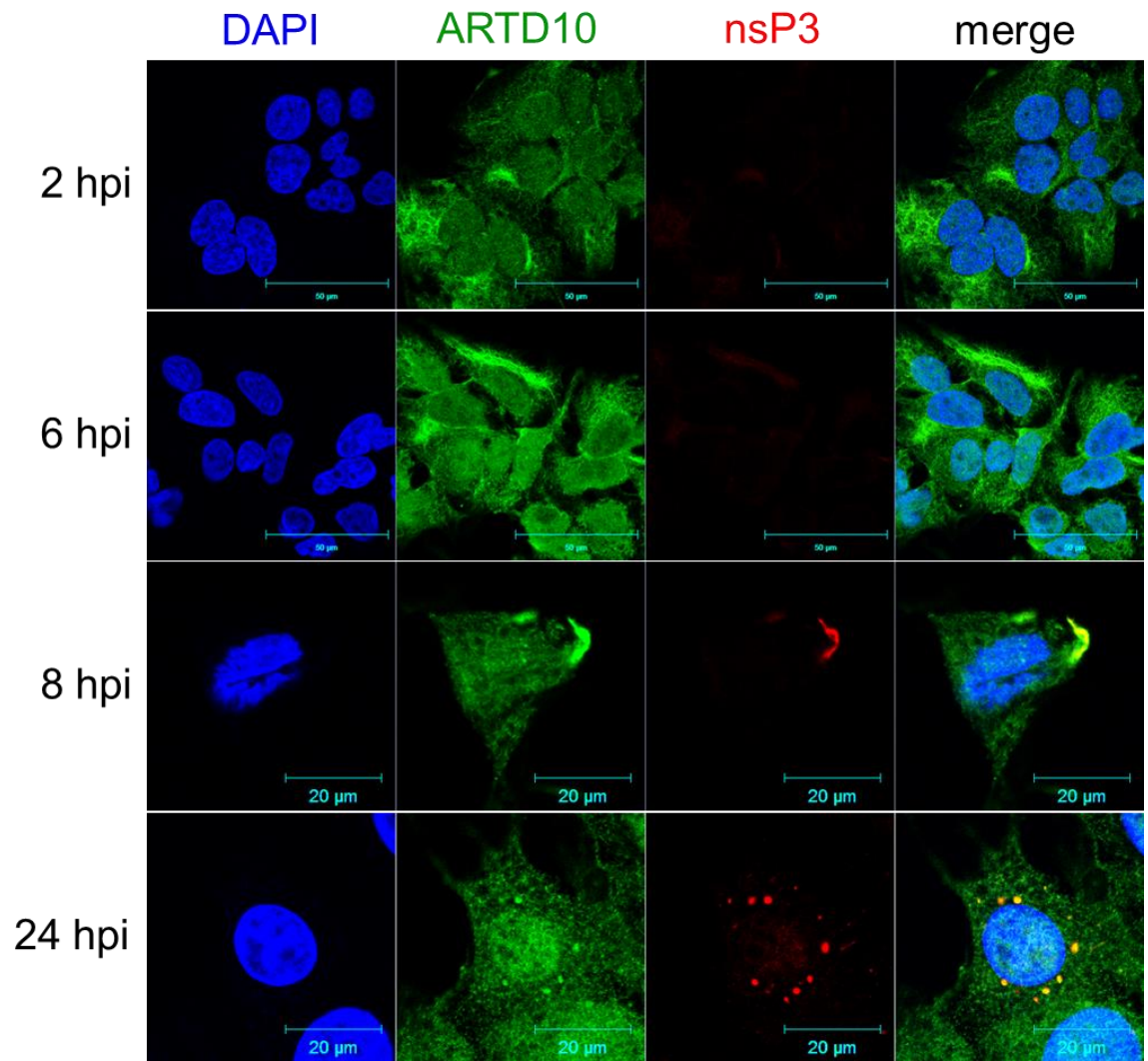
Figure 5.23 Immunofluorescence for ARTD10 and nsP3. Huh7 cells were infected with CHIKV at MOI=10. Cells were fixed over a 24 h period and stained for ARTD10 (green) and nsP3 (red). Detectable levels of nsP3 were not seen until 8 hpi where co-localisation with ARTD10 was observed.

5.3 Discussion

5.3.1 The NFκB pathway in CHIKV infection

CHIKV is known to induce a highly inflammatory environment in infected cells. In particular, it has been well defined that CHIKV infected cells produce a robust IFN response and that this response is critical for survival from infection (Her *et al.*, 2010; Priya *et al.,* 2014; Nair *et al.*, 2017). Inhibition of the IFN pathway can enhance CHIKV replication. CHIKV is capable of inhibition of the IFN pathway, to some extent, via nsP2 which is able to promoting the nuclear export of STAT1, therefore reducing JAK-STAT signalling (Wichit *et al.*, 2017; Göertz *et al.*, 2018).

Only one publication to date has examined the role of NFκB in CHIKV infection. Selvamani *et al.* demonstrated that CHIKV did not activate the NFκB pathway and linked this lack of activation with overexpression of microRNA-146a. However, the mechanism of how CHIKV induced upregulation of this miRNA was not elucidated. This chapter therefore aimed to reiterate these findings and investigate whether the nsP3 macro domain played a role in the disruption of the NFκB pathway.

5.3.1.1 CHIKV infection does not activate the NFκB pathway

Prior to investigating any potential roles nsP3 may have in subverting the NFκB pathway, firstly the relationship between the NFκB pathway and CHIKV was investigated. In agreement with Selvamani *et al*, here it was demonstrated that CHIKV does not induce an NFκB response in infected cells. This was confirmed by both luciferase assay, using NFκB reporter plasmids, and by IF of the NFκB subunit p65 in infected cells. In both these data, it was shown that CHIKV infection does not induce the activation of the NFκB pathway.

It was further sought to determine whether the IKK complex, the central component of the NFκB pathway, was active in CHIKV infected cells. This was assessed by western blot of phosphorylated-p105. The IKK complex phosphorylates NFκB (p105) rapidly after activation. Here, the CHIKV infected cells resembled the mock-infected cells with little phospho-p105 being detected. This indicates that the NFκB pathway is either not being activated, or, potentially, the pathway is activated but is inhibited prior to the formation of the IKK complex.

5.3.1.2 CHIKV cannot inhibit an exogenously activated NFκB pathway

As it had been established that CHIKV does not activate the NFκB pathway, it was sought to determine whether CHIKV could inhibit an activated NFκB pathway. Through luciferase assay with the NFκB reporter plasmids, it was shown that CHIKV infection could not inhibit the NFκB pathway once activated exogenously via TNFα. This was further confirmed by IF of p65 where CHIKV infected, TNFα treated cells contained nuclear p65, much like the TNFα-treated, mock-infected cells. This indicates that whilst CHIKV does not induce an NFκB response in infected cells, its potentially inhibitory activity is not sufficient enough to overcome the NFκB pathway once activated by external stimuli.

5.3.1.2.1 CHIKV production is reduced when cells are TNFα treated

Since CHIKV infection does not induce the NFκB pathway, nor is the virus capable of inhibiting an activated pathway, what effect an active pathway would have on CHIKV replication was investigated. A time of addition study using TNFα showed that, regardless of time of stimulation, CHIKV titres were reduced when titred at 24 hpi. However, this reduction was only significant with cells treated either at the time of infection, or 1 h post infection. It is not immediately obvious why treatment with TNFα significantly reduced CHIKV production when cells were treated at or 1 h post infection, but not at 6 h prior to infection. This could suggest that CHIKV is better able to disrupt the pathway once later stages of the pathway have been reached, but is not able to establish infection during the early stages of the pathway being stimulated. Alternatively, presence of CHIKV proteins or RNA at the time of TNFα treatment could be inducing an innate response better tailed to counter CHIKV infection. As shown in the schematic of the NFκB pathway (Figure 5.1), TNFα is detected via a cell surface receptor, whereas RNA viruses, such as CHIKV are mostly detected through dsRNA sensing in endosomes and the cytoplasm (Jensen and Thomsen, 2012). These different mechanisms of detection result in the triggering of different pathways to ultimately activate the IKK complex and trigger the NFκB pathway. Due to a complex variety of interactions with other pathways, the different routes of the pathway induced by different stimuli produce altered inflammatory responses depending on the method of activation (Akira and Takeda, 2004; Sen and Smale,

2010). It therefore may be that, the TNFα stimulus in combination with the presence of the virus in early stages of replication may alter the pathway and therefore tailor the response to be more effective against CHIKV. In contrast, when cells are pre-treated, by the time of CHIKV infection they have only been exposed to TNFα for a substantial amount of time. Therefore these cells have a fully activated NFκB pathway, though, since this inflammatory state was formed in the absence of any virus, may be less specifically anti-viral and therefore allow more replication once infected than the cells treated with TNFα in combination with early stages of replication.

5.3.2 nsP3 inhibits the NFκB pathway

Once it had been established that CHIKV does not activate the NFκB pathway and that an activated pathway reduces viral replication, the potential role of nsP3 as an inhibitor of the NFκB pathway was investigated. It was therefore necessary to engineer an appropriate expression construct for nsP3. Initially, wt, untagged nsP3 was engineered into a mammalian expression vector. Despite producing encouraging results where it was shown that cells transfected with the wt nsP3 expression construct had consistently reduced NFκB activation in the luciferase assay system, it was challenging to consistently detect expression of nsP3, both wt and mutant, in these cells via western blot. In the literature, it has been shown that nsP3, and in particular, full length nsP3 is particularly unstable and is quickly degraded in cells (Varjak *et al.*, 2010). It was therefore decided that using a tagged nsP3 may increase stability and detection of the protein.

There is a variety of different protein tags in the literature each with their advantages and disadvantages. There are a wide range of fluorescent tags which are advantageous as they allow easy detection of the tagged protein via fluorescence microscopy. However these tags do tend to be quite large and therefore may affect protein folding or function, so care must be taken over selecting an appropriate tag and ensuring the resulting expressed protein is not affected by the tag (Thorn, 2017).

Initially, a ZsGreen tag was adopted and placed in the HVD of the nsP3 expression construct. The use of ZsGreen, a 26 kDa protein isolated from *Zoanthus* species, as a fluorescent tag was reported in 1999 and was found to

be more stable and less toxic to cells than the conventional EGFP (Matz *et al.*, 1999). This tag was chosen as it has been used in replicon and infectious CHIKV systems with no apparent adverse effects on CHIKV replication (Remenyi *et al.*, 2018). It also allowed for checking successful transfection before proceeding with the experiments, as cells could be quickly checked under a fluorescent microscope to observe nsP3-ZsGreen expression. Additionally, it improved detection of nsP3 via western blot. It may be that the addition of a large, stable tag was able to limit degradation of the protein. However, when repeating the luciferase assay with the tagged versions of nsP3, both wt and mutant, different results were produced. Unlike in experiments using untagged nsP3, ZsGreen-tagged D10A nsP3 exhibited some inhibition of the NFκB pathway, though this was not as strong an inhibition as wt nsP3. When using the ZsGreen constructs to analyse the sub-cellular localisation of p65, it became apparent that the expression of ZsGreen alone was able to block nuclear translocation of p65. Therefore the expression of ZsGreen in cells results in inhibition the NFκB pathway, and explains the difference seen in the luciferase data between the untagged and ZsGreen-tagged nsP3 expression. ZsGreen was therefore considered an unsuitable control for these experiments and a different tagging strategy was required.

The next attempt at tagging nsP3 was using a Flag tag. A Flag tag is an artificial protein tag, specifically designed to be as small as possible whilst being large enough to be a specific epitope for a monoclonal antibody (Hopp *et al.*, 1988). A Flag tag is the protein sequence DYKDDDDK, which is recognised by a highly specific monoclonal antibody termed M1. It is a hydrophilic tag that has shown to be less likely to denature the protein it is fused to. Use of a Flag tag to tag nsP3 would also be consistent with the B14 positive control which is Flag tagged at the N terminus. The Flag tag was therefore engineered at the C terminal end of nsP3. Prior to conducting any further experiments, it was firstly assessed whether the Flag tag helped stabilise and detect nsP3 by western blot and, more importantly, whether the tagged nsP3 behaved in a similar way to untagged nsP3. Therefore, the nsP3-F expression construct was compared to the nsP3-untagged construct in the context of the NFκB reporter plasmid system. Fortunately, there was no significant difference between the untagged and the

flag-tagged nsP3 in terms of their effects of the NFκB pathway. The addition of the Flag tag to the C-terminus of nsP3 enhanced stability and detection of the protein as nsP3 could be clearly be detected via western blot, using the anti-nsP3 antibody. The tagged protein could also be detected using the anti-Flag antibody but to a lesser extent. This reduction could potentially be due to the anti-Flag antibody being monoclonal and, since nsP3-F only contains a single flag tag at the C terminus, it would have fewer epitopes to detect per nsP3-F molecule. The stronger signal produced by the nsP3 antibody is likely to be due to it being polyclonal and therefore able to bind multiple epitopes per protein molecule. Therefore the anti-nsP3 antibody was used to detect nsP3-F for further experiments.

5.3.2.1 Expression of nsP3-F inhibits the NFκB pathway

The nsP3-F construct was then used in experiments to determine nsP3 inhibition of the NFκB pathway. By this point in the project, a positive control had been acquired – a Flag-tagged B14 expression construct (F-B14, kindly provided by Geoffrey Smith, as described in Chen *et al.*, 2008). B14 is a vaccinia protein that is a well characterised inhibitor of the NFκB pathway. B14 is able to bind to, and inhibit, IKKβ; a key component of the IKK complex. In addition, another negative control was also engineered; pcDNA3.1+ GFP to ensure that excessive protein expression was not the cause of the inhibitory effect on the NFκB pathway observed for nsP3 expression. The nsP3-F alongside the empty vector, GFP and F-B14 controls were used in the NFκB reporter system as before. The GFP negative control behaved in a similar manner as the empty vector, showing its suitability as a negative control, unlike with ZsGreen. The F-B14 positive control exhibited an inhibitory effect for both conditions as expected. The expression of nsP3-F also inhibited the NFκB pathway under both stimulated and basal conditions. The nsP3-F construct was able to inhibit the NFκB pathway to similar levels as F-B14. Protein expression of F-B14 and nsP3-F were confirmed by western blot. Unfortunately it was not possible to detect GFP via western blot with the reagents available, therefore GFP expression was confirmed by fluorescence microscopy instead. This data shows, for the first time, that nsP3 is significantly inhibiting the NFκB pathway, and the expression of nsP3 was confirmed successfully by western blotting.

Similarly to previously experiments, immunofluorescence of p65 in protein-expressing cells was performed to confirm the findings of the luciferase assay. In agreement with the luciferase data and previous experiments, in cells expressing nsP3, when stimulated, p65 remained cytoplasmic. This indicates that the presence of nsP3 in cells is able to prevent the translocation of NFκB to the nucleus and therefore inhibit activation of the NFκB pathway. This was further confirmed by imaging the samples via tile scan and performing quantification. In nsP3 expressing cells, approximately 20% exhibited nuclear p65 whereas for GFP expressing cells, nuclear p65 was observed in over 70% of cells. This further clarifies that the restriction of nuclear translocation of p65 by nsP3 is not an uncommon occurrence.

5.3.2.2 The macro domain of nsP3 contributes to NFκB inhibition

It was then sought to determine whether the macro domain of nsP3 had a role in the inhibition of the NFκB pathway. The initial untagged-nsP3 expression experiment indicated that wt nsP3 could prevent activation of the NFκB pathway whereas the mutant D10A could not. This indicated that the macro domain may be important in this inhibition. Though many attempts were made, it was not possible to express either the macro domain by itself or a Flag-tagged macro domain. This may be due to degradation as macro domains are often parts of much larger, multi-domain proteins (Li *et al.*, 2013). In the case of CHIKV nsP3, the macro domain is the N-terminal domain, with two further domains downstream which are likely to improve stability. Therefore, expression of the macro domain was abandoned and a different approach used. The six macro domain mutants as described in chapter 4 were engineered in the nsP3-Flag expression construct and similarly to previous experiment, the NFκB luciferase reporter assay was performed. Reassuringly, in this experiment, the flag tagged D10A mutant behaved in a similar manner to the previous experiments that used untagged nsP3 expression constructs. Again confirming the that the Flag tag was not disrupting nsP3 functions. When activated by TNFα, two mutants significantly reduced activation: V113A and Y114A. In contrast, in the mock treated cells (indicating basal levels of NFκB activation) all mutants except D10A, G112A and Y114A demonstrated a significant reduction in activation of the pathway. This shows that most mutations of the macro domain cannot inhibit the NFκB pathway

when activated, though when not activated, most mutants were able to induce some reduction of the pathway. This indicates that a TNFα-activated pathway is effective in overcoming the actions of mutated nsP3 in terms of its inhibition of the innate immune system. Though when the pathway is inactive, even mutated nsP3 can exert some effects. This may indicate that the interaction required for inhibition is weaker for the nsP3 mutants compared to wt and is therefore easier for the innate immune system of the cells to overcome when the pathway is activated by external stimuli. It is surprising that Y114A significantly reduced the pathway when externally activated, but not at basal levels. However, given the large error bars for the Y114A samples at basal levels, this implies there may have been an outlier in the data. Due to time constraints, this experiment was only performed once at n=3. Ideally more repeats of this experiment would have been performed to confirm the outcomes.

When comparing the biochemical properties of the macro domain mutants, (previously published by McPherson *et al.*, 2017) to their ability to inhibit the NFκB pathway, there is some indication of what may be responsible for the inhibitory effect. The hydrolase activity of the mutants, has little correlation with NFκB inhibition. There is, however, some correlation with the macro domain mutants ability to bind ADPR. Mutants D10A, T111A and G112A were the least inhibitory of the NFκB pathway when activated and were the three mutants with no, or extremely low affinity for ADPR. This implies that, in agreement with the original hypothesis, ADPR binding is responsible for the macro domain mediated inhibition of the NFKB pathway, possibly via binding an ADP-ribosylated component of the pathway. However, not all the mutants correlated so well. Both G32A, which had similar ADPR affinity to wt, and Y114A, which had a much higher affinity than wt, only mildly inhibited the NFκB pathway, with the inhibition by Y114A not being significant. This may indicate that ADPR binding is only one aspect of the method of inhibition.

5.3.2.3 Investigating the stage of the NFκB pathway where nsP3 is enacting its inhibitory function

Now it has been well established that nsP3 is able to inhibit the NFκB pathway and restricts nuclear translocation of NFκB, of which the macro domain is partly

responsible for, it was sought to determine at what stage in the pathway nsP3 exerted its inhibitory affects. It was originally hypothesised that nsP3 could interact with the NFκB pathway through either ARTD10 or NEMO – both of which are ADP-ribosylated, and are involved in the central IKK step of the pathway. It therefore seemed logical to investigate whether the active complex could form in nsP3–expressing cells. This was assessed by western blotting for phosphor-p105 where the IKK complex appears as active in nsP3-expressing cells as it is in the GFP-expressing and empty vector-transfected cells. In contrast, F-B14 expressing cells have a delayed, muted response which was expected due to its direct inhibitory effect on the complex. This demonstrated that nsP3 is inhibiting the pathway at some point after IKK activation but before nuclear translocation of p65. Though this narrows down the part of the pathway of which nsP3 is causing inhibition, it does not necessarily confirm a lack of interaction with either ARTD10 or NEMO. Unfortunately, it was not possible using available reagents to visualise NEMO through IF. However, it was possible to perform IF for nsP3 and ARTD10 which demonstrated co-localisation between the two proteins. Though co-localisation between two proteins via IF does not confirm a definite interaction, it does indicate that, at the very least, ARTD10 is interacting with the virus machinery, in areas where nsP3 is present.

Originally, it was postulated that if nsP3 was capable of hydrolysing the ADPR moiety from ARTD10 or NEMO *in vivo*, it would lead to activation of the NFκB pathway. However, since it has been shown repeatedly, that CHIKV does not activate the NFκB pathway, this now seems an unlikely hypothesis. It could be that nsP3 is capable of interacting with either of these proteins through the ADPR but without hydrolysis. Also, the interaction between nsP3 and ARTD10 could be unrelated to the NFκB pathway. ARTD10 is a highly multifunctional protein that is involved in many cellular pathways. In addition to innate immunity, ARTD10 has been implicated in apoptosis, DNA repair, and cell cycle regulation (Kaufmann *et al.*, 2014). It is a highly dynamic protein within cells and has been shown to form discrete bodies within the cytoplasm. The function of these ARTD10 bodies is unknown but they are not associated with either p-bodies or stress granules (Kleine *et al.*, 2012). As a result, Kleine *et al.* hypothesised that ARTD10 may have a role in RNA transport, but not RNA processing. ARTD10

has also been shown to interact with p62 which has a role in autophagy (Johansen and Lamark, 2011; Kleine *et al.*, 2012). Both of these roles of ARTD10 may be advantageous for an RNA virus to exploit, as CHIKV is known to induce autophagy to delay apoptosis (Joubert *et al.*, 2012). It may be that the CHIKV nsP3 macro domain interacts with ARTD10, independent of the role of nsP3 in NFκB inhibition, in order to disrupt other pathways or hijack the RNA shuttling function of ARTD10 in order to promote virus replication. More research is required to confirm an interaction between nsP3 and ARTD10 and to determine the function of this interaction.

In this work, it was necessary to produce many expression constructs of nsP3 and the macro domain as none were available at the time. These constructs were generated with a variety of tags and mutants which may prove useful for further work in this field.

5.3.3 Chapter summary

Looking specifically of what cellular functions the nsP3 macro domain may possess, it was hypothesised that this N-terminal domain may be capable of interacting with the ribosylated proteins involved in the NFκB pathway in order to interfere with inflammation. More specifically, the nsP3 macro domain could potentially interact with NEMO, a component of the IKK complex and ARTD10, which is auto-ribosylated and regulates NEMO through ADP-ribosylation.

Here, an agreement with the literature, it has been demonstrated that CHIKV infection does not activate the NFκB pathway. Looking more specifically at nsP3, it has been shown that expression of the protein inhibits the NFκB pathway to similar levels of B14, a vaccinia virus protein, well characterised as an NFκB inhibitor. Immunofluorescence revealed that p65, a subunit of NFκB, was unable to translocate to the nucleus of activated cells expressing nsP3. When using a panel of macro domain mutants to assess their ability to inhibit the pathway, it revealed that the nsP3 macro domain is at least partly responsible for NFκB inhibition. The mutants produced a range of inhibitory phenotypes with some mutants exhibiting inhibition similar to wt levels, and others having no inhibitory effects at all. When comparing these inhibitory phenotypes to the known biochemical properties of the macro domain mutants, it suggested that the ADPR-binding capability may be responsible for the macro domain's inhibitory effects.

When attempting to determine the stage at which nsP3 exerts its inhibition of the NFκB pathway, it was shown that this effect occurs after IKK complex activation but prior to NFκB nuclear translocation. Due to time constraints it was not possible to further determine the step of inhibition.

Due to the original hypothesis, it was investigated whether nsP3 interacted with ARTD10. IF showed co-localisation between the two proteins across different stages of infection, indicating that an interaction does indeed occur between ARTD10 and the virus machinery. Unfortunately, due to time constraints, it was not possible to determine the nature or purpose of this interaction. Although this would be an interesting line of inquiry for future research.

Chapter 6 Discussion and future perspectives

Macro domains are found in the proteins of all species including many positive sense single stranded viruses. In CHIKV, as with all alphaviruses, there is a macro domain at the N-terminus of nsP3. At the start of this project, it was known that nsP3 is required for CHIKV replication, but the function of nsP3, and specifically of the macro domain was unclear.

Recent studies by others have assessed the biochemical properties of the CHIKV macro domain which has been shown to possess both ADP-ribose hydrolase and ADP-ribose 1"–phosphatase activities as well as affinity for ADR-ribose and RNA. However, it was unclear which processes these properties relate to in the context of infected cells. The macro domain had also been shown to be a virulence factor as certain mutations within the domain exhibited a less severe morbidity in mice.

In order to facilitate study of the nsP3 macro domain in this project, optimisation was required to determine suitable cell lines for use for CHIKV research and optimal methods for us of the replicon and the infectious virus systems available to us. Prior to this study, very little work had been conducted on establishing suitable cell lines for CHIKV research. In humans, is has been established that CHIKV replicates to high titres within the lymphoid tissues, muscles, liver, joints and brain in infected individuals. Other studies have aimed to define specific cell types in the body that become infected with CHIKV, in order to determine spread of the virus through the lymphatic and cardiovascular systems. However, in practise, many studies examining the molecular biology of CHIKV have utilised cells that are not physiologically relevant to the *in vivo* infection such as Vero cells, BHK cells and HeLa cells. Being an arbovirus, it is also important to study CHIKV in the mosquito vectors; *Aedes aegypti* and *Aedes albopictus*. In both vector species, it has been shown that CHIKV replicates in most tissues, producing high titres in the midgut and salivary glands in particular. In this study, we aimed to determine a set of physiologically-relevant cell lines that supported the replication of CHIKV in order to study the molecular and cellular biology of the virus.

From a large panel of cell lines, including those that were physiologically relevant and other cells previously utilised in the literature, four mammalian and two

mosquito cell lines were shown here to support both replicon and virus replication, and allowed expression of nsP3 to detectable levels via western blotting and IF.

Now that a range of appropriate and useful cell lines had been established, and replicon and virus system had been optimised, the project could then focus on the aim of determining the function of the macro domain in CHIKV replication.

At the start of this project, little work had been conducted specifically on the CHIKV nsP3 macro domain, however the three-dimensional structure of the domain had been previously solved by x-ray crystallography (Malet *et al.*, 2009). This structure revealed the binding pocket of the domain, and, in the same study, revealed some of the properties of the domain. It was shown that the CHIKV nsP3 macro domain binds ADP-ribose (both monomeric and polymeric forms) and RNA. In addition, it possessed ADP-ribose 1″-phosphate phosphatase enzymatic activity.

Informed by the available structures, sequence homology between various macro domains, and limited mutagenesis work from the literature (Malet *et al.*, 2009), here, a panel of mutants were generated in the binding pocket of the nsP3 macro domain and their replicative phenotypes assessed in both replicon and infectious virus. These mutants exhibited a range of replicative phenotypes, some of which varied greatly between cell lines. This indicated that the macro domain may have some cell-specific functions. In addition, for certain mutants, the difference in phenotypes between the two mosquito cell lines used here indicated a potential role for the macro domain in inhibiting the RNAi pathway, in agreement with the literature (Mathur *et al.*, 2016).

Over the course of this study, several publications that studied the CHIKV nsP3 macro domain became available (McPherson *et al.*, 2017; Abraham *et al.*, 2018). Of note, it was shown that the macro domain possessed hydrolase activity, similar to that previously demonstrated for the hepatitis E macro domain. In addition, other groups had generated a similar set of mutations within the macro domain binding pocket and assessed each mutant for ADP-ribose affinity and hydrolase activity.

Combining the phenotypic data from this study with those in the literature revealed a strong correlation between ADP-ribose affinity and virus replication. Mutants with undetectable ADP-ribose affinity were those less able to produce infectious virus in most cell lines.

McPherson *et al.* suggested that hydrolase activity is also important for CHIKV replication, although the data presented here suggests it is not as essential as several macro domain mutants with low hydrolase activity were tolerated, producing virus whilst maintaining the mutation. These data are summarised in Figure 6.1.
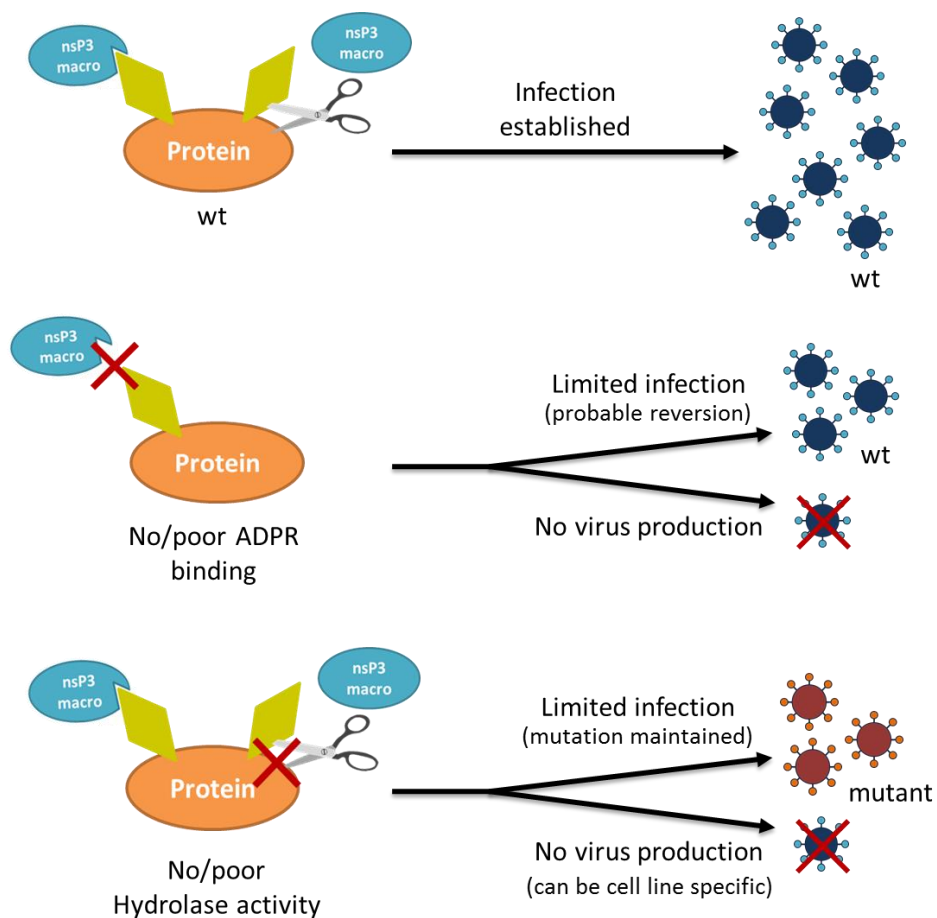
Figure 6.1 Summary of macro domain mutants biochemical and resulting replicative phenotypes. Mutants that possess poor or no ADP-ribose affinity either did not produce virus or were capable to low levels. The literature indicates this is probably through reversion. Mutants with poor hydrolase activity were able to produce virus in most cell types and, where possible to assess the sequence of resulting virus RNA, the mutation was maintained.

However, as several mutants possessed poor ADP-ribose binding and poor hydrolase activity in combination, it is difficult to draw conclusive conclusions from this work alone. Further mutagenesis experiments, using specific mutations that affect either hydrolase activity or ADP-ribose binding would be useful in determining the importance of these properties. Though this may prove difficult as it is likely that hydrolase activity is reliant on ADP-ribose binding.

Much like with other studies examining the roles of viral macro domains, the data produced here indicated that the ADP-ribose 1″-phosphate phosphatase activity is not required for replication. Other groups have demonstrated viral macro domains such as that of SARS-coronavirus and SFV possess no detectable phosphatase activity (Egloff *et al.*, 2006; Malet *et al.*, 2009). The CHIKV macro domain mutant Y114A was shown here to replicate broadly to wt levels, yet in the literature it was shown to have no detectable phosphatase activity. This provides further evidence to the theory that ADP-ribose 1″-phosphate phosphatase activity is not the primary function of viral macro domains.

The data produced by the mutagenesis experiments, and by others in the literature, suggested a role for the CHIKV nsP3 macro domain in antagonising the innate immunity of infected cells. Recently, it had been shown that ADP-ribosylation is important in many signalling pathways, including the NFκB pathway. Mono-ribosylation of NEMO, a key IKK component, by ARTD10 (which is auto-ribosylated), results in suppression of the NFκB pathway as ribosylation prevents NEMO from forming an active IKK complex (Verheugd *et al.*, 2013). It was therefore investigated whether the CHIKV nsP3 macro domain was able to interfere with this pathway potentially through binding and/or hydrolysis of ADP-ribosylated proteins in this pathway.

Prior to focussing on nsP3, it was investigated whether the NFκB pathway is activated upon CHIKV infection. In agreement with the literature, it was demonstrated in the studies described here that the NFκB pathway is not activated at any point during CHIKV infection. It was further shown that CHIKV cannot suppress an exogenously activated pathway and that, when the pathway was activated, CHIKV titres were reduced.

A major finding of this project is that nsP3 is capable of inhibiting the NFκB pathway. Using expression constructs, tagged nsP3 was expressed in cells that were co-transfected with NFκB reporter plasmids. When these cells were exogenously activated, those expressing nsP3 demonstrated significantly lower levels of NFκB activation. This was reiterated via IF where, in the presence of nsP3, the NFκB subunit p65 remained in the cytoplasm, unable to translocate to the nucleus.

In this project, it was not possible to confirm expression of the macro domain (both untagged or flag-tagged) in cells. Therefore, to confirm involvement of the macro domain in NFκB inhibition, the macro domain mutants described in chapter 4 were engineered into the flag-tagged nsP3 expression construct and used alongside the NFκB reporter plasmid system. This luciferase assay revealed that the different mutants produced a range of inhibitory phenotypes – when the pathway was activated, some nsP3 mutants were completely unable to inhibit the pathway, with only one mutant capable of significant inhibition. However, the majority of mutants were able to suppress the basal levels of NFκB activation.

When comparing the biochemical data available in the literature as described previously to the levels of inhibition exerted by the macro domain mutants, there is a strong correlation between ADP-ribose binding and inhibition of the NFκB pathway. The three mutants with the lowest affinity for ADP-ribose were also the three mutants least capable of NFκB inhibition. The V113A mutant which was the only macro domain mutant able to significantly inhibit the NFκB pathway has poor hydrolase activity (15% wt) indicating that ADP-ribose hydrolysis is not required for this inhibitory affect.

Further investigation into at what stage in the pathway this inhibition was being enacted by the nsP3 macro domain revealed that, contrary to the initial hypothesis, the IKK complex was active in nsP3-expressing cells. This indicates that inhibition of the NFκB pathway by nsP3 occurs after the formation of an active IKK complex but prior to the nuclear translocation of NFκB as summarised Figure 6.2. Further work would be required to determine at which stage in the pathway the nsP3 macro domain is exerting its inhibitory effects.
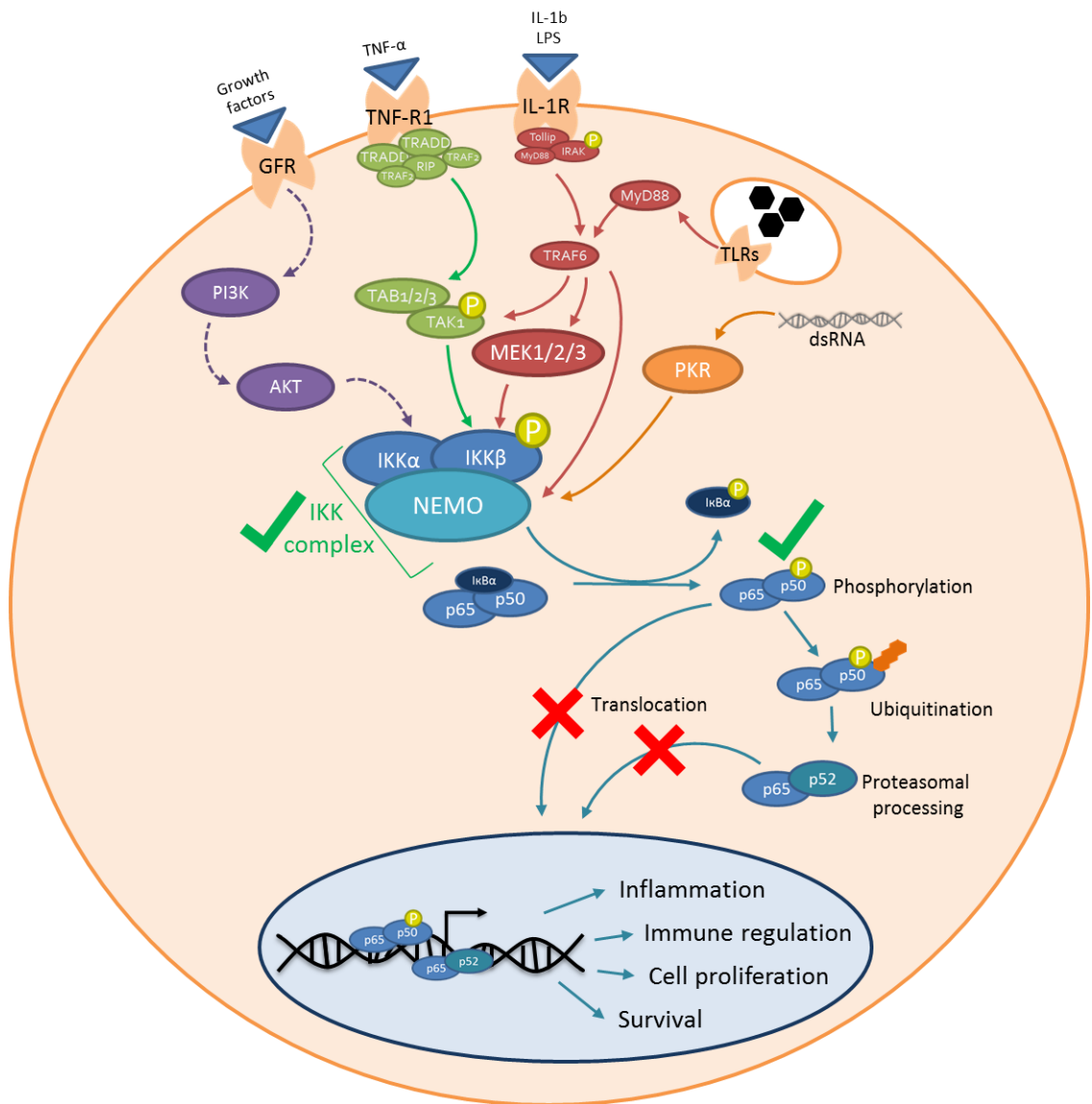
Figure 6.2 Summary of the effect of nsP3 on the NFκB pathway. It has been shown that in nsP3 expressing cells, the IKK complex is active and the phosphorylated form of p105 can be detected. It is also known that NFκB is not able to translocate to the nucleus in the presence of nsP3. This indicates that the stage of inhibition enacted by nsP3 is after p105 phosphorylation but prior to, or at the stage of nuclear translocation.

It was demonstrated in this work that at no point in CHIKV infection is the NFκB pathway activated, nor was an active IKK complex detected in infected cells. This implies that CHIKV may have other mechanisms to inhibit or evade detection by the NFκB pathway other than via the nsP3 macro domain. Most viruses activate the pathway through TLR detection in endosomes, an early stage in CHIKV infection prior to translation of the non-structural proteins. Therefore, further work

examining other CHIKV proteins, such as the structural proteins, may reveal other inhibitors of innate immune pathway, other +ssRNA viruses express structural proteins that have been shown to inhibit the NFκB pathway (see Table 6.1).

Though it has been clearly demonstrated here that the CHIKV nsP3 macro domain is capable of NFκB inhibition, the precise mechanism of action is yet to be determined. Many viruses express proteins that are capable of inhibiting the NFκB pathway. Multiple DNA viruses express specific proteins that inhibit the NFκB pathway. For example, the vaccinia protein B14, used in this study, is capable of binding IKKβ and inhibits the IKK complex, is one of seven proteins expressed by Vaccinia virus that inhibit the NFκB pathway by various methods. Of the +ssRNA viruses, hepatitis C virus, West Nile Virus, Poliovirus, and SARS coronavirus all express proteins that inhibit the NFκB pathway, as detailed in Table 6.1. For all these proteins, they block the pathway at, or prior to the formation of an active IKK complex.

Virus	Protein	Mechanism of inhibition
Hepatitis C virus	NS5A	Inhibits TRAF2 signalling (Park *et al.,* 2003)
	NS5B	Inhibits IKKα (Choi *et al.,* 2006)
	Core	Inhibits IKKβ (Joo *et al.,* 2005)
West Nile virus	NS1	Blocks TLR3 activation of NFκB pathway (Wilson *et al.,* 2008)
Poliovirus	3C protease	Cleaves p65 (Neznanov *et al.,* 2005)
SARS-coronavirus	M	Binds IKKβ (Fang *et al.,* 2007)

Table 6.1 Proteins expressed by +ssRNA viruses that inhibit the NFκB pathway. Reviewed in Rahman and McFadden, 2011.

There are very few examples in the literature of virus proteins that inhibit the NFκB pathway past the IKK complex/IκB degradation stage. One example is the N protein of Hantaan virus (HTNV), a segmented, negative sense RNA virus. This protein has been shown to block nuclear translocation of the NFκB p65 subunit through an interaction with nuclear pore protein importin α (Taylor *et al.,*

2009). Though this protein has little in common with nsP3, and with a distinctly different cellular localisation to that of nsP3, this mechanism of inhibition highlights that not all inhibitory effects of viral proteins are due to direct interactions of components of specific pathways.

With viruses such as varicella-zoster virus (VZV), it has been observed that NFκB transiently translocates to the nucleus and is then sequestered back into the cytoplasm through an unknown mechanism (Jones and Arvin, 2006). A more detailed time course observing the localisation of p65 could reveal whether this occurs with CHIKV. However, it is unlikely that the NFκB inhibition exerted by nsP3 is by this mechanism as nsP3 has never exhibited nuclear localisation.

Many bacterial toxins are ADP-ribosyltransferases, which MARylate various cellular proteins to enhance infection and interact with cellular innate immune pathways (Cohen and Chang, 2018). This highlights the likelihood of ADP-ribosylation being a common occurrence in cellular innate immunity pathways. It is therefore possible that there are other, currently undiscovered, ribosylation events that regulate NFκB pathway. As shown in Figure 6.2, depending on the mechanism of activation the p50 subunit of NFκB can be K63-ubiquitinated, which signals for proteasome processing of p50 to produce p52 for nuclear translocation. There are many instances where ADP-ribose and ubiquitination counteract each other, much like with the regulation of NEMO, described in chapter 5. It may be possible that the CHIKV nsP3 macro domain interacts with, and inhibits the pathway another ADPR-dependent stage.

Though other viral macro domains have been implicated in antagonising cellular innate immunity, none have been implicated in the NFκB pathway. The hepatitis E virus macro domain has been shown to inhibit the IFN pathway by blocking IRF-3 phosphorylation (Nan *et al.*, 2014). The SARS-coronavirus macro domain has also been implicated in the inhibition of the IFN response though the precise mechanism is unknown (Kuri *et al.*, 2011). Though CHIKV is known to induce a robust IFN response in infected cells, it was not investigated in this project whether the nsP3 macro domain interfered with the IFN response, though this may be an interesting line of inquiry. No other viral macro domains to date have been implicated with the NFκB response. Further work would be required, using

similar experiments performed here, to determine whether other viral macro domains have similar inhibitory functions to those demonstrated by the nsP3.

This work highlights the potential for therapeutics to be developed that target the nsP3 macro domain. If a therapeutic were capable of inhibiting the macro domain from exerting its effects on the NFκB pathway, infected cells may be able to successfully eliminate the virus. Alternatively, as it was shown that an activated NFκB pathway reduces CHIKV titres, modulation of the immune response could potentially be used to treat CHIKV infection.

Currently, ongoing work within the Harris group and with collaborators is being conducted to design small molecular inhibitors for the CHIKV nsP3 macro domain. As it is an essential domain required for CHIKV replication that possesses a small binding pocket, it was identified as a potential drug target. There are, however, some concerns over the potential toxicity, or off-target effects of any macro domain inhibitor, as many cellular proteins also possess macro domains required for essential functions. However, the macro domains of alphaviruses are highly conserved and, although there is some sequence homology between the alphavirus macro domains and those found in human proteins, it is probable that, via high throughput screening for small molecule inhibitors, some will be identified that are specific to the CHIKV macro domain. In addition, any compounds found to have potential inhibitory effects can be further chemical modification can be performed to enhance effectivity and specificity.

It is important to acknowledge that nsP3 is likely to be a highly multifunctional protein. Having investigated the role of the macro domain of nsP3 in isolation, future work would be useful to assess the function of the macro domain in combination with the other domains; the AUD and HVD as all alphavirus nsP3s have evolved to contain these three domains, suggesting shared functions. However, several +ssRNA viruses, other than alphaviruses, contain macro domains within multi-domained proteins with very little resemblance to nsP3. This suggests some shared function of the macro domain across species of viruses. Further work would be required to determine whether the findings shown

here for the CHIKV macro domain, are shared by the macro domains of other viral species.

In conclusion, work here has not only increased the general knowledge of the cellular and molecular biology of CHIKV, but also that of viral macro domains across different virus families. The macro domain of nsP3 has been shown to be a virulence factor, capable of inhibiting the NFκB pathway. This highlights the potential of the nsP3 macro domain as a drug target. Alternatively, immune modulation via therapeutics that activate the NFκB pathway may be another potential treatment for CHIKV infected patients.

Chapter 7 Appendix

7.1.1 Primers

Primer name	Template DNA	Destination vector	Primer sequence	Ann temp (°C)	Elong. time (min:sec)
P11 BamHI nsP3 FWD	CHIKV nsP3-ZsGreen/SG-Gluc replicon Or CHIKV ICRES wt	pcDNA3.1+	CCG TAC GGA TCC ACC ATG GCA CCG TCG TAC CGG GTA AAA CGC ATG	66	1:40 (nsP3) 2:10 (nsP3-ZsG)
P21 XhoI REVnsP3	CHIKV nsP3-ZsGreen/SG-Gluc replicon Or CHIKV ICRES wt	pcDNA3.1+	CAC TAG CTC GAG TTA CCC ACC TGC CCT GTC TAG TCT TAA C	66	1:40 (nsP3) 2:10 (nsP3-ZsG)
P58 nsP3 FWD BamHI	CHIKV ICRES (wt/mutant)	pcDNA3.1+	CCG TAC GGA TCC ACC ATG GCA CCG TCG TAC CGG GTA	60	1:40
P59 nsP3 stop Flag NotI	CHIKV ICRES (wt/mutant)	pcDNA3.1+	AGC TCA CTG CGG CCG CTT ACT TGT CGT CAT CGT CTT TGT AGT CCC CAC CTG CCC TGT CTA G	60	1:40

Table 7.1 Primers used for the cloning of various nsP3 expression constructs

Mutant	Primer name	Template DNA	Primer sequence	Ann temp (°C)	Elong. time (min:sec)
Macro domain D10A	P26 nsP3 macro D10A FWD	WT CHIKV ICRES	AAA ACG CAT GGC CAT CGC GAA GAA CG	68	14:30
	P27 nsP3 macro D10A FWD	WT CHIKV ICRES	ACC CGG TAC GAC GGT GCC	68	14:30
Macro domain G32A	P30 G32A Q5 FWD	WT CHIKV ICRES	AAC CCG CGA GGG TTA GCG	70	14:30
	P31 G32A Q5 REV	WT CHIKV ICRES	ACC GGG TGG CGC AGT TTG CAA GG	70	14:30
Macro domain T111A	P32 nsP3 macro T111A FWD	WT CHIKV ICRES	TCT CCT CTC CGC AGG TGT ATA CT	58	14:30
	P33 nsP3 macro T111A FWD	WT CHIKV ICRES	GGT ATA GCT ACA CTA TTT ACT CC	58	14:30
Macro domain G112A	P34 nsP3 macro G112A FWD	WT CHIKV ICRES	CCT CTC CAC AGC TGT ATA CTC AG	57	14:30
	P35 nsP3 macro G112A FWD	WT CHIKV ICRES	AGA GGT ATA GCT ACA CTA TTT AC	57	14:30
Macro domain V113A	P36 nsP3 macro V113A FWD	WT CHIKV ICRES	CTC CAC AGG TGC ATA CTC AGG AG	62	14:30
	P37 nsP3 macro V113A FWD	WT CHIKV ICRES	AGG AGA GGT ATA GCT ACA C	62	14:30
Macro domain Y114A	P38 nsP3 macro Y114A FWD	WT CHIKV ICRES	CAC AGG TGT AGC CTC AGG AGG GAA AG	62	14:30
	P39 nsP3 macro Y114A FWD	WT CHIKV ICRES	GAG AGG AGA GGT ATA GCT AC	62	14:30
nsP4 GAA	P43 nsP4 GAA Q5 FWD	WT CHIKV ICRES	CGC CAA CAT AAT ACA TGG AGT CGT CTC CGA TG	68	14:30
	P44 nsP4 GAA Q5 REV	WT CHIKV ICRES	GCG CCG ATG AAG GCC GCG CAC GC	68	14:30

Table 7.2 Primers used for Q5 mutagenesis.

Primer name	Forward primer	Reverse primer	Ann temp (°C)	Reference
E1 qRT-PCR primers	GCATCAGCTAAGCTCCGCGTC	GGTGTCCAGGCTGAAGACATTG	56 °C	(Pongsiri *et al.*, 2012)
AUD qRT-PCR primers	GCGCGTAAGTCCAAGGGAAT	AGCATCCAGGTCTGACGGG	56 °C	(Chiam *et al.*, 2013)

Table 7.3 Primers used for qRT-PCR.

Primer name	Template DNA	Primer sequence	Ann temp (°C)	Elong. time (min:sec)
P62 Macro PCR Prod for seq FWD	cDNA from RNA TRIzol extracted from infected cells	GGG ACG CAA GTT TAG ATC G	57	1:00
P63 Macro PCR Prod for seq REV	cDNA from RNA TRIzol extracted from infected cells	CGC AGT CTA TGG AGA TGT G	57	1:00

Table 7.4 Primers used for amplification of macro-domain coding sequence containing fragment from cDNA for sequencing.

Primer name	Used to sequence	Primer sequence
P1 nsP3 macro SeqP	Macro domain of replicon and virus constructs	CATGTGTCACCAGCAACACTGAGATG
T7 FWD seq	pcDNA3.1+ constructs	TAATACGACTCACTATAGGG
P62 Macro PCR Prod for seq FWD	PCR product formed from cDNA for sequencing	GGGACGCAAGTTTAGATCG

Table 7.5 Primers used for DNA sequencing

7.1.2   Plasmid maps

Figure 7.1 Plasmid map of pcDNA3.1+. Enzyme set shown are unique cutters. Plasmid map created using SnapGene software.

Figure 7.2 Dual luciferase (dLuc) CHIKV replicon plasmid map. Enzyme set shown are unique and double cutters. Plasmid map created using SnapGene software.

Figure 7.3 CHIKV wt ICRES virus construct plasmid map. Enzyme set shown are unique and double cutters. Plasmid map created using SnapGene software.

7.1.3 Supplementary figures

A

```
                                            10
gcaccgtcgtaccgggtaaaacgcatgMgacatcgcgaagaacgatgaagagtgcgtagtc 60
A  P  S  Y  R  V  K  R  M  D  I  A  K  N  D  E  E  C  V  V    20

                                            32
aacgccgctaaccctcgcgggttaccgggtggcggtgtttgcaaggcagtatacaaaaaa 120
N  A  A  N  P  R  G  L  P  G  G  G  V  C  K  A  V  Y  K  K    40

tggccggagtcctttaagaacagtgcaacaccagtgggaaccgcaaaaacagttatgtgc 180
W  P  E  S  F  K  N  S  A  T  P  V  G  T  A  K  T  V  M  C    60

ggtacgtatccagtaatccacgctgttggaccaaacttctctaattattcggagtctgaa 240
G  T  Y  P  V  I  H  A  V  G  P  N  F  S  N  Y  S  E  S  E    80

ggggaccgggaattggcagctgcctatcgagaagtcgcaaaggaagtaactaggctggga 300
G  D  R  E  L  A  A  A  Y  R  E  V  A  K  E  V  T  R  L  G    100

                              111 112 113 114
gtaaatagtgtagctatacctctcctctccacaggtgtatactcaggagggaaagacagg 360
V  N  S  V  A  I  P  L  L  S  T  G  V  Y  S  G  G  K  D  R    120

ctgacccagtcactgaaccacctctttacagccatggactcgacggatgcagacgtggtc 420
L  T  Q  S  L  N  H  L  F  T  A  M  D  S  T  D  A  D  V  V    140

atctactgccgcgacaaagaatgggagaagaaaatatctgaggccatacagatgcggacc 480
I  Y  C  R  D  K  E  W  E  K  K  I  S  E  A  I  Q  M  R  T    160
```

B

```
                                            10
gcaccgtcgtaccgggtaaaacgcatggccatcgcgaagaacgatgaagagtgcgtagtc 60
A  P  S  Y  R  V  K  R  M  A  I  A  K  N  D  E  E  C  V  V    20

                                            32
aacgccgctaaccctcgcgggttaccgggtggcgcagtttgcaaggcagtatacaaaaaa 120
N  A  A  N  P  R  G  L  P  G  G  A  V  C  K  A  V  Y  K  K    40

tggccggagtcctttaagaacagtgcaacaccagtgggaaccgcaaaaacagttatgtgc 180
W  P  E  S  F  K  N  S  A  T  P  V  G  T  A  K  T  V  M  C    60

ggtacgtatccagtaatccacgctgttggaccaaacttctctaattattcggagtctgaa 240
G  T  Y  P  V  I  H  A  V  G  P  N  F  S  N  Y  S  E  S  E    80

ggggaccgggaattggcagctgcctatcgagaagtcgcaaaggaagtaactaggctggga 300
G  D  R  E  L  A  A  A  Y  R  E  V  A  K  E  V  T  R  L  G    100

                              111 112 113 114
gtaaatagtgtagctatacctctcctctccgcagctgcagcctcaggagggaaagacagg 360
V  N  S  V  A  I  P  L  L  S  A  A  A  A  S  G  G  K  D  R    120

ctgacccagtcactgaaccacctctttacagccatggactcgacggatgcagacgtggtc 420
L  T  Q  S  L  N  H  L  F  T  A  M  D  S  T  D  A  D  V  V    140

atctactgccgcgacaaagaatgggagaagaaaatatctgaggccatacagatgcggacc 480
I  Y  C  R  D  K  E  W  E  K  K  I  S  E  A  I  Q  M  R  T    160
```

Figure 7.4 Nucleotide and amino acid sequences of wt macro domain and mutations generated. (A) wt macro domain sequence with codons and corresponding residues selected for mutagenesis highlighted in green. (B) Mutations (generated into the infectious CHIKV construct individually) in the nucleotide sequence are highlighted in blue, alongside resulting residue changes; D10A, G32A, T111A, G112A, V113A and Y114A.

Chapter 8 Bibliography

Abdelnabi, R., Neyts, J. and Delang, L. (2016) 'Antiviral Strategies Against Chikungunya Virus', *Methods in molecular biology*, pp. 243–253. doi: 10.1007/978-1-4939-3618-2_22.

Abdul-Sada, H. et al. (2017) 'The PP4R1 sub-unit of protein phosphatase PP4 is essential for inhibition of NFκB by merkel polyomavirus small tumour antigen', *Oncotarget*, 8(15), pp. 25418–25432. doi: 10.18632/oncotarget.15836.

Abraham, R. et al. (2018) 'ADP-ribosyl-binding and hydrolase activities of the alphavirus nsP3 macrodomain are critical for initiation of virus replication.', *Proceedings of the National Academy of Sciences*, p. 201812130. doi: 10.1073/pnas.1812130115.

Ahn, A., Gibbons, D. L. and Kielian, M. (2002) 'The fusion peptide of Semliki Forest virus associates with sterol-rich membrane domains.', *Journal of virology*, 76(7), pp. 3267–75.

Ahola, T. and Kääriäinen, L. (1995) 'Reaction in alphavirus mRNA capping: formation of a covalent complex of nonstructural protein nsP1 with 7-methyl-GMP.', *Proceedings of the National Academy of Sciences*. 92(2), pp. 507–11.

Akahata, W. et al. (2010) 'A virus-like particle vaccine for epidemic Chikungunya virus protects nonhuman primates against infection', *Nature Medicine*, 16(3), pp. 334–338. doi: 10.1038/nm.2105.

Akhrymuk, I., Kulemzin, S. V and Frolova, E. I. (2012) 'Evasion of the innate immune response: the Old World alphavirus nsP2 protein induces rapid degradation of Rpb1, a catalytic subunit of RNA polymerase II.', *Journal of virology*. 86(13), pp. 7180–91. doi: 10.1128/JVI.00541-12.

Akira, S. and Takeda, K. (2004) 'Toll-like receptor signalling', *Nature Reviews Immunology*. 4(7), pp. 499–511. doi: 10.1038/nri1391.

Albulescu, I. C. et al. (2014) 'An in vitro assay to study chikungunya virus RNA synthesis and the mode of action of inhibitors', *Journal of General Virology*. 95(Pt_12), pp. 2683–2692. doi: 10.1099/vir.0.069690-0.

Alphey, L. (2014) 'Genetic Control of Mosquitoes', *Annual Review of Entomology*. 9(1), pp. 205–224. doi: 10.1146/annurev-ento-011613-162002.

Alvarez, M. F. et al. (2017) 'Cardiovascular involvement and manifestations of systemic Chikungunya virus infection: A systematic review.', *F1000Research*. 6, p. 390. doi: 10.12688/f1000research.11078.2.

Amaya, M. et al. (2014) 'The Role of IKKβ in Venezuelan Equine Encephalitis Virus Infection', *PLoS ONE*. 9(2), p. e86745. doi: 10.1371/journal.pone.0086745.

Amaya, M. et al. (2016) 'Venezuelan equine encephalitis virus non-structural protein 3 (nsP3) interacts with RNA helicases DDX1 and DDX3 in infected cells', *Antiviral Research*. 131, pp. 49–60. doi: 10.1016/j.antiviral.2016.04.008.

Anang, S. et al. (2016) 'Identification of critical residues in Hepatitis E virus macro domain involved in its interaction with viral methyltransferase and ORF3 proteins.', *Scientific reports*. 6, p. 25133. doi: 10.1038/srep25133.

Andersson, N. et al. (2015) 'Evidence based community mobilization for dengue prevention in Nicaragua and Mexico (Camino Verde, the Green Way): cluster randomized controlled trial.', *British medical journal*. 351, p. h3267. doi: 10.1136/BMJ.H3267.

Atasheva, S., Frolova, E. I. and Frolov, I. (2014) 'Interferon-stimulated poly(ADP-Ribose) polymerases are potent inhibitors of cellular translation and virus replication.', *Journal of virology*. 88(4), pp. 2116–30. doi: 10.1128/JVI.03443-13.

Auteri, M. et al. (2018) 'Insecticide Resistance Associated with kdr Mutations in Aedes albopictus: An Update on Worldwide Evidences.', *BioMed research international*. p. 3098575. doi: 10.1155/2018/3098575.

Bernard, E. et al. (2010) 'Endocytosis of Chikungunya Virus into Mammalian Cells: Role of Clathrin and Early Endosomal Compartments', *PLoS ONE*. 5(7), p. e11479. doi: 10.1371/journal.pone.0011479.

Bick, M. J. et al. (2003) 'Expression of the zinc-finger antiviral protein inhibits alphavirus replication.', *Journal of virology*, 77(21), pp. 11555–62.

Boppana, S. B. et al. (1997) 'Neuroradiographic findings in the newborn period and long-term outcome in children with symptomatic congenital cytomegalovirus infection.', *Pediatrics*, 99(3), pp. 409–14.

Bordi, L. et al. (2011) 'Chikungunya virus isolates with/without A226V mutation show different sensitivity to IFN-a, but similar replication kinetics in non human primate cells.', *The new microbiologica*. 34(1), pp. 87–91.

Borgherini, G. et al. (2007) 'Outbreak of Chikungunya on Reunion Island: Early Clinical and Laboratory Features in 157 Adult Patients', *Clinical Infectious Diseases*. 44(11), pp. 1401–1407. doi: 10.1086/517537.

Boylan, B. T. et al. (2017) 'Mosquito cell-derived West Nile virus replicon particles mimic arbovirus inoculum and have reduced spread in mice', *PLOS Neglected Tropical Diseases*. 11(2), p. e0005394. doi: 10.1371/journal.pntd.0005394.

Brackney, D. E. et al. (2010) 'C6/36 Aedes albopictus Cells Have a Dysfunctional Antiviral RNA Interference Response', *PLoS Neglected Tropical Diseases*. 4(10). doi: 10.1371/JOURNAL.PNTD.0000856.

Brault, A. C. et al. (2000) 'Re-emergence of chikungunya and o'nyong-nyong viruses: evidence for distinct geographical lineages and distant evolutionary relationships', *Journal of General Virology*. 81(2), pp. 471–479. doi: 10.1099/0022-1317-81-2-471.

Briolant, S. et al. (2004) 'In vitro inhibition of Chikungunya and Semliki Forest viruses replication by antiviral compounds: synergistic effect of interferon-α and ribavirin combination', *Antiviral Research*. 61(2), pp. 111–117. doi: 10.1016/J.ANTIVIRAL.2003.09.005.

Bron, R. et al. (1993) 'Membrane fusion of Semliki Forest virus in a model system: correlation between fusion kinetics and structural changes in the envelope glycoprotein.', *The EMBO journal*, 12(2), pp. 693–701.

Burattini, S. et al. (2004) 'C2C12 murine myoblasts as a model of skeletal muscle development: morpho-functional characterization.', *Eur J Histochem*. 48(3), pp. 223–33.

Buschbeck, M. and Di Croce, L. (2010) 'Approaching the molecular and physiological function of macroH2A variants', *Epigenetics*. 5(2), pp. 118–123. doi: 10.4161/epi.5.2.11076.

Candé, C. et al. (2002) 'Apoptosis-inducing factor (AIF): a novel caspase-independent death effector released from mitochondria', *Biochimie*. 84(2–3), pp. 215–222. doi: 10.1016/S0300-9084(02)01374-3.

Chakravarthy, S. et al. (2005) 'Structural Characterization of the Histone Variant macroH2A', *Molecular and Cellular Biology*, 25(17), pp. 7616–7624. doi: 10.1128/MCB.25.17.7616-7624.2005.

Chambon, P., Weill, J. D. and Mandel, P. (1963) 'Nicotinamide mononucleotide activation of a new DNA-dependent polyadenylic acid synthesizing nuclear enzyme', *Biochemical and Biophysical Research Communications*. 11(1), pp. 39–43. doi: 10.1016/0006-291X(63)90024-X.

Chandak, N. H. et al. (2009) 'Neurological complications of Chikungunya virus infection.', *Neurology India*. 57(2), pp. 177–80. doi: 10.4103/0028-3886.51289.

Chang, A. Y. et al. (2018) 'Frequency of Chronic Joint Pain Following Chikungunya Virus Infection', *Arthritis & Rheumatology*, 70(4), pp. 578–584. doi: 10.1002/art.40384.

Chang, L.-J. et al. (2014) 'Safety and tolerability of chikungunya virus-like particle vaccine in healthy adults: a phase 1 dose-escalation trial', *The Lancet.* 384(9959), pp. 2046–2052. doi: 10.1016/S0140-6736(14)61185-5.

Charlier, C. et al. (2017) 'Arboviruses and pregnancy: maternal, fetal, and neonatal effects', *The Lancet Child & Adolescent Health.* 1(2), pp. 134–146. doi: 10.1016/S2352-4642(17)30021-4.

Chatel-Chaix, L. et al. (2011) 'Y-Box-Binding Protein 1 Interacts with Hepatitis C Virus NS3/4A and Influences the Equilibrium between Viral RNA Replication and Infectious Particle Production', *Journal of Virology,* 85(21), pp. 11022–11037. doi: 10.1128/JVI.00719-11.

Chen, D. et al. (2011) 'Identification of Macrodomain Proteins as Novel O -Acetyl-ADP-ribose Deacetylases', *Journal of Biological Chemistry.* 286(15), pp. 13261–13271. doi: 10.1074/jbc.M110.206771.

Chen, K. C. et al. (2013) 'Comparative analysis of the genome sequences and replication profiles of chikungunya virus isolates within the East, Central and South African (ECSA) lineage.', *Virology journal.* 10, p. 169. doi: 10.1186/1743-422X-10-169.

Chen, R. et al. (2013) 'Chikungunya Virus 3′ Untranslated Region: Adaptation to Mosquitoes and a Population Bottleneck as Major Evolutionary Forces', *PLoS Pathogens.* 9(8), p. e1003591. doi: 10.1371/journal.ppat.1003591.

Chen, R. et al. (2018) 'ICTV Virus Taxonomy Profile: Togaviridae', *Journal of General Virology.* 99(6), pp. 761–762. doi: 10.1099/jgv.0.001072.

Chen, R. A.-J. et al. (2008) 'Inhibition of IκB Kinase by Vaccinia Virus Virulence Factor B14', *PLOS Pathogens.* 4(2), p. e22. doi: 10.1371/JOURNAL.PPAT.0040022.

Chen, Z. J. (2012) 'Ubiquitination in signalling to and activation of IKK', *Immunological Reviews.* (10.1111), 246(1), pp. 95–106. doi: 10.1111/j.1600-065X.2012.01108.x.

Chiam, C. W. et al. (2013) 'Real-time polymerase chain reaction for diagnosis and quantitation of negative strand of chikungunya virus', *Diagnostic Microbiology and Infectious Disease.* 77(2), pp. 133–137. doi: 10.1016/j.diagmicrobio.2013.06.018.

Chiarugi, A. and Moskowitz, M. A. (2002) 'Cell biology: PARP-1--a Perpetrator of Apoptotic Cell Death?', *Science*, 297(5579), pp. 200–201. doi: 10.1126/science.1074592.

Chin, P. A. et al. (2018) 'Differential Effects of Temperature and Mosquito Genetics Determine Transmissibility of Arboviruses by Aedes aegypti in Argentina', *The American Journal of Tropical Medicine and Hygiene,* 99(2), pp. 417–424. doi: 10.4269/ajtmh.18-0097.

Ching Hua Lee, R. et al. (2013) 'Mosquito Cellular Factors and Functions in Mediating the Infectious entry of Chikungunya Virus'. *PLoS Neglected Tropical Diseases.* 7(2), p. 2050. doi: 10.1371/journal.pntd.0002050.

Cho, C.-C. et al. (2016) 'Macro Domain from Middle East Respiratory Syndrome Coronavirus (MERS-CoV) Is an Efficient ADP-ribose Binding Module', *Journal of Biological Chemistry.* 291(10), pp. 4894–4902. doi: 10.1074/jbc.M115.700542.

Choi, H.-K. et al. (1991) 'Structure of Sindbis virus core protein reveals a chymotrypsin-like serine proteinase and the organization of the virion', *Nature.* 354(6348), pp. 37–43. doi: 10.1038/354037a0.

Choi, S.-H. et al. (2006) 'Hepatitis C Virus Nonstructural 5B Protein Regulates Tumor Necrosis Factor Alpha Signaling through Effects on Cellular I B Kinase', *Molecular and Cellular Biology.* 26(8), pp. 3048–3059. doi: 10.1128/MCB.26.8.3048-3059.2006.

Choi, S. et al. (2009) 'Characterization of increased drug metabolism activity in dimethyl sulfoxide (DMSO)-treated Huh7 hepatoma cells', *Xenobiotica*, 39(3), pp. 205–217. doi: 10.1080/00498250802613620.

Chopra, A., Saluja, M. and Venugopalan, A. (2014) 'Effectiveness of Chloroquine and Inflammatory Cytokine Response in Patients With Early Persistent Musculoskeletal Pain and Arthritis Following Chikungunya Virus Infection', *Arthritis & Rheumatology*, 66(2), pp. 319–326. doi: 10.1002/art.38221.

Chow, A. et al. (2011) 'Persistent Arthralgia Induced by Chikungunya Virus Infection is Associated with Interleukin-6 and Granulocyte Macrophage Colony-Stimulating Factor', *The Journal of Infectious Diseases.* 203(2), pp. 149–157. doi: 10.1093/infdis/jiq042.

Chretien, J.-P. and Linthicum, K. J. (2007) 'Chikungunya in Europe: what's next?', *The Lancet.* 370(9602), pp. 1805–1806. doi: 10.1016/S0140-6736(07)61752-8.

Cohausz, O. and Althaus, F. R. (2009) 'Role of PARP-1 and PARP-2 in the expression of apoptosis-regulating genes in HeLa cells', *Cell Biology and Toxicology*. 25(4), pp. 379–391. doi: 10.1007/s10565-008-9092-8.

Cohen, M. S. and Chang, P. (2018) 'Insights into the biogenesis, function, and regulation of ADP-ribosylation.', *Nature chemical biology*. 14(3), pp. 236–243. doi: 10.1038/nchembio.2568.

Couderc, T. et al. (2008) 'A Mouse Model for Chikungunya: Young Age and Inefficient Type-I Interferon Signaling Are Risk Factors for Severe Disease', *PLoS Pathogens,* 4(2), p. e29. doi: 10.1371/journal.ppat.0040029.

Couderc, T. et al. (2008) 'Cell and tissue tropisms of Chikungunya virus and its dissemination to the central nervous system', *BMC Proceedings.* p. S7. doi: 10.1186/1753-6561-2-s1-s7.

Cunha, R. V. da and Trinta, K. S. (2017) 'Chikungunya virus: clinical aspects and treatment - A Review.', *Memorias do Instituto Oswaldo Cruz.* 112(8), pp. 523–531. doi: 10.1590/0074-02760170044.

Dani, N. et al. (2009) 'Combining affinity purification by ADP-ribose-binding macro domains with mass spectrometry to define the mammalian ADP-ribosyl proteome.', *Proceedings of the National Academy of Sciences*. 106(11), pp. 4243–8. doi: 10.1073/pnas.0900066106.

Das, B. B. et al. (2014) 'PARP1–TDP1 coupling for the repair of topoisomerase I–induced DNA damage', *Nucleic Acids Research*, 42(7), pp. 4435–4449. doi: 10.1093/nar/gku088.

Das, T. et al. (2015) 'Multifaceted innate immune responses engaged by astrocytes, microglia and resident dendritic cells against Chikungunya neuroinfection', *Journal of General Virology,* 96(Pt_2), pp. 294–310. doi: 10.1099/vir.0.071175-0.

Dé, I. et al. (2003) 'Functional analysis of nsP3 phosphoprotein mutants of Sindbis virus.', *Journal of virology.* 77(24), pp. 13106–16. doi: 10.1128/JVI.77.24.13106-13116.2003.

DeFilippis, R. A. et al. (2003) 'Endogenous Human Papillomavirus E6 and E7 Proteins Differentially Regulate Proliferation, Senescence, and Apoptosis in HeLa Cervical Carcinoma Cells', *Journal of virology.* 69(12), pp. 7791–7799. doi: 10.1128/jvi.77.2.1551-1563.2003.

Delang, L. et al. (2014) 'Mutations in the chikungunya virus non-structural proteins cause resistance to favipiravir (T-705), a broad-spectrum antiviral',

Journal of Antimicrobial Chemotherapy. 69(10), pp. 2770–2784. doi: 10.1093/jac/dku209.

Delisle, E. et al. (2015) 'Chikungunya outbreak in Montpellier, France, September to October 2014.', *Euro surveillance : bulletin Europeen sur les maladies transmissibles (European communicable disease bulletin),* 20(17).

Desmyter, J. et al. (1968) 'Defectiveness of interferon production and of rubella virus interference in a line of African green monkey kidney cells (Vero).', *Journal of virology.* 2(10), pp. 955–61. doi: 10.1128/jvi.00949-10.

Devhare, P. B. et al. (2013) 'Analysis of Antiviral Response in Human Epithelial Cells Infected with Hepatitis E Virus', *PLoS ONE.* 8(5), p. e63793. doi: 10.1371/journal.pone.0063793.

Dhanwani, R. et al. (2012) 'Characterization of Chikungunya virus infection in human neuroblastoma SH-SY5Y cells: Role of apoptosis in neuronal cell death', *Virus Research*, 163(2), pp. 563–572. doi: 10.1016/j.virusres.2011.12.009.

Diagne, C. T. et al. (2014) 'Vector competence of Aedes aegypti and Aedes vittatus (Diptera: Culicidae) from Senegal and Cape Verde archipelago for West African lineages of chikungunya virus.', *The American journal of tropical medicine and hygiene.* 91(3), pp. 635–41. doi: 10.4269/ajtmh.13-0627.

Díaz, Y. et al. (2015) 'Chikungunya virus infection: first detection of imported and autochthonous cases in Panama.', *The American journal of tropical medicine and hygiene.* 92(3), pp. 482–5. doi: 10.4269/ajtmh.14-0404.

Doceul, V. et al. (2016) 'Zoonotic Hepatitis E Virus: Classification, Animal Reservoirs and Transmission Routes.', *Viruses.*, 8(10). doi: 10.3390/v8100270.

Dong, J. et al. (2010) 'Constitutively active NF- B triggers systemic TNF - dependent inflammation and localized TNF -independent inflammatory disease', *Genes & Development.* 24(16), pp. 1709–1717. doi: 10.1101/gad.1958410.

Douet, J. et al. (2017) 'MacroH2A histone variants maintain nuclear organization and heterochromatin architecture', *Journal of Cell Science*, 130(9), pp. 1570–1582. doi: 10.1242/jcs.199216.

Ducheyne, E. et al. (2018) 'Current and future distribution of Aedes aegypti and Aedes albopictus (Diptera: Culicidae) in WHO Eastern Mediterranean Region', *International Journal of Health Geographics,* 17(1), p. 4. doi: 10.1186/s12942-018-0125-0.

van Duijl-Richter, M. K. S. et al. (2015) 'Chikungunya virus fusion properties elucidated by single-particle and bulk approaches', *Journal of General Virology*, 96(8), pp. 2122–2132. doi: 10.1099/vir.0.000144.

Dutta, S. K. and Myrup, A. C. (1983) 'Infectious center assay of intracellular virus and infective virus titer for equine mononuclear cells infected in vivo and in vitro with equine herpesviruses.', *Canadian journal of comparative medicine : Revue canadienne de medecine comparee.* 47(1), pp. 64–9.

Eckei, L. et al. (2017) 'The conserved macrodomains of the non-structural proteins of Chikungunya virus and other pathogenic positive strand RNA viruses function as mono-ADP-ribosylhydrolases', *Scientific Reports.* 7(1), p. 41746. doi: 10.1038/srep41746.

Economopoulou, A. et al. (2009) 'Atypical Chikungunya virus infections: clinical manifestations, mortality and risk factors for severe disease during the 2005-2006 outbreak on Réunion.', *Epidemiology and infection*, 137(4), pp. 534–41. doi: 10.1017/S0950268808001167.

Egloff, M.-P. et al. (2006) 'Structural and functional basis for ADP-ribose and poly(ADP-ribose) binding by viral macro domains.', *Journal of virology.* 80(17), pp. 8493–502. doi: 10.1128/JVI.00713-06.

Eliseeva, I. A. et al. (2011) 'Y-box-binding protein 1 (YB-1) and its functions', *Biochemistry.* 76(13), pp. 1402–1433. doi: 10.1134/S0006297911130049.

Ember, S. W. J. et al. (2012) 'Vaccinia virus protein C4 inhibits NF-κB activation and promotes virus virulence.', *The Journal of general virology*, 93(Pt 10), pp. 2098–108. doi: 10.1099/vir.0.045070-0.

Erbay, E. and Chen, J. (2001) 'The Mammalian Target of Rapamycin Regulates C2C12 Myogenesis via a Kinase-independent Mechanism', *Journal of Biological Chemistry.* 276(39), pp. 36079–36082. doi: 10.1074/JBC.C100406200.

Eriksson, K. K. et al. (2008) 'Mouse Hepatitis Virus Liver Pathology Is Dependent on ADP-Ribose-1''-Phosphatase, a Viral Function Conserved in the Alpha-Like Supergroup', *Journal of Virology*, 82(24), pp. 12325–12334. doi: 10.1128/JVI.02082-08.

Esu, E. et al. (2010) 'Effectiveness of peridomestic space spraying with insecticide on dengue transmission; systematic review', *Tropical Medicine & International Health*, 15(5), pp. 619–31. doi: 10.1111/j.1365-3156.2010.02489.x.

Fang, X. et al. (2007) 'The membrane protein of SARS-CoV suppresses NF-кB activation', *Journal of Medical Virology,* 79(10), pp. 1431–1439. doi: 10.1002/jmv.20953.

Fehr, A. R. et al. (2016) 'The Conserved Coronavirus Macrodomain Promotes Virulence and Suppresses the Innate Immune Response during Severe Acute Respiratory Syndrome Coronavirus Infection'. *mBio*, doi: 10.1128/mBio.01721-16.

Feijs, K. L. H., Verheugd, P. and Lüscher, B. (2013) 'Expanding functions of intracellular resident mono-ADP-ribosylation in cell physiology', *FEBS Journal,* 280(15), pp. 3519–3529. doi: 10.1111/febs.12315.

Ferguson, N. M. (2018) 'Challenges and opportunities in controlling mosquito-borne infections', *Nature.* 559(7715), pp. 490–497. doi: 10.1038/s41586-018-0318-5.

Firth, A. E. et al. (2008) 'Discovery of frameshifting in Alphavirus 6K resolves a 20-year enigma', *Virology Journal.* 5(1), p. 108. doi: 10.1186/1743-422X-5-108.

Fongsaran, C. et al. (2014) 'Involvement of ATP synthase β subunit in chikungunya virus entry into insect cells', *Archives of Virology*, 159(12), pp. 3353–3364. doi: 10.1007/s00705-014-2210-4.

Foy, N. J. et al. (2013) 'Hypervariable domains of nsP3 proteins of New World and Old World alphaviruses mediate formation of distinct, virus-specific protein complexes.', *Journal of virology.* 87(4), pp. 1997–2010. doi: 10.1128/JVI.02853-12.

Frolov, I., Frolova, E. and Schlesinger, S. (1997) 'Sindbis virus replicons and Sindbis virus: assembly of chimeras and of particles deficient in virus RNA.', *Journal of virology*, 71(4), pp. 2819–29.

Fros, J. J. et al. (2010) 'Chikungunya Virus Nonstructural Protein 2 Inhibits Type I/II Interferon-Stimulated JAK-STAT Signaling', *Journal of Virology*, 84(20), pp. 10877–10887. doi: 10.1128/JVI.00949-10.

Fros, J. J. et al. (2012) 'Chikungunya Virus nsP3 Blocks Stress Granule Assembly by Recruitment of G3BP into Cytoplasmic Foci', *Journal of Virology*, 86(19), pp. 10873–10879. doi: 10.1128/JVI.01506-12.

Fros, J. J. et al. (2013) 'The C-terminal domain of chikungunya virus nsP2 independently governs viral RNA replication, cytopathicity, and inhibition of interferon signaling.', *Journal of virology.* 87(18), pp. 10394–400. doi: 10.1128/JVI.00884-13.

Fros, J. J. and Pijlman, G. P. (2016) 'Alphavirus Infection: Host Cell Shut-Off and Inhibition of Antiviral Responses.', *Viruses*, 8(6), p. 166. doi: 10.3390/v8060166.

Froshauer, S., Kartenbeck, J. and Helenius, A. (1988) 'Alphavirus RNA replicase is located on the cytoplasmic surface of endosomes and lysosomes.', *The Journal of cell biology,* 107(6 Pt 1), pp. 2075–86.

Fullman, N. et al. (2013) 'Nets, spray or both? The effectiveness of insecticide-treated nets and indoor residual spraying in reducing malaria morbidity and child mortality in sub-Saharan Africa', *Malaria Journal*, 12(1), p. 62. doi: 10.1186/1475-2875-12-62.

Gabrieli, P., Smidler, A. and Catteruccia, F. (2014) 'Engineering the control of mosquito-borne infectious diseases', *Genome Biology.* 15(11), p. 535. doi: 10.1186/s13059-014-0535-7.

Galizi, R. et al. (2014) 'A synthetic sex ratio distortion system for the control of the human malaria mosquito', *Nature Communications.* 5(1), p. 3977. doi: 10.1038/ncomms4977.

Gao, Y. et al. (2018) 'Multiple roles of the non-structural protein 3 (nsP3) alphavirus unique domain (AUD) during Chikungunya virus genome replication and transcription', *bioRxiv.* p. 377127. doi: 10.1101/377127.

Gardner, C. L. et al. (2012) 'Interferon-alpha/beta deficiency greatly exacerbates arthritogenic disease in mice infected with wild-type chikungunya virus but not with the cell culture-adapted live-attenuated 181/25 vaccine candidate', *Virology.* 425(2), pp. 103–112. doi: 10.1016/J.VIROL.2011.12.020.

Gérardin, P. et al. (2008) 'Multidisciplinary Prospective Study of Mother-to-Child Chikungunya Virus Infections on the Island of La Réunion', *PLoS Medicine.* 5(3), p. e60. doi: 10.1371/journal.pmed.0050060.

Gérardin, P. et al. (2014) 'Neurocognitive Outcome of Children Exposed to Perinatal Mother-to-Child Chikungunya Virus Infection: The CHIMERE Cohort Study on Reunion Island', *PLoS Neglected Tropical Diseases.* 8(7), p. e2996. doi: 10.1371/journal.pntd.0002996.

Göertz, G. P. et al. (2018) 'The Methyltransferase-Like Domain of Chikungunya Virus nsP2 Inhibits the Interferon Response by Promoting the Nuclear Export of STAT1', *Journal of Virology.* 92(17). doi: 10.1128/JVI.01008-18.

Gokhale, M. D. et al. (2015) 'Chikungunya virus susceptibility and variation in populations of Aedes aegypti (Diptera: Culicidae) mosquito from India.', *The*

Indian journal of medical research. 142 Suppl(Suppl 1), pp. S33-43. doi: 10.4103/0971-5916.176614.

Goo, L. et al. (2016) 'A Virus-Like Particle Vaccine Elicits Broad Neutralizing Antibody Responses in Humans to All Chikungunya Virus Genotypes', *Journal of Infectious Diseases.* 214(10), pp. 1487–1491. doi: 10.1093/infdis/jiw431.

Goodier, J. L. et al. (2015) 'The Broad-Spectrum Antiviral Protein ZAP Restricts Human Retrotransposition', *PLOS Genetics.* 11(5), p. e1005252. doi: 10.1371/journal.pgen.1005252.

Gorbalenya, A. E., Koonin, E. V and Lai, M. M. (1991) 'Putative papain-related thiol proteases of positive-strand RNA viruses. Identification of rubi- and aphthovirus proteases and delineation of a novel conserved domain associated with proteases of rubi-, alpha- and coronaviruses.', *FEBS letters,* 288(1–2), pp. 201–5.

Gorchakov, R. et al. (2004) 'PKR-Dependent and-Independent Mechanisms Are Involved in Translational Shutoff during Sindbis Virus Infection', *Journal of virology,* 78(16), pp. 8455–8467. doi: 10.1128/JVI.78.16.8455-8467.2004.

Gorchakov, R. et al. (2008) 'Different types of nsP3-containing protein complexes in Sindbis virus-infected cells.', *Journal of virology.* 82(20), pp. 10088–101. doi: 10.1128/JVI.01011-08.

Götte, B., Liu, L. and McInerney, G. M. (2018) 'The Enigmatic Alphavirus Non-Structural Protein 3 (nsP3) Revealing Its Secrets at Last.', *Viruses.* 10(3). doi: 10.3390/v10030105.

Griffin, D. E. and Hardwick, and J. M. (1997) 'Regulators of apoptosis on the road to persistent alphavirus infection.', *Annual Review of Microbiology*, 51(1), pp. 565–592. doi: 10.1146/annurev.micro.51.1.565.

Guo, L. et al. (2011) 'Similarities and Differences in the Expression of Drug-Metabolizing Enzymes between Human Hepatic Cell Lines and Primary Human Hepatocytes', *Drug Metabolism and Disposition*, 39(3), pp. 528–538. doi: 10.1124/dmd.110.035873.

Guo, X. et al. (2004) 'The zinc finger antiviral protein directly binds to specific viral mRNAs through the CCCH zinc finger motifs.', *Journal of virology.* 78(23), pp. 12781–7. doi: 10.1128/JVI.78.23.12781-12787.2004.

Gupte, R., Liu, Z. and Kraus, W. L. (2017) 'PARPs and ADP-ribosylation: recent advances linking molecular functions to biological outcomes', *Genes & Development*, 31(2), pp. 101–126. doi: 10.1101/gad.291518.116.

Haese, N. N. et al. (2016) 'Animal Models of Chikungunya Virus Infection and Disease', *The Journal of Infectious Diseases*. 214(Suppl 5), p. S482. doi: 10.1093/INFDIS/JIW284.

Haist, K. C. et al. (2017) 'Inflammatory monocytes mediate control of acute alphavirus infection in mice', *PLOS Pathogens.* 13(12), p. e1006748. doi: 10.1371/journal.ppat.1006748.

Hallengard, D. et al. (2014) 'Novel Attenuated Chikungunya Vaccine Candidates Elicit Protective Immunity in C57BL/6 mice', *Journal of Virology*, 88(5), pp. 2858–2866. doi: 10.1128/JVI.03453-13.

Haller, O., Kochs, G. and Weber, F. (2006) 'The interferon response circuit: Induction and suppression by pathogenic viruses', *Virology.* 344(1), pp. 119–130. doi: 10.1016/J.VIROL.2005.09.024.

Hartman, Z. C., Black, E. P. and Amalfitano, A. (2007) 'Adenoviral infection induces a multi-faceted innate cellular immune response that is mediated by the toll-like receptor pathway in A549 cells', *Virology.* 358(2), pp. 357–372. doi: 10.1016/J.VIROL.2006.08.041.

Hawman, D. W. et al. (2013) 'Chronic joint disease caused by persistent Chikungunya virus infection is controlled by the adaptive immune response.', *Journal of virology.* 87(24), pp. 13878–88. doi: 10.1128/JVI.02666-13.

Hayden, M. S. and Ghosh, S. (2008) 'Shared Principles in NF-κB Signaling', *Cell.* 132(3), pp. 344–362. doi: 10.1016/J.CELL.2008.01.020.

Hengstler, J. G. et al. (2005) 'Generation of human hepatocytes by stem cell technology: definition of the hepatocyte', *Expert Opinion on Drug Metabolism & Toxicology.* 1(1), pp. 61–74. doi: 10.1517/17425255.1.1.61.

Her, Z. et al. (2010) 'Active infection of human blood monocytes by Chikungunya virus triggers an innate immune response.', *Journal of immunology.* 184(10), pp. 5903–13. doi: 10.4049/jimmunol.0904181.

Her, Z. et al. (2015) 'Loss of TLR3 aggravates CHIKV replication and pathology due to an altered virus-specific neutralizing antibody response', *EMBO Molecular Medicine.* 7(1), pp. 24–41. doi: 10.15252/emmm.201404459.

Hinson, A. R. P. et al. (2013) 'Human Rhabdomyosarcoma Cell Lines for Rhabdomyosarcoma Research: Utility and Pitfalls', *Frontiers in Oncology.* 3. doi: 10.3389/FONC.2013.00183.

Honório, N. A. et al. (2018) 'Chikungunya virus vector competency of Brazilian and Florida mosquito vectors.', *PLoS neglected tropical diseases*. 12(6), p. e0006521. doi: 10.1371/journal.pntd.0006521.

Hoornweg, T. E. et al. (2016) 'Dynamics of Chikungunya Virus Cell Entry Unraveled by Single-Virus Tracking in Living Cells.', *Journal of virology*. 90(9), pp. 4745–4756. doi: 10.1128/JVI.03184-15.

Hopp, T. P. et al. (1988) 'A Short Polypeptide Marker Sequence Useful for Recombinant Protein Identification and Purification', *Bio/Technology*. 6(10), pp. 1204–1210. doi: 10.1038/nbt1088-1204.

Horstick, O. et al. (2010) 'Dengue vector-control services: how do they work? A systematic literature review and country case studies', *Transactions of the Royal Society of Tropical Medicine and Hygiene*. 104(6), pp. 379–386. doi: 10.1016/j.trstmh.2009.07.027.

Hottiger, M. O. et al. (2010) 'Toward a unified nomenclature for mammalian ADP-ribosyltransferases', *Trends in Biochemical Sciences*. 35(4), pp. 208–219. doi: 10.1016/J.TIBS.2009.12.003.

Hugo, L. E. et al. (2016) 'Chikungunya virus transmission between Aedes albopictus and laboratory mice', *Parasites & Vectors*. 9(1), p. 555. doi: 10.1186/s13071-016-1838-1.

Hyde, J. L. et al. (2014) 'A viral RNA structural element alters host recognition of nonself RNA.', *Science*. 343(6172), pp. 783–7. doi: 10.1126/science.1248465.

Hyde, J. L. et al. (2015) 'The 5' and 3' ends of alphavirus RNAs--Non-coding is not non-functional.', *Virus research*. 206, pp. 99–107. doi: 10.1016/j.virusres.2015.01.016.

Ivashkiv, L. B. and Donlin, L. T. (2014) 'Regulation of type I interferon responses.', *Nature reviews immunology*. 14(1), pp. 36–49. doi: 10.1038/nri3581.

Janeway, C. (2001) Immunobiology 5 : the immune system in health and disease. *Garland Pub.*

Garland Pub. Jensen, S. and Thomsen, A. R. (2012) 'Sensing of RNA viruses: a review of innate immune receptors involved in recognizing RNA virus invasion.', *Journal of virology*. 86(6), pp. 2900–10. doi: 10.1128/JVI.05738-11.

Jiang, Z. et al. (2004) 'Toll-like receptor 3-mediated activation of NF- B and IRF3 diverges at Toll-IL-1 receptor domain-containing adapter inducing IFN-',

Proceedings of the National Academy of Sciences, 101(10), pp. 3533–3538. doi: 10.1073/pnas.0308496101.

Jiggins, F. M. (2017) 'The spread of Wolbachia through mosquito populations', *PLOS Biology.* 15(6), p. e2002780. doi: 10.1371/journal.pbio.2002780.

Johansen, T. and Lamark, T. (2011) 'Selective autophagy mediated by autophagic adapter proteins', *Autophagy*, 7(3), pp. 279–96.

Johansson, M. A. (2015) 'Chikungunya on the move.', *Trends in parasitology.* 31(2), pp. 43–5. doi: 10.1016/j.pt.2014.12.008.

Jones, J. E. et al. (2017) 'Disruption of the Opal Stop Codon Attenuates Chikungunya Virus-Induced Arthritis and Pathology.', *mBio.* 8(6), pp. e01456-17. doi: 10.1128/mBio.01456-17.

Jones, J. O. and Arvin, A. M. (2006) 'Inhibition of the NF-kappaB pathway by varicella-zoster virus in vitro and in human epidermal cells in vivo.', *Journal of virology.* 80(11), pp. 5113–24. doi: 10.1128/JVI.01956-05.

Joo, M. et al. (2005) 'Hepatitis C Virus Core Protein Suppresses NF- B Activation and Cyclooxygenase-2 Expression by Direct Interaction with I B Kinase', *Journal of Virology*, 79(12), pp. 7648–7657. doi: 10.1128/JVI.79.12.7648-7657.2005.

Josseran, L. et al. (2006) 'Chikungunya disease outbreak, Reunion Island.', *Emerging infectious diseases.* 12(12), pp. 1994–5. doi: 10.3201/eid1212.060710.

Joubert, P.-E. et al. (2012) 'Chikungunya virus–induced autophagy delays caspase-dependent cell death', *The Journal of Experimental Medicine,* 209(5), pp. 1029–1047. doi: 10.1084/jem.20110996.

Judith, D. et al. (2013) 'Species-specific impact of the autophagy machinery on Chikungunya virus infection', *EMBO reports*, 14(6), pp. 534–544. doi: 10.1038/embor.2013.51.

Justman, J., Klimjack, M. R. and Kielian, M. (1993) 'Role of spike protein conformational changes in fusion of Semliki Forest virus.', *Journal of virology*, 67(12), pp. 7597–607.

Kagawa, S. et al. (2001) 'Deficiency of Caspase-3 in MCF7 Cells Blocks Bax-mediated Nuclear Fragmentation but not Cell Death', *Clinical Cancer Research.* 7(5), pp. 1474–1480.

Kam, Y.-W. et al. (2009) 'Immuno-biology of Chikungunya and implications for disease intervention', *Microbes and Infection,* 11(14–15), pp. 1186–1196. doi: 10.1016/j.micinf.2009.09.003.

Kaneko, T., Li, L. and Li, S. S.-C. (2008) 'The SH3 domain--a family of versatile peptide- and protein-recognition module.', *Frontiers in bioscience.* 13, pp. 4938–52.

Karras, G. I. et al. (2005) 'The macro domain is an ADP-ribose binding module.', The *EMBO journal.* 24(11), pp. 1911–20. doi: 10.1038/sj.emboj.7600664.

Kaufmann, M., Feijs, K. L. H. and Lüscher, B. (2014) 'Function and Regulation of the Mono-ADP-Ribosyltransferase ARTD10', *Current topics in microbiology and immunology.* 384 pp. 167–188. doi: 10.1007/82_2014_379.

Kelvin, A. A. et al. (2011) 'Inflammatory cytokine expression is associated with chikungunya virus resolution and symptom severity.', *PLoS neglected tropical diseases.* 5(8), p. e1279. doi: 10.1371/journal.pntd.0001279.

Khan, M. et al. (2010) 'Assessment of in vitro prophylactic and therapeutic efficacy of chloroquine against chikungunya virus in vero cells', *Journal of Medical Virology.* 82(5), pp. 817–824. doi: 10.1002/jmv.21663.

Khong, J. J. et al. (2016) 'Association of Polymorphisms in MACRO Domain Containing 2 With Thyroid-Associated Orbitopathy', *Investigative Opthalmology & Visual Science.* 57(7), p. 3129. doi: 10.1167/iovs.15-18797.

Kim, D. Y. et al. (2011) 'Design of chimeric alphaviruses with a programmed, attenuated, cell type-restricted phenotype.', *Journal of virology.* 85(9), pp. 4363–76. doi: 10.1128/JVI.00065-11.

Kim, D. Y. et al. (2016) 'New World and Old World Alphaviruses Have Evolved to Exploit Different Components of Stress Granules, FXR and G3BP Proteins, for Assembly of Viral Replication Complexes', *PLOS Pathogens.* 12(8), p. e1005810. doi: 10.1371/journal.ppat.1005810.

Kleine, H. et al. (2012) 'Dynamic subcellular localization of the mono-ADP-ribosyltransferase ARTD10 and interaction with the ubiquitin receptor p62', *Cell Communication and Signalling.* 10(1), p. 28. doi: 10.1186/1478-811X-10-28.

Ko, H. L. and Ren, E. C. (2012) 'Functional Aspects of PARP1 in DNA Repair and Transcription.', *Biomolecules.* 2(4), pp. 524–48. doi: 10.3390/biom2040524.

Krejbich-Trotot, P., Gay, B., et al. (2011) 'Chikungunya triggers an autophagic process which promotes viral replication', *Virology Journal,* 8(1), p. 432. doi: 10.1186/1743-422X-8-432.

Krejbich-Trotot, P., Denizot, M., et al. (2011) 'Chikungunya virus mobilizes the apoptotic machinery to invade host cell defences', *The FASEB Journal*, 25(1), pp. 314–325. doi: 10.1096/fj.10-164178.

Kumaran, D. et al. (2005) 'Structure and mechanism of ADP-ribose-1″-monophosphatase (Appr-1″-pase), a ubiquitous cellular processing enzyme', *Protein Science.* 14(3), p. 719. doi: 10.1110/PS.041132005.

Kuri, T. et al. (2011) 'The ADP-ribose-1''-monophosphatase domains of severe acute respiratory syndrome coronavirus and human coronavirus 229E mediate resistance to antiviral interferon responses', *Journal of General Virology*. 92(8), pp. 1899–1905. doi: 10.1099/vir.0.031856-0.

Kutchko, K. M. et al. (2018) 'Structural divergence creates new functional features in alphavirus genomes', *Nucleic Acids Research.* 46(7), pp. 3657–3670. doi: 10.1093/nar/gky012.

Lambert, A. J. and Lanciotti, R. S. (2016) 'Phylogenetic Analysis of Chikungunya Virus Strains Circulating in the Western Hemisphere', *The American Journal of Tropical Medicine and Hygiene*, 94(4), pp. 800–803. doi: 10.4269/ajtmh.15-0375.

Landry, J. J. M. et al. (2013) 'The Genomic and Transcriptomic Landscape of a HeLa Cell Line', *Genes|Genomes|Genetics*, 3(8), pp. 1213–1224. doi: 10.1534/g3.113.005777.

Lani, R. et al. (2015) 'Antiviral activity of silymarin against chikungunya virus', *Scientific Reports.* 5(1), p. 11421. doi: 10.1038/srep11421.

LaStarza, M. W., Lemm, J. A. and Rice, C. M. (1994) 'Genetic analysis of the nsP3 region of Sindbis virus: evidence for roles in minus-strand and subgenomic RNA synthesis.', *Journal of virology.* 68(9), pp. 5781–91.

Lawson, M. A. and Purslow, P. P. (2000) 'Differentiation of Myoblasts in Serum-Free Media: Effects of Modified Media Are Cell Line-Specific', *Cells Tissues Organs.* 167(2–3), pp. 130–137. doi: 10.1159/000016776.

Lee, H.-J. et al. (1991) 'The complete sequence (22 kilobases) of murine coronavirus gene 1 encoding the putative proteases and RNA polymerase', *Virology.* 180(2), pp. 567–582. doi: 10.1016/0042-6822(91)90071-I.

Lemm, J. A. et al. (1994) Polypeptide requirements for assembly of functional Sindbis virus replication complexes: a model for the temporal regulation of minus-and plus-strand RNA synthesis,'*, The EMBO journal*. 13(12), pp 2925-2934

Leparc-Goffart, I. et al. (2014) 'Chikungunya in the Americas.', *Lancet*. 383(9916), p. 514. doi: 10.1016/S0140-6736(14)60185-9.

Leung, A. K. L. (2017) 'PARPs', *Current Biology*, 27(23), pp. R1256–R1258. doi: 10.1016/j.cub.2017.09.054.

Leung, A. K. L., McPherson, R. L. and Griffin, D. E. (2018) 'Macrodomain ADP-ribosylhydrolase and the pathogenesis of infectious diseases', *PLOS Pathogens*. 14(3), p. e1006864. doi: 10.1371/journal.ppat.1006864.

Lhomme, S. et al. (2014) 'Influence of Polyproline Region and Macro Domain Genetic Heterogeneity on HEV Persistence in Immunocompromised Patients', *The Journal of Infectious Diseases*. 209(2), pp. 300–303. doi: 10.1093/infdis/jit438.

Li, C. et al. (2016) 'Viral Macro Domains Reverse Protein ADP-Ribosylation.'*, Journal of virology*. 90(19), pp. 8478–86. doi: 10.1128/JVI.00705-16.

Li, L. et al. (2018) 'PARP12 suppresses Zika virus infection through PARP-dependent degradation of NS1 and NS3 viral proteins.', *Science signalling*. 11(535), p. eaas9332. doi: 10.1126/scisignal.aas9332.

Li, X., Wu, Z. and Han, W. (2013) 'The macrodomain family: Rethinking an ancient domain from evolutionary perspectives', *Chinese Science Bulletin*. 58(9), pp. 953–960. doi: 10.1007/s11434-013-5674-9.

Li, Y.-G. et al. (2012) 'Poly (I:C), an agonist of toll-like receptor-3, inhibits replication of the Chikungunya virus in BEAS-2B cells', *Virology Journal*. 9(1), p. 114. doi: 10.1186/1743-422X-9-114.

La Linn, M. et al. (2001) 'Arbovirus of marine mammals: a new alphavirus isolated from the elephant seal louse, Lepidophthirus macrorhini.', *Journal of virology*. 75(9), pp. 4103–9. doi: 10.1128/JVI.75.9.4103-4109.2001.

Long, K. M. and Heise, M. T. (2015) 'Protective and Pathogenic Responses to Chikungunya Virus Infection.', *Current tropical medicine reports*. 2(1), pp. 13–21. doi: 10.1007/s40475-015-0037-z.

Lumsden, W. H. . (1955) 'An epidemic of virus disease in Southern Province, Tanganyika territory, in 1952–1953 II. General description and epidemiology',

Transactions of the Royal Society of Tropical Medicine and Hygiene. 49(1), pp. 33–57. doi: 10.1016/0035-9203(55)90081-X.

Malet, H. et al. (2006) 'Expression, purification and crystallization of the SARS-CoV macro domain.', *Acta crystallographica.* 62(Pt 4), pp. 405–8. doi: 10.1107/S1744309106009274.

Malet, H. et al. (2009) 'The crystal structures of Chikungunya and Venezuelan equine encephalitis virus nsP3 macro domains define a conserved adenosine binding pocket.', *Journal of virology.* 83(13), pp. 6534–45. doi: 10.1128/JVI.00189-09.

Mathur, K. et al. (2016) 'Analysis of chikungunya virus proteins reveals that non-structural proteins nsP2 and nsP3 exhibit RNA interference (RNAi) suppressor activity', *Scientific Reports.* 6(1), p. 38065. doi: 10.1038/srep38065.

Matz, M. V. et al. (1999) 'Erratum: Fluorescent proteins from nonbioluminescent Anthozoa species', *Nature Biotechnology.* 17(10), pp. 969–973. doi: 10.1038/13657.

McFarlane, M. et al. (2014) 'Characterization of Aedes aegypti Innate-Immune Pathways that Limit Chikungunya Virus Replication', *PLoS Neglected Tropical Diseases.* 8(7), p. e2994. doi: 10.1371/journal.pntd.0002994.

McHugh, J. (2018) 'Acute inflammatory arthritis: Long-term effects of chikungunya', *Nature Reviews Rheumatology*, 14(2), pp. 62–62. doi: 10.1038/nrrheum.2017.223.

McPherson, R. L. et al. (2017) 'ADP-ribosylhydrolase activity of Chikungunya virus macrodomain is critical for virus replication and virulence.', *Proceedings of the National Academy of Sciences.* 114(7), pp. 1666–1671. doi: 10.1073/pnas.1621485114.

McWilliam, H. et al. (2013) 'Analysis Tool Web Services from the EMBL-EBI', *Nucleic Acids Research.* 41(W1), pp. W597–W600. doi: 10.1093/nar/gkt376.

Mehta, R. et al. (2018) 'The neurological complications of chikungunya virus: A systematic review.', *Reviews in medical virology.* 28(3), p. e1978. doi: 10.1002/rmv.1978.

Metz, S. W. et al. (2011) 'Functional processing and secretion of Chikungunya virus E1 and E2 glycoproteins in insect cells', *Virology Journal*, 8(1), p. 353. doi: 10.1186/1743-422X-8-353.

Miller, J. R. et al. (2018) 'Analysis of the Aedes albopictus C6/36 genome provides insight into cell line utility for viral propagation', *GigaScience.* 7(3). doi: 10.1093/GIGASCIENCE/GIX135.

Moller-Tank, S. et al. (2013) 'Role of the Phosphatidylserine Receptor TIM-1 in Enveloped-Virus Entry', *Journal of Virology,* 87(15), pp. 8327–8341. doi: 10.1128/JVI.01025-13.

Morazzani, E. M. et al. (2012) 'Production of Virus-Derived Ping-Pong-Dependent piRNA-like Small RNAs in the Mosquito Soma', *PLoS Pathogens.* 8(1), p. e1002470. doi: 10.1371/journal.ppat.1002470.

Moreira, L. A. et al. (2009) 'A Wolbachia Symbiont in Aedes aegypti Limits Infection with Dengue, Chikungunya, and Plasmodium', *Cell*, 139(7), pp. 1268–1278. doi: 10.1016/j.cell.2009.11.042.

Moyes, C. L. et al. (2017) 'Contemporary status of insecticide resistance in the major Aedes vectors of arboviruses infecting humans', *PLOS Neglected Tropical Diseases.* 11(7), p. e0005625. doi: 10.1371/journal.pntd.0005625.

Nair, S. et al. (2017) 'Interferon Regulatory Factor 1 Protects against Chikungunya Virus-Induced Immunopathology by Restricting Infection in Muscle Cells', *Journal of Virology.* 91(22). doi: 10.1128/JVI.01419-17.

Nan, Y. et al. (2014) 'Hepatitis E virus inhibits type I interferon induction by ORF1 products.', *Journal of virology.* 88(20), pp. 11924–32. doi: 10.1128/JVI.01935-14.

Napetschnig, J. and Wu, H. (2013) 'Molecular Basis of NF-κB Signaling', *Annual Review of Biophysics.* 42(1), pp. 443–468. doi: 10.1146/annurev-biophys-083012-130338.

Narayanan, A. et al. (2012) 'Curcumin Inhibits Rift Valley Fever Virus Replication in Human Cells', *Journal of Biological Chemistry*, 287(40), pp. 33198–33214. doi: 10.1074/jbc.M112.356535.

Nasar, F. et al. (2012) 'Eilat virus, a unique alphavirus with host range restricted to insects by RNA replication', *Proceedings of the National Academy of Sciences.* 109(36), pp. 14622–14627. doi: 10.1073/pnas.1204787109.

Nayak, T. K. et al. (2017) 'Regulation of Viral Replication, Apoptosis and Pro-Inflammatory Responses by 17-AAG during Chikungunya Virus Infection in Macrophages.', *Viruses.* 9(1). doi: 10.3390/v9010003.

Neuvonen, M. et al. (2011) 'SH3 Domain-Mediated Recruitment of Host Cell Amphiphysins by Alphavirus nsP3 Promotes Viral RNA Replication', *PLoS Pathogens*. 7(11), p. e1002383. doi: 10.1371/journal.ppat.1002383.

Neuvonen, M. and Ahola, T. (2009) 'Differential Activities of Cellular and Viral Macro Domain Proteins in Binding of ADP-Ribose Metabolites', *Journal of Molecular Biology,* 385(1), pp. 212–225. doi: 10.1016/j.jmb.2008.10.045.

Neznanov, N. et al. (2005) 'Proteolytic Cleavage of the p65-RelA Subunit of NF-κB during Poliovirus Infection', *Journal of Biological Chemistry*, 280(25), pp. 24153–24158. doi: 10.1074/jbc.M502303200.

Nuckols, J. T. et al. (2014) 'pH-Dependent entry of chikungunya virus fusion into mosquito cells', *Virology Journal*. 11(1), p. 215. doi: 10.1186/s12985-014-0215-y.

O'Neill, S. L. et al. (2018) 'Scaled deployment of Wolbachia to protect the community from Aedes transmitted arboviruses', *Gates Open Research*, 2, p. 36. doi: 10.12688/gatesopenres.12844.1.

Okudela, K. et al. (2004) 'K-ras Gene Mutation Enhances Motility of Immortalized Airway Cells and Lung Adenocarcinoma Cells via Akt Activation: Possible Contribution to Non-Invasive Expansion of Lung Adenocarcinoma', *The American Journal of Pathology*. 164(1), p. 91. doi: 10.1016/S0002-9440(10)63100-8.

Olagnier, D. et al. (2014) 'Inhibition of dengue and chikungunya virus infections by RIG-I-mediated type I interferon-independent stimulation of the innate antiviral response.', *Journal of virology*. 88(8), pp. 4180–94. doi: 10.1128/JVI.03114-13.

Paessler, S. et al. (2003) 'Recombinant sindbis/Venezuelan equine encephalitis virus is highly attenuated and immunogenic.', *Journal of virology*. 77(17), pp. 9278–86. doi: 10.1128/JVI.77.17.9278-9286.2003.

Pal, P. et al. (2013) 'Development of a Highly Protective Combination Monoclonal Antibody Therapy against Chikungunya Virus', *PLoS Pathogens*. 9(4), p. e1003312. doi: 10.1371/journal.ppat.1003312.

Paranjape, S. M. and Harris, E. (2007) 'Y Box-binding Protein-1 Binds to the Dengue Virus 3′-Untranslated Region and Mediates Antiviral Effects', *Journal of Biological Chemistry,* 282(42), pp. 30497–30508. doi: 10.1074/jbc.M705755200.

Park, E. and Griffin, D. E. (2009) 'The nsP3 macro domain is important for Sindbis virus replication in neurons and neurovirulence in mice', *Virology*. 388(2), pp. 305–314. doi: 10.1016/J.VIROL.2009.03.031.

Park, K.-J. et al. (2003) 'Hepatitis C Virus NS5A Protein Modulates c-Jun N-terminal Kinase through Interaction with Tumor Necrosis Factor Receptor-associated Factor 2', *Journal of Biological Chemistry*, 278(33), pp. 30711–30718. doi: 10.1074/jbc.M209623200.

Parquet, M. del C. et al. (2002) 'Complete nucleotide sequence of chikungunya virus and evidence for an internal polyadenylation site', *Journal of General Virology*, 83(12), pp. 3075–3084. doi: 10.1099/0022-1317-83-12-3075.

Pasque, V. et al. (2012) 'Histone variant macroH2A marks embryonic differentiation in vivo and acts as an epigenetic barrier to induced pluripotency.', *Journal of cell science.* 125(Pt 24), pp. 6094–104. doi: 10.1242/jcs.113019.

Pehrson, J. R. and Fuji, R. N. (1998) 'Evolutionary conservation of histone macroH2A subtypes and domains.', *Nucleic acids research*, 26(12), pp. 2837–42.

Peränen, J. and Kääriäinen, L. (1991) 'Biogenesis of type I cytopathic vacuoles in Semliki Forest virus-infected BHK cells.', *Journal of virology.* 65(3), pp. 1623–7.

Perera, R. et al. (2001) 'Alphavirus nucleocapsid protein contains a putative coiled coil alpha-helix important for core assembly.', *Journal of virology.* 75(1), pp. 1–10. doi: 10.1128/JVI.75.1.1-10.2001.

Perez-Ruiz, M. (2003) 'Human rhabdomyosarcoma cells for rapid detection of enteroviruses by shell-vial assay', *Journal of Medical Microbiology*, 52(9), pp. 789–791. doi: 10.1099/jmm.0.05237-0.

Perkins, N. D. (2006) 'Post-translational modifications regulating the activity and function of the nuclear factor kappa B pathway', *Oncogene*, 25(51), pp. 6717–6730. doi: 10.1038/sj.onc.1209937.

Peyrefitte, C. N. et al. (2007) 'Chikungunya virus, Cameroon, 2006.', *Emerging infectious diseases.* 13(5), pp. 768–71. doi: 10.3201/eid1305.061500.

Pingen, M. et al. (2016) 'Host Inflammatory Response to Mosquito Bites Enhances the Severity of Arbovirus Infection', *Immunity.* 44(6), pp. 1455–1469. doi: 10.1016/j.immuni.2016.06.002.

Pohjala, L. et al. (2011) 'Inhibitors of Alphavirus Entry and Replication Identified with a Stable Chikungunya Replicon Cell Line and Virus-Based Assays', *PLoS ONE.* 6(12), p. e28923. doi: 10.1371/journal.pone.0028923.

Pongsiri, P. et al. (2012) 'Multiplex real–time RT–PCR for detecting chikungunya virus and dengue virus', *Asian Pacific Journal of Tropical Medicine*, 5(5), pp. 342–346. doi: 10.1016/S1995-7645(12)60055-8.

Powers, A. M. (2018) 'Vaccine and Therapeutic Options To Control Chikungunya Virus.', *Clinical microbiology reviews.* 31(1), pp. e00104-16. doi: 10.1128/CMR.00104-16.

Prabhu, L. et al. (2015) 'Role of post-translational modification of the Y box binding protein 1 in human cancers', *Genes & Diseases.* 2(3), pp. 240–246. doi: 10.1016/J.GENDIS.2015.05.001.

Priya, R., Patro, I. K. and Parida, M. M. (2014) 'TLR3 mediated innate immune response in mice brain following infection with Chikungunya virus', *Virus Research,* 189, pp. 194–205. doi: 10.1016/j.virusres.2014.05.010.

Prokic, I., Cowling, B. S. and Laporte, J. (2014) 'Amphiphysin 2 (BIN1) in physiology and diseases', *Journal of Molecular Medicine.* 92(5), pp. 453–463. doi: 10.1007/s00109-014-1138-1.

Protter, D. S. W. and Parker, R. (2016) 'Principles and Properties of Stress Granules.', *Trends in cell biology.* 26(9), pp. 668–679. doi: 10.1016/j.tcb.2016.05.004.

Rahman, M. M. and McFadden, G. (2011) 'Modulation of NF-κB signalling by microbial pathogens.', *Nature reviews microbiology.* 9(4), pp. 291–306. doi: 10.1038/nrmicro2539.

Rajapakse, S., Rodrigo, C. and Rajapakse, A. (2010) 'Atypical manifestations of chikungunya infection', *Transactions of the Royal Society of Tropical Medicine and Hygiene.* 104(2), pp. 89–96. doi: 10.1016/j.trstmh.2009.07.031.

Rausalu, K. et al. (2016) 'Chikungunya virus infectivity, RNA replication and non-structural polyprotein processing depend on the nsP2 protease's active site cysteine residue.' *Scientific Reports.* 6(1), p. 37124. doi: 10.1038/srep37124.

Ray Chaudhuri, A. and Nussenzweig, A. (2017) 'The multifaceted roles of PARP1 in DNA repair and chromatin remodelling', *Nature Reviews Molecular Cell Biology,* 18(10), pp. 610–621. doi: 10.1038/nrm.2017.53.

Remenyi, R. et al. (2018) 'Persistent Replication of a Chikungunya Virus Replicon in Human Cells Is Associated with Presence of Stable Cytoplasmic Granules Containing Nonstructural Protein 3.', *Journal of virology.* 92(16), pp. e00477-18. doi: 10.1128/JVI.00477-18.

Reynaud, J. M. et al. (2015) 'IFIT1 Differentially Interferes with Translation and Replication of Alphavirus Genomes and Promotes Induction of Type I Interferon', *PLOS Pathogens*. 11(4), p. e1004863. doi: 10.1371/journal.ppat.1004863.

Rikkonen, M. (1996) 'Functional Significance of the Nuclear-Targeting and NTP-Binding Motifs of Semliki Forest Virus Nonstructural Protein nsP2', *Virology*, 218(2), pp. 352–361. doi: 10.1006/viro.1996.0204.

Roberts, G. C. et al. (2017) 'Evaluation of a range of mammalian and mosquito cell lines for use in Chikungunya virus research', *Scientific Reports*. 7(1), p. 14641. doi: 10.1038/s41598-017-15269-w.

Rupp, J. C. et al. (2015) 'Alphavirus RNA synthesis and non-structural protein functions.', *The Journal of general virology*. 96(9), pp. 2483–500. doi: 10.1099/jgv.0.000249.

Rupp, J. C., Jundt, N. and Hardy, R. W. (2011) 'Requirement for the amino-terminal domain of sindbis virus nsP4 during virus infection.', *Journal of virology*. 85(7), pp. 3449–60. doi: 10.1128/JVI.02058-10.

Russo, A. T., White, M. A. and Watowich, S. J. (2006) 'The Crystal Structure of the Venezuelan Equine Encephalitis Alphavirus nsP2 Protease', *Structure*. 14(9), pp. 1449–1458. doi: 10.1016/j.str.2006.07.010.

Sainz, B. and Chisari, F. V. (2006) 'Production of Infectious Hepatitis C Virus by Well-Differentiated, Growth-Arrested Human Hepatoma-Derived Cells', *Journal of Virology,* 80(20), pp. 10253–10257. doi: 10.1128/JVI.01059-06.

Sakthianandeswaren, A. et al. (2018) 'MACROD2 Haploinsufficiency Impairs Catalytic Activity of PARP1 and Promotes Chromosome Instability and Growth of Intestinal Tumors.', *Cancer discovery*. 8(8), pp. 988–1005. doi: 10.1158/2159-8290.CD-17-0909.

Sanz, M. A. and Carrasco, L. (2001) 'Sindbis virus variant with a deletion in the 6K gene shows defects in glycoprotein processing and trafficking: lack of complementation by a wild-type 6K gene in trans.', *Journal of virology*. 75(16), pp. 7778–84. doi: 10.1128/JVI.75.16.7778-7784.2001.

Schilte, C. et al. (2010) 'Type I IFN controls chikungunya virus via its action on nonhematopoietic cells.', *The Journal of experimental medicine*. 207(2), pp. 429–42. doi: 10.1084/jem.20090851.

Schoggins, J. W. et al. (2011) 'A diverse range of gene products are effectors of the type I interferon antiviral response.', *Nature*. 472(7344), pp. 481–5. doi: 10.1038/nature09907.

Schütze, S. et al. (1995) 'TNF-Induced Activation of NF-κB', *Immunobiology*. 193(2–4), pp. 193–203. doi: 10.1016/S0171-2985(11)80543-7.

Schwartz, O. and Albert, M. L. (2010) 'Biology and pathogenesis of chikungunya virus', *Nature Reviews Microbiology*. 8(7), pp. 491–500. doi: 10.1038/nrmicro2368.

Selvamani, S. P., Mishra, R. and Singh, S. K. (2014) 'Chikungunya Virus Exploits miR-146a to Regulate NF-κB Pathway in Human Synovial Fibroblasts', *PLoS ONE*. 9(8), p. e103624. doi: 10.1371/journal.pone.0103624.

Sen, R. and Smale, S. T. (2010) 'Selectivity of the NF-{kappa}B response.', *Cold Spring Harbor perspectives in biology*. 2(4), p. a000257. doi: 10.1101/cshperspect.a000257.

Severini, F. et al. (2018) 'Vector competence of Italian Aedes albopictus populations for the chikungunya virus (E1-226V)', *PLOS Neglected Tropical Diseases*. 12(4), p. e0006435. doi: 10.1371/journal.pntd.0006435.

Shi, C., Zhang, G.-B. and Yin, S.-W. (2015) 'Effect of bortezomib on migration and invasion in cervical carcinoma HeLa cell', *Asian Pacific Journal of Tropical Medicine*. 8(6), pp. 485–488. doi: 10.1016/J.APJTM.2015.05.004.

Shin, G. et al. (2012) 'Structural and functional insights into alphavirus polyprotein processing and pathogenesis', *Proceedings of the National Academy of Sciences*, 109(41), pp. 16534–16539. doi: 10.1073/pnas.1210418109.

Shirako, Y. and Strauss, J. H. (1998) 'Requirement for an aromatic amino acid or histidine at the N terminus of Sindbis virus RNA polymerase.', *Journal of virology*. 72(3), pp. 2310–5.

Shull, N. P., Spinelli, S. L. and Phizicky, E. M. (2005) 'A highly specific phosphatase that acts on ADP-ribose 1''-phosphate, a metabolite of tRNA splicing in Saccharomyces cerevisiae', *Nucleic Acids Research*. 33(2), pp. 650–660. doi: 10.1093/nar/gki211.

Silva, L. A. et al. (2014) 'A Single-Amino-Acid Polymorphism in Chikungunya Virus E2 Glycoprotein Influences Glycosaminoglycan Utilization', *Journal of Virology*, 88(5), pp. 2385–2397. doi: 10.1128/JVI.03116-13.

Simmons, G. et al. (2016) 'High Incidence of Chikungunya Virus and Frequency of Viremic Blood Donations during Epidemic, Puerto Rico, USA, 2014', *Emerging Infectious Diseases*, 22(7), pp. 1221–1228. doi: 10.3201/eid2207.160116.

Singh, A. et al. (2018) 'Deciphering the dark proteome of Chikungunya virus', S*cientific Reports.* 8(1), p. 5822. doi: 10.1038/s41598-018-23969-0.

Sleijfer, S. et al. (2005) 'Side Effects of Interferon-α Therapy', Pharmacy World & *Science.* 27(6), pp. 423–431. doi: 10.1007/s11096-005-1319-7.

Smit, J. M., Bittman, R. and Wilschut, J. (1999) 'Low-pH-dependent fusion of Sindbis virus with receptor-free cholesterol- and sphingolipid-containing liposomes.', *Journal of virology*, 73(10), pp. 8476–84.

Smith, T. J. et al. (1995) 'Putative receptor binding sites on alphaviruses as visualized by cryoelectron microscopy.', *Proceedings of the National Academy of Sciences.* 92(23), pp. 10648–52.

Solignat, M. et al. (2009) 'Replication cycle of chikungunya: a re-emerging arbovirus.', *Virology.* 393(2), pp. 183–97. doi: 10.1016/j.virol.2009.07.024.

Solt, L. A. and May, M. J. (2008) 'The IkappaB kinase complex: master regulator of NF-kappaB signaling.', *Immunologic research.* 42(1–3), pp. 3–18. doi: 10.1007/s12026-008-8025-1.

Sourisseau, M. et al. (2007) 'Characterization of Reemerging Chikungunya Virus', *PLoS Pathogens.* 3(6), p. e89. doi: 10.1371/journal.ppat.0030089.

Spuul, P. et al. (2007) 'Role of the amphipathic peptide of Semliki forest virus replicase protein nsP1 in membrane association and virus replication.', *Journal of virology.* 81(2), pp. 872–83. doi: 10.1128/JVI.01785-06.

Spuul, P. et al. (2010) 'Phosphatidylinositol 3-Kinase-, Actin-, and Microtubule-Dependent Transport of Semliki Forest Virus Replication Complexes from the Plasma Membrane to Modified Lysosomes', *Journal of Virology*, 84(15), pp. 7543–7557. doi: 10.1128/JVI.00477-10.

Sreejith, R. et al. (2012) 'Mapping interactions of Chikungunya virus nonstructural proteins', *Virus Research*, 169(1), pp. 231–236. doi: 10.1016/j.virusres.2012.08.006.

Staples, J. E., Breiman, R. F. and Powers, A. M. (2009) 'Chikungunya Fever: An Epidemiological Review of a Re-Emerging Infectious Disease', *Clinical Infectious Diseases.* 49(6), pp. 942–948. doi: 10.1086/605496.

Steenbergen, R. H. G. et al. (2013) 'Human serum leads to differentiation of human hepatoma cells, restoration of very-low-density lipoprotein secretion, and a 1000-fold increase in HCV Japanese fulminant hepatitis type 1 titers', *Hepatology*, 58(6), pp. 1907–1917. doi: 10.1002/hep.26566.

Stobart, C. C. and Moore, M. L. (2014) 'RNA virus reverse genetics and vaccine design.', *Viruses.* 6(7), pp. 2531–50. doi: 10.3390/v6072531.

Stollar, V. and Thomas, V. L. (1975) 'An agent in the Aedes aegypti cell line (Peleg) which causes fusion of Aedes albopictus cells', *Virology.* 64(2), pp. 367–377. doi: 10.1016/0042-6822(75)90113-0.

Strauss, J. H. and Strauss, E. G. (1994) 'The alphaviruses: gene expression, replication, and evolution.', *Microbiology and Molecular Biology Reviews*, 58(3).

Suhrbier, A., Jaffar-Bandjee, M.-C. and Gasque, P. (2012) 'Arthritogenic alphaviruses—an overview', *Nature Reviews Rheumatology*, 8(7), pp. 420–429. doi: 10.1038/nrrheum.2012.64.

Sun, S. et al. (2013) 'Structural analyses at pseudo atomic resolution of Chikungunya virus and antibodies show mechanisms of neutralization', *eLife*, 2. doi: 10.7554/eLife.00435.

Suomalainen, M., Liljeström, P. and Garoff, H. (1992) 'Spike protein-nucleocapsid interactions drive the budding of alphaviruses.', *Journal of virology.* 66(8), pp. 4737–47.

Szemiel, A. M., Failloux, A.-B. and Elliott, R. M. (2012) 'Role of Bunyamwera Orthobunyavirus NSs Protein in Infection of Mosquito Cells', *PLoS Neglected Tropical Diseases.* 6(9). doi: 10.1371/JOURNAL.PNTD.0001823.

Tagliamonte, M. et al. (2017) 'Virus-Like Particles', *Micro and Nanotechnology in Vaccine Development.* pp. 205–219. doi: 10.1016/B978-0-323-39981-4.00011-7.

Takata, M. A. et al. (2017) 'CG dinucleotide suppression enables antiviral defence targeting non-self RNA', *Nature*, 550(7674), pp. 124–127. doi: 10.1038/nature24039.

Tang, B. L. (2012) 'The cell biology of Chikungunya virus infection', *Cellular Microbiology.* (10.1111), 14(9), pp. 1354–1363. doi: 10.1111/j.1462-5822.2012.01825.x.

Taylor, S. L. et al. (2009) 'Hantaan Virus Nucleocapsid Protein Binds to Importin Proteins and Inhibits Tumor Necrosis Factor Alpha-Induced Activation of Nuclear Factor Kappa B', *Journal of Virology*, 83(3), pp. 1271–1279. doi: 10.1128/JVI.00986-08.

Teo, T.-H. et al. (2013) 'A pathogenic role for CD4+ T cells during Chikungunya virus infection in mice.', *Journal of immunology.* 190(1), pp. 259–69. doi: 10.4049/jimmunol.1202177.

Thaa, B. et al. (2015) 'Differential Phosphatidylinositol-3-Kinase-Akt-mTOR Activation by Semliki Forest and Chikungunya Viruses Is Dependent on nsP3 and Connected to Replication Complex Internalization', *Journal of Virology.* 89(22), pp. 11420–11437. doi: 10.1128/JVI.01579-15.

Thio, C. L.-P. et al. (2013) 'Differential Proteome Analysis of Chikungunya Virus Infection on Host Cells', *PLoS ONE.* 8(4), p. e61444. doi: 10.1371/journal.pone.0061444.

Thon-Hon, V. G. et al. (2012) 'Deciphering the differential response of two human fibroblast cell lines following Chikungunya virus infection'. *Virology Journal.* 9(1), p. 213. doi: 10.1186/1743-422X-9-213.

Thorn, K. (2017) 'Genetically encoded fluorescent tags.', *Molecular biology of the cell.* 28(7), pp. 848–857. doi: 10.1091/mbc.E16-07-0504.

Timinszky, G. et al. (2009) 'A macrodomain-containing histone rearranges chromatin upon sensing PARP1 activation', *Nature Structural & Molecular Biology.* 16(9), pp. 923–929. doi: 10.1038/nsmb.1664.

Toné, S. et al. (2007) 'Three distinct stages of apoptotic nuclear condensation revealed by time-lapse imaging, biochemical and electron microscopy analysis of cell-free apoptosis', *Experimental Cell Research*, 313(16), pp. 3635–3644. doi: 10.1016/j.yexcr.2007.06.018.

van Tong, H. et al. (2016) 'Hepatitis E Virus Mutations: Functional and Clinical Relevance', *EBioMedicine.* 11, pp. 31–42. doi: 10.1016/J.EBIOM.2016.07.039.

Torres, J. R. et al. (2015) 'Chikungunya fever: Atypical and lethal cases in the Western hemisphere: A Venezuelan experience', *IDCases.* 2(1), pp. 6–10. doi: 10.1016/J.IDCR.2014.12.002.

Tsetsarkin, K. A. et al. (2007) 'A Single Mutation in Chikungunya Virus Affects Vector Specificity and Epidemic Potential', *PLoS Pathogens*, 3(12), p. e201. doi: 10.1371/journal.ppat.0030201.

Tuittila, M. and Hinkkanen, A. E. (2003) 'Amino acid mutations in the replicase protein nsP3 of Semliki Forest virus cumulatively affect neurovirulence', *Journal of General Virology.* 84(6), pp. 1525–1533. doi: 10.1099/vir.0.18936-0.

Turner, T. (2012) 'Development of the Polio Vaccine: A Historical Perspective of Tuskegee University's Role in Mass Production and Distribution of HeLa Cells', *Journal of health care for the poor and underserved*. 23(4 0), p. 5. doi: 10.1353/HPU.2012.0151.

Uematsu, S. and Akira, S. (2007) 'Toll-like receptors and Type I interferons.', The Journal of biological chemistry. 282(21), pp. 15319–23. doi: 10.1074/jbc.R700009200.

Ulmanen, I., Söderlund, H. and Kääriäinen, L. (1976) 'Semliki Forest virus capsid protein associates with the 60S ribosomal subunit in infected cells.', *Journal of virology*, 20(1), pp. 203–10.

Vancini, R. et al. (2013) 'Alphavirus Genome Delivery Occurs Directly at the Plasma Membrane in a Time- and Temperature-Dependent Process', *Journal of Virology,* 87(8), pp. 4352–4359. doi: 10.1128/JVI.03412-12.

Varjak, M., Zusinaite, E. and Merits, A. (2010) 'Novel Functions of the Alphavirus Nonstructural Protein nsP3 C-Terminal Region', *Journal of Virology*, 84(5), pp. 2352–2364. doi: 10.1128/JVI.01540-09.

Vasiljeva, L. et al. (2000) 'Identification of a Novel Function of the Alphavirus Capping Apparatus', *Journal of Biological Chemistry*, 275(23), pp. 17281–17287. doi: 10.1074/jbc.M910340199.

Vaux, D. L. and Häcker, G. (1995) 'Hypothesis: apoptosis caused by cytotoxins represents a defensive response that evolved to combat intracellular pathogens.', *Clinical and experimental pharmacology & physiology*, 22(11), pp. 861–3.

Vega-Rua, A. et al. (2014) 'High Level of Vector Competence of Aedes aegypti and Aedes albopictus from Ten American Countries as a Crucial Factor in the Spread of Chikungunya Virus', *Journal of Virology*, 88(11), pp. 6294–6306. doi: 10.1128/JVI.00370-14.

Venkatesan, A. et al. (2013) 'Case Definitions, Diagnostic Algorithms, and Priorities in Encephalitis: Consensus Statement of the International Encephalitis Consortium', *Clinical Infectious Diseases*, 57(8), pp. 1114–1128. doi: 10.1093/cid/cit458.

Verheugd, P. et al. (2013) 'Regulation of NF-κB signalling by the mono-ADP-ribosyltransferase ARTD10', *Nature Communications*, 4(1), p. 1683. doi: 10.1038/ncomms2672.

Villoing, S. et al. (2000) 'Rainbow trout sleeping disease virus is an atypical alphavirus.', *Journal of virology*. 74(1), pp. 173–83. doi: 10.1128/JVI.74.1.173-183.2000.

Vyas, S. et al. (2014) 'Family-wide analysis of poly(ADP-ribose) polymerase activity', *Nature Communications,* 5(1), p. 4426. doi: 10.1038/ncomms5426.

Wahid, B. et al. (2017) 'Global expansion of chikungunya virus: mapping the 64-year history'. *International Journal of Infectious Diseases*, 58, pp. 69–76. doi: 10.1016/j.ijid.2017.03.006.

Welsby, I. et al. (2014) 'PARP12, an interferon-stimulated gene involved in the control of protein translation and inflammation.', *The Journal of biological chemistry*. 289(38), pp. 26642–57. doi: 10.1074/jbc.M114.589515.

Wengler, G., Würkner, D. and Wengler, G. (1992) 'Identification of a sequence element in the alphavirus core protein which mediates interaction of cores with ribosomes and the disassembly of cores.', *Virology*, 191(2), pp. 880–8.

Werneke, S. W. et al. (2011) 'ISG15 Is Critical in the Control of Chikungunya Virus Infection Independent of UbE1L Mediated Conjugation', *PLoS Pathogens*. 7(10), p. e1002322. doi: 10.1371/journal.ppat.1002322.

Weston, J. H. et al. (1999) 'Salmon Pancreas Disease Virus, an Alphavirus Infecting Farmed Atlantic Salmon, Salmo salar L.', *Virology*, 256(2), pp. 188–195. doi: 10.1006/viro.1999.9654.

White, J. and Helenius, A. (1980) 'pH-dependent fusion between the Semliki Forest virus membrane and liposomes.', *Proceedings of the National Academy of Sciences*. 77(6), pp. 3273–7.

White, L. K. et al. (2011) 'Chikungunya virus induces IPS-1-dependent innate immune activation and protein kinase R-independent translational shutoff.', *Journal of virology*. 85(1), pp. 606–20. doi: 10.1128/JVI.00767-10.

Wichit, S. et al. (2017) 'Aedes Aegypti saliva enhances chikungunya virus replication in human skin fibroblasts via inhibition of the type I interferon signalling pathway', *Infection, Genetics and Evolution*, 55, pp. 68–70. doi: 10.1016/j.meegid.2017.08.032.

Willison, H. J., Jacobs, B. C. and van Doorn, P. A. (2016) 'Guillain-Barré syndrome', *The Lancet*. 388(10045), pp. 717–727. doi: 10.1016/S0140-6736(16)00339-1.

Wilson, J. R. et al. (2008) 'West Nile Virus Nonstructural Protein 1 Inhibits TLR3 Signal Transduction', *Journal of Virology,* 82(17), pp. 8262–8271. doi: 10.1128/JVI.00226-08.

Wintachai, P. et al. (2012) 'Identification of prohibitin as a Chikungunya virus receptor protein', *Journal of Medical Virology*, 84(11), pp. 1757–1770. doi: 10.1002/jmv.23403.

Xu, W.-D. et al. (2012) 'Association of MicroRNA-146a with Autoimmune Diseases', *Inflammation*, 35(4), pp. 1525–1529. doi: 10.1007/s10753-012-9467-0.

Yamada, H. et al. (2007) 'Amphiphysin 1 is important for actin polymerization during phagocytosis.', *Molecular biology of the cell*. 18(11), pp. 4669–80. doi: 10.1091/mbc.e07-04-0296.

Yao, J. S., Strauss, E. G. and Strauss, J. H. (1996) 'Interactions between PE2, E1, and 6K required for assembly of alphaviruses studied with chimeric viruses.', *Journal of virology,* 70(11), pp. 7910–20.

Yap, M. L. et al. (2017) 'Structural studies of Chikungunya virus maturation.', *Proceedings of the National Academy of Sciences*. 114(52), pp. 13703–13707. doi: 10.1073/pnas.1713166114.

Yat-Sing Leung, J., Mah-Lee Ng, M. and Jang Hann Chu, J. (2011) 'Replication of Alphaviruses: A Review on the Entry Process of Alphaviruses into Cells', *Advances in Virology*. 2011. doi: 10.1155/2011/249640.

Yoshiko, Y., Hirao, K. and Maeda, N. (2002) 'Differentiation in C2C12 myoblasts depends on the expression of endogenous IGFs and not serum depletion', *American Journal of Physiology-Cell Physiology,* 283(4), pp. C1278–C1286. doi: 10.1152/ajpcell.00168.2002.

Yu, S.-W. et al. (2002) 'Mediation of poly(ADP-ribose) polymerase-1-dependent cell death by apoptosis-inducing factor.', *Science*. 297(5579), pp. 259–63. doi: 10.1126/science.1072221.

Zaid, A. et al. (2018) 'Review: Chikungunya Arthritis: Implications of Acute and Chronic Inflammation Mechanisms on Disease Management', *Arthritis & Rheumatology*, 70(4), pp. 484–495. doi: 10.1002/art.40403.

Zeng, X., Mukhopadhyay, S. and Brooks, C. L. (2015) 'Residue-level resolution of alphavirus envelope protein interactions in pH-dependent fusion', *Proceedings of the National Academy of Sciences,* 112(7), pp. 2034–2039. doi: 10.1073/pnas.1414190112.

Zhang, G. et al. (2017) 'Cell fusing agent virus and dengue virus mutually interact in Aedes aegypti cell lines', *Scientific Reports*. 7. doi: 10.1038/S41598-017-07279-5.

Zhang, R. et al. (2011) '4.4 Å cryo-EM structure of an enveloped alphavirus Venezuelan equine encephalitis virus.', *The EMBO journal*. 30(18), pp. 3854–63. doi: 10.1038/emboj.2011.261.

Zhang, R. et al. (2018) 'Mxra8 is a receptor for multiple arthritogenic alphaviruses'. *Nature*. 557(7706), pp. 570–574. doi: 10.1038/s41586-018-0121-3.

Zhang, Y. et al. (2011) 'RNF146 is a poly(ADP-ribose)-directed E3 ligase that regulates axin degradation and Wnt signalling', *Nature Cell Biology*. 13(5), pp. 623–629. doi: 10.1038/ncb2222.

Zhang, Y. et al. (2018) 'Y-shaped copolymers of poly(ethylene glycol)-poly(ε-caprolactone) with ketal bond as the branchpoint for drug delivery', *Materials Science and Engineering*. 93, pp. 554–564. doi: 10.1016/J.MSEC.2018.08.021.

Zug, R. and Hammerstein, P. (2012) 'Still a Host of Hosts for Wolbachia: Analysis of Recent Data Suggests That 40% of Terrestrial Arthropod Species Are Infected', *PLoS ONE*. 7(6), p. e38544. doi: 10.1371/journal.pone.0038544.

Zumla, A. (2010) 'Mandell, Douglas, and Bennett's principles and practice of infectious diseases,' 7th edition (vols 1 and 2), GL Mandell, JE Bennett, Dolin R. Churchill (Eds.), *Livingstone* (2010), ISBN: 978-0-443-06839-3'.